Journal Information

Maejo International Journal of Science and Technology (ISSN 1905-7873 © 2011), the international journal for preliminary communications in Science and Technology is the first peerrefereed scientific journal of Maejo University (www.mju.ac.th). Intended as a medium for communication, discussion, and rapid dissemination of important issues in Science and Technology, articles are initially published online in an open access format, which thereby gives authors the chance to communicate with a wide range of readers in an international community.

Publication Information

MIJST is published triannually. Articles are available online and can be accessed free of charge at http://www.mijst.mju.ac.th. Printed and bound copies of each volume are produced and distributed to authors and selected groups or individuals.

Abstracting/Indexing Information

MIJST is covered and cited by Science Citation Index Expanded, SCOPUS, Journal Citation Reports/Science Edition, Zoological Record, Chemical Abstracts Service (CAS), SciFinder Scholar, Directory of Open Access Journals (DOAJ) and Google Scholar.

Contact Information

Editorial office: Maejo International Journal of Science and Technology (MIJST), 1st floor, Orchid Building, Maejo University, San Sai, Chiang Mai 50290, Thailand

Tel: +66-53-87-3880
E-mails: duang@mju.ac.th

MAEJO INTERNATIONAL JOURNAL OF SCIENCE AND TECHNOLOGY

MAEJO INTERNATIONAL JOURNAL OF SCIENCE AND TECHNOLOGY

The International Journal for the Rapid Publication of Preliminary Communications in Science and Technology

http://www.mijst.mju.ac.th
ISSN 1905-7873

MAEJO INTERNATIONAL JOURNAL OF SCIENCE AND TECHNOLOGY

Volume 5, Issue 3 (September – December 2011)

CONTENTS

Page

ISSN 1905-7873

MAEJO INTERNATIONAL JOURNAL OF SCIENCE AND TECHNOLOGY

Volume 5, Issue 3 (September – December 2011)

Author Index

Instructions for Authors

A proper introductory e-mail page containing the title of the submitted article and certifying its originality should be sent to the editor (Duang Buddhasukh, e-mail : duang@mju.ac.th). The manuscript proper together with a list of suggested referees should be attached in separate files. The list should contain at least 3 referees (one or more non-native) with appropriate expertise. Each referee's academic/professional position, scientific expertise, affiliation and e-mail address must be given. The referees should not be affiliated to the same university/institution as any of the authors, nor should any two referees come from the same university/institution.

Failure to conform to the above instructions will result in non-consideration of the submission.

Please also ensure that English and style is properly edited before submission. Authors who would like to consult a professional service can visit www.journalexperts.com, www.proof-reading-service.com, www.editage.com, www.enago.com, www.bioedit.co.uk (bioscience and medical papers), www.bioscienceeditingsolutions.com, www.scribendi.com, or www.letpub.com.

Important : Manuscript with substandard English and style will not be considered.

Warning : Plagiarism (including self-plagiarism) may be checked for at *the last* stage of processing and, if detected, will result in a rejection and blacklisting.

Manuscript Preparation

Manuscripts should be prepared in English using a word processor. MS Word for Macintosh or Windows, and .doc or .rtf files are preferred. Manuscripts may be prepared with other software provided that the full document (with figures, schemes and tables inserted into the text) is exported to a MS Word format for submission. Times or Times New Roman font is preferred. The font size should be 12 pt and the line spacing 'at least 17 pt'. A4 paper size is used and margins must be 1.5 cm on top, 2.0 cm at the bottom and 2.0 cm on both left and right sides of the paper. Although our final output is in .pdf format, authors are asked NOT to send manuscripts in this format as editing them is much more complicated. Under the above settings, a manuscript submitted should not be longer than **15 pages** for a full paper or **20 pages** for a review paper.

A template file may be downloaded from the *Maejo Int. J. Sci. Technol.* homepage. (DOWNLOAD HERE)

Authors' full mailing addresses, homepage addresses, phone and fax numbers, and e-mail addresses homepages can be included in the title page and these will be published in the manuscripts and the Table of Contents. The corresponding author should be clearly identified. It is the corresponding author's responsibility to ensure that all co-authors are aware of and approve of the contents of a submitted manuscript.

A brief (200 word maximum) Abstract should be provided. The use in the Abstract of numbers to identify compounds should be avoided unless these compounds are also identified by names.

A list of three to five keywords must be given and placed after the Abstract. Keywords may be single words or very short phrases.

Although variations in accord with contents of a manuscript are permissible, in general all papers should have the following sections: Introduction, Materials and Methods, Results and Discussion, Conclusions, Acknowledgments (if applicable) and References.

Authors are encouraged to prepare Figures and Schemes in colour. Full colour graphics will be published free of charge.

Tables and Figures should be inserted into the main text, and numbers and titles supplied for all Tables and Figures. All table columns should have an explanatory heading. To facilitate layout of large tables, smaller fonts may be used, but in no case should these be less than 10 pt in size. Authors should use the Table option of MS Word to create tables, rather than tabs, as tab-delimited columns are often difficult to format in .pdf for final output.

Figures, tables and schemes should also be placed in numerical order in the appropriate place within the main text. Numbers, titles and legends should be provided for all tables, schemes and figures. Chemical structures and reaction schemes should be drawn using an appropriate software package designed for this purpose. As a guideline, these should be drawn to a scale such that all the details and text are clearly legible when placed in the manuscript (i.e. text should be no smaller than 8-9 pt).

For bibliographic citations, the reference numbers should be placed in square brackets, i.e. [ ], and placed before the punctuation, for example [4] or [1-3], and all the references should be listed separately and as the last section at the end of the manuscript

Format for References

Journal :

1. D. Buddhasukh, J. R. Cannon, B. W. Metcalf and A. J. Power, ″ Synthesis of 5-n-alkylresorcinol dimethyl ethers and related compounds *via* substituted thiophens", *Aust. J. Chem.*, **1971**, *24*, 2655-2664.

Text :

2. A. I. Vogel, "A Textbook of Practical Organic Chemistry", 3rd Edn., Longmans, London, **1956,** pp. 130-132.

Chapter in an edited text :

3. W. Leistritz, "Methods of bacterial reduction in spices ", in "Spices: Flavor Chemistry and Antioxidant Porperties" (Ed. S. J. Risch and C-T. Ito), American Chemical Society, Washington, DC, **1997**, Ch. 2.

Thesis / Dissertation :

4. W. phutdhawong, “Isolation of glycosides by electrolytic decolourisation and synthesis of pentinomycin”, *PhD. Thesis*, **2002**, Chiang Mai University, Thailand.

Patent :

5. K. Miwa, S. Maeda and Y. Murata, "Purification of stevioside by electrolysis", *Jpn. Kokai Tokkyo Koho 79 89,066* (**1979**).

Proceedings :

6. P. M. Sears, J. Peele, M. Lassauzet and P. Blackburn, "Use of antimicrobial proteins in the treatment of bovine mastitis", Proceedings of the 3rd International Mastitis Seminars, **1995**, Tel-Aviv, Israel, pp. 17-18.

Maejo Int. J. Sci. Technol. **2011**, *5*(03), 292-311

Maejo International Journal of Science and Technology

ISSN 1905-7873
Available online at www.mijst.mju.ac.th

Full Paper

Personalised learning object based on multi-agent model and learners' learning styles

Noppamas Pukkhem* and Wiwat Vatanawood

Department of Computer Engineering, Chulalongkorn University, Bangkok 10400, Thailand

* Corresponding author, e-mail: noppamas.p@student.chula.ac.th

Received: 3 November 2010 / Accepted: 19 September 2011 / Published: 21 September 2011

Abstract: A multi-agent model is proposed in which learning styles and a word analysis technique to create a learning object recommendation system are used. On the basis of a learning style-based design, a concept map combination model is proposed to filter out unsuitable learning concepts from a given course. Our learner model classifies learners into eight styles and implements compatible computational methods consisting of three recommendations: i) non-personalised, ii) preferred feature-based, and iii) neighbour-based collaborative filtering. The analysis of preference error (PE) was performed by comparing the actual preferred learning object with the predicted one. In our experiments, the feature-based recommendation algorithm has the fewest PE.

Keywords: collaborative filtering, content-based recommendation, learning object, learning style, multi-agent model

---

INTRODUCTION

The e-learning community commonly refers to online digital learning resources as learning objects. They offer a new way of thinking about learning content. Learning objects can be educational components presented in any format. Learning objects are commonly stored in learning object repositories that facilitate various functions such as learning object creation, submission, search, comment, review and so on. Rapidly evolving internet and web technologies have facilitated the use of learning objects in learning management systems (LMS), but the LMS does not offer personalised services. All learners are given access to the same set of learning objects and tools

without considering the difference in interest, prior knowledge, experience, motivation and goals. This causes a 'one-size-fits-all' problem owing to a lack of individual learner information that can be used to perform accurate predictions of the most suitable learning object for a particular learner.

Our focus is to build a recommendation method for providing personalised learning for learners. Learning style is used as the adaptation criterion since it is one of the individual differences that plays an important role in learning according to experts.

BACKGROUND AND RELATED WORK

Learning Object

Learning objects are a new way of thinking about learning content design, development, and delivery. Instead of providing all of the material for an entire course or lecture, a learning object seeks to provide material only for a single lesson or lesson-topic within a course. Examples of learning objects include simulations, interactive data sets, quizzes, surveys, annotated texts, and adaptive learning modules. In general, learning objects have the following characteristics [1-4]:

Self-contained—each learning object can be used independently;
Reusable—a single learning object has the potential to be used in multiple contexts for multiple purposes on multiple campuses;
Aggregable—learning objects can be grouped into larger collections, allowing for their inclusion within a traditional course structure;
Tagged with metadata—every learning object has descriptive information that allows it to be found easily by a search, which facilitates the object's use;
Just enough—if a learner needs only a part of a course, he/she can use only the learning objects needed;
Just in time—learning objects are searchable; a learner can quickly find and use the content needed;
Customisable—learning objects allow for easy customisation of courses for a whole organisation or even for each individual.

A learning object does not have a predetermined size. Granularity of a learning object can extend from sub-topics to topics to lessons and to their associated media elements. A collection of learning object topics are aggregated to form lessons, modules, courses and curriculum libraries.

Learning Object Metadata (LOM)

There have been international efforts to develop learning object standards and specifications since the late 1990s. The IEEE Learning Technology Standards Committee, the IMS Global Learning Consortium Inc. and the CanCore Initiative [5] are organisations active in this area.

The IEEE learning object metadata (LOM) [6] standard is a multipart standard composed of the standard for LOM data model, the standard for extensible markup language (XML) binding, and the standard for resource description language (RDF) binding. The first part of the standard, namely IEEE 1484.12.1 LOM data model standard, has been approved and published. The LOM data model is the core of existing metadata specifications and it defines a hierarchical structure for describing a learning object. In the LOM instance, relevant characteristics of learning objects are represented by data elements that are grouped into nine top-level categories, each of which is described in Table 1.

Table 1. Top-level LOM categories [6]

Category	Description
General	The general category groups the general information that describes the resource as a whole.
Lifecycle	The lifecycle category groups the features related to the history and current state of this resource and those that have affected this resource during its evolution.
Meta-metadata	The meta-metadata category groups information about the meta-data record itself (rather than the resource that the record describes).
Technical	The technical category groups the technical requirements and characteristics of the resource.
Educational	The educational category groups the educational and pedagogic characteristics of the resource.
Rights	The rights category groups the intellectual property rights and conditions of use for the resource.
Relation	The relation category groups features that define the relationship between this resource and other targeted resources.
Annotation	The annotation category provides comments on the educational use of the resource and information on when and by whom the comments were created.
Classification	The classification category describes where this resource falls within a particular classification system.

Learning Style

Learning style is an important criterion used in providing personalisation since it has a significant influence on the learning process. Attempts to represent the learning styles of learner and to adapt the learning object to best suit these learning styles are challenging research goals. Learning style includes every type of learning that is characteristic of an individual, i.e. a specific manner of approaching a learning activity, or the learning strategies used in order to fulfill the task.

The Felder-Silverman's learning style model [7] is one of the most widely used learning style in adaptive hypermedia systems. A model for finding the learning style of learners, according to Brown et al.[8], should be suitable for use with multimedia and adaptive web-based education system. The model should display a good degree of validity and reliability/internal consistency and thus provide accurate evaluations of the learning style. The model should also be easily administered to university students.

Another important remark by Sangineto et al. [9] was that the Felder-Silverman learning style model is widely used and validated on an engineering and science student population. Furthermore, this model contains useful pragmatic recommendations for customising teaching according to student profiles.

Related Work

The TANGOW (task-based adaptation learner guidance on the WWW) system [10] is based on an adaptation approach similar to that used by Felder and Silverman but employs only two of the Felder-Silverman learning style dimensions, i.e. sensing/intuitive and sequential/global, and only two types of modules, i.e. 'example' and 'exposition'. For instance, in the case of sensing learners, the students are first presented with an example and only after that they are presented with an exposition regarding that concept.

The Heritage Alive Learning System [11] provides an adaptively customised learning interface. It contains three pairs of widget placeholders (text/image, audio/video and Q&A board/bulletin board). Each pair consists of a primary and a secondary information area. The space allocated on the screen for each widget varies according to the student's Felder-Silverman learning styles. For example, for a visual learner, the image data widget is located in the primary information area, which is larger than the area of text data widget.

Bajraktarevic and Shonam [12] present the course content in a specific layout, corresponding to the Felder-Silverman learning styles (only sequential/global preference). Pages for global learners contain diagrams, table of contents, overview of information and summaries, while pages for sequential learners include only small pieces of information and forward and back buttons.

Graf et al. [13] use adaptation features such as the order of examples, exercises, self-assessment tests, content objects, number of presented examples, and exercises to adapt the course to the four Felder-Silverman learning styles.

In our previous work [14], we implemented a method for generating a course concept map called the course concept map combination model (CMCM) (see the right box in Figure 1). The course concept map is a domain model that represents all possible sequences of learning concepts for a specific course [15]. The domain model stores the knowledge about course preferences and instructor's characteristics and experiences. The main concept map was implemented using CmapTools [16], which is a suite of tools for generating and sharing concept maps in an electronic form. CmapTools supports the generation and modification of concept maps as well as the addition of navigational links from individual concepts to other concept maps and multi-media material such as images, diagrams and video clips, thereby enabling the construction of rich knowledge models. The tools facilitate storage of and access to concept maps on multiple servers, providing the network services required to support knowledge sharing across geographically distant sites. The concept map can be used as the structure of contents that support the learning object recommendation method (Figure 1) described in this paper.

LEARNER MODEL

A learner model is one constructed by observing the interaction between a learner and a learning system in an instructional environment. Building the learner model (Figure 1) starts with an analysis of the learner's learning style using an index of learning styles (ILS) questionnaire.

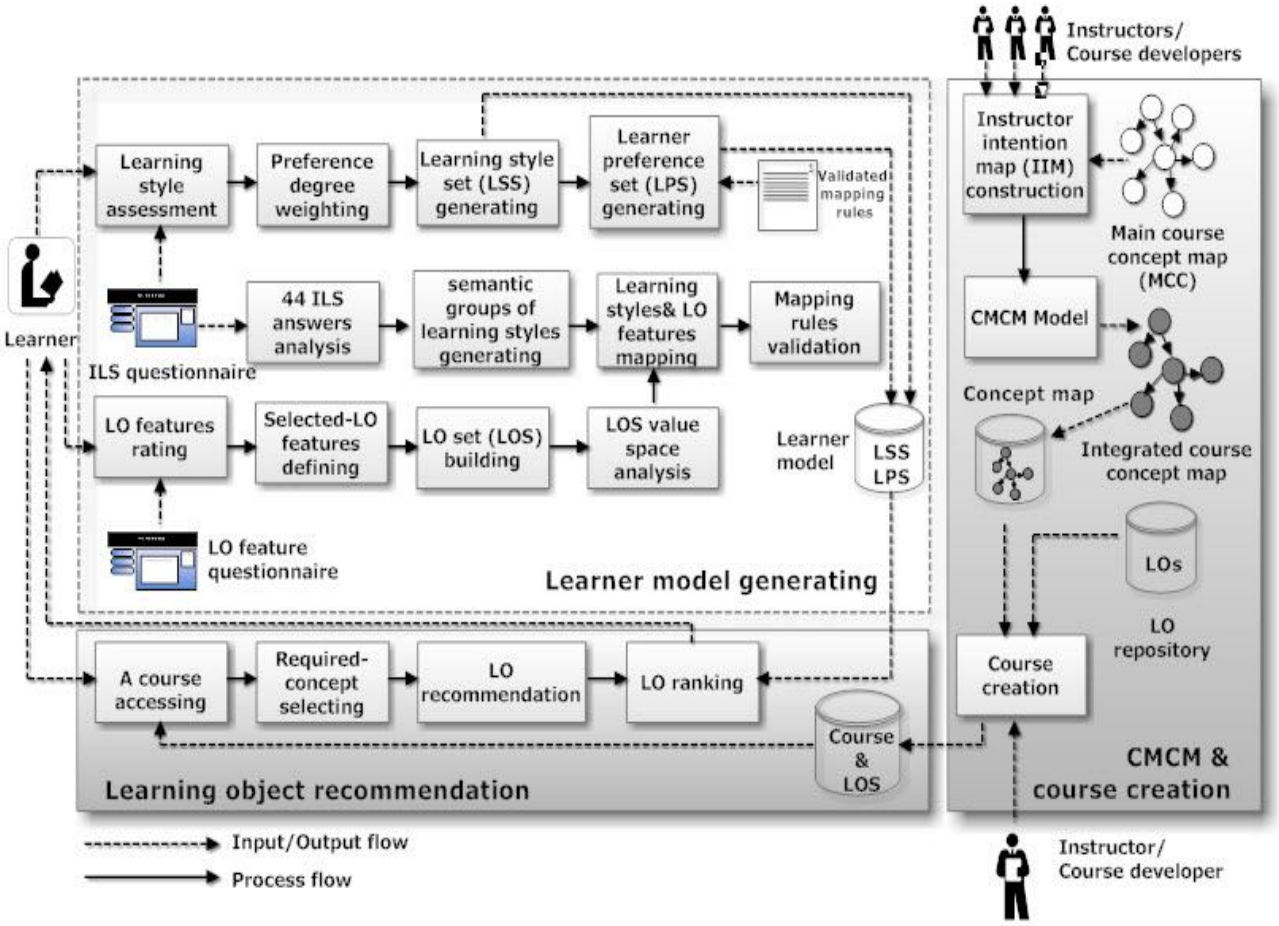

Figure 1. Abstract of recommended model for learning object based on learning styles

The ILS is a 44-question instrument designed to assess preference on the four dimensions of the Felder-Silverman learning style model [17]. The learner's responses are evaluated by the learning style indicator. Then learners are classified using a learner style set (LSS) that contains the learning styles of each learner by assigning a weight parameter (0, 0.5 and 1). In our study, preference scores (PS) are scaled into three groups:

Strong preference: learner strongly prefers to learn with this learning style. The score ranges between 8 and 11 (weight = 1);

Medium preference: learner quite prefers to learn with this learning style. The score ranges between 4 and 7 (weight=0.5);

Weak preference: learner does not prefer or does not like this learning style. The score ranges between 0 and 3 (weight = 0).

The LSS is a combination of each learning style and its weight. The learning object selection rules are used to identify the preferred learning object features for each learner and to create a learner preference set (LPS) that contains the preference of each learner. Both the LSS and LPS are stored in the learner model database.

Learner Analysis Experiment

Learner analysis is the first step in developing a learner model because the learning styles of learners need to be known in order to develop an appropriate learner model in our system. We examined the learning styles of third- and fourth-year students majoring in computer science (CS) and information technology (IT) at Thaksin University (Thailand) during the academic year 2009.

The Thai-version ILS was administered to all participants. Students were asked to complete a self-administered questionnaire at the end of one lecture period during the first semester. Each dimension of the ILS has a two-pan scale, with each pan representing one of the two categories of the dimension (e.g. sensing and intuiting) and weight in a pan representing the skills associated with that category. The indications of the ILS are shown in Table 2. If a learner has a preference for sensing, for example, it means he/she has more weight in the sensing pan than the intuitive pan.

Of the learners in the 2009 cohort, 142 participated in the study by completing the ILS. In active/reflective (D1) category, the majority of learners preferred the strong active learning style (80 learners) and 16 learners preferred the strong reflective style. In visual/verbal (D3) category, many learners preferred the strong visual style (77 learners) and fewer learners preferred the strong verbal style (28 learners). There was not much difference in the strong preferences in D2 and D4 learning styles. In the former, 53 learners preferred the strong sensing style and 47 learners preferred the strong intuitive style. In the latter, 21 learners preferred the strong sequential style and 25 learners preferred the strong global style. Thus, we could define those features of learning objects that were related to both active/reflective and visual/verbal categories. This is the implicit information to be used in matching the learning style of the learner and the learning object.

Table 2. Indications of the ILS [17]

Dimension No.	Question No.	Symbol
D1	1, 5, 9, 13, 17, 21, 25, 29, 33, 37, 41	**A-A**ctive/**R-R**eflective
D2	2, 6, 10, 14, 18, 22, 26, 30, 34, 38, 42	**S-S**ensing/**I-I**ntuitive
D3	3, 7, 11, 15, 19, 23, 27, 31, 35, 39, 43	**U**-Vis**U**al/**B**-Ver**B**al
D4	4, 8, 12, 16, 20, 24, 28, 32, 36, 40, 44	**Q-**Se**Q**uential/ **G-G**lobal

Learner's Learning Style Set (LSS)

The result of the learner's learning style analysis from the above subsection was used to create the learner's LSS. We define the LSS of learners in Definition 1.

Definition 1: *Learner style set* $LSS(L) = \{(P_i, Pw_i)\} \mid P_i \in \{A, R, S, I, U, B, Q, G\}$, *where* Pw_i *is the weight with interval [0–1] for each* P_i *and i is the number of learning styles.* For example, for a particular learner L_1, we might have $LSS(L_1)$ = *{(A,1), (R,0), (S,0.5), (I,0.5), (U,1), (B, 0), (Q,0), (G,1)}*

Learner Preference Set (LPS)

For generating the LPS that describes the preferred learning object features of the learner, we developed the learning object selection rules for matching the learner preference with suitable features of learning objects (LO-learner preference matching). The features and their value space, based on the IEEE LOM metadata in the proposed recommendation algorithm, are identified in Table 3.

Table 3. Selected features for learning object recommendation

ID	Name	Element path	Value space
F1	Format	LOM/Technical/Format	Video, Image, Text, Audio, Animation
F2	Interactivity type	LOM/Educational/Interactivity_Type	Active, Expositive, Mixed
F3	Interactivity level	LOM/Educational/Interactivity_Level	Very low (0), Low (1), Medium (2), High (3), Very high (4)
F4	Semantic density	LOM/Educational/Semantic_Density	Very low (5), Low (6), Medium (7), High (8), Very high (9)
F5	Learning resource type	LOM/Educational/Learning_Resource_Type	Exercise, Simulation, Experiment, Definition, Algorithm, Example, Slide, Index

This feature set was used in the feature-based recommendation algorithm. Definition 2 is the feature set used to describe a learning object.

Definition 2: *Learning object set, LOS_{LO} , is a discrete set of all selected learning object features necessary to describe the characteristics of a specific learning object:*

$$LOS_{LO} = \{F_1, F_2, F_3, F_4, F_5 \mid \forall F_i \in LOM, F_i \neq F_j\}$$

For example, three learning objects in Table 3 were explained by Definition 2 as follows:

LOS_{LO001} = {*F1, F2, F3, F4, F5*} = {*animation, active, 4, 8, simulation*}

LOS_{LO002} = {*F1, F2, F3, F4, F5*} = {*text, expositive, 2, 7, algorithm*}

LOS_{LO003} = {*F1, F2, F3, F4, F5*} = {*video, active, 4, 7, definition*}

Mapping Selected Learning Object Features to Learners' Learning Style

Felder and Silverman [17] defined eight learning styles: active, reflective, sensing, intuitive, visual, verbal, sequential and global. Examples of semantic group (SG) associated with the ILS answers are explained in Table 4.

Table 4. Examples of 'A-Active' learning style's SG associated with ILS answers

Learning Style	SG	ILS questionnaire indicator No.		Extracted words for validating mapping rule
		Answer 'a'	Answer 'b'	
A-Active	Trying something out (SG1)	1 17 25 29	-	Try out Start solution immediately Try out Practice
	Social oriented (SG2)	5 9 13 21 33 37 41	-	Talk Contribute idea Group Group Group Group, outgoing Group

The values of these properties constitute the input for the planner to generate a recommendation adjusted to the learner's preferences and learning styles. However, this process is only possible if there is an implicit relationship between the learners' characteristics and the different kinds of learning objects and activities associated with the learning design. If these learning objects are characterised by the metadata, rules can be applied to assign the learning objects to the learners' learning style in the LMS. In this study, the IEEE LOM was used to characterise learning objects. An appropriate learning object is one that addresses at least one characteristic of the learner.

Grouping of Learning Style Preferences

The SGs within the dimensions provide relevant information used to identify learning styles. For example, if a learner has a preference for trying things out and tends to be more impersonal oriented, the learner would have a balanced learning style on the active/reflective dimension. However, a learner also has a balanced learning style if he/she prefers to think about the material and tends to be more socially oriented. Although both learners have different preferences and therefore different behaviour in an online course, both are viewed according to the result of the ILS. Therefore, considering the proposed SGs leads to providing more accurate information about

learners' preferences and thereby developing a more accurate model for identifying their learning styles based on their behaviour in an online course.

In this analysis, we define the learner characteristics required to generate recommendations according to learning styles and related competence. Furthermore, we describe the mechanism to link those features with the learning objects and resources used to create the learning object selection rules.

Table 5 presents the domain knowledge of the learning object set (LOS). We may infer from LOS definition 2 that $LOS_{LO} = \{F_1, F_2, F_3, F_4, F_5 \mid \forall F_i \in LOM, F_i \neq F_j\}$. Since LOS $\subseteq$ LOM, where LOM always describes every learning object, LO_i, the result implies that LOS always describes every learning object, LO_i. If we define the mapping rules that cover all LOS features, every LO_i can be accessed. Table 5 presents the LOM value space analysis in the LOS domain. Vi is defined as the LOM value space, where i is value space (V) number. This knowledge is used in mapping rule construction and validation.

Table 5. Examples of LOM value space analysis in the LOS domain [5-6]

Feature of LOS	LOM value space	LOS domain
Format (F1)	Video (V1)	"I see," "moving eye picture," "a recording of both the visual and audible components"
	Image (V2)	"two-dimensional figure," "map," "graph," "pie chart," "abstract painting," "computer graphic," "drawing," "painting," "photograph," "visual media," "picture," "idea"
	Text (V3)	"set of writing," "message"
	Audio (V4)	"hear," "listen," "sound"
	Animation (V5)	"motion picture," "the act of animating," "spirit," "liveliness," "airiness," "sequence of image"

The valid mapping rule is the one that is a member of the intersection set of word meaning or semantic between SGs and LOS features. Figure 2 presents the mapping process between learning style and LOS.

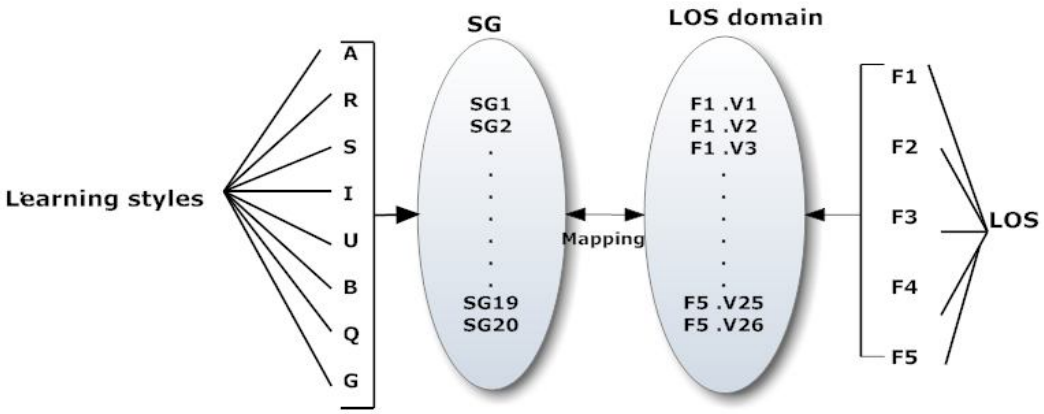

Figure 2. Semantic mapping between learning style and LOS features

Mapping Rules with Word Analysis Construction and Validation

A common way to perform the analysis of mapping is to allow the domain knowledge of learning styles and learning object features to perform this task with word analysis support. Figure 3 shows the mapping rules for this building process.

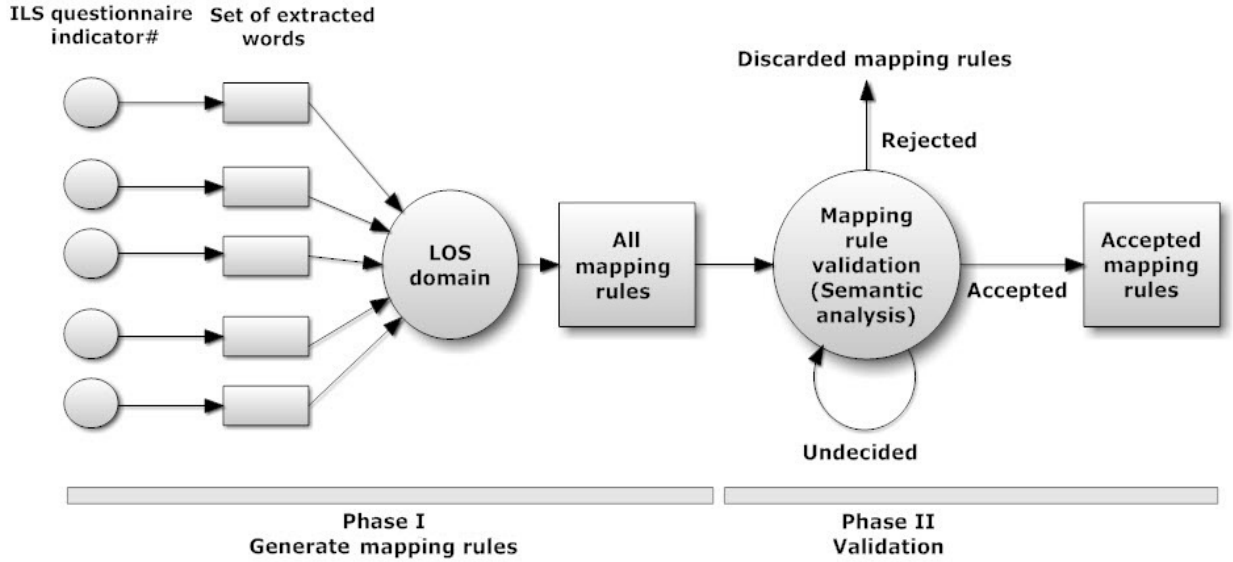

Figure 3. Learning object mapping rules for the building process

In the proposed approach, learning styles and learning object feature mapping rules are discovered and the LOS domain validated by an expert. Depending on how well the rules represent the actual behaviour of the learner, some rules are 'accepted' and some are 'rejected' by the expert.

In Phase I, mapping rule generation constitutes mapping rules describing the learning object preferences of individual learners that are generated from the learners' ILS answer as described in

the subsection below. Phase II constitutes the mapping rule validation process. Mapping rule validation, unlike rule discovery (Phase I), is not performed separately for each learner, but rather performed for all learners at once. The reason we perform mapping rule validation collectively (rather than individually) is that there are usually many similar or even identical rules across different learners.

All mapping rules are collected into one set. The mapping rule validation process is performed as the second part of Phase II as described in Figure 3. At this stage, all the mapping rules are considered invalid. We analyse the meaning of extracted words from 44 ILS answers and compare them with the learning object features in the LOS. Then the validation mapping as O is defined and successively applied to the set of invalid mapping rules. The validation mapping results in the validation of some of the rules. In particular, some mapping rules are accepted and some are rejected (sets O_{accept} and O_{reject} according to Algorithm 1).

Algorithm 1: Mapping rules validation process

INPUT: Set of all discovered mapping rules MR_{all}
OUTPUT: Set of mapping rules MR_{accept}, MR_{reject}, $MR_{invalid}$ such that
$MR_{all} = MR_{accept} \cup MR_{reject} \cup MR_{invalid}$
METHODS:
$MR_{invalid} = MR_{all}$, $MR_{accept} = \phi$, $MR_{reject} = \phi$
WHILE (not TerminateValidationProcess())
BEGIN Expert selects a validation operator (called O) from the set of available validation mapping. O is applied to $MR_{invalid}$, Result: disjoint sets O_{accept} and O_{reject}
$MR_{invalid} = MR_{invalid} - O_{accept} - O_{reject}$,
$MR_{accept} = MR_{accept} \cup O_{accept}$,
$MR_{reject} = MR_{reject} \cup O_{reject}$
END

Next, the validation mapping is applied to the remaining set of invalid rules (set $MR_{invalid}$). This validation process stops when the terminate validation process condition is met. In this study, this condition is that the set of validated mapping rules are covered by the LOS domain (all learning object features are referred). After the validation process is stopped, the set of all the discovered rules (MR_{all}) is split into three sets: accepted rules (MR_{accept}), rejected rules (MR_{reject}), and possibly some remaining rules that have not been invalidated ($MR_{invalid}$). At the end of Phase II, all the accepted mapping rules are used to transform the LSS to the LPS.

Based on the Felder-Silverman learning style model, the association between each learning style and learning object features is analysed. Examples of validated mapping rule selection from all possible mapping rules are presented as follows:

Mapping rule 1. *Recommend learning object for "**A-A**ctive" learner*

If "A" ∈ LSS(L)

Then LOM.educational.interactivity_type = "active" or "mixed"

And LOM.educational.LearningResourceType = "exercise" or "simulations" or "experiment"

Mapping rule 2. *Recommend learning object for "**R-R**eflective" learner*

If "R" ∈ LSS(L)

Then LOM.educational.interactivity_type = "expositive"

And LOM.educational.ResourceType = "definition" or "algorithm" or "example"

Mapping rule 3. *Recommend learning object for "**S-S**ensing" learner*

If "S" ∈ LSS(L)

Then LOM.educational.semanticDensity = "high" or very "high"

And LOM.educational.learningResourceType = simulation or experiment

Mapping rule 4. *Recommend learning object for "**I-I**ntuitive" learner*

If "I" ∈ LSS(L)

Then LOM.educational.semanticDensity = "very low" or "low or medium"

And LOM.educational.learningResourceType = "definition" or "exercise"

Mapping rule 5. *Recommend learning object for "**U-**vis**U**al" learner*

If "U" ∈ LSS(L)

Then LOM.technical.format = "video" or "image" or "animation"

And LOM.educational.interactivity_level= "high" or "very high"

And LOM.educational.learningResourceType = "simulation"

Mapping rule 6. *Recommend learning object for "**B-**ver**B**al" learner*

If "B" ∈ LSS(L)

Then LOM.technical.format = "text" or "audio"

And LOM.educational.interactivity_level= "medium" or "low" or" very low"

And LOM.educational.learningResourceType = "definition" or "exercise"

Mapping rule 7. *Recommend learning object for "**S-**se**Q**uential" learner*

If "Q" ∈ LSS(L)

Then LOM.technical.format = "text" or "audio"

And LOM.educational.learningResourceType = "exercise" or "algorithm" or "slide"

Mapping rule 8. *Recommend learning object for "**G-G**lobal" learner*

If "G" ∈ LSS(L)

Then LOM.technical.format = "image"

And LOM.educational.learningResourceType = "index"

Based on the word analysis process, an example of accepting the proposed mapping rules (validation mappings O in Algorithm 1) is shown as follows:

Example of Mapping

Active *= {try out, start solution immediately, practice, talk, contribute idea}*

Map to:

Interactivity type

Interactivity type = "active" = {simulation, questionnaire, exercise, problem, practice}

Interactivity type = "mixed"= {video, simulation}

Interactivity type = "expositive" = {hypertext, graphics, audio, essay}

Learning resource type

Learning resource type = "exercise"= {planned sequence of actions, assignment, worksheet, tutorial}

Learning resource type = "simulation"= {behaviour of some situation, behaviour of process}

Learning resource type = "experiment"= {discover unknown, test hypothesis, establish some known truth}

Learning resource type= "definition"= {explanation, give meaning, objective}

Learning resource type= "example"= {case study, show how to act}

Learning resource type= "index"= {glossary, reference, list of contents}

…

Next, the LSS is considered with mapping rules to create the LPS. The definition of the LPS is shown in Definition 3.

Definition 3: *Learner preference set, LPS, is a set of learning object features by which the learner prefers to learn, and its preferred weight.*
LPS = {({PF$_i$}, Pw$_i$)| PF$_i$ ∈ F$_i$, Fw$_i$ ∈ {0, 0.5, 1}},
where PF is the preference feature and denoted by PF= {A, R, S, I, U, B, Q, G},
Fw is the feature weight and i is the number of feature.

PROPOSED RECOMMENDATION MODEL

A learning object recommendation model provides learners with personalised learning object selection service. There are four intelligent agents in this model: learner interface, feedback, learner model and learning object recommendation.

Using XML messaging, we define a generic architecture for agent-based course brokering in order to represent the agent's roles in the recommendation process. The main agents participating (Figure 4) are described as follows:

Learner Interface Agent: This agent detects any user interaction with the learner interface and records the results, if any, of these interactions.

Learner Model Agent: This agent is for maintaining, updating, and analysing the learner profile. The learner model agent employs a learning object selection rule to create the LPS.

Learning Object Recommendation Agent: This agent uses the learner's information from the learner model agent to compute the PS of each learning object.

Feedback Agent: For system modification, the feedback agent obtains the learner's feedback and sends it to the recommended learning object. If the learner is not satisfied with the learning object, the learning object selection rule or the learner model will be updated and the process of recommendation restarted.

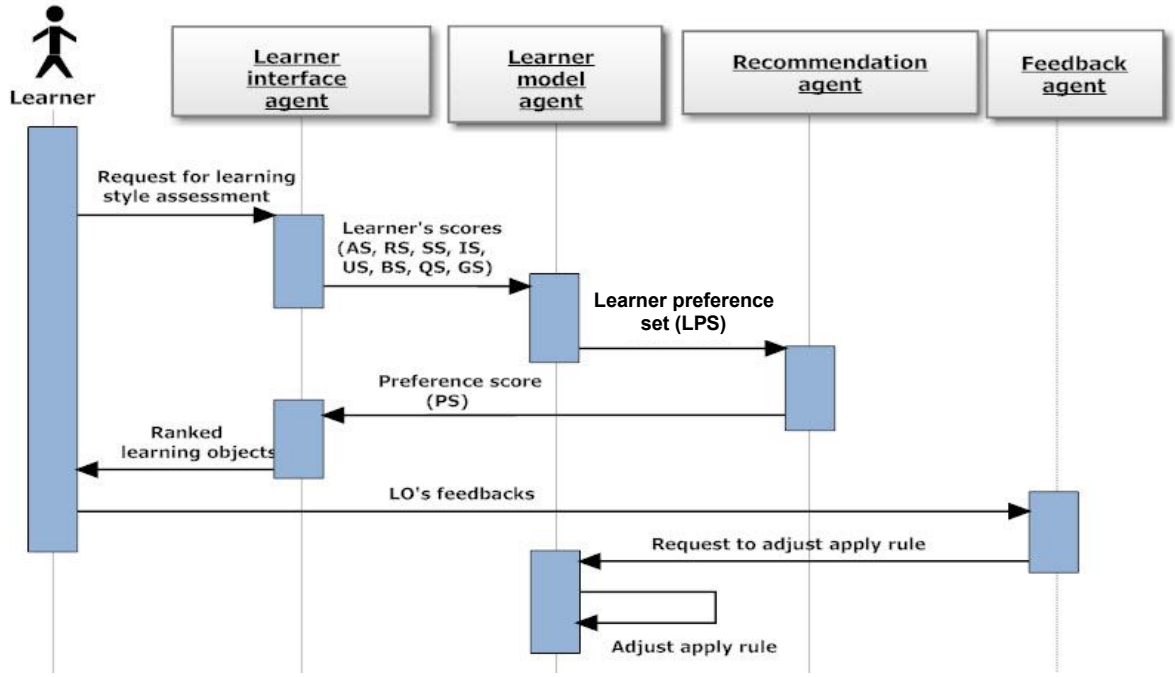

Figure 4. Sequence of personalised learning object selection

Non-personalised Recommendation Algorithms

Next, we examine the non-personalised algorithms to provide the results of learning object selection when learners do not use any of their LPS. There are two sub-algorithms. First, the random algorithm (Rand) randomly selects learning objects in the same topic, independent from the evaluation of the learner. Second, the arithmetic mean (AriMean) calculates a recommendation as the arithmetic mean of each learning object that other learners prefer, independent of how similar the other users are to the learner. The most popular learning object in the same concept will be chosen for the learner.

Preferred Feature-Based Recommendation Algorithm

The preferred feature-based (PFB) algorithm is to bias learning objects towards a learner's preferences. Learning objects tending to suit a learner's preference will get a higher priority when it is matched to the learner. Two variations of the PFB recommendation algorithm, namely non-weighting feature PFB (NWF-PFB) and weighted feature PFB (WF-PFB), are proposed.

NWF-PFB recommendation

In NWF-PFB recommendation, the PS is calculated by the NWF-PFB algorithm. The results show the suitability of each learning object for the learner, independent of the feature weighting. In this algorithm, we define a feature frequency weight of the learning object's features as 1 ($\omega = 1$) for every learning object feature.

WF-PFB recommendation

In WF-PFB recommendation, the learning object feature is weighted by using the frequency that the target feature is given by the learning object selection rule. We note that the frequencies of learning object features, which are referred to in learning object selection rules, are different. In the WF-PFB, ω is computed by $\omega = \frac{1}{\sum F_i \text{ appearing in each Rule}}$ and the results for ω of the learning object features are shown in Algorithm 2. Both the NFW-PFB and the FW-PFB algorithms are described using the PFB algorithm, but they are different in variations of ω. The information of learner model used in our experiment is used as an input for the learning object recommendation. An example of learner id 001 (LSS_{L001}) is described as follows:

LSS_{L001}= *{(A,1), (R,0), (S,0.5), (I,0.5), (U,1,), (B, 0), (Q,0), (G,1)}*

From the rules presented in Definition 3, the LSS of learner 001 (LSS_{L001}) can be converted to the LPS of learner 001 (LPSL001) as follows:

LPS_{L001} = *{({exercise, simulations, experiment, active, mixed},1), ({simulation, experiment, 8, 9}, 0.5), {definition, exercise, 5, 6, 7}, 0.5), ({video, image, animation, simulation, 3, 4, 5},1), ({image, index},1)}*

Both the LSS and LPS is used as input values in the PFB algorithm.

Algorithm 2: The PFB algorithm

INPUT: LPS, LOS,
Two choices of variation of feature frequency weight (ω)
- NWF-PFB, ω = 1 for each learning object feature i, or
- WF-PFB, $\omega = \frac{1}{\#of\ RF_i}$, RF is the frequency of referred feature.

OUTPUT: PS of specific LO
FUNCTION**:** Preference_Score_Calculation () //compute PS of all learners
  FOR EACH LPS // compute PS of learner with all learning objects
    FOR EACH LOS of learning object i
    INT PS = 0
    //compute all of learner styles {A, R, S, I, B, U, Q, G} in LPS
     FOR EACH $PF_i \in$ LPS (L)
          IF ($PF_i = F_i$) and FWi<>0
          THEN PS = PS + ω FW_i
        BREAK
RETURN Preference_Score_Calculation()=PS
END FUNCTION

To demonstrate the program of PFB algorithm, the concept called "Process" in the operating systems course has five learning objects that are used to show the learning object recommendation

for a learner. The example shown in Figure 5 presents PS after a recommendation program has been run.

When the PFB algorithm is used to compute the PS of each LO of learner ID 001, the results are: $PS(LO_{001}) = 1.8125$, $PS(LO_{002}) = 0.75$, $PS(LO_{003}) = 1.0625$, $PS(LO_{004}) = 1.75$, and $PS(LO_{005}) = 1.375$. Therefore, the recommendation order is LO1, LO4, LO5, LO3 and LO2.

```
run:
Learner ID >> 001
Active : Mixed : Execise : Simulation : Experiment : 1.0
8 : 9 : Simulation : Experiment : 0.5
5 : 6 : 7 : Definition : Example : 0.5
Video : Image : Animation : 2 : 3 : 4 : Simulation : 1.0
Image : Index : 1.0
=======================
Learner ID >> 002
Active : Mixed : Execise : Simulation : Experiment : 0.5
Expositive : Definition : Algorithm : Example : 0.5
8 : 9 : Simulation : Experiment : 0.5
5 : 6 : 7 : Definition : Example : 0.5
Video : Image : Animation : 2 : 3 : 4 : Simulation : 0.5
Text : Audio : 0 : 1 : Definition : Exercise : 0.5
Text : Audio : 5 : 6 : Exercise : Algorithm : Slide : 0.5
Image : Index : 0.5
=======================
Learner ID >> 003
Active : Mixed : Execise : Simulation : Experiment : 0.5
Expositive : Definition : Algorithm : Example : 0.5
8 : 9 : Simulation : Experiment : 1.0
Video : Image : Animation : 2 : 3 : 4 : Simulation : 1.0
Text : Audio : 5 : 6 : Exercise : Algorithm : Slide : 0.5
Image : Index : 0.5
=======================
...
=======================
Learner ID >> 001
LO_id = 001 >> 1.8125
LO_id = 002 >> 0.75
LO_id = 003 >> 1.0625
LO_id = 004 >> 1.75
LO_id = 005 >> 1.375

Learner ID >> 002
LO_id = 001 >> 1.0625
LO_id = 002 >> 1.125
LO_id = 003 >> 0.8125
LO_id = 004 >> 1.0625
LO_id = 005 >> 1.3125

Learner ID >> 003
LO_id = 001 >> 1.8125
LO_id = 002 >> 1.0
LO_id = 003 >> 0.8125
LO_id = 004 >> 1.1875
LO_id = 005 >> 0.9375
...
```

Figure 5. Output examples of PS calculated by PFB algorithm

Neighbour-based Collaborative Filtering Recommendation Algorithm (NBCF)

The neighbour-based collaborative filtering (NBCF) recommendation algorithm predicts how helpful a learning object will be for a learner by analysing feedback from similar learners. A similar learner group is defined as a group of learners who have used the same learning objects in the past and returned similar feedback.

The result of this algorithm is an average ranking of the three most similar neighbours

between the learners (SL) and the learner who prefers LO (PL). The detail of NBCF algorithm is shown in Algorithm 3.

Algorithm 3: The NBCF algorithm

INPUT: Preferred learning object ID, LSS of learner (SL)
LSS of preferred learner (PL) of preferred LO
n = number of learner style preference
k = number of nearest neighbours (k = 1, k = 3, k = 5, k = 7, k =9)
OUTPUT: Neighbour Score (NS) of preferred LO
FUNCTION: Neighbour_Score_Calculation()
FOR EACH LSS of SL
FLOAT DIS = 0, MDIS = 0
// compute distance between SP and PL by using learner style
FOR EACH LSS of PL of preferred LO
FOR EACH (P_i in LSS)
$DIS_{(SL,PL)} = DIS_{(SL,PL)} + Sqr((P_{SL}\wedge 2) - (P_{PL}\wedge 2))$
// return k learners who have the least distance of all PLs
FOR ALL $DIS_{(SL,PL)}$ between SL and PLs
Rank($DIS_{(SL,PL)}$)
RETURN Last k of $DIS_{(SL,PL)}$)
MDIS = SUM($DIS_{(SL,PL)}$)/k
RETURN Neighbour_Score_Calculation()=1-MDIS
END FUNCTION

EXPERIMENT AND RESULTS

Experimental Setting

In all experiments, learning objects were recommended to learners using different learning object recommendation algorithms based on their learning styles. Candidate learning objects were filtered by a concept map that was created by the concept map combination model (CMCM) and represented in terms of LOS. Then the actual feedback preferences from learners were evaluated according to the PS and the neighbour score (NS) that were computed by the recommendation algorithms. For the content-based approach, the PS represented the suitability of a learning object according to the learner's degree of preference for each learning object feature. Therefore, the learning object with the highest PS was recommended to the learner. For the collaborative filtering approach, the NS showed a degree of similarity between learners. The learning object that was preferred by other learners who were similar to the learner would be recommended.

Participants and Learning Object Candidates

For experiments, participants were 142 undergraduate students majoring in CS and IT at Thaksin University (Phattalung campus). We divided the undergraduate students into four groups according to their year and study major. Group 1 had 31 third-year students majoring in CS (3CS, n = 31); Group 2 had 48 third-year students majoring in IT (3IT, n = 48); Group 3 had 29 fourth-year students majoring in CS (4CS, n = 29); and Group 4 had 31 fourth-year students majoring in IT (4IT, n = 31). The default number of candidate learning objects for our experiment was 54 in the concept operating systems course. Examples of the LOS of the candidate learning objects are described as follows:

LOS_{L001} = {*animation, active, very high, high, simulation*}
LOS_{L002} = {*text, expositive, low, medium, algorithm*}
LOS_{L003} = {*video, active, very high, medium, definition*}

To understand how the recommendation results affect learners, both feedback analysis and PE between the real learner's preference and the system predictions were compared. Observing the learner's feedback directly indicated whether the proposed model recommended learning objects in accordance with the learner's preference, while calculated PE showed whether the model could accurately infer the learner's preference and interest. The prediction accuracy was good when the PE value was low. In our experiments, different algorithms showed different results. PE could be calculated by using $PE = 1 - \frac{\sum_{i=1}^{N}(LO_{ac} \cap LO_{pd})}{N}$, where LO_{ac} is an actual preferred learning object, LO_{pd} is the recommended learning object, and N is the number of learners.

As a final evaluation of the proposed algorithms, the predicted results of each algorithm were compared with the actual results. The comparison of average PE results among recommendation algorithms is shown in Table 3. It can be concluded that the WF-PFB algorithm has the highest accuracy followed by the NFW-PFB and NBCF, with Rand having the lowest performance (predicted with average PE = 0.8279).

Table 3. Comparison of evaluation results for every algorithm

Algorithm	Variation	PE				Average PE
		3CS	3IT	4CS	4IT	
Rand	-	0.8670	0.8203	0.8190	0.8051	0.8279
AriMean	-	0.3871	0.4792	0.5172	0.3824	0.4415
PFB	Non-weighting feature (NWF)	0.2903	0.2917	0.2759	0.3235	0.2954
	Weighted feature (WF)	**0.2258**	**0.2083**	**0.2414**	**0.2353**	**0.2277**
NBCF	k=1	0.6774	0.5484	0.5517	0.4138	0.5478
	k=3	0.4194	0.4516	0.5172	0.3448	0.4333
	k=5	0.4194	0.4516	0.4138	0.3103	0.3988
	k=7	0.3871	0.5806	0.4483	0.3448	0.4402
	k=9	0.3871	0.4516	0.4483	0.3448	0.4080

CONCLUSIONS

Our model is multi-agent-based with continuous interaction among involved agents. Such an activity is facilitated by the choice of XML for both representing agent ontologies and handling data exchange. Then, based on the learning object features and the results of the learner preference analysis, the learner model that consists of LSS and LPS is created. Both the LSS and the LPS are used as criterion in the recommendation algorithms and are generated by mapping rules on the basis of a word analysis technique. When the three recommendations to learn objects and their variations were compared to determine PE, it was found that the PFB algorithm with weighted feature variation (WF-PFB) has the lowest PE result.

From a research point of view, learning style diagnosis is a prerequisite for adaptation provisioning. Because we provide both the content-based and collaborative filtering techniques, the 'one-size-fits-all' problem is solved. Finally, the efficiency of the proposed model was proved experimentally, and the accuracy of students' satisfaction was very high. In future research, we plan to apply the model on a larger scale, repeated in different domains and for longer periods of time, with a larger number of learners who have different backgrounds and knowledge levels and are in different areas of study.

ACKNOWLEDGEMENTS

The authors sincerely thank the Computer Graphic and Computer Imaging (CGCI) laboratory and Software Engineering laboratory, Faculty of Computer Engineering, Chulalongkorn University. We also thank Thailand's Office of the Higher Education Commission for the financial support.

REFERENCES

1. Blackboard Inc., "Blackboard launches enterprise learning object repository", **2004**, http://investor.blackboard.com/phoenix.zhtml?c=177018&p=irol-newsArticle&ID=604710&highlight= (Accessed: Feb. 3, 2010).
2. Moodle, http://moodle.org (Accessed: Jan. 20, **2010**).
3. ATutor, "Learning management tools", **2010,** http://www.atutor.ca (Accessed: Jan. 20, 2010).
4. dotLRN, "User's manual dotLRN platform", http://eva.unicauca.edu.co/dotLRN%20Manual/ (Accessed: Jan. 20, **2010**).
5. CanCore, http://es.athabascau.ca/Organisations/cancore.htm/view (Accessed: Jan. 3, **2010**).
6. IEEE, "Draft standard for learning object metadata", **2002**, http://ltsc.ieee.org/wg12/20020612-Final-LOM-Draft.html (Accessed: Jan. 20, 2010).
7. R. M. Felder and J. Spurlin, "Application, reliability and validity of the index of learning styles", *Int. J. Eng. Edu.*, **2005,** *21*, 103-112.
8. E. Brown, T. Brailsford, T. Fisher, A. Moore and H. Ashman, "Reappraising cognitive styles in adaptive web applications", Proceedings of the 15th International Conference on World Wide Web, **2006**, Edinburgh, Scotland, pp.327-335.
9. E. Sangineto, N. Capuano, M. Gaeta and A. Micarelli, "Adaptive course generation through learning styles representation", *Univers. Access Inf. Soc.*, **2008**, *7*, 1-23.

10. R. M. Carro, E. P. Pulido and P. Rodriguez, "TANGOW: A model for internet-based learning", *Int. J. Continu. Eng. Edu. Life Long Learning*, **2001**, *11*, 25-34.
11. H. J. Cha, Y. S. Kim, S. H. Park, T. B. Yoon, Y. M. Jung and J. H. Lee, "Learning styles diagnosis based on user interface behaviors for the customization of learning interfaces in an intelligent tutoring system", Proceedings of International Conference on Intelligent Tutoring Systems, LNCS, **2006**, Jhongli, Taiwan, pp.513-524.
12. M. Balabanovic and Y. Shoham, "Fab: Content-based collaborative recommendation", *Comm. ACM,* **1997**, *40*, 66-72.
13. S. Graf, S. R. Viola and T. Leo, "In-depth analysis of the Felder-Silverman learning style dimensions", *J. Res. Technol. Edu.*, **2007,** *40*, 79-93.
14. N. Pukkhem and W. Vatanawood, "Using ontological modeling in multi-expert guiding based learning object recommendation", Proceedings of International Conference on Computer Engineering and Application, **2009**, Manila, Philippines, pp.73-77.
15. H. Y. Shyu, S. H. Hsieh and Y. H. Chou, "Integrating concept map into designing a courseware management system", Proceedings of the Learning Objects 2003 Symposium, **2003**, Honolulu, USA, June, pp.51-60.
16. J. Novak and A. Caňas, "The theory underlying concept maps and how to construct and use them", Florida Institute for Human and Machine Cognition, **2008**, http://cmap.ihmc.us/publications/researchpapers/theorycmaps/theoryunderlyingconceptmaps.htm (Accessed: Jan. 30, 2009).
17. R. M. Felder and B. A. Soloman, "Index of learning styles", http:www.ncsu.edu/felder-public/ILSpage.html (Accessed: June 15, **2007**).

Maejo Int. J. Sci. Technol. **2011**, *5*(03), 312-330

Maejo International Journal of Science and Technology

ISSN 1905-7873
Available online at www.mijst.mju.ac.th

Report

Impact assessment of soil and water conservation measures at Medego watershed in Tigray, northern Ethiopia

Kirubel Mekonen [1] and Gebreyesus Brhane Tesfahunegn [1, 2, *]

[1] Faculty of Agriculture and Rural Development, Aksum University, Aksum, Ethiopia
[2] Present address: Centre for Development Research, University of Bonn, Walter-Flex-Str. 3, D-53113 Bonn, Germany
* Corresponding author, e-mail: gebre042001@yahoo.com; Tel: +49 (0)15 225 262 887; Fax: +49 (0)228-73-5097

Received: 24 September 2010 / Accepted: 23 September 2011 / Published: 26 September 2011

Abstract: The aim of this study is to assess the impact of various physical and biological soil and water conservation (SWC) measures implemented during the past 2–3 decades in combating land degradation caused by soil erosion in the Medego watershed, northern Ethiopia. Such evaluation is essential to understanding the success or failure of previous conservation measures and readjusting accordingly in the future planning. Data collected through semi-structured interviews, transect walks, field observation and field measurements demonstrated that terraces and check dams were filled with soil up to 1.5 m deep, gullies started to stabilise, irrigation and other water supplies increased many folds, the seedling survival rate rose to over 45%, and the vegetation composition and coverage density improved by more than 30%. Water levels increased in hand-dug wells by up to 2 m, and in a number of springs and shallow wells by more than 100 times as a result of the positive impact of SWC measures implemented in this watershed. Existing SWC measures should be improved for continued maintenance and also expanded further to restore critically degraded areas to their full potential through integrated intervention.

Keywords: land degradation, impact assessment, soil and water conservation, Medego watershed, northern Ethiopia

INTRODUCTION

Land degradation is a serious global problem. Of the world's 8.7 billion ha of agricultural land, pasture, forest and woodland, nearly 2 billion ha (22.5%) have been degraded since 1950 [1-2], and 5-10 million ha (0.36–0.71% of global arable land) are lost every year to severe degradation [2-

3]. If such a trend continues, 1.4-2.8% of the total agricultural, pasture and forest land will be lost by 2020 [1]. In addition, estimates show that degradation of crop land and pasture appears to be most extensive in Africa, affecting 65% of crop land area and 31% of pasture land, compared to 51% and 14% in Latin America and 38% and 20% in Asia respectively [1].

It has also been indicated that nowhere is the severe effect of poverty and environmental degradation more evident than in Ethiopia [4]. In this country, out of the estimated 60 million ha of agriculturally productive areas, nearly 27 million ha experience erosion, 14 million ha are considered eroded and requiring rehabilitation, and 2 million ha are considered lost with an estimated total loss of 2 million m^3 of top soil per year and with an average annual soil loss from cultivated lands of 100 t ha^{-1} [4]. The economic impact of soil erosion is more significant in developing countries such as Ethiopia due to lack of capacities to protect existing nutrients and replace lost nutrients [5]. If land degradation continues at the present rates, the consequence will be a challenge for sustainable future productivity and food security of many developing countries [1]. Soil erosion is the main cause of land degradation that affects soil properties and ecosystems in Ethiopia more than anywhere else [6-7].

The immediate consequence of land degradation is reducing crop yields, which leads to economic decline and increasing social stress [6, 8-9]. Periodic low soil moisture due to erratic and poorly distributed rainfall, severe soil loss by run-off and resultant low soil fertility are the prominent factors associated with land degradation causing low agricultural production [7]. In addition, subsistence agriculture that has extended into marginal lands due to increasing population is also aggravating land degradation as well as damaging and threatening the long-term viability of the environment and agricultural production [10]. Soil erosion, which affects about 30 per cent of the cropland, leads to a grain loss of about 7,000 tons per year in Ethiopia[11]. According to Bojö and Cassells [11], the value of grain lost in 1994 due to soil erosion was estimated to be about 10 million Ethiopian Birr (1 USD ~ 2 ETB at that time). The cost of decreased livestock feed availability due to soil erosion leading to lower crop yields was estimated to be 0.8 million ETB in 1994. The total gross annual loss due to both erosion and nutrient loss was estimated at 637 million ETB, which amounted to 3 per cent of the agricultural gross domestic production at that time [11]. Land degradation in the form of soil erosion and declining soil quality seriously challenges agricultural productivity and overall economic growth of the country [12]. The Tigray region, which is in the northernmost part of Ethiopia, suffers from extreme land degradation since steep slopes have been cultivated for many centuries and are subjected to serious soil erosion [13-14].

In coping with these problems, soil and water conservation (SWC) measures have been implemented to alleviate both the problems of erosion and low crop productivity, which are symptoms of two different extremes of rainfall conditions in Ethiopia since the 1970s. The impacts of physical SWC measures can be classified into short- and long-term effects based on the time needed to become effective against soil erosion [15-16]. According to Bosshart [16], the short-term effects of stone bunds are the reduction in slope length and the creation of small retention basins for run-off and sediment. These reduce the quantity and eroding capacity of overland flow. Such effects appear immediately after construction of the stone bunds and reduce soil loss. The medium- and long-term effects include the reduction in slope angle by formed bench terraces, development of vegetation

cover on the bunds and gullies, and change in land management [16]. Based on the studies of the soil conservation research project in other parts of Ethiopia, Herweg and Stillhardt [17] stated that well-established mechanical SWC measures retain most of the soil eroded in between the structures. Such studies, however, may not be applicable to old conservation measures on a catchment scale as most of these studies were conducted on erosion plots that concerned well-managed and young structures.

Several studies have shown that methods employed to reduce soil loss and run-off to negligible amounts are usually based on a combination of practices that help to maintain soil infiltration rates at sufficiently high levels and efficient water run-off [18-20]. Other studies also indicated that SWC practices undoubtedly have a significant role in increasing agricultural production in arid and semi-arid areas where agriculture is hampered by drought, erosion, low soil fertility and moisture stress [7-8, 21]. Such practices have been implemented in the semi-arid areas of Ethiopia since the 1970s. However, little information is documented on the impact of the various long-term SWC measures implemented in watersheds in northern Ethiopia. The objective of this study is to assess the impact of the SWC measures implemented to reduce land degradation in the Medego watershed, northern Ethiopia, and to realise the results so far achieved. This could lead to further improvement of policies implemented in the future.

STUDY AREA DESCRIPTION

This study was carried out from August 2007 to June 2008 to assess the various impacts of SWC measures implemented in the Medego watershed in the Tigray region, northern Ethiopia (Figure 1). Elevation varies between 2000-2700 m above sea level and the watershed has a total area of 1090 ha. The number of households and total population in the watershed were 97 and 637 respectively. The land holding size of most farmers in the study area was less than 1.3 ha. The rainfall is unimodal but erratic in variability and amount within and among seasons. The main rainy season is very short and extends from June to the first week of September. The mean annual rain fall is 700 mm and the mean monthly temperature during the growing season ranges between 15-20^{o}C [22].

Medego watershed is characterised by different landforms which range from flat or undulating plains and rolling land to steep mountains and very steep escarpments (Table 1). This topography terminology is adopted from the slope capability classification by Chekun [23]. The slope aspect and area are also presented in Table 1. Topography influences the type and intensity of SWC measures to be used. The degradation severity also varies as one moves from flat to steep areas. The bedrock of the watershed is mostly of volcanic origin. Alluvial and colluvial deposits on flat plains are also common in the watershed. The soil types vary according to the landform. The main soil types are cambisols on undulating plains and rolling land, lithosols on hilly and steep to very steep lands, and vertisols on flat and plateau landforms [22].

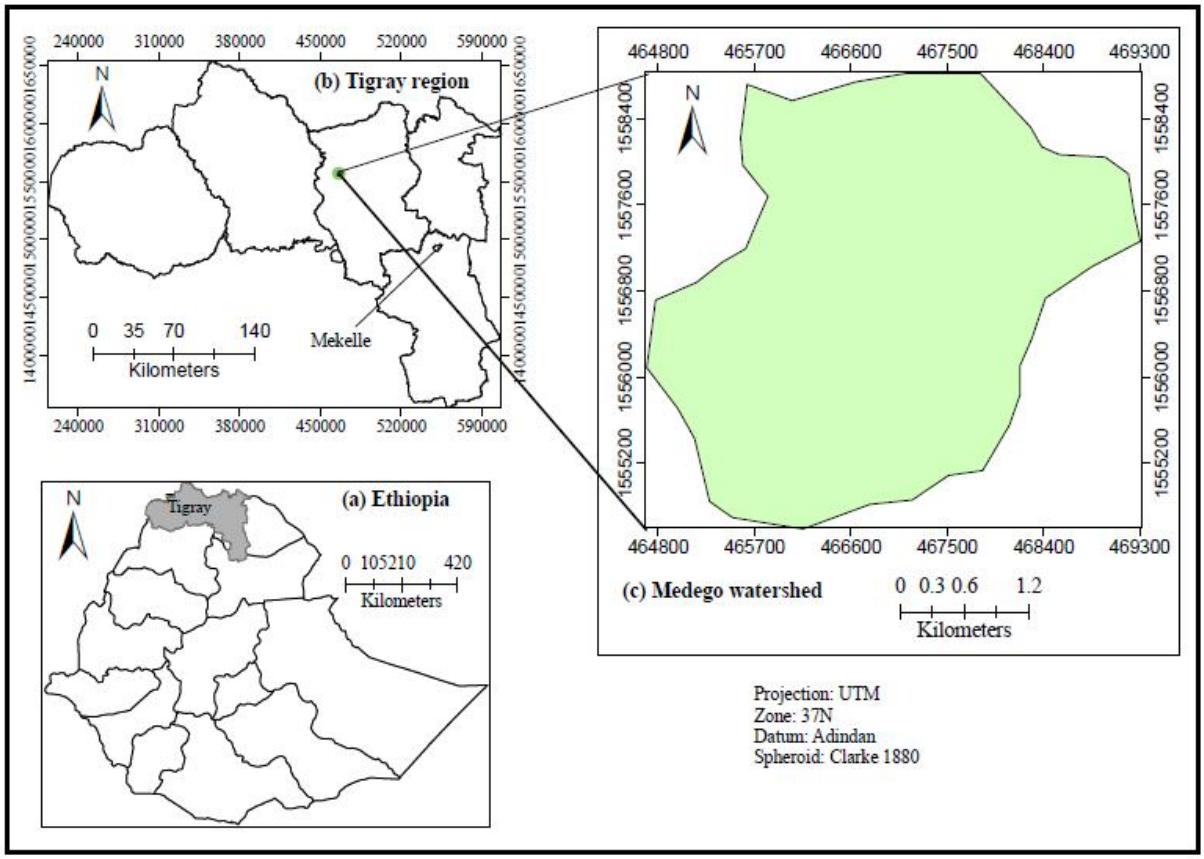

Figure 1. (a) Map of Ethiopia, (b) Tigray region, and (c) Medego watershed

Table 1. Landforms and their area coverage in the Medego watershed

Landform	Slope range (%)	Area (ha)
Flat plain	< 2	200
Undulating plain	2-8	300
Rolling land	8-15	50
Hilly to rolling	15-30	290
Steep mountains	30-50	200
Very steep escarpment	>50	50
Flat, flood-prone area	< 2	1.50
Total		1091

According to the respondents and our field observation, the farming system is principally crop-oriented. Teff cultivation *(Eragrostis tef*) accounts for the majority of the cultivated lands followed by wheat *(Triticum vulgare)*. Other crops such as faba bean *(Vicia faba*), field pea *(Pisum sativum*), lentil *(Lens culinaris*), chick pea *(Cicer arietinum*), flax *(Linum usitatissimum*), barley *(Hordeum vulgare*) and maize *(Zea mays*) are also important crops. Irrigation is also widely practiced here. Despite the high crop diversification in the watershed, we observed that there is still a

need for crop productivity to be improved using appropriate cropping systems and soil and water management practices. Livestock rearing is also essential in the farming system, but stock numbers are being reduced due to feed shortages.

The vegetation is sparse and has been overexploited for centuries and consists of shrubs and small trees with little economic value. The vegetation in the study area includes 'seraw' (*Acacia etbaica*), 'chea' (*Acacia abyssinica*), 'acacha' (*Acacia decurrence*) and 'awhi' (*Cordia africana*) on most uncultivated land, and 'momona' (*Acacia albida*), 'tambock' (*Croton machostachys*), 'keyih bahrizaf' (*Eucalyptus camaldulensis*) and some 'seraw' (*Acacia etbaica*) in both cultivated and marginalised areas. Leucena (*Leuceana leucocephala*), sesbania (*Sesbania sesban*) and some grasses are also commonly found in gullies.

METHODOLOGY

Primary and secondary data were collected related to the environmental impact assessment of SWC measures in the watershed. Primary data were gathered from farmers (topographic transect walks, semi-structured questionnaire interviews, group discussions) and field measurements and observations. The approaches described in Table 2, such as before and after or with and without SWC, down stream and upper stream, and comparisons of indicators of environmental impact, were used during data collection. Secondary data such as climate, demographic and other related data in this study were collected from the Bureau of Agriculture.

The topographic transect walk method was employed for the assessment of natural resources and existing SWC measures in the watershed. In order to obtain as much information as possible, the transect walk was done in two direction: east to west and south to north. In both directions, the walks started at the top margin (divider) of the watershed and then all the way downhill to the other side of the watershed. During the transect walk, observations and appraisals of the vegetation and density, impact of the existing SWC measures, level of erosion before and after the SWC program, and levels of SWC measures at different parts of the landscape were recorded. Land use and slope was taken into account during these walks. The transect walks also provided an opportunity for informal discussions with farmers working on their land. Informal interviews of the farmers were carried out using a combination of participatory rural appraisal (PRA) techniques such as semi-structured interviews and group discussions. The focus group discussions were supplemented by secondary data from knowledgable people in the Bureau of Agriculture.

A total of 49 household heads were used for the semi-structured interviews. The observations and informal participatory discussions with individuals and groups that represented men and women from different socio-economic categories led to the formation of focus groups. Such groups met as a team for discussions for three consecutive days during the holidays. Among the samples, six women-headed households were purposely involved throughout the interviews and group discussions. These were the only women household heads in the watershed. The distribution of men respondents were 15, 15 and 13 for low, medium and high wealth status respectively, on the basis of the local wealth criterion. These were selected randomly from each wealth category. Economic status and sex difference did not show any significant difference in this study. The aim of the semi-structured interview was to assess the role of the existing SWC measures on environmental degradation

Table 2. Ideal and operational performance indicators of the SWC measures after and before implementation in the Medego watershed

Performance criterion	Ideal indicator	Operational indicator used in this study
Level of soil erosion	- Measurement of erosion and associated yield loss - Sediment deposition rate - Presence, expansion and development of new active erosion features by slope, soil and land use types	- Visual assessment of rill and gully erosion status - Impact on soil fertility and soil moisture through vegetation and yield indicators - Qualitative comparison before and after the SWC program implementation - Quantifying sediment deposits
Measures taken to arrest erosion	- Inventory of the types of soil and water conservation practices	- Visual assessment of SWC investments -Intensity or level of the SWC measures across the landscape using farmer view and apparent effectiveness on rehabilitation
Water recharge	- Surface water storage amount - Levels ground water before and after SWC measures	- Approximate change in number of wells - Change in well depths to get water - Change in irrigated area - Change in village level water supply
Soil moisture retention	- Time series, intra- and inter-year variations in soil moisture using measuring instruments	- Change in cropping patterns - Change in cropping intensity - Relative change in yields and biomass using farmer opinions and field observations
Productivity of non-arable lands	- Change in production of plantation lands (actual biomass quantities) - Value added to social, economic and environmental situations	- Relative change in farm land area, biomass and soil cover (more than, same as or less than the pre-program) - Extent of erosion and SWC in such areas using local farmers' views

rehabilitation and find out ways that improve its role in the watershed in particular, and in other similar semi-arid areas in general. The potential and limitations of the existing SWC measures in the watershed were evaluated from environmental factors' (soil, water, microclimate, irrigation, vegetation) points of view.

In support of the data collected using Table 2, the transect walk field observations, and the interviews and group discussions, the accumulated sediment rate (t ha^{-1} yr^{-1}) behind stone bunds was estimated by adopting the equations described by Gebrermichael et al. [24] as:

$$A_A = 10M_A/(T*D) \quad \text{..... (1)}$$

$$M_A = BD*V_A \quad \text{..... (2)}$$

$$V_A = W_A*H_A \quad \text{..... (3)}$$

where: A_A is the annual sediment accumulation behind stone bund (t ha^{-1} yr^{-1}); M_A, mass of accumulated sediment per unit length (kg m^{-1}); T, age of stone bund (yr); D, average spacing between stone bunds (m); BD, dry bulk density of sediment accumulated behind stone bund (kg m^{-3}); V_A, the unit volume of accumulated sediment (m^3 m^{-1}); H_A = depth of the accumulated sediment (m); W_A, width of the sediment zone; and *, multiplication symbol.

The value of D was calculated as a mean of the spacing between consecutive bunds on different fields in the watershed. The mean value of D was taken as 70 m between consecutive fields for gentle sloping areas in this study. The average bulk density value of 1143 kg m^{-3} for deposited sediment behind bunds was adopted from a similar condition in the Tigray highlands as reported by Nyssen [25]. The H_A was determined at field level as a mean of the sampled plot lands having stone bunds of similar age and topography on the cultivated lands of the watershed. Similarly, the width of the sediment zone (W_A) was also calculated as a mean of the field measurements. A mean value of 0.80 m for H_A and 6 m for W_A was observed with the aged stone bunds (average of 12 years).

Different field materials were used, e.g. a GPS receiver to locate ground control points, elevation and delineated area, a metric tape measure for measuring changes in sediment depth accumulated behind the SWC facilities and water level differences in the wells, a clinometer to measure slope gradient, and a digital camera to take photographs. The data were subjected to analysis using SPSS 17.0 version software [26]. Percentages, cross-tabulations and nonparametric test (chi-square/χ^2 test) were used. The data were also subjected to qualitative analysis and interpretation.

RESULTS AND DISCUSSION

Experience of Land Management in the Watershed

Under the SWC program, various types of physical and biological SWC measures have been undertaken in the watershed with full participation of the communities since the 1980s. According to the survey results, most (90%) of the respondents had a positive response on check dams installed to stabilise gullies and transported 0.25 m^3 of stones per person to build them. This was organised by the Food for Work campaign program as part of the contribution to food security for SWC with voluntary labour from the farmers. According to the respondents, farmers were not only taking some incentives, but also developed more commitment and awareness to rehabilitate as well as stabilise gullies in order to reduce soil loss and stop gully development and expansion.

According to our field observation, some of the check dams constructed in both the up-stream and down-stream parts of the landscape collapsed due to faulty construction. There was less tendency to integrate the physical and biological SWC measures, particularly in the up-stream part of the watershed. Most respondents (80%) felt that the Bureau of Agriculture as well as the Food for Work campaign program coordinators did not give enough follow-up and monitoring of check dam maintenance. The local community did not adopt participatory feelings to repair these community resources. In spite of this, many farmers believed that they had benefited much from check dams constructed in the watershed. Some of the farmers (~30%) planted vegetable crops such as tomato, potato, onion and carrot as well as citrus with water accumulated on the check dam floor (Figure 2). Farmers not having land near a water supply used shallow and deep wells with increased ground water as a result of improved soil conservation measures.

Figure 2. Small-scale irrigation expansion: (a) fruits; (b) vegetables intercropped with maize after implementation of SWC measures using water retained in check dams and shallow and deep wells (March 2008)

The recommended spacing between check dams is 4.6 m, but actual spacing was up to 30 to 80 m even if the height and width of the check dam correlated well with the recommended spacing. As a result of this, the amount of run-off from the up-slope areas of the watershed could not be readily dissipated by the existing check dams, which caused their collapse. This also led to the formation of incisions on the gully floor and sides. According to the field observation, many of the check dams were not constructed well in that the spill way was too wide, an apron was lacking, and also the head was apart from the wall of the gully (Figure 3). Figure 3 shows that the depression behind the check dam and bund has been filled with soil so there is no more space to trap sediment. Lack of available rocks to increase the height of the dam above ground level in the cultivated fields was also a problem. Other biological conservation measures such as planting perennial grasses should be done to increase the sediment trapping efficiency of the bunds. Regular maintenance and appraisal of SWC measures is necessary to maintain the effectiveness of the programme.

Information from the respondents and development agents showed that the check dam and the stone bund in Figure 3 were constructed more than 12 years ago. At that time the check dam was constructed with an apron, which had been buried by soil deposits. This was due to a lack of maintenance and the fact that SWC measures were not targeted to the sources of high run-off and sediment in the upper part of the watershed. Wide spacing between check dams was also a cause. As shown in Figure 3, the space between check dams is wide so that the check dam above it cannot be seen. Generally, gullies become stabilised as vegetation grows on the sides and floor. However, the risk of damage by erosion is still possible since the check dam can be destroyed by water erosion. Preventive maintenance is essential to help conserve soil resources rather than investing heavily after erosion occurs.

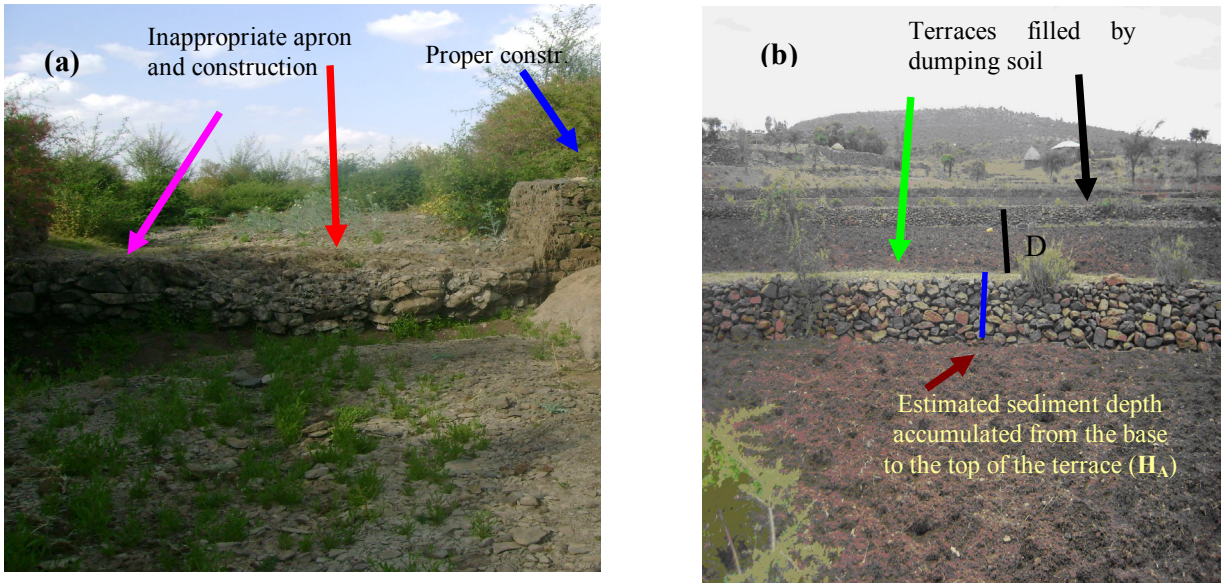

Figure 3. Watershed rehabilitation after the implementation of SWC measures: (a) check dam without apron and proper construction caused collapse; (b) stone bunds around a village filled with soil (indicated by arrows). D is the space between two consecutive bunds. (January 2008)

The farmers in the area noted that the gully did not stabilise and had no vegetation before the implementation of SWC measures, which resulted in high biomass productivity. This clearly demonstrated the advantages of using SWC measures for environmental rehabilitation. Other SWC measures on cultivated land also showed that terraces that can accumulate much soil (Figure 3b). A rough calculation to estimate the sediment accumulated in the stone bunds in Figure 3b was carried out. It was about 65.3 t ha^{-1} y^{-1}. This is higher than the 59 t ha^{-1} y^{-1} estimated from a similar environmental condition in the Tigray region reported by Gebrernichael et al [24]. This difference might be attributed to fewer sample plots used in our study. In addition, the annual sediment accumulated could be large after installation of the bund because of the capacity (space) to retain soil (Figure 3b), which older bunds lack. The inclusion of some older stone bunds that do not have the capacity to accumulate sediment could also reduce the annual rate of sedimentation. Further studies on the differences between young and old bunds in the same slope range, soil and land use types should be conducted to evaluate the impact in order to help decision makers to improve SWC implementation.

Since stones were cleared from cultivated fields for other purposes, no terrace height increment was observed for many fields. In such situations, the integration of biological SWC measures with terraces could help conserve the soil and increase biomass production. All respondents agreed on the point that farmers having farmland on flat plains in the watershed were more reluctant to use SWC measures compared to those on steep areas. They even destroyed improvements constructed for fear of being waterlogged during heavy rainfall. If the SWC measures on the steep parts of the watershed were good enough to reduce run-off, waterlogged and related problems of erosion on flat areas could be minimised. Our study revealed that there is still room for

further implementation and intensification of SWC measures in the Medego watershed. The farmers should be made to realise how to increase overall biomass production by integrating grasses or fruit trees in the bunds and improve crop yield by SWC.

Our analysis of the opinions generated a Chi-square ($\chi 2$) test which revealed that there was a significant difference ($P<0.05$) among the levels of SWC measures implemented in the studied catchment (Table 3). The level of SWC measures in the watershed was rated by more than half of the respondents as low in flat slope (<3%) and moderate in high slope (>15%) areas. The respondents who rated SWC measures as intensive were few in number, and no respondent rated the existing SWC level as very intensive. Table 3 also indicates that the high number of respondents perceived that SWC measures were more commonly implemented on higher slopes than on lower slopes. This is logical because steeper areas are the sources of erosion. Despite this fact, even in higher slopes the conservation measures were not intensive and not good enough to stop run-off and erosion. This implies that there is a need to implement intensively or very intensively the physical and biological SWC measures in the Medego watershed in particular and the northern Ethiopia in general. Several studies have shown that watershed management using integrated SWC measures can increase infiltration, directy decrease run-off and improve soil productivity [27-29].

Table 3. Rating (%) by the farmers on the level of existing SWC measures on different slopes in the Medego watershed

Average slope (%)	Estimated level of existing SWC measures				χ^2 probability
	Low [a]	Moderate [b]	Intensive [c]	Very intensive [d]	
2	75	23	2	0	0.005
7	52	41	7	0	0.002
15	43	55	2	0	0.001
30	36	55	9	0	0.002
60	24	64	12	0	0.04

[a] This is rated as low by farmers if there is no practice or if the spacing between consecutive measures is too wide.
[b] Implies SWC measures are addressed only to the degraded areas.
[c] Implies many conservation measures are constructed regardless of the appropriateness in spacing.
[d] Implies the conservation measures are appropriate in space so as to solve soil erosion.

Impact of SWC on Soil Moisture, Soil Depth, Soil Fertility and Crop Yields

For the last two decades, the problem of soil erosion has been of great concern in the Tigray region in general and the Medego watershed in particular. This is due to the fact that inappropriate land management practices coupled with intensive rainfall and steep terrains resulted in big gullies, topsoil erosion and poor soil fertility. To minimise the effects of soil erosion, the governments of the region and country have allowed the implementation of SWC programmes at a watershed level. The consequences of different measures were assessed in this study in different land uses to evaluate the positive impact on soil, water (moisture), fertility, biomass and reduction of soil and water losses with run-off by comparison with the situation before/without the programme (Table 4).

Table 4. Measured, observed and farmer-rated impact of SWC measures on soil, moisture, fertility, biomass and erosion (run-off, soil loss) in the Medego watershed

Land use	Performance indicator			
	Soil conserved	Moisture conservation	Soil fertility	Erosion reduction
Cultivated	Terraces filled by soil ranging from 0.2-0.90 m (e.g. see Fig. 3b)	Yield increased by 25% while rainfall is similar as before	Yield increment of 25% with some fertiliser input	Formation of rills and inter-rills decreased by 60%
Natural forest	Soil deposition increased by 0.3-0.9 m after implementation of SWC measures	Greenness increased from time to time by 50% compared to before SWC implementation	Regeneration rate of plant species increased by 5-58% depending on soil conditions	Expansion of gullies decreased by 95% compared to before SWC implementation
Reforestation	Erosion decreased but soil deposition increased by 0.3-0.9 m depth	Survival rate of seedlings increased by 55%	High survival rate of seedlings (increased by more than 55%)	Rainfall drops dissipated by soil cover increased
Grazing	Extent of soil loss by erosion decreased by soil deposit of 0.2-0.6 m	Growth and species diversity of the grasses increased by > 30%	Biomass of grass species increased by 65%	Infiltration increases due to water stored in SWC measures
Area closure	Extent of soil erosion decreased as evidenced by 0.3-1.2 m soil depth deposition	Grass, trees and bush biomass and diversity increased by 18-87% depending on slope	Grass, trees and bush biomass and diversity increase by 18-87%	No further new erosion channels are created or expanded.
Marginal land	Poorly maintained terraces but contributed to soil accumulation from 0.1-0.4 m depth	Plant diversity and regeneration increased by 10%	Plant diversity increased by 10% compared to before the program	Low run-off amount decreases the number of erosion channels.
Gully	Check-dam-accumulated soil ranges 0.4-1.5 m depth.	Plants spread for most part of gullies by 5-90%.	Fast plant growth rate and highly diversified species	Little gully expansion and development (Fig. 3)

Soil accumulated along the bunds and check dams was up to 1.5 m deep. The sediment depth varied according to land use, slope and sediment source area. For example, more than 1.5-m soil was deposited in the gullies with check dams integrated with biological SWC measures (Figure 3a). On cultivated land with stone terrace (Figure 3b), sediment depth was more than 0.80 m. In closed areas, up to 1.2 m and in degraded grazing land, about 0.6 m of soil accumulated. Positive effects of individual SWC measures (both physical and biological) on hydrology and soil loss were reported for a variety of agro-ecological zones and under various land uses in the region [30-31]. However, assessing the overall impact of different SWC measures at watershed level seems more appropriate for practical decision-making processes for further improvements of the measures, rather than using a single conservation measure at plot level.

According to the respondents, the impact of SWC measures on biomass yield (grain and biomass) also showed an increment of more than 25% for grain and 30% for biomass (including cover grass) yields. This was as a result of the SWC measures that contributed to enhancing soil moisture and soil fertility (added or restored), and also to reducing the expansion and development of gullies (Table 4). The contribution of the measures varied across different land uses and slopes in

the area (Table 4), which could help identify target priorities. This does not mean that the SWC measures are always appropriate or targeted to achieve the intended goal of sustainable natural resources management. It needs further consideration on spacing, appropriateness and maintenance besides awareness of local farmers to adopt and handle the technologies sustainably by themselves.

Scientifically documented data that described the watershed before the implementation of the SWC programme was not available. As a result, the results of this study were based on our investigation: visually, field measurements and information collected from farmers (Table 4). According to the respondents, the age of most of the SWC measures in Medego watershed ranged from 8-20 years and some of them were younger than this.

The farmers were also able to classify their land into different levels of erosion based on the degree of erosion severity before the implementation of SWC measures (Table 5) and after their implementation (Table 6). These opinions were based on qualitative factors, but this seems to be a quicker and less expensive approach for fact finding and decision making. This study shows that there is a significantly different ($P < 0.05$) chi-square test among the erosion levels described by the farmers in the same slope category (Table 5). The majority of the respondents (>59%) indicated that the level of erosion was severe in the absence of conservation measures at all parts of the landscape, the severity being higher on steepest slopes than on lower slopes (Table 5).

Table 5. Rating (%) of levels of erosion impact *before* the implementation of SWC measures at different steepness from the respondents' point of view in the Medego watershed

Average slope (%)	Level of erosion before implementation of SWC measures				χ^2 probability
	Insignificant [1]	Slight [2]	Moderate [3]	Severe [4]	
2	8	11	22	59	0.04
7	7	9	11	73	0.02
15	4	7	9	80	0.003
30	2	4	8	86	0.002
60	0	2	3	95	0.001

[1] Respondents consider the effect of erosion on land productivity as negligence as they assume that erosion is redistributed soils within or among the same fields.
[2] Somewhat decreased agricultural suitability but is still proper for local farming conditions as the original biotic functions are not destroyed. Restoration can be easily achieved to its full productivity using appropriate soil management practices and measures.
[3] Soil highly reduces its productivity but is still continued for use in local farming. Major soil amendments are required to restore original biotic resources that are partially degraded.
[4] Soil almost denuded of topsoil and is not appropriate for agricultural production as the original soil resources are largely degraded. This needs large investment and/or SWC engineering work to restore to its full production capacity.

We also demonstrated that the chi-square test shows a significantly difference ($P<0.01$) in the reduction of soil erosion levels after the SWC measures were implemented (Table 6). Most respondents (about 90%) noted less soil erosion after conservation measures. Similarly, most respondents replied that severe erosion was not noticed after the implementation of the conservation

measures in many parts of the watershed. According to 95% of the respondents (Table 5), severe soil erosion was observed on steep slopes before the implementation of SWC measures. The majority of the respondents (>59%) indicated that the degree of soil erosion was less severe in the presence of the existing conservation measures in many places (Table 6). The respondents also understood the most important causes and effects of soil erosion. Deforestation and inappropriate land use and soil management practices were rated as the most important causes of environmental degradation. Among the most frequently reported effects of soil erosion by farmers was an immediate reduction in crop and straw yields.

Table 6. Rating (%) of level of erosion impact *after* the implementation of SWC measures according to the respondents in Medego watershed

Average slope (%)	Level of erosion after implementation of SWC measures				χ^2 probability
	Less	Same	More	More severe	
2	59	31	10	0	0.002
7	87	8	5	0	0.001
15	98	2	0	0	0.001
30	94	5	1	0	0.000
60	100	0	0	0	0.000

Water Resource Development

The impact of the SWC measures such as bunds and check dams increased the availability of surface and subsurface water for traditional irrigation and other uses. The same trend was also observed for available soil water for rain-fed crops. Water availability by rehabilitating the gullies using check dams was the main source of surface irrigation water, which was supplemented by shallow and deep ground water wells. All of the respondent farmers were convinced that bunds and gullies greatly increased the amount of surface water. Groundwater levels in the wells increased up to 2.5 m while irrigation area increased many times and the number of hand-dug wells also significantly increased (Table 7). Newly emerging springs and irrigated fields as well as increasing crop diversity and yields were some of the indicators for the improved water resources and supply as a result of SWC measures. Arid condition of the area has also been changed to a moister one because of improved water resources in the watershed (Figure 4). The areas in Figure 4 used to be bare land with barren gullies, without water, and with sparse vegetation before the implementation of SWC measures. Livestock in the areas in Figure 4 is strictly forbidden, which has enhanced its successful rehabilitation. Achievements are noticable but are more concentrated along gullies. More effort should be done to expand and sustain the watershed and other similar areas to achieve successful SWC measures.

Table 7. Indicators of the impact of SWC measures on water resources development according to farmers in the Medego watershed

Performance criterion	Indicator *
Surface water storage capacity and spring development	Increased many times from almost nil to the present situation
Extent of irrigated area	Increased by more than 300 times
Water level in wells	Increased by 0.5 m to 2.5 m
Ground water recuperation rate	Increased 15 times

* Comparing between pre- and post-implementation of the SWC measures according to farmers' qualitative evaluation

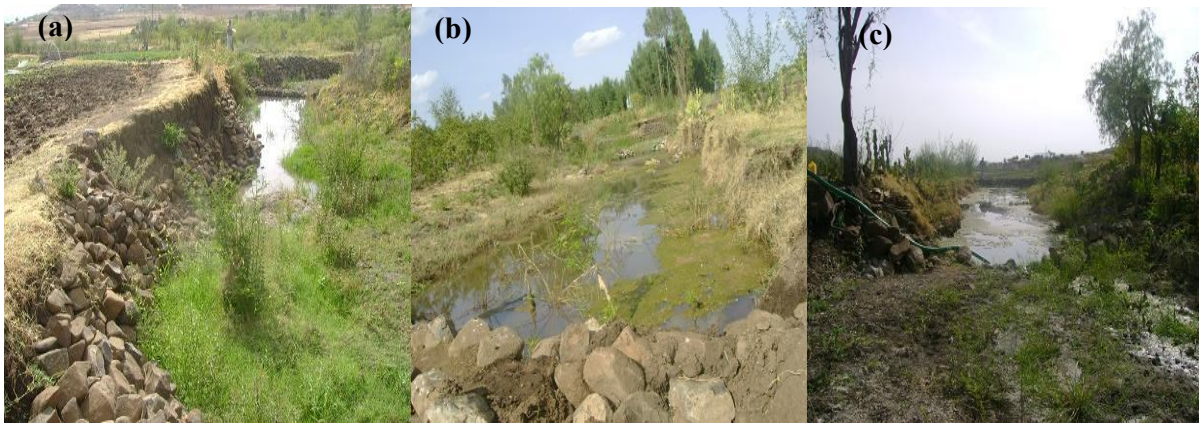

Figure 4. Water resources developed and used for small-scale irrigation and other purposes as a result of long-term impact of the SWC measures implemented in the Medego watershed: (a) deep gully rehabilitated; (b) shallow but wide gully rehabilitated; (c) deep and wide gully after rehabilitation (January 2008)

The increases in crop yield, biomass and diversity are due to more water availability and soil fertility restoration after the SWC measures for both irrigation and rain-fed crops. The duration of rain-fed crops and grass cover is also prolonged by improvement in soil water content as witnessed by the farmers in the area. Additional indicators of the positive effects of the SWC measures are the rapid recharge of the water table and development of new springs. This is because the time for infiltration has increased after installation of the stone/soil bunds and check dams, which raises the water table level. Farmers described this fact as follows: "Ten years ago, it was difficult to get water by digging 3-4 metres deep, but now the possibility of having water at this depth is high". There are many more opportunities for farmers to use their natural resources sustainably by introducing appropriate plant species on the steep slopes and degraded areas to enhance soil fertility and also as a source of fodder for livestock and pollen for bees. Apiculture is possible in the area and needs to be proven so that farmers can enhance their incomes and at the same time improve the ecosystem in severely degraded landscapes.

Greenness of the Environment

After the implementation of different SWC measures, especially check dams in gullies and bunds in steep streams, the climate of the area improves as a result of increasing vegetation cover (Figures 2-5). The respondents confirmed that the hot and dry air that previously dominated the watershed has been replaced by moist and cooler air. This is because by of increasing vegetation cover in the catchment, which is a direct reflection of the improvement of available water and soil fertility in the area. More biomass after SWC conservation measures has resulted (Figure 5). The vegetables and fruits cultivated in irrigated fields in the watershed have also contributed towards the greenness and humidity in the area.

Figure 5. The impact of SWC measures on greenness, increasing biomass and climate improvement after gully rehabilitation in the Medego watershed (February 2008)

Impact of SWC Measures on Seedling Survival

The farmers were fully dedicated and inspired to work hard towards environmental improvement by planting more trees and vowing to maintain the naturally-growing ones. The respondents (93%) had indicated the low survival rate of newly planted seedlings due to moisture stress and the associated poor soil fertility. However, they said that such problem started to reduce after the implementation of some SWC measures in the area. Barbier and Bishop [32] reported that increasing seedling survival is an advantage of SWC as a long-term incentive to farmers.

Table 8 demonstrates a trend in the increasing survival rate of seedlings for different plantations. The survival rate of seedlings planted in the community and private plantations during 1993–1999 was about 53% and 68% respectively, whereas in 2005 it increased to about 88% and 89% respectively. The 35% increase in survival rate for community plantations and 21% for private plantations was due to the implementation of SWC. Such an achievement is encouraging and offers hope to the people living in this watershed. Poor management of the plantations, such as human and animal interference, has destroyed many of the seedlings. Regulation and rules should be made with the involvement of local communities to successfully maintain planted trees.

Table 8. Inventory of survival rate approximation of tree seedlings planted at the administrative unit of Laelay Maychew where Medego watershed is located [22]

Year	Afforestation/Community			Individual plantation			Agro-forestry plantation		
	Number of seedlings planted	Surviving seedlings		Number of seedlings planted	Surviving seedlings		Number of seedlings planted	Surviving seedlings	
		Number	%		Number	%		Number	%
1993-1999	2,599,497	1,366,884	52.9	3,716,261	2,672,298	68.0	21,822	7,394	72.7
2000	695,611	475,696	68.4	594,781	468,593	78.7	14,576	10,728	73.6
2001	608,899	420,141	69.0	547,004	421,193	77.0	18,117	16,015	88.4
2002	579,209	411,239	71.0	396,588	310,132	78.2	96,488	86,743	89.9
2003	419,811	335,796	79.9	282,070	237,821	84.3	- *	-	-
2004	257,312	210,934	82.0	484,481	428,249	88.4	-	-	-
2005	985,778	867,485	88.2	374,188	333,028	89.0	-	-	-
Total	6,146,117	4,088,175	-	6,395,373	4,871,314	-	51,003	130,880	-

* Not applicable or data not available

CONCLUSIONS

This study assessed the impact of various SWC measures implemented for soil, water, vegetation and climate qualitatively and quantitatively in the Medego watershed, northern Ethiopia. The study indicated that there has been success in maintaining and improving land resources, viz. soil, water, vegetation and humidity due to the implementation of SWC measures. Many issues need to be improved on the existing SWC measures, such as maintenance of terraces, appropriate spacing and integrating with biological conservation measures, in all parts of the watershed landscape in order to restore degraded land to its full potential. A long-term solution in improving infiltration, spreading run-off, and increasing biomass production requires an integrated effort with the full involvement of farmers. More efforts should be directed towards increasing the water retention capacity and improving the organic matter content of the soil, along with the restoration of flora and fauna for ecological and economic benefits in many parts of the watershed. This is because a soil rehabilitation should go beyond the application of natural fertilisers to replace chemical ones or only terraces to reduce soil loss. Such community-based watershed rehabilitation programmes can transfer sustainable and restored landscape to future generations. Development and research work should be focused on introducing alternative management options that can rehabilitate degraded areas to its full potential by considering the existing weaknesses of the SWC measures. This research should include testing techniques appropriate to specific local conditions to identify areas prone to severe degradation, sources of high run-off, and sedimentation that has priority, while taking action using the limited resources available.

ACKNOWLEDGEMENTS

We appreciate the financial support by the Ethiopia Science and Technology Agency Research Support Program and field work assistance from Aksum University, Ethiopia. The assistance given by the participating farmers and extension agents during the study is also acknowledged. The reviewers are thanked for their important comments and suggestions.

REFERENCES

1. S. J. Scherr and S. N. Yadav, "Land degradation in the developing world: Implications for food, agriculture, and the environment to 2020", Food, Agriculture and the Environment Discussion Paper 14, International Food Policy Research Institute, Washington, D.C., U.S.A, **1996**.
2. A. Buckwell, "Rise task force on public goods from private land. Rise rural investment support for Europe", **2009**, http://www.agriculture.gov.ie/media/migration/agri-foodindustry/foodharvest2020/foodharvest2020/submissionsreceived/Rise%20Task%20Force.pdf (Accessed: Aug. 5, 2011).
3. World Economic Forum, "Biodiversity and business risk-A global risks network briefing", A briefing paper for participants engaged in biodiversity-related discussions at the World Economic Forum Davos-Klosters Annual Meeting, Cologny/Geneva, Switzerland, **2010.**
4. FAO, "Highlands reclamation study: Ethiopia", Final Report, **1986**, pp.166-169.
5. O. C. A. Erenstein, "The Economics of soil conservation in developing countries: The case of crop residue mulching", *PhD Thesis*, **1999,** Wageningen University, The Netherlands.

6. H. Hurni, K. Tato and G. Zeleke, "The implications of changes in population, land use, and land management for surface runoff in the upper Nile Basin Area of Ethiopia", *Mountain Res. Dev.*, **2005***, 25*, 147–154.
7. H. Tamirie, "The role of improved soil, water and crop management practices in increasing agricultural production in Ethiopia", National Workshop on Food Strategies for Ethiopia, December **1986**, Alemaya University of Agriculture, Alemaya, Ethiopia.
8. N. Hudson, "Land Husbandry", Batsford Ltd., London, **1992**.
9. Y. Tilahun, "Impacts of conservation bunds on crop yields in Degua Tembien, northern Ethiopia", *MSc Thesis,* **1996**, Agricultural University of Norway, Norway.
10. R. C. Muchow and J. A. Bellamy, "Climatic risk in crop production: Models and management for the semiarid tropics and subtropics", Proceedings of International Symposium on Climatic Risk in Crop Production, **1990**, Brisbane, Australia, pp.56–57.
11. J. Bojö and D. Cassells, "Land degradation and rehabilitation in Ethiopia: A reassessment", Working Paper No. 17, World Bank, **1995**, pp.36.
12. M. Lemenin, E. Karltun and M. Olsson, "Assessing soil chemical and physical property responses to deforestation and subsequent cultivation in smallholders farming system in Ethiopia", *Agric. Ecosys. Environ.*, **2005**, 105, 373–386.
13. L. Tamene, "Reservoir siltation in the drylands of northern Ethiopia: Causes, source areas and management options", *PhD Thesis,* **2005**, University of Bonn, Germany.
14. W. Mekuria, E. Veldkamp, M. Haile, J. Nyssen, B. Muys and K. Gebrehiwot, "Effectiveness of exclosures to restore degraded soils as a result of overgrazing in Tigray, Ethiopia", *J. Arid Environ.*, **2007**, 69, 270–284.
15. R. P. C. Morgan, "Soil erosion and conservation", 3rd Edn., Blackwell Publishing Ltd, Malden, **2005**, pp.25–29.
16. U. Bosshart, "Catchment discharge and suspended sediment transport as indicators of physical soil and water conservation in the Minchet catchment, Anjemi research unit: A case study in the north-western highlands of Eritrea", Research Report 39, Soil Conservation Research Project, Centre for Development and Environment, University of Bern, **1997**, p.137.
17. K. Herweg and B. Stillhardt, "The variability of soil erosion in the highands of Ethiopia and Eritrea", Research Report 42, Soil Conservation Research Project, Centre for Development and Environment, University of Berne, **1999**, p.81.
18. K. Herweg and E. Ludi, "The performance of selected soil and water conservation measures - Case studies from Ethiopia and Eritrea", *Catena*, **1999**, *36*, 99–114.
19. R. Lal, "Soil degradation by erosion", *Land Degrad. Dev.*, **2001,** *6*, 519–539.
20. A. Zenebe, "Assessment of spatial and temporal variability of river discharge, sediment yield and sediment-fixed nutrient export in Geba River catchment, northern Ethiopia", *PhD Thesis,* **2009**, Katholieke Universiteit Leuven, Belgium.
21. H. Gebrekidan, "Grain yield response of sorghum (*Sorghum bicolor*) to tied ridges and planting methods on Entisols and Vertisols of Alemaya area, eastern Ethiopia highlands", *J. Agric. Rural Dev. Trop. Subtrop.*, **2003**, *104*, 113–128.

22. "Soil and water conservation", Annual report (in Tigrigna), Bureau of Agriculture and Natural Resources (BoANR), Aksum, Ethiopia, **2007**, pp.4–18.
23. T. C. Awoke, "Vetiver in rehabilitation of the degraded ZegZeg watershed in Ethiopia", Project Report, Coffee and Tea Authority, Addis Ababa, Ethiopia, **2002,** p.31.
24. D. Gebrernichael, J. Nyssen, J. Poesen, J. Deckers, M. Haile, G. Govers and J. Moeyersons, "Effectiveness of stone bunds in controlling soil erosion on cropland in the Tigray Highlands, northern Ethiopia", *Soil Use Manage.*, **2005**, *21*, 287–297.
25. J. Nyssen, "Erosion processes and soil conservation in a tropical mountain catchments under threat of anthropogenic desertification - A case study from Northern Ethiopia", *PhD Thesis,* **2001**, Katholieke Universiteit Leuven, Belgium.
26. SPSS Inc., International Business Machines (IBM) Company**, 2010**.
27. M. Huang and L. Zhang, "Hydrological responses to conservation practices in a catchment of the Loess Plateau, China", *Hydrol. Process.*, **2004***, 18*, 1885–1898.
28. X. Mu, L. Zhang, T. R. McVicar, B. Chille and P. Gau, "Analysis of the impact of conservation measures on stream flow regime in catchments of the Loess Plateau, China'', *Hydrol. Process.*, **2007**, *21*, 2124–2134.
29. G. Lacombe, B. Cappelaere and C. Leduc, "Hydrological impact of water and soil conservation works in the Merguellil catchment of central Tunisia", *J. Hydrol.*, **2008***, 359*, 210–224.
30. A. S. Collick, "Community water use in the Yeku watershed and hydrological modeling in watersheds of the upper Nile basin, northern Ethiopia", *PhD Thesis*, **2008**, Cornell University, USA.
31. K. Descheemaeker, J. Nyssen, J. Rossi, J. Poesen, M. Haile, D. Raes, B. Muys, J. Moeyersons and J. Deckers, "Sediment deposition and pedogenesis in exclosures in the Tigray Highlands, Ethiopia", *Geoderma,* **2006***, 132*, 291–314.
32. E. B. Barbier and J.B. Bishop, "Economic values and incentives affecting soil and water conservation in developing countries", *J. Soil Water Conserv.*, **1995**, *50***,** 133–137.

Maejo Int. J. Sci. Technol. **2011**, *5*(03), 331-349

Maejo International Journal of Science and Technology

ISSN 1905-7873
Available online at www.mijst.mju.ac.th

Full Paper

Deposition of platinum-group metals in sediment and water bodies along the coastal belt of Ghana

David K. Essumang * and Christian K. Adokoh

Environmental Research Group, Department of Chemistry, University of Cape Coast, Cape Coast, Ghana

* Corresponding author, e-mail: kofiessumang@yahoo.com

Received: 11 June 2010 / Accepted: 5 October 2011 / Published: 6 October 2011

Abstract: Water and sediment samples from seven water bodies along the coastal belt of Ghana were assessed for the deposition of platinum-group metals (PGM), i.e. platinum, palladium and rhodium. Source analysis of the results indicated probable anthropogenic origins which had a strong linkage to automobile and marine vessel emissions. In the sediment samples, pollution indicators revealed that all the seven water bodies along the coast had elevated levels of PGM above the background values. Significant correlation between the metals indicated a common anthropogenic origin of the PGM. Rhodium metal measured at Pra River estuary demonstrated opposite correlation with PGM to the other six sampling sites, which indicated another source other than automobile and marine vessel emissions of rhodium.

Keywords: platinum-group metals deposition, metal pollution, coastal belt of Ghana

INTRODUCTION

In recent years, environmental analyses have revealed the presence of elevated levels of platinum-group metals (PGM) in road side soils, water, biota, and sediment samples not only in developed countries, but also in developing countries. Most of these studies which were done in the developed countries have demonstrated the existence of increasing concentration of PGM in roadside environments, presenting undoubtful evidence that the automobile catalytic converters are the predominant source of these heavy metal pollutants in the environment [1-5].

PGM in the environment have been linked to the emission of these metals used as active metal catalysts in internal combustion engines to reduce the emission of hydrocarbons, carbon

monoxide and nitrogen oxides [3-5]. The total extent of the emission, its composition in terms of relative concentrations of these elements, and the average size of the emitted particles strongly depend on the catalytic converter type and the traffic condition, although the age of the catalytic converter may also in part be another factor [6]. Also, it was previously believed that the soluble fraction of the emitted PGM was low, but recent studies have demonstrated that this fraction has increased tremendously [7].

Ghana relies heavily on the import of used vehicles (5-12 years old), which may constitute about 70% of the vehicular fleet in this country [8]. This situation raises fears of possible deposition of PGM in the environment, which may end up in water bodies and soils (along the roadways). Also, studies on the Ghanaian environment have shown the presence of elevated levels of PGM in sediment and some biological species [9-10]. It is believed that in addition to the availability of PGM in terrestrial ecosystems, these metals are also introduced passively in aquatic biotopes by road run-off into lakes and rivers, where the metals accumulate in the sediment [11].

Although PGM are not yet considered a serious health risk, studies suggest that they can potentially pose danger in the future as worldwide car sales keep increasing [4]. The accumulation of Pd and Pt should be of great concern as they are known to have some mutagenic and toxic effects, even at very low concentrations [12]. PGM are known to have very good catalytic properties and therefore their presence in the environment may trigger several chemical and biochemical processes which may affect the environment. The chemistry of platinum compounds in aqueous solutions is dominated by the formation of complex compounds. Many of the salts of PGM, particularly those with halogen or nitrogen-donor ligands, are water-soluble. Platinum (as well as the other platinum group metals) has a pronounced tendency to react with carbon compounds such as alkenes and alkynes, forming Pt(II) coordination complexes [13].

Although Pt does not corrode in air, it can be affected by halogens, cyanides, sulphur and other heavy metals and hydroxides, which makes it mobile in the environment [14]. In soil, the mobility of platinum depends on the pH, redox potential, chloride concentration, and the chemical form of Pt in the primary rock. The soluble forms of the PGM are absorbed by plants, raising the possibility of its presence in the food chain [8].

This study was done to assess the levels, transport, distribution and source of PGM in water and sediment samples from seven water bodies along the coastal belt of Ghana.

MATERIALS AND METHODS

The study area lies between latitudes 5-6^{o}N and longitudes 1^{o}7'-1^{o}45'W as shown in Figure 1. The sites are: Pra estuary at Shama (western region), Benya lagoon at Elmina, Fosu lagoon in Cape Coast, Narkwa lagoon at Narkwa (all in the central region of Ghana), Sakumono 2 lagoon near Tema (Greater Accra), Volta estuary at Anyanuin and Keta lagoon (easternmost, both in the Volta region). Each of these water bodies plays a significant role as far as fishery activities are concerned in Ghana. Two sampling sites A and B, about 1 kilometre apart, were chosen at each study area where samples A and B were taken.

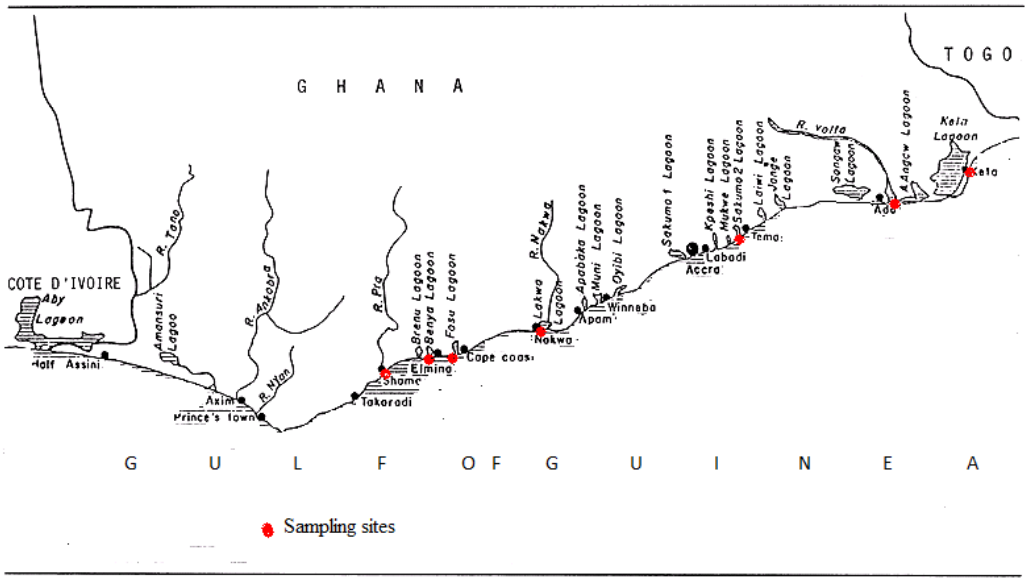

Figure 1. Map showing the sampling sites

Two sediment samples (riverbed soil), labelled A and B, were collected from the middle part of the river/lagoon (about 100 metres from the bank) at each site. Using a fishing boat, each sediment sample (about 200 g) was scooped into a black polyethylene container. Samples were further prepared for laboratory analysis by air drying at room temperature for three days.

Two water samples in 1-litre polyethylene bottles, labelled A and B, were also collected at the same sampling points where sediment A and B respectively were taken. The bottles were pre-washed with acetone to remove any grease, then with dilute nitric acid to dissolve any metal before rinsing with distilled water. The labelled sediment and water samples were kept in the refrigerator and later sent to the Ghana Atomic Energy Commission laboratory for neutron activation analysis (NAA) with a 30-kW miniature neutron source reactor supplied by the international atomic energy agency (IAEA).

The physicochemical variables determined for the water samples were pH, dissolved oxygen (DO), refractive index, salinity and turbidity. The DO was determined with an oxygen meter (model: AZ8403, A.W.R. Smith Process Instrumentation). The pH was measured using a bench-top pH meter (model AZ86555, Eztech Instruments). The pH meter was calibrated with pH tablets (pH 4 and 8). The refractive index was measured in the laboratory with an Abbe refractometer (model AR2008, A. Krüss Optronics). The salinity was measured on-site using an Abbe refractometer (model AR2008, A. Krüss Optronics) with an in-built salinity scale. The turbidity was determined on-site using a Micro1000 turbidimeter (model HFS-20014, Preiser Scientific). All measurements were done in duplicate and averaged.

For the INAA of the PGM, exactly 0.5 mL of each water sample was transferred using a calibrated Eppendorf-tip ejector pipette to a clean pre-weighed 1.5-mL rabbit capsule (sample vial),

reweighed and heat-sealed. Four of these sample vials were packed into 7.0-mL rabbit capsule and heat-sealed for irradiation [15].

Each sediment sample was air-dried for 3 days in a clean environment and organic debris, shells, stones and some organisms physically removed. It was then crushed with an agate mortar and pestle, sieved through an 85-µm-mesh sieve and homogenised. About 100 mg was weighed onto a clean polyethylene film, which was then wrapped and heat-sealed. It was then packed into a 7-mL volume rabbit capsule and heat-sealed for irradiation. Certified reference material, SARM 7 (platinum ore), prepared by the National Institute for Metallurgy and distributed by South African Bureau of Standards Reference Materials, was treated the same way as the samples [15].

The determination of the trace PGM was done by NAA method using thermal neutron from a low-flux Am-Be radioisotope. Theoretically, NAA is based on the measurement of characteristic gamma-ray from radionuclei formed from a specific neutron reaction which can be used to measure the amount of the elements using the usual radioactive decay law [16-17]. The irradiation source was a 20-curie Am-Be radioactive neutron source and the thermal neutron flux at the irradiation site was 5.0×10^{11} $ns^{-1}cm^{-2}$. Each of the samples was sent by the pneumatic transfer system into the Am-Be source for a 1-hour irradiation and left overnight to cool or for decaying process to take place. The irradiated sample was placed on top of the detector and counts were accumulated for pre-selected time to obtain the spectral intensities. For short and medium irradiation, 600-second counting time was chosen and the intensities of the photo peaks recorded for further analysis.

Counting of signals was done by an ENERTEC high germanium (HPGe) detector of 3000 (+ve) bias with a resolution of 2.55 keV for 1332 KeV photo peak of Co-60. A Microsoft Windows-based software (MAESTRO) was used for qualitative and quantitative spectrum analyses [17-18]. Validation of the analytical procedure was undertaken by irradiating an IAEA standard reference material (SARM 7 platinum ore) and counting under identical experimental conditions. The analytical values of the reference material obtained from this study were compared with the recommended values (in ppm).

The pollution load index (PLI), contamination factor (CF) and geo-accumulation index (Igeo) were used to assess and quantify the levels of pollution of the monitored element in the sediment and water samples of the study areas [19-24]. The mean concentrations, standard deviations and correlation matrices for the sediment data were determined using SPSS version 16 software. According to Tomlinson et al. [19], the indices enable the quality of the environment to be easily understood by a non-specialist. The CF (= element concentration in soil / background value in the earth crust) was computed for the sediment using the average elemental concentration and the maximum corresponding value in the world-average abundance of metals in the earth crust (0.005, 0.005 and 0.0002 ppm for Pt, Pd and Rh respectively) [25-26].

The resultant CF values of the elements were used to compute the PLI as a measure of the mutual pollution effect on the soils [17, 19, 27]. In this case, $PLI = 3\sqrt{CF_{Pt} \times CF_{Pd} \times CF_{Rh}}$ (3=number of metals studied).

The Igeo approach was used to quantify the degree of anthropogenic contamination in soils with regard to the different elements monitored [22]. The Igeo for each element was calculated using the formula: $Igeo = \log 2 (Cn/1.5 \times Bn)$, where Cn is the measured element concentration in the soil

(sediment) sample and Bn is the geochemical background value in a world-average shale, or the maximum corresponding value in the world-average abundance of the metal in the earth crust reported [25-26, 28].

For water samples, the contamination degree was used to assess an excessive contamination value of the monitored element. This was calculated using the expression: $CD = \sum Cfi$, where CD is the contamination degree and *Cfi* (the contamination factor for the i^{th} element) = (Cn/Cb)-1, where Cn is the analytical value of the i^{th} element and Cb is the upper permissible limit of the element in water [29].

In this study, guideline values for the dietary intake (0.20 µg/g/day for Pt and Rh, and 1.00 µg/g/day for Pd) [30-31] were selected for the calculation of the contamination degree of the water samples since it was difficult to get guideline values for drinking water.

RESULTS AND DISCUSSION

The accuracy and precision of the analytical technique (NAA) was measured by simultaneous activation of the certified reference material SARM 7 (platinum ore). Table 1 shows the analytical results obtained for the reference material compared with the standard concentration values. The values compare favourably well with the standard values for Pt, Pd and Rh with less than 6% bias. The precision was calculated as a per cent relative standard deviation (%RSD) of three replicated samples of the prepared standard, which were found to be less than 5% with recovery of about 98% (Table 1).

Table 1. Result of the quality control analysis of SARM 7

PGM	Standard concentration (SARM 7)	Results obtained after NAA analysis of the standards Std.1	Std. 2	Std. 3	Mean	Recovery (%)
Pt (µg/g)	3.74±0.045	3.65±0.55	3.70±0.56	3.71±0.56	3.69±0.56	98.6
Pd (µg/g)	1.53±0.032	1.49± 0.22	1.51±0.23	1.49±0.23	1.50±0.23	98.0
Rh (µg/g)	0.24±0.013	0.23± 0.04	0.22±0.033	0.20±0.04	0.23±0.04	96.95

The results of the analysis of the sediment samples (wet and dry season) showed the presence of the platinum group metals at all the seven sampling sites. The dry-season samples generally recorded higher PGM levels as shown in Appendix 1, which presents details of mean concentration at each sampling site (A and B). Table 2 presents mean PGM concentrations (mean of A and B (n = 2)) of the seven water bodies studied. The mean PGM values ranged between 0.0002 µg/g (Rh) and 0.095 µg/g (Pd) for sediment, and 0.001µg/L (Rh) and 0.019 µg/L (Pd) for water samples (Table 2). The Keta lagoon recorded the highest PGM mean concentrations for both sediment and water samples. The general trend of the distribution of PGM in the sediment followed a decreasing order of Keta > Narkwa > Benya > Pra > Fosu > Sakumono 2 > Volta estuary.

Table 2. Mean concentrations of PGM in sediment and water samples of 7 water bodies along the coastal belt of Ghana

Sampling site	Mean PGM value		
	Pt	**Pd**	**Rh**
Sediment (µg/g)			
Pra estuary	0.034	0.052	0.0002
Benya lagoon	0.056	0.076	0.005
Fosu lagoon	0.032	0.027	0.001
Narkwa lagoon	0.054	0.073	0.003
Sakumono 2 lagoon	0.027	0.034	0.001
Volta estuary	0.007	0.024	0.003
Keta lagoon	0.047	0.095	0.010
Water (µg/L)			
Pra estuary	0.005	0.003	0.002
Benya lagoon	0.005	0.008	0.002
Fosu lagoon	0.004	0.013	0.002
Narkwa lagoon	0.004	0.009	0.001
Sakumono 2 lagoon	0.005	0.009	0.001
Volta estuary	0.012	0.017	0.002
Keta lagoon	0.011	0.019	0.002

The high concentrations of the metals recorded at Keta lagoon might be attributed to its direct contact with the sea and close proximity to highways with heavy traffic, resulting in a higher vehicular PGM deposition [11]. The situation was different at the Narkwa lagoon where even though there was not much vehicular activities close to the lagoon, yet it recorded elevated mean values of PGM (0.001–0.073 µg/g) for the sediment. In this case, there was an extensive use of outboard motors and some marine vessels, which might have contributed to the elevated PGM [32-33]. Sites which are far away from the sea but close to highways (Volta Lake, River Pra estuary and Benya lagoon in Elmina) also recorded appreciable levels of PGM. A study in Ghana by Essumang et al. [8] also reported similar elevated PGM results.

Palladium metal recorded the highest concentrations and rhodium the lowest. This trend was also observed by Essumang et al. [8-9] in their PGM study on the Pra River estuary. Thus, Pd seems to be the most distributed PGM with a distribution gradient of Pd ≥ Pt > Rh. Other studies have reported similar results which showed a higher proportion of Pd, which matched the recent change in the composition of the metal mixtures in catalytic converters used in automobile exhaust purification [11, 34]. The proportion of Pd in the catalyst has increased to approximately 96%, showing a dominant use of Pd in catalytic converters in recent years [35-36]. In addition, palladium in the biosphere can exist in metallic or oxide forms which are sparingly soluble in water, resistant to most reactions in the biosphere (e.g. abiotic degradation, UV-initiated reactions and oxidation by hydroxyl radicals) and do not volatilise [37], thus resulting in their greater accumulation in soil. The levels of

all the examined metals in the riverine sediment and water column might result in the reduction in the benthic biodiversity [4, 22].

Table 3 shows the physicochemical properties of the water samples from the seven sampling sites. The DO values in various water bodies did not show significant difference between the seasons. The values indicated moderate DO content, attributable to the build-up of organic waste in the lagoons. There was also no significant difference in the pH and refractive index values of the water bodies. The pH values were mostly on the slightly basic side and that might have contributed to the very low PGM values in the water column as a basic medium does not support metal dissolution.

High values of pH: 8.37, 8.12 and 8.80 were recorded in the dry season at Sakumono 2, Narkwa and Keta respectively. This situation should be due to the fact that these lagoons are the 'open' types and always open to the ocean where the average pH of sea water is 8.2 [38] Similar high pH has been reported for a lagoon open to the ocean and filled with a high population of algae [38]. In the case of salinity, significant differences were observed as a result of influx from the ocean for some sites. Turbidity values were slightly higher during the rainy season for some sites while lower for others. This could be attributed to the diurnal variations and different environmental pollution state of these water bodies.

Table 3. Summary of average physicochemical properties studied in rainy and dry seasons in various coastal water bodies

Physicochemical property	Pra	Benya	Fosu	Narkwa	Sakumono 2	Volta	Keta
DO (%)							
Dry season	8.90	6.30	7.50	7.14	7.60	6.20	7.60
Wet season	7.79	7.28	7.38	7.38	7.55	6.75	7.50
Mean	8.35	6.79	7.44	7.26	7.58	6.48	7.55
pH							
Dry season	7.67	7.33	7.12	8.37	8.12	7.93	8.80
Wet season	6.15	7.54	8.15	7.54	7.21	7.25	7.74
Mean	6.91	7.44	7.64	7.96	7.67	7.59	8.27
Refractive index							
Dry season	1.332	1.336	1.335	1.338	1.336	1.334	1.336
Wet season	1.333	1.338	1.335	1.338	1.334	1.334	1.337
Mean	1.333	1.337	1.338	1.338	1.335	1.334	1.337
Salinity (%)							
Dry season	0.00	27.70	0.50	25.50	2.80	1.50	2.00
Wet season	0.00	26.80	9.30	27.00	6.50	10.50	21.00
Mean	0.00	27.25	4.90	26.25	4.65	6.00	11.50
Turbidity (ppm)							
Dry season	36.50	26.00	66.30	31.80	46.50	29.80	10.30
Wet season	52.00	48.80	43.80	29.00	50.50	23.00	22.30
Mean	44.25	37.40	55.05	30.40	48.50	26.40	16.30

CF, PLI and Igeo for sediment and water samples are presented in Table 4. Keta lagoon sediment had the highest CF values for Pd and Pt (35.40 and 34.96 respectively) in the dry season, followed by Sukumono 2 lagoon with Pd CF value of 28.96 in the wet season. Pra estuary, Narkwa lagoon and Benya lagoon recorded CF values of 20.08, 27.56 and 21.48 respectively for Pd and Pt, which were all less than 100 (Table 4).

Table 4. Contamination factor (CF), pollution load index (PLI) and geo-accumulation index (Igeo) of PGM in sediment and water

Sediment	Season	CF(Pt)	CF(Pd)	CF(Rh)	PLI	Igeo(Pt)	Igeo(Pd)	Igeo(Rh)
Pra Estuary								
A	Dry	7.88	13.48	0.48	3.71	1.58	2.71	0.00
	Wet	0.00	6.92	0.08	0.74	0.00	1.39	2.40
B	Dry	8.96	20.08	0.04	1.93	1.79	4.03	0.20
	Wet	2.20	1.24	0.04	0.48	0.44	0.25	0.20
Benya lagoon								
A	Dry	0.00	16.2	0.24	1.97	0.00	3.25	1.20
	Wet	0.00	16.4	0.16	1.62	0.00	3.29	0.80
B	Dry	7.56	21.48	1.56	0.33	1.52	4.31	7.83
	Wet	14.68	5.92	0.00	9.32	2.95	1.18	0.00
Fosu lagoon								
A	Dry	3.48	2.04	0.00	1.12	0.69	0.41	0.00
	Wet	1.48	16.52	0.20	1.69	0.29	3.32	1.00
B	Dry	2.04	1.28	0.04	0.47	0.41	0.26	0.20
	Wet	18.68	0.00	0.00	0.91	3.75	0.00	0.00
Narkwa lagoon								
A	Dry	27.56	13.68	1.96	9.04	5.53	2.74	9.83
	Wet	3.32	4.80	0.16	1.37	0.67	0.96	0.80
B	Dry	0.16	15.16	0.08	0.58	0.03	3.04	0.40
	Wet	11.36	24.36	0.00	16.64	2.28	4.89	0.40
Sakumono 2 lagoon								
A	Dry	5.56	8.32	0.00	6.80	1.12	1.67	0.00
	Wet	0.00	4.08	0.12	0.69	0.00	0.82	0.60
B	Dry	4.68	6.52	0.24	1.94	0.94	1.31	1.20
	Wet	0.00	28.96	0.16	2.15	0.00	5.81	0.80
Volta estuary								
A	Dry	0.96	2.88	0.08	0.60	0.19	0.58	0.40
	Wet	0.00	0.00	0.02	0.09	0.00	0.00	0.08
B	Dry	3.24	3.88	0.00	3.55	0.65	0.78	0.00
	Wet	5.56	9.32	0.04	1.28	1.12	1.87	0.20
Keta lagoon								
A	Dry	34.96	35.40	1.48	12.24	7.02	7.10	7.43
	Wet	2.32	6.92	0.04	0.86	0.47	1.39	0.20
B	Dry	0.00	21.44	0.88	4.34	0.00	4.30	4.41
	Wet	0.00	11.56	0.00	0.77	0.00	2.32	0.00

Table 4. (Continued)

Water	Season	CF(Pt)	CF(Pd)	CF(Rh)	PLI	Igeo(Pt)	Igeo(Pd)	Igeo(Rh)
Pra estuary								
A	Dry	1.36	0.36	0.20	0.46	-1.45	-1.58	-1.56
	Wet	0.32	0.40	0.32	0.46			
B	Dry	1.52	1.04	0.32	0.79			
	Wet	0.44	0.36	0.12	0.27			
Benya lagoon								
A	Dry	1.28	3.04	0.68	1.38	-1.42	-1.54	-1.55
	Wet	0.28	0.36	0.24	0.29			
B	Dry	1.96	1.72	0.16	0.81			
	Wet	0.16	0.76	0.08	0.21			
Fosu lagoon								
A	Dry	0.00	4.20	0.68	1.69	-1.53	-1.49	-1.56
	Wet	0.08	3.76	0.08	0.29			
B	Dry	2.48	1.88	0.12	0.82			
	Wet	0.12	0.44	0.00	0.23			
Narkwa lagoon								
A	Dry	0.92	3.88	0.00	1.89	-1.47	-1.53	-1.58
	Wet	0.28	1.44	0.00	0.64			
B	Dry	1.84	1.96	0.36	1.09			
	Wet	0.48	0.00	0.00	0.27			
Sakumono 2 lagoon								
A	Dry	0.40	1.48	0.40	0.62	-1.42	-1.54	-1.56
	Wet	0.16	0.32	0.16	0.20			
B	Dry	3.00	4.08	0.16	1.25			
	Wet	0.16	0.64	0.04	0.16			
Volta estuary								
A	Dry	3.44	3.72	0.00	3.58	-1.01	-1.49	-1.59
	Wet	1.12	1.68	0.00	1.37			
B	Dry	3.00	4.08	0.14	1.19			
	Wet	1.12	3.76	0.12	0.79			
Keta lagoon								
A	Dry	3.24	3.68	0.00	3.45	-1.23	-1.49	-1.56
	Wet	1.52	1.60	0.32	0.92			
B	Dry	2.44	4.00	0.40	1.58			
	Wet	0.24	1.20	0.08	0.29			

Note: A and B are two sampling sites at each water body under study.

The CF assessment of the quality of sediment of the lagoons studied indicated contamination mainly with Pt and Pd. It also showed that Rh did not seem to contaminate the sediment in any of the sites. CF values of Pt and Pd were generally greater than 3, indicating high contamination in the sediment at most sampling sites. This result is not surprising since most of the sites are close to highways except Volta and Narkwa lagoons. However, the rivers of these estuaries (Volta and Narkwa) go through several urban communities, thereby carrying some PGM to the sediment.

The CF values of water samples were generally lower than those of the sediment with Pt and Pd contributing to moderate pollution in the water bodies. Most of the Pt and Pd CF values recorded were slightly above 3 except for the Pra estuary. In the case of Rh, all the sampling sites recorded CF values of less than 3, indicating no pollution of the water bodies by Rh.

The PLI values of the sediment and water from all the studied sites were between 0.09–16.64, with the highest value of 16.64 at Narkwa lagoon, followed by Keta lagoon (12.24) and Benya lagoon (9.32), while the range for water samples was 0.16–3.58. Several sediment and water samples had PLI values greater than 1, demonstrating progressive deterioration of the environment by PGM. Also, most samples with PLI values greater than 1 were collected in the dry season. These values indicate that Pra, Benya, Narkwa, Sakumono and Keta sites underwent progressive environmental deterioration while Fosu lagoon and Volta estuary showed baseline levels of PGM pollutants in sediment. In the case of water samples, Pra, Benya, Fosu Narkwa and Sakumono 2 showed baseline levels of pollutants present while Keta and Volta estuary sites showed some degree of progressive deterioration of the water bodies [19–21].

The Igeo values in sediment ranged between 0.00–7.02 for Pt, 0.00–7.10 for Pd, and 0.00-9.83 for Rh. The two highest Igeo values of 9.83 and 7.83 (Rh) were recorded at Narkwa and Benya lagoons respectively for dry season samples. Overall, the Igeo values for Pd were the highest followed by Pt and Rh from site-to-site comparison (Table 4). These values for the sediment samples indicate that the presence of PGM in the environment was probably from anthropogenic sources. The values varied across the sampling sites and indicated moderate to strong pollution situations. Most of the values were less than 5, above which a situation of very high pollution is indicated [39]. Sites which registered values greater than 5 for sediment samples were Benya lagoon (Rh), Narkwa lagoon (Pt and Rh) and Keta lagoon (Pt, Pd and Rh).

For water samples, however, CD was used to assess the pollution status of the water bodies. The CD for all the elements recorded values less than 1, signifying low pollution of the metals in the water columns at the sampling sites [29].

The correlation matrices of the elements from the sampling sites demonstrated good positive interrelationships between the three elements studied. These elements showed correlation at 0.01 level (99%), suggesting their common source in the studied areas [17]. However, there was no correlation between the PGM in the water columns and those in the sediments (Table 5), indicating that the accumulation of these elements in the sediment might not depend on the amount received by the water column. This therefore suggests that there was another source influencing the distribution of the metals between water and sediment. However, it was also possible that such environmental factors as water current and pH contributed to such situation. Only one positive correlation between Pt and Rh in the sediment and water (0.637) at 0.05 level was observed. This demonstrates that the

distribution of the metals in the water and sediment could be altered by environmental factors such as geological area or soil type, acidity and alkalinity. The metal-to-metal relationships at all the sampling sites seem to correlate perfectly at 0.01 level as expected for the metals in both sediment and water.

Table 5. Pearson correlation between elements in water and sediment

Element	Pt (water)	Pd (water)	Rh (water)	Pt (sed.)	Pd (sed.)	Rh (sed.)
Pt (water)	1					
Pd (water)	0.256	1				
Rh (water)	-0.448	0.071	1			
Pt (sediment)	0.129	-0.139	-0.129	1		
Pd (sediment)	0.135	0.06	0.202	0.357	1	
Rh (sediment)	0.001	0.031	-0.341	0.637*	0.453	1

* Correlation is significant at the 0.05 level.

The interrelationships among the PGM in sediment and water at each sampling site were also investigated (Table 6). The elements showed positive significant correlation from site to site at both 0.01 and 0.05 levels. Platinum from Benya lagoon showed a strong correlation (1.00) at 0.01 level with platinum and palladium at Keta lagoon as well as palladium from Pra River estuary and Sakumono 2 lagoon. Palladium from Benya lagoon correlated well with that of Keta lagoon and Pra River estuary at 0.998 and 0.985 respectively. At 0.05 level, another strong positive correlation ranging between 0.990-0.999 was also observed between platinum at Pra, Fosu, Benya and Narkwa lagoons as well as Volta estuary. In addition, palladium to platinum and rhodium correlations were also recorded at the same range and level (Table 6). The general strong correlations between PGM concentrations in the study areas suggest a common anthropogenic source, most likely automobile emissions, of these elements.

It was also observed from the Pearson's correlation analysis that rhodium at Pra estuary correlated negatively with platinum at Benya, Fosu and Volta, palladium at Sakumono 2 and Volta, and Rh at Benya, with values ranging between 0.9270–0.990 at 0.05 level (Table 6). Platinum concentration at Benya also recorded a negative correlation with Pd at Narkwa and Benya, which suggested another possible source of PGM. A possible source of Rh other than vehicular emissions was gold mine waste discharged into Pra River as rhodium has been found to be associated with gold ore [40]. This situation was possible as Ghana is covered by the Paleoprotoerozoic rocks of the Birimian Super group and the overlying clastic sedimentary [41]. Placer gold deposits, also referred to as 'alluvial gold', were found in the stretch of the Pra River, in which Rh occurred as a by-product. Also, PGM may occur naturally in the alluvial sand [42]. All these water bodies deposit their debris into the Gulf of Guinea, hence the possibility of contributing to Rh level in the Pra River estuary. The correlation coefficients for the PGM in sediment and water in the study areas suggest

Maejo Int. J. Sci. Technol. **2011**, *5*(03), 331-349

Table 6. Pearson correlation matrix of PGM in samples from each site

	Pra Pt	By Pt	Fs Pt	Nk Pt	Sak Pt	Vt Pt	Kt Pt	Pra Pd	By Pd	Fs Pd	Nk Pd	Sak Pd	Vt Pd	Kt Pd	Pra Rh	By Rh	Fs Rh	Nk Rh	Sak Rh	Vt Rh	Kt Rh
Pra Pt	1.000																				
By Pt	0.999*	1.000																			
Fs Pt	0.503	0.997*	1.000																		
Nk Pt	0.943*	0.997*	0.186	1.000																	
Sak Pt	0.864	0.990*	0.866	0.650	1.000																
Vt Pt	-0.074	0.994*	0.815	-0.400	0.419	1.000															
Kt Pt	0.781	1.00**	-0.245	0.960	0.301	-0.759	1.000														
Pra Pd	0.953*	1.00**	0.738	0.790	0.969*	0.233	0.509	1.000													
By Pd	0.988**	0.998*	0.609	0.890	0.913*	0.069	0.676	0.99**	1.000												
Fs Pd	0.615	-0.491	-0.335	0.820	0.143	-0.740	0.926	0.377	0.532	1.000											
Nk Pd	0.680	0 .998*	0.965*	0.396	0.937*	0.683	-0.081	0.869	0.776	-0.085	1.000										
Sak Pd	0.510	1.00**	0.998**	0.194	0.866	0.817	-0.261	0.746	0.621	-0.311	0 .973*	1.000									
Vt Pd	0.224	0.961	0.942*	-0.110	0.683	0.904*	-0.422	0.492	0.332	-0.621	0.821	0.928*	1.000								
Kt Pd	0 .996**	1.00**	0.560	0.915*	0.891	0.000	0.730	0.972*	0.99**	0.576	0.733	0.571	0.280	1.000							
Pra Rh	-0.260	-0.992*	-0.965*	0.075	-0.708	-.927*	0.455	-0.535	-0.380	0.568	-0.868	-0.959*	-0.99**	-0.323	1.000						
By Rh	0.248	0.964	0.914*	-0.076	0.649	.931*	-0.62	0.527	0.392	-0.443	0.872	0.928*	0.877	0.328	-0.934*	1.000					
Fs Rh	-0.424	-0.692	-0.747	-0.209	-0.717	-0.477	-0.115	-0.554	-0.443	0.370	-0.640	-0.708	-0.799	-0.428	0.729	-0.453	1.000				
Nk Rh	0.557	-1.00**	-0.629	0.828	-0.085	-0.902	1.00**	0.205	0.399	0.959	-0.370	-0.598	-0.879	0.472	0.816	-0.681	0.969	1.000			
Sak Rh	0.220	0.974	0.917*	-0.108	0.638	0.946*	-0.623	0.504	0.364	-0.486	0.860	0.929*	0.897	0.300	-0.948*	0.99**	-0.48	-0.720	1.000		
Vt Rh	-0.908	-1.00**	-0.669	-0.684	0.971	-0.286	1.00**	-0.99*	-0.968	-0.431	-0.860	-0.697	-0.334	-0.945	0.442	-0.616	0.091	-0.157	-0.577	1.000	
Kt Rh	0.898	0.990*	0.796	0.711	0.963*	0.354	0.362	0.98**	0.955*	0.304	0.922*	0.810	0.552	0.933*	-0.611	0.647	-0.500	0.070	0.620	-0.990*	1.000

* Correlation is significant at the 0.05 level

** Correlation is significant at the 0.01 level

Note: PraPt = Pra Platinum, ByPt = Benya Platinum, FSPt = Fosu Platinum, NkPt = Narkwa Platinum, SakPt = Sakumono 2 Platinum, VtPt = Volta Platinum and KtPt = Keta Platinum
PraPd = Pra Palladium, ByPd = Benya Palladium, FsPd = Fosu Palladium, NkPd = Narkwa Palladium, SakPd= Sakumono 2 Palladium, VtPdt = Volta Palladium and KtPd= Keta Palladium
PraRh = Pra Rhodium, ByRh = Benya Rhodium, FsRh = Fosu Rhodium, NkRh = Narkwa Rhodium, SakRh = Sakumono 2 Rhodium, VtRh= Volta Rhodium, and KtRh = Keta Rhodium

both strong negative and positive correlations within the sampling sites, implying that sources other than vehicular emissions, such as hospital effluent and gold mining activities might also contribute. The effect of gold mining operations should be investigated further to ascertain its influence on environmental PGM.

CONCLUSIONS

This study shows that there was moderate to high platinum-group-metal contamination along the coast of Ghana, which was most likely attributed to anthropogenic activities. The degree of contamination among the three metals was generally in the order: Pd > Pd > Rh, the most mobile element being Pd. The study suggests a distribution gradient: Pd ≥ Pt > Rh. The pollution indices showed moderate to high contamination at all the study sites in the case of sediment while there was less pollution of water. The study has provided useful information on the water quality status of some of our lagoons and estuaries along the coastal belt and may serve as a reference for future research studies.

ACKNOWLEDGEMENTS

This work was supported under contract with the Ghana Atomic Energy Commission Reactor 1 (GHAER 1). The authors would like to thank the technical workers of GHAER 1 and staff and research team of the Chemistry Department, University of Cape Coast, for their support and contributions. Finally, the authors wish to thank the government of Ghana for financial support.

REFERENCES

1. E. J. Hutchinson, M. E. Farago and P. R. Simpson, "Changes in platinum concentrations in soils and dusts from UK cities", in "Anthropogenic Platinum-Group Element Emission. Their Impact on Man and Environment" (Ed. F. Zereini and F. Alt), Springer Verlag, Berlin, **2000**, pp.57–64.
2. J. D. Whiteley and F. Murray, "Anthropogenic platinum group element (Pt, Pd and Rh) concentrations in road dusts and roadside soils from Perth, Western Australia", *Sci. Total Environ.*, **2003,** *317*, 121–135.
3. H. E. Kristine, G. M. Morrison and S. Rauch, "Environmental routes for platinum group elements to biological materials - A review", *Sci. Total Environ.*, **2004**, *334-335*, 21–38.
4. I. K. Kalavrouziotis and P. H. Koukoulakis, "The Environmental impact of the platinum group elements (Pt, Pd, Rh) emitted by the automobile catalyst converters", *Water Air Soil Pollut.*, **2009,** *196*, 393–402.
5. B. Sures, S. Zimmermann, J. Messershmidt and A. Von Bohlen, "Relevance and analysis of traffic related platinum group metals (Pt, Pd, Rh) in the aquatic biosphere, with emphasis on palladium", *Ecotoxicol.*, **2002,** *11*, 385–392.
6. H. P. Känig, R. F. Hertel, W. Koch and G. Rosner, "Determination of platinum emissions from a three-way catalyst-equipped gasoline engine", *Atmos. Environ. A*, **1992,** *26*, 741–745.

7. M. Moldovan, M. A. Palacios, M. M. Gomez, G. Morrison, S. Rauch, C. McLeod, R. Ma, S. Caroli, A. Alimonti, F. Petrucci, B. Bocca, P. Schramel, M. Zischka, C. Pettersson, U. Wass, M. Luna, J. C. Saenz and J. Santamara, "Environmental risk of particulate and soluble platinum group elements released from gasoline and diesel engine catalytic converters", *Sci. Total Environ.*, **2002,** *296*, 199–208.
8. D. K. Essumang, D. K. Dodoo and C. K. Adokoh, "The Impact of vehicular fallout on the Pra estuary of Ghana (A case study of the impact of platinum group metals (PGMs) on the marine ecosystem)", *Environ. Monit. Assess.*, **2008,** *145*, 283–294.
9. D. K. Essumang, D. K. Dodoo, C. K. Adokoh, A. Sam and N. G. Doe, "Bioaccumulation of platinum group metals (PGMs) on some fish species (*Oreochromis niloticus*, *Penaeus laspisulcates*, *Scylla serrate*, *Galaxias brevipinnis* and *Mollusc*) in the Pra estuary of Ghana", *J. Toxicol. Environ. Chem.*, **2008,** *90*, 625–638.
10. D. K. Essumang "Bioaccumulation of platinum group metals in dolphins, *Stenella* sp., caught off Ghana", *Afr. J. Aqua. Sci.*, **2008,** *33*, 255–259.
11. B. Sures, S. Zimmermann, J. Messershmidt, A. Von Bohlen and F. Alt, "First report on the uptake of automobile catalyst emitted palladium by European eels (*Anguilla anguilla*) following experimental exposure to road dust", *Environ. Pollut.*, **2001,** *113*, 341–345.
12. K. Hoppstock and B. Sures, "Platinum group metals", in "Elements and Their Compounds in the Environment" (Ed. E. M. Anke, M. Ihnat and M. Stoeppler), Wiley-VCH, Weinheim, **2004,** pp.1047–1086.
13. R. R. Barefoot, "Determination of platinum at trace levels in environmental and biological materials", *Environ. Sci. Technol.*, **1997,** *31*, 309–314.
14. International Programme on Chemical Safety, "Platinum Environmental Health Criteria", World Health Organization, Geneva, **1991**, http://www.inchem.org/documents/ehc/ehc/ehc125.htm (Accessed: Sept. 29, 2011).
15. D. K. Essumang, "First determination of the levels of platinum group metals in *Manta birostris* (Manta Ray) caught along the Ghanaian coastline", *Bull. Environ. Contam. Toxicol.*, **2010**, *84*, 720–725.
16. J. Tolgyessy and M. Kyrs, "Radioanalytical Chemistry 1 and 2", Ellis Horwood Ltd., Chichester, **1989**.
17. D. Adomako, B. J. B. Nyarko, S. B. Dampare, Y. Serfor-Armah, S. Osae, J. R. Fianko and E. H. K. Akaho, "Determination of toxic elements in water and sediments from River Subin in the Ashanti region of Ghana", *Environ. Monit. Assess.*, **2008,** *141*, 165–175.
18. Y. Katoh, T. Sato and Y. Yamamoto, "Use of instrumental neutron activation analysis to determine concentrations of multiple trace elements in human organs", *Arch. Environ. Health*, **2003**, *58*, 1–9.
19. D. L. Tomlinson, J. G. Wilson, C. R. Harris and D. W. Jeffrey, "Problems in the assessment of heavy-metal levels in estuaries and the formation of a pollution index", *Helgol Meeresunters*, **1980,** *33*, 566–575.

20. B. J. B. Nyarko, D. Adomako, Y. Serfor-Armah, S. B. Dampare, D. K. Adotey and E. H. K. Akaho, "Biomonitoring of atmospheric trace element deposition around an industrial town in Ghana", *Radiat. Phys. Chem.*, **2006,** *75*, 954–958.
21. E. Angulo, "The Tomlinson pollution load index applied to heavy metal, 'Mussel-watch' data: A useful index to assess coastal pollution", *Sci. Total Environ.*, ***1999,*** *187*, 19–56.
22. Y. Ji, Y. Feng, J. Wu, T. Zhu, Z. Bai and C. Duan, "Using geoaccumulation index to study source profiles of soil dust in China", *J. Environ. Sci.*, **2008,** *20*, 571–578.
23. H. Lokeshwari and G. T. Chandrappa, "Effects of heavy metal contaminatal impact and health effect", **2007**, http:www.lenntech.com/aluminium(al)andwater.htm (Accessed: May 11, 2009).
24. W. Grzebisz, L. Cieoela, J. Komisarek and J. Potarzycki, "Geochemical assessment of heavy metals pollution of urban soils", *Polish J. Environ. Stud.*, **2002,** *11*, 493-499.
25. B. Mason, "Principles of Geochemistry", 3rd Edn., Wiley, New York, **1966**.
26. N. N. Greenwood and A. Earnshaw, "Chemistry of the Elements", Pergamon Press, Oxford, **1984.**
27. F. Cabrera, L. Clemente, D. E. Barrientos, R. Lopez and J. M. Murillo, "Heavy metal pollution of soils affected by Guandiamar toxic flood", *Sci. Total Environ.*, **1999,** *242*, 117–129.
28. A. R. Karbassi, S. M. Monvari, G. R. N. Bidhendi, J. Nouri and K. Nemapour, "Metal pollution assessment of sediment and water in the Shurr River", *Environ. Monit. Assess.*, **2008,** *147*, 107–116.
29. Y. Teng, S. Ni, P. Jiao, J. Deng, C. Zhang and J. Wang, "Eco-environmental geochemistry of heavy metal pollution in Dexing mining area", *Chinese J. Geochem.*, **2004,** *23*, 349–358.
30. G. Ysart, P. Miller, H. Crews, P. Robb, M. Baxter, C. de L'Argy, S. Lofthouse, C. Sargent and N. Harrison, "Dietary exposure estimates of 30 elements from the UK total diet study", *Food Addit. Contam.*, **1999,** *16*, 391–403.
31. S. Rauch and G. M. Morrison, "Environmental relevance of the platinum-group elements", *Mineralog. Soc. America*, **2008,** *4*, 259–263.
32. (a) New Hampshire Department of Environmental Services, "Outboard marine engines and the environment: New technology engines reduce air and water pollution", **2000**, http://des.nh.gov/organization/commissioner/pip/factsheets/ard/documents/ard-31.pdf (Accessed: Sept. 29, 2011).
    (b) US Environmental Protection Agency (EPA), "Program announcement: Marine engine manufacturer develops low emission inboard marine engines", **2006**, http://www.epa.gov/otaq/regs/nonroad/marine/si/420f06057.htm (Accessed: Sept. 29, 2011).
33. L. Russel, "Two strokes and you're out. (Air pollution from pleasure craft caused by two-stroke engines)", *Earth Island J.*, **1997**, *12*, 1-3.
34. J. Schäfer and H. Puchelt, "Platinum-group-metals (PGM) emitted from automobile catalytic converters and their distribution in roadside soils", *J. Geochem. Explor.*, **1998,** *64*, 307–314.
35. L. S. Wiseman-Clare, "Palladium from catalytic converters: Exposure levels and human risk of palladium emissions in the environment", *Earth Environ.*, **2006,** 5, 565–574.

36. S. Lustig, R. Schierl, F. Alt, E. Helmers and K. Kümmerer,"Schwerpunktthema: Platin in umweltkompartimenten-deposition, verteilung sowie bedeutung für den munched und sein nahrungsnetz", *UWSF- Z Umweltchem. Ökotox* , **1997,** *9*, 149–152.
37. H. Renner and G. Schmuckler, "Platinum-group metals", in "Metals and Their Compounds in the Environment", (Ed. E. Merian), VCH Verlagsgesellschaft, Weinheim, **1991,** pp.1115–1136.
38. J. Wilson and P. Evans, "Likely cause of poor water quality and fish kills in Cockrone lagoon", Centre for Natural Resources Department Land and Water Conservation, Newcastle NSW, **2002**, http://www.gosford.nsw.gov.au/customer/document_gallery/public_studies/fishkills.pdf (Accessed: Aug. 28, 2011).
39. S. M. Praveena, M. Radojevic and M. H. Abdullah, "The assessment of mangrove sediment quality in Mengkabong lagoon: An index analysis approach", *Int. J. Environ. Sci. Edu.*, **2007**, *2*, 60–68.
40. S. Draggan, "Platinum", in "Encyclopedia of Earth" (Ed. C. J. Cleveland), **2008**, http://www.eoearth.org/article/Platinum (Accession date: March 3, 2010).
41. T. Oberthür, T. Weiser, J. A. Amanor and S. L. Chryssoulis, "Mineralogical siting and distribution of gold in quartz veins and sulfide ores of the Ashanti mine and other deposits in the Ashanti belt of Ghana: Genetic implications", *Mineral. Deposita*, **1997,** *32*, 2–15.
42. G. Hilson "A contextual review of the Ghanaian small-scale mining industry", *Mining Miner. Sustain. Dev.*, **2001,** *76*, 2–29.

APPENDIX 1. PGM mean concentration in sediment and water samples at sampling sites A and B along the coastal belt of Ghana

Sampling site		Season	Mean PGM		
			Pt	**Pd**	**Rh**
Pra estuary					
	A	Dry	0.039±0.006	0.067±0.010	0.002±0.000
		Wet	nd	0.035±0.005	0.0004±0.001
Sediment (µg/g)		**Mean**	**0.039±0.006**	**0.051**	**0.0012**
		SD	**0.000**	**0.023**	**0.001**
	B	Dry	0.0448±0.007	0.100±0.000	0.0002±0.000
		Wet	0.011±0.002	0.006±0.015	0.0002±0.000
		Mean	**0.028**	**0.053**	**0.0002±0.000**
		SD	**0.024**	**0.066**	**0.000**
	A	Dry	0.007±0.001	0.002±0.000	0.001±0.000
		Wet	0.002±0.000	0.002±0.000	0.002±0.000
Water (µg/L)		**Mean**	**0.005**	**0.002**	**0.0015**
		SD	**0.004**	**0.000**	**0.001**
	B	Dry	0.008±0.001	0.005±0.001	0.002±0.000
		Wet	0.002±0.000	0.002±0.000	0.001±0.000
		Mean	**0.005**	**0.004**	**0.002**
		SD	**0.004**	**0.002**	**0.001**
Benya lagoon					
	A	Dry	nd	0.081±0.012	0.001±0.000
		Wet	nd	0.082±0.012	0.001±0.000
Sediment (µg/g)		**Mean**	**nd**	**0.082**	**0.001±0.000**
		SD	**0.000**	**0.001**	**0.000**
	B	Dry	0.038±0.001	0.107±0.016	0.008±0.001
		Wet	0.073±0.011	0.030±0.004	nd
		Mean	**0.056**	**0.069**	**0.008±0.001**
		SD	**0.025**	**0.054**	**0.000**
	A	Dry	0.006±0.001	0.015±0.002	0.003±0.001
		Wet	0.001±0.000	0.002±0.000	0.001±0.000
Water (µg/L)		**Mean**	**0.004**	**0.009**	**0.002**
		SD	**0.004**	**0.009**	**0.001**
	B	Dry	0.010±0.000	0.009±0.001	0.001±0.000
		Wet	0.001±0.000	0.004±0.001	0.0004±0.000
		Mean	**0.006**	**0.007**	**0.001**
		SD	**0.006**	**0.004**	**0.0004**
Fosu lagoon					
	A	Dry	0.017±0.003	0.010±0.002	nd
		Wet	0.007±0.001	0.083±0.012	0.001±0.000
Sediment (µg/g)		**Mean**	**0.012**	**0.047**	**0.001±0.000**
		SD	**0.007**	**0.052**	**0.00**
	B	Dry	0.010±0.002	0.006±0.01	0.0002±0.000
		Wet	0.093±0.014	nd	nd
		Mean	**0.052**	**0.006**	**0.0002**
		SD	**0.059**	**0.000**	**0.00**
	A	Dry	nd	0.021±0.003	0.003±0.000
		Wet	0.0004±0.000	0.019±0.003	0.0004±0.000
Water (µg/L)		**Mean**	**0.0004**	**0.020**	**0.002**
		SD	**0.000**	**0.001**	**0.002**
	B	Dry	0.012±0.002	0.009±0.001	0.001±0.000
		Wet	0.001±0.000	0.002±0.000	nd
		Mean	**0.007**	**0.006**	**0.001±0.000**
		SD	**0.008**	**0.005**	**0.000**

Sampling site		Season		Mean PGM	
Narkwa lagoon					
	A	Dry	0.139±0.021	0.068±0.010	0.010±0.001
		Wet	0.017±0.002	0.024±0.004	0.001±0.000
Sediment (µg/g)		**Mean**	**0.078**	**0.046**	**0.006**
		SD	**0.086**	**0.031**	**0.006**
	B	Dry	0.001±0.000	0.076±0.011	0.0004±0.000
		Wet	0.057±0.009	0.122±0.015	nd
		Mean	**0.029**	**0.099**	**0.0004**
		SD	**0.039**	**0.033**	**0.000**
	A	Dry	0.001±0.000	0.007±0.001	nd
		Wet	0.001±0.000	0.007±0.001	nd
Water (µg/L)		**Mean**	**0.001**	**0.007**	**nd**
		SD	**0.000**	**0.000**	**-**
	B	Dry	0.009±0.001	0.010±0.002	0.002±0.000
		Wet	0.002±0.000	nd	nd
		Mean	**0.006**	**0.010**	**0.002**
		SD	**0.005**	**0.000**	**0.000**
Sakumono 2 lagoon					
	A	Dry	0.028±0.004	0.042±0.006	nd
		Wet	nd	0.020±0.003	0.001±0.000
Sediment (µg/g)		**Mean**	**0.028**	**0.031**	**0.001**
		SD	**0.000**	**0.016**	**0.000**
	B	Dry	0.023±0.004	0.033±0.005	0.001±0.000
		Wet	0.028±0.004	0.042±0.006	nd
		Mean	**0.026**	**0.038**	**0.001**
		SD	**0.004**	**0.006**	**0.000**
	A	Dry	0.002±0.000	0.007±0.001	0.002±0.000
		Wet	0.001±0.000	0.002±0.000	0.001±0.000
Water (µg/L)		**Mean**	**0.002**	**0.005**	**0.0015**
		SD	**0.001**	**0.004**	**0.001**
	B	Dry	0.015±0.003	0.020±0.002	0.001±0.000
		Wet	0.001±0.000	0.003±0.001	0.0002±0.000
		Mean	**0.008**	**0.012**	**0.001**
		SD	**0.009**	**0.012**	**0.001**
Volta estuary					
	A	Dry	0.005±0.001	0.014±0.002	0.001±0.000
		Wet	nd	nd	nd
Sediment (µg/g)		**Mean**	**0.005**	**0.014**	**0.001**
		SD	**0.00**	**0.00**	**0.000**
	B	Dry	0.016±0.002	0.019±0.003	0.003±0.000
		Wet	0.028±0.004	0.047±0.007	0.006±0.001
		Mean	**0.022**	**0.033**	**0.0045**
		SD	**0.008**	**0.019**	**0.002**
	A	Dry	0.017±0.003	0.019±0.003	0.003±0.000
		Wet	0.006±0.001	0.008±0.001	0.001±0.000
Water (µg/L)		**Mean**	**0.012**	**0.014**	**0.002**
		SD	**0.008**	**0.008**	**0.001**
	B	Dry	0.015±0.002	0.020±0.003	0.003±0.000
		Wet	0.006±0.001	0.019±0.003	0.001±0.000
		Mean	**0.011**	**0.020**	**0.002**
		SD	**0.006**	**0.001**	

Sampling site		Season		Mean PGM	
Keta lagoon					
	A	Dry	0.175±0.026	0.177±0.027	0.035±0.004
		Wet	0.012±0.002	0.035±0.003	0.0002±0.000
Sediment (µg/g)		**Mean**	**0.094**	**0.106**	**0.015**
		SD	**0.115**	**0.100**	**0.025**
	B	Dry	nd	0.107±0.016	0.004±0.001
		Wet	nd	0.058±0.001	nd
		Mean	**nd**	**0.083**	**0.004**
		SD	**-**	**0.035**	**0.00**
	A	Dry	0.016±0.002	0.018±0.003	0.003±0.000
		Wet	0.008±0.001	0.008±0.001	0.002±0.000
Water (µg/L)		**Mean**	**0.012**	**0.013**	**0.0025**
		SD	**0.006**	**0.007**	**0.001**
	B	Dry	0.012±0.002	0.020±0.002	0.002±0.000
		Wet	0.006±0.001	0.030±0.005	0.002±0.000
		Mean	**0.009**	**0.025**	**0.002**
		SD	**0.004**	**0.007**	**0.000**

Note: nd = not detected

Maejo Int. J. Sci. Technol. **2011**, *5*(03), 350-357

Maejo International Journal of Science and Technology

ISSN 1905-7873
Available online at www.mijst.mju.ac.th

Communication

A good conversion loss and a very high LO-to-RF isolation of 24-GHz single balanced mixer for RF front-end receiver

Mouloud Challal [1, 2,*] and Arab Azrar [1]

[1]Department of Electronics, Institute of Electrical Engineers and Electronics, University of Boumerdes, Avenue de l'indépendance, B-35000, Boumerdes, Algeria

[2] Electrical Engineering, Institute of Information and Communication Technologies, Electronics and Applied Mathematics, Université catholique de Louvain, Bâtiment Maxwell, 3 place du Levant, B-1348, Louvain-la-Neuve, Belgium

* Corresponding author, e-mail: mchallal@gmail.com

Received: 29 November 2010 / Accepted: 14 October 2011 / Published: 17 October 2011

Abstract: This work describes the design, analysis and fabrication of a 24-GHz microwave single balanced down-conversion mixer based on Schottky diode, hybrid ring coupler and a wide and deep stopband low-pass filter (LPF). The LPF is composed of three uniform defected ground structures along with a compensated microstrip line. The selected frequencies are 24.125 GHz for RF signal and 24 GHz for LO signal. When the LO and RF signals are injected as 10 dBm and 0 dBm respectively, a conversion loss of 12.85 dB with an LO-to-RF isolation greater than 38 dB is obtained. The measured results agree well with the simulated results and the reported design.

Keywords: Schottky diode, low pass filter, signal balanced mixer

INTRODUCTION

One of the important blocks in the radio frequency (RF) front-end receiver is the down-conversion mixer which forms a critical part of the system. The down-conversion mixer converts an RF signal at the input to an intermediate frequency (IF) at the output through the use of a local oscillator (LO) signal. Single balanced diode mixers have a benefit of low-level of LO signal to produce a high RF/IF isolation. A Schottky diode can be used to produce an output spectrum consisting of sum and difference frequencies of two input signals. It has received considerable attention from the researchers due to its simplicity and efficiency of application in mixing signals. Mixer circuits have been much

presented in the literature [1-8]. However, only Roselli et al. [6] have designed a hybrid mixer at 24 GHz but have not investigated all its characteristics.

This paper presents and proposes a reasonably good conversion loss (CL) and a very high LO-to-RF isolation of a hybrid single balanced down-conversion mixer (SBDCM) with and without DC power supply. The designed, optimised and tested SBDCM, with two silicon Schottky diodes [9], five-port hybrid coupler and an low-pass filter (LPF), is intended to be implemented in a radar receiver front-end system. The novelty of the proposed down-conversion mixer is the use of an LPF with a wide and deep stopband microstrip with and without DC power supply. The LPF is composed of three defected ground structures (DGS) etched on the backside metallic ground plane under a microstrip line [10], and a compensated microstrip line to reject the unwanted harmonics of the designed 24-GHz SBDCM. The relative permittivity and thickness of the substrate are 3.63 and 0.25 mm respectively for all designs. The complete circuit was designed and analysed using an Agilent's advanced design system (ADS) circuit simulator, then prototyped and verified by measurements. The input signal frequencies of the RF and the LO are 24.125 GHz and 24 GHz respectively. The design goals are: (i) conversion loss of less than 15 dB and (ii) isolation of greater than 25 dB.

CIRCUIT DESIGN, THEORETICAL ANALYSIS AND FABRICATION

A down-conversion mixer operates on a theoretical basis of trigonometric identities where the input signal (called RF signal, $V_{RF}(t)$) coming from the receiver antenna is filtered, amplified and multiplied at the mixer by another signal (called LO signal, $V_{LO}(t)$) generated by a local oscillator to be down converted to the intermediate frequency (called IF signal, $V_{IF}(t)$). However, this conversion process causes a set of difficulties which affect the overall mixer performances such as gain, noise, power consumption, linearity, isolation and cost. In practice, the mixing operation is performed using non-linear components. Besides, although mathematically simple, the multiplication operation is virtually impossible to be achieved.

In a non-linear system, a response may be in the form [11]:

$$v_{out}(t) = av_{in}(t) + bv_{in}^{2}(t) + cv_{in}^{3}(t) + \ldots \quad (1)$$

where a, b and c are constant and v_{in} is the co-sinusoidal signals of the combined excitation input of the form:

$$v_{in}(t) = V_{RF}\cos(w_{RF}t) + V_{LO}\cos(w_{LO}t) \quad (2)$$

where V_{RF} and w_{RF} are the voltage and angular frequency of the RF signal respectively, and V_{LO} and w_{LO} are the voltage and angular frequency of the LO signal respectively.

It has been shown that the generated frequency is given as follows [11]:

$$f_{mn} = |mf_{RF} \pm nf_{LO}| \quad (3)$$

where $m, n = \ldots, -3, -2, -1, 0, 1, 2, 3, \ldots.$. The term f_{mn} is called a mixing frequency and f_{RF} and f_{LO} are the RF signal and LO signal frequencies respectively.

The MA4E2502 silicon Schottky diodes (SSD) is selected for its extremely low parasitic capacitance and inductance, mountable surface in microwave circuits and lower susceptibility to electrostatic discharge (ESD) damage. Its spice model is given as [9]: I_S = 5E-1 nA, C_{JO} = 1E-02 pF,

V_J= 8E-2 V, BV=5 V, IBV= 1E-2 mA, N=1.2, RS= 9.6 Ω, M=0.5, Ik=10 mA, C_{jpar}= 9E-2 pF, FC=0.5, and it is implemented in our circuit simulator.

To suppress the spurious responses present at the IF output mixer, several researchers have demonstrated that with the use of low-pass filter based on DGS, the obtained performance considerably improves with wider and deeper stopband characteristics than the conventional LPF [12-22]. To reject the undesirable harmonics and take only the IF signal, a unit cell of well-known dumb-bell shaped DGS with 50-Ω microstrip line is used [10, 12]. In this paper, the designed LPF is based on three DGS units of dumb-bell shaped DGS integrated to the mixer circuit. In the mixer, both RF and LO signals are mixed in the two diodes to generate signals which are combined through the ring and taken out through a DGS-LPF. A photograph of the fabricated 24-GHz SBDCM is shown in Figure 1. It consists of a hybrid coupler, two DC blocks, two Schottky diodes (D_1 and D_2) and an LPF. In order to increase the output power and decrease the losses, the designed mixer is also biased with low DC voltage (V_{DC}) as shown in Figure 1.

Figure 2 shows simulation results of the output power in a spectral domain at the IF port with RF power of 0 dBm at 24.125 GHz and LO power of 10 dBm at 24 GHz (input power at the mixer RF and LO ports is -11.75 dBm and -6.78 dBm respectively). When the diodes are biased, the biased current (I_d) is equal to 2 mA from a 0.2 V power supply. Figures 3 and 4 show the measured output power with and without bias respectively.

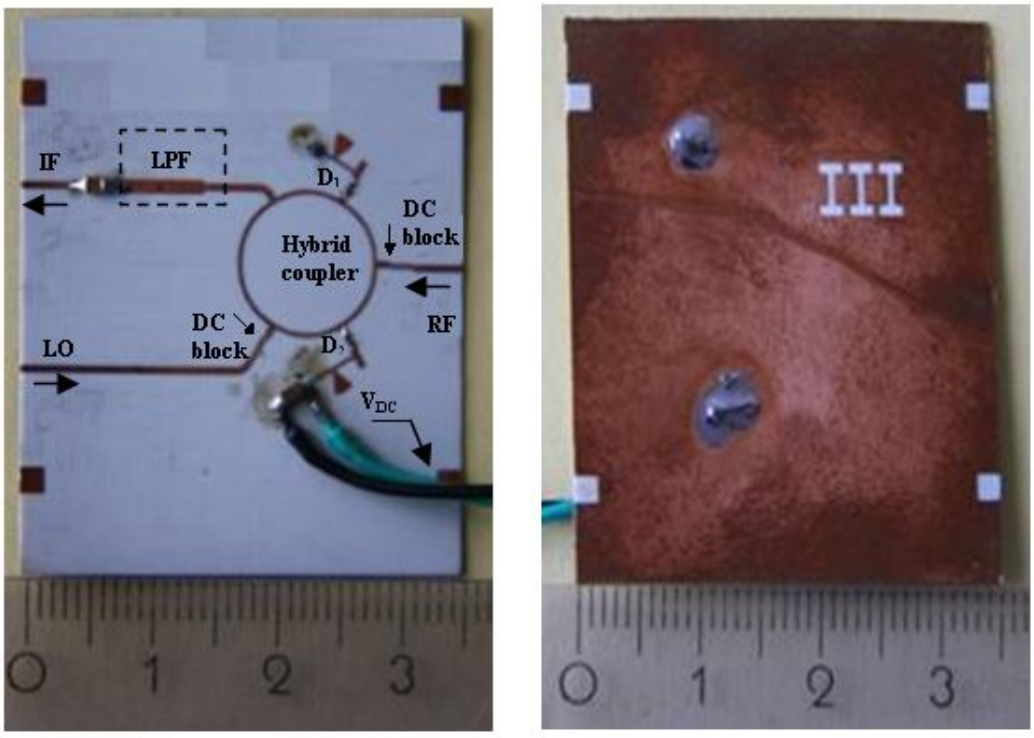

(a) (b)

Figure 1. Photograph of the fabricated down-conversion mixer: (a) top view, (b) bottom view

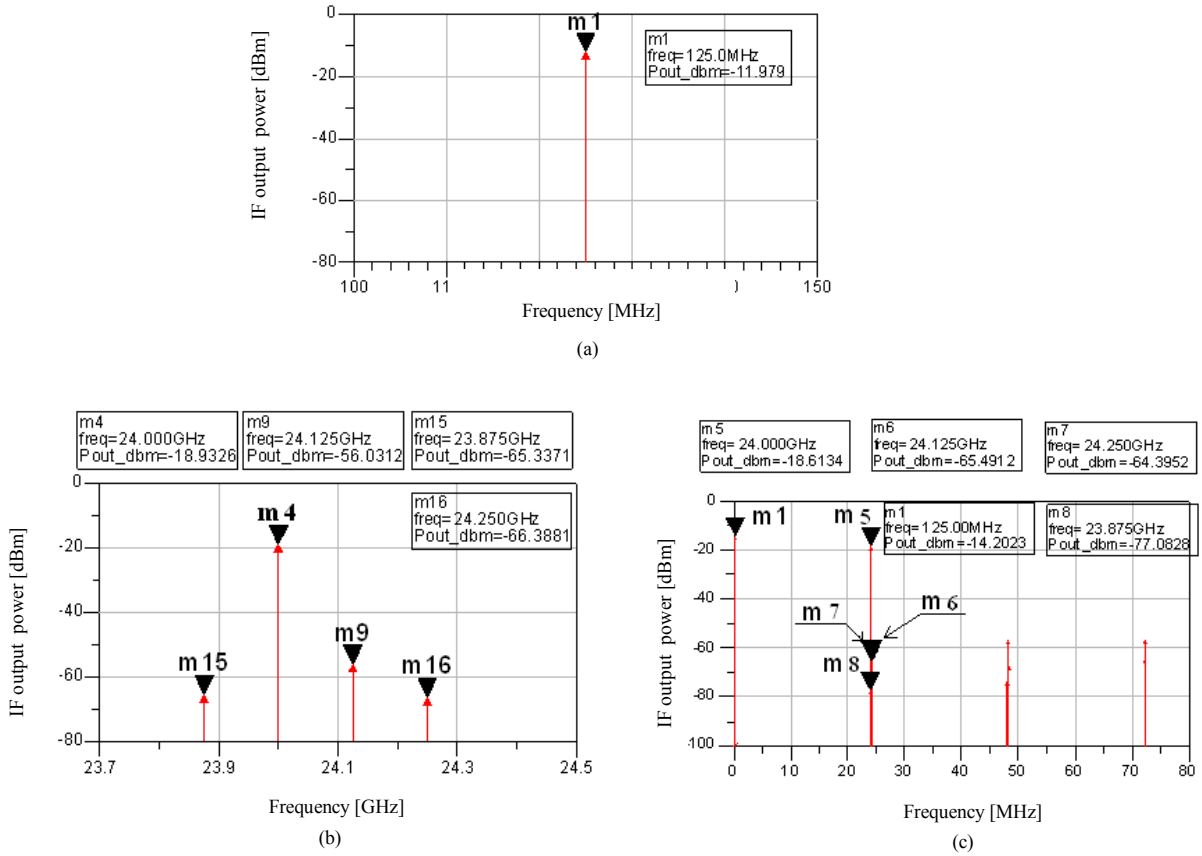

Figure 2. Simulated IF output spectrum: (a) f_{IF} = 125 MHz (I_d = 2 mA), (b) other harmonics (I_d = 2 mA), (c) f_{IF} = 125 MHz along with other harmonics (without bias)

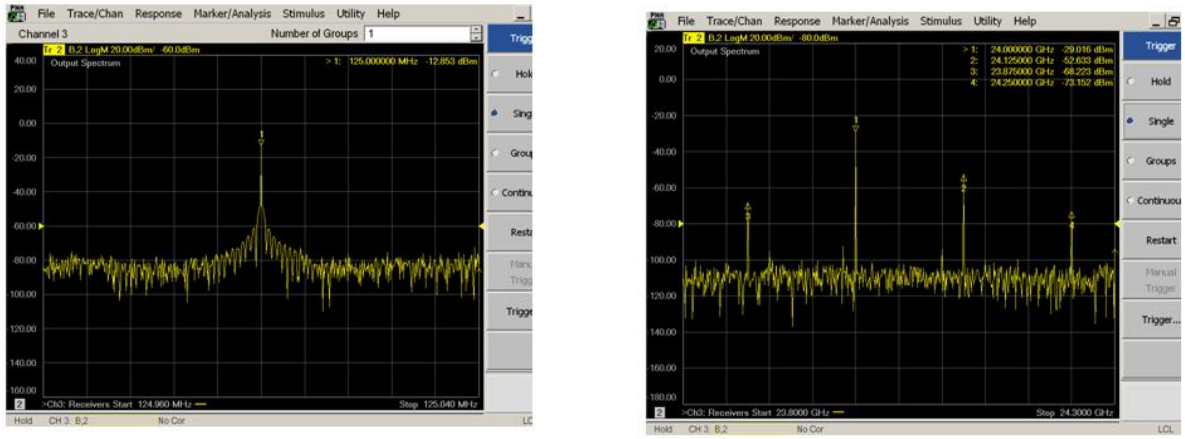

Figure 3. Measured IF output spectrum (in dBm) versus frequency (I_d =2 mA): (a) f_{IF} =125 MHz, (b) other harmonics

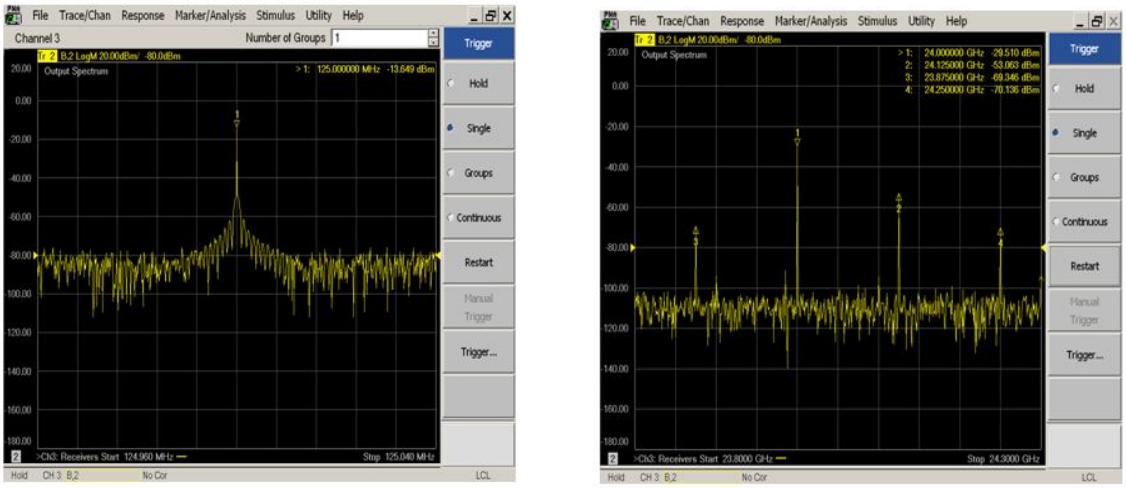

(a) (b)

Figure 4. Measured IF output spectrum (in dBm) versus frequency (without bias): (a) f_{IF} =125 MHz, (b) other harmonics

As shown in Figures 3-4, the mixer demonstrates a good down-conversion of f_{RF} and f_{LO} to f_{IF}. It can be seen that a good agreement is achieved between the simulated and measured data results. Furthermore, by adding a DC bias to the mixer, it is observed that the output power is increased: the measured IF power is equal to -13.64 dBm (before bias) and then equal to -12.85 dBm (after bias).

Figure 5 shows the simulation and the measurement of 1-dB compression point, which is approximately equal to 5 dBm.

The simulated and measured CL are shown in Figures 6(a) and 6(b) respectively. From the measured results, the maximum CL of a mixer is equal to 12.85 dBm with a 2-mA diode biased current. It can be seen that it is constant below 0 dBm (power at RF port) and then decreases due to the non-linearity of the mixer. Therefore, the CL decreases from 13.64 to 12.85 dBm when the mixer is biased.

In order to determine the isolations between different ports, the power at RF port was also measured and is shown in Figure 7. From Figure 5 and Figure 7, the LO-to-IF, LO-to-RF and RF-to-IF isolations are 39.01 dB, 38.38 dB and 52.63 dB respectively.

The 24-GHz SBDCM presented here was compared with another circuit in terms of performance and the results are summarised in Table 1, which shows a good agreement in CL. The literature result shows that when a DC bias is added to the mixer, the CL decreases from 15 dBm to 12 dBm, whereas in our circuit it decreases from 13.64 dBm to 12.85 dBm under a 2-mA diode biased current.

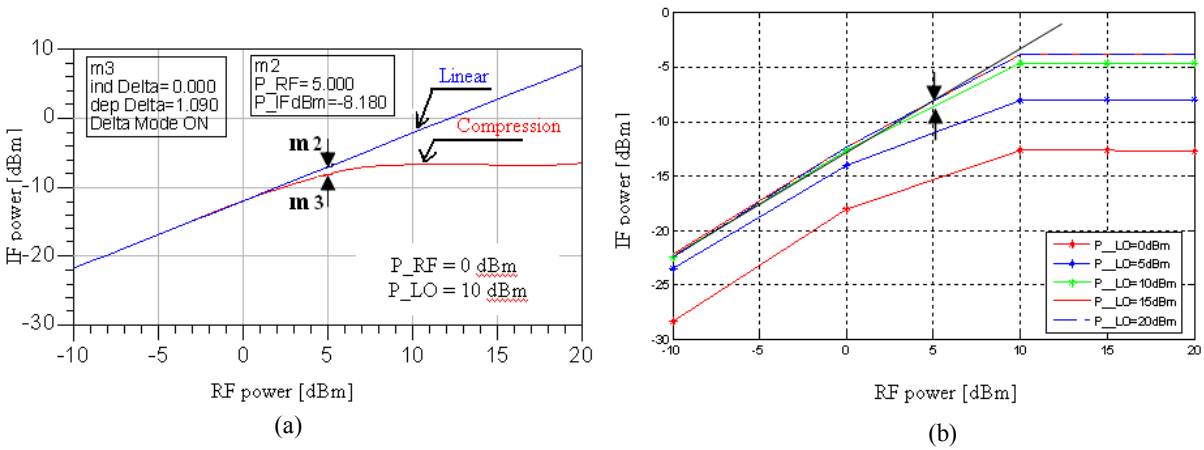

Figure 5. 1-dB Compression point: (a) simulated, (b) measured for different values of P_LO

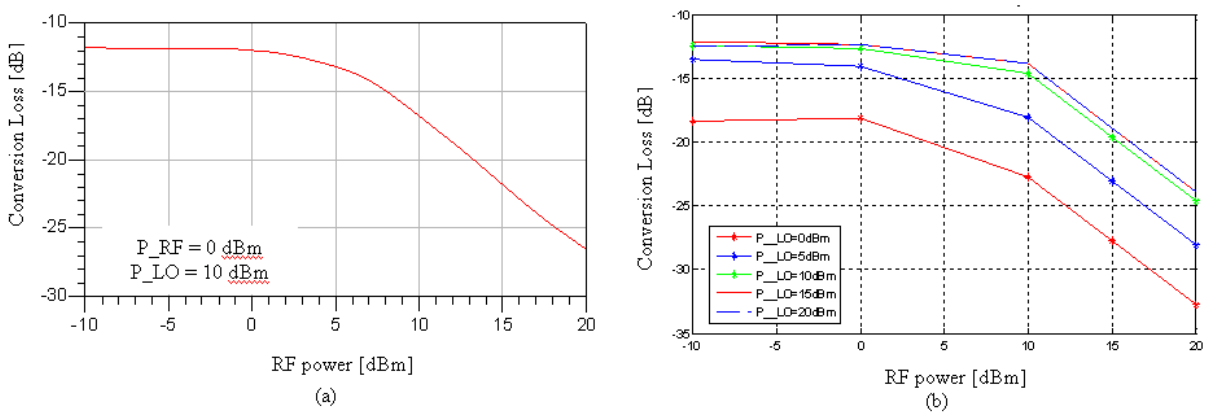

Figure 6. Conversion loss: (a) simulated, (b) measured for different values of P_LO

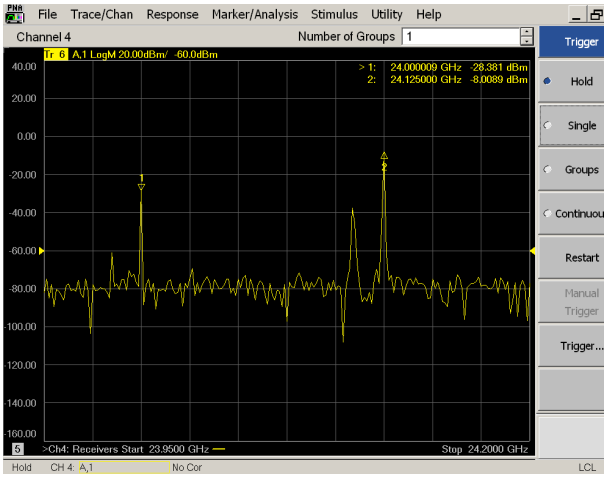

Figure 7. Measured power (in dBm) at RF port versus frequency

Table 1. Comparison of reported designs

Ref.	f_{RF} [GHz]	f_{LO} [GHz]	f_{IF} [MHz]	P_RF [dBm]	P_LO [dBm]	V_{DC} [V]		I_{DC} [mA]	CL [dB]	1-dB [dBm]	Isol. [dB]
Roselli et al. [6]	–	24.15	0.18	- 30	- 3	–		2.5	12	–	–
						Without bias			15	–	–
This work	24.125	24	125	- 11.75	- 6.78	Simul.	0.2	2	11.97	5	> 38
							Without bias		14.2	–	–
						Meas.	0.2	2	12.85	~ 5	> 38
							Without bias		13.64	–	–

CONCLUSIONS

A 24-GHz single balanced diode mixer has been designed, analysed and fabricated. It shows good optimised performance in terms of DC power supply, conversion loss (CL) and isolation. We obtained a CL of 12.85 dB, a 1-dB compression point of 5 dBm and isolations greater than 38 dB. It was demonstrated that when a DC bias is added, the mixer performance is affected positively. Measured results agreed well with the simulated data.

REFERENCES

1. K. S. von Behren, D. Pienkowski and G. Boeck, "77 GHz Si-Schottky diode harmonic mixer", Proceedings of the 32nd European Microwave Conference, **2002**, Amsterdam, Netherlands, pp.1-4.
2. E. Chan, "Design of a 5-6 GHz single balanced Schottky diode mixer ", Proceedings of the Asia-Pacific Conference on Applied Electromagnetics, **2003**, Penang, Malaysia , pp.67-71.
3. S. Douss, F. Touati and M. Loulou, "An RF-LO current-bleeding doubly balanced mixer for IEEE 802.15.3a UWB MB-OFDM standard receivers", *Int. J. Electron. Commun.*, **2008**, *62*, 490-495.
4. C. H. Lin, H. Z. Liu, C. K. Chu, H. K. Huang, C. C. Liu, C. H. Chang, C. L. Wu, C. S. Chang and Y. H. Wang, "A PHEMT diode single-balanced mixer for K/K-band application ", *Microw. Optic. Technol. Lett.*, **2007,** *49*, 2692-2694.
5. J. Jaiyen, A. Namahoot and P. Akkaraekthalin, "A 2.4-2.5 GHz singly balanced diode mixer for up and down conversions", Proceedings of the 06th International Symposium on Communications and Information Technologies, **2006,** Bangkok, Thailand, pp.1109-1112**.**
6. L. Roselli, F. Alimenti, M. Comez, V. Palazzari, F. Placentino, N. Porzi and A. Scarponi, "A cost driven 24 GHz Doppler radar sensor development for automotive applications", Proceedings of the 35th European Microwave Conference, **2005**, Paris, France, pp.335-338.
7. M. A. Nassef, E. A. Hosny and M. I. Sobhy, "Practical design of microstrip mixer circuits", Proceedings of the 32nd Midwest Symposium on Circuits and System, **1989,** Champaign, USA, *2*, pp.1046-1049.
8. B. Schuppert, "Analysis and design of microwave balanced mixers", *IEEE Trans. Microw. Theo. Tech.*, **1986**, *34*, 120-128**.**

9. M/A-COM Technology Solutions Inc., "Surmount™ low, medium, and high barrier silicon Schottky diodes", http://www.macomtech.com/datasheets/MA4E2502%20Series.pdf (Accessed: **2009**).
10. D. Ahn , J. S. Park, C. S. Kim, J. Kim, Y. Qian and T. Itoh, "A design of the low-pass filter using the novel microstrip defected ground structure", *IEEE Trans. Microw. Theo. Tech.*, **2001,** *49*, 86-93.
11. S. A. Mass, "Nonlinear Microwave and RF Circuit ", 2nd Edn., Artech House, London, **2003**, pp. 4-8.
12. A. Boutejdar, A. Elsherbini and A. Omar, "Design of a novel ultra-wide stopband lowpass filter using H-defected ground structure", *Microw. Optic. Technol. Lett.*, **2008,** *50*, 771-775**.**
13. J. S. Lim, C. S. Kim, Y. T. Lee, D. Ahn and S. Nam, "Design of lowpass filters using defected ground structure and compensated microstrip line", *Electron. Lett.*, **2002,** *38*, 1357-1358**.**
14. X. Q. Chen, R. Li, S. J. Shi, Q. Wang, L. Xu and X. W. Shi, "A novel low pass filter using elliptic shape defected ground structure", *Progr. Electromag. Res. B*, **2008,** *9*, 117-126**.**
15. A. Boutedjar and A. Omar, "Design of microstrip bandpass and lowpass filters using coupling matrix method and a new hairpin defected ground structure", *Microw. Optic. Technol. Lett.*, **2008,** *50*, 2898-2901**.**
16. Y. Sun, R. Xu and Y. Zhang, "A design of the novel lowpass filter using defected ground structure", Proceedings of the Asia-Pacific Microwave Conference, **2005**, Suzhou, China. pp.4-7.
17. A. B. Abdel-Rahman, A. K. Verma, A. Boutejdar and A. S. Omar, "Control of bandstop response of Hi–Lo microstrip low-pass filter using slot in ground plane", *IEEE Trans. Microw. Theo. Tech.*, **2004**, *52*, 1008-1013.
18. F. Wei, X. W. Shi, B. Li, Q. L. Huang and X. H. Wang, "Design of a compact microstrip low-pass filter using defected ground structure", *Microw. Optic. Technol. Lett.*, **2008**, *50*, 3157-3160.
19. X. Q. Chen, L. X. Wang, L. H. Weng and X. W. Shi, "Compact low pass filter using novel elliptic shape DGS", *Microw. Optic. Technol. Lett.*, **2009**, *51*, 1088-1091.
20. S. K. Parui and S. Das, "A novel asymmetric defected ground structure for implementation of elliptic filters", Proceedings of the IEEE MTT-S International Conference on Microwave and Optoelectronics, **2007**, Salvador, Brazil, pp.946-949.
21. H. J. Chen, T. H. Huang, C. S. Chang, L. S. Chen, N. F. Wang, Y. H Wang and M. P. Houng, "A novel cross-shaped DGS applied to design ultra-wide stopband low-pass filters", *IEEE Microw. Wireless Comp. Lett.*, **2006**, *16*, 252-254.
22. S. W. Ting, K. W. Tam and R. P. Martins, "Miniaturized microstrip lowpass filter with wide stopband using double equilateral U-shaped defected ground structure", *IEEE Microw. Wireless Comp. Lett.*, **2006**, *16*, 240-242.

Maejo Int. J. Sci. Technol. **2011**, *5*(03), 358-364

Maejo International Journal of Science and Technology

ISSN 1905-7873
Available online at www.mijst.mju.ac.th

Report

Phenology of *Exacum bicolor* Roxb., an endangered medicinal herb of Kannur and Wayanad districts, Kerala, India

Meethaley V. Jeeshna and Subramaniam Paulsamy*

Post Graduate and Research Department of Botany, Kongunadu Arts and Science College, Coimbatore-641 029, India

* Corresponding author, e-mail: paulsami@yahoo.com

Received: 2 November 2010 / Accepted: 28 October 2011 / Published: 28 October 2011

Abstract: The deciduous herbaceous plant, *Exacum bicolor* Roxb. (Gentianaceae), is endangered in peninsular India and is distributed in grasslands and scrub forests of Kerala between the elevations of 50 and 1350 m. We investigated four variants on basis of leaf blade shape in the grasslands of Kannur and Wayanad districts, Kerala. The detailed study of these variants for various phenophases such as vegetative growth, leaf flushing, flowering, flowering with fruit development, fruiting and seed dispersal was done during May–November 2009. The development of tillers of all four variants happened in May and the leaf formation took place during June. The flowering period occurred generally during June and July. During August and September, flowering with fruit formation for all variants was followed by the fruiting stage and seed dispersal stage during October and November. As this species completes its flowers-to-seeds period within seven months, collection and sowing of seeds in appropriate time is suggested to enhance subsequent establishment and minimise extirpation.

Keywords: *Exacum bicolor* Roxb., phenophases, Kerala, Western Ghats

INTRODUCTION

Exacum bicolor Roxb. (Gentianaceae), an endangered plant species [1] locally called Ceti in Tamil and Kanamthali in Malayalam, is distributed in scrub forests and grasslands of Western Ghats and plateaus from Konkan coast to the southern tip of India. In northern Kerala, this species is distributed in nine districts which include Kannur and Wayanad. The plant is very popular in Kerala as it is one of the choice flowers to adorn *Trikkakkarayappan*, the earth deity worshipped during Onam, an important regional Hindu festival. It is used traditionally for the ailments from many diseases such as eye and skin problems and stomachic and urinary disorders [2–6]. On the basis of

variation in leaf blade shape, four ecological variants, viz. linear-lanceolate, ovate-elliptic, oblanceolate and ovate, were identified in the population of *E. bicolor* in Kannur and Wayanad districts of Kerala [7] (Figure 1). This species is more common in seasonally dry grasslands in the plains of Kannur and Kasargode districts compared to high-elevation grasslands in Wayanad district. The population of this species is severely affected due to habitat destruction caused by urbanisation and plantation [7]. The over-exploitation of this species by complete uprooting for its medicinal uses by the local public and herb gatherers may also be a factor for its diminishing population size [2]. In addition, phenophases, particularly the fruit-seed phase, is essential for species distribution and perpetuation in natural communities [8-9]. Hence, to diagnose the factors apart from heavy exploitation, an attempt in analysing the phonological behaviour of this species is made in the present study. As the ecological variants are generally environment-controlled [9], all the four variants of *E. bicolor* were observed for phenophases.

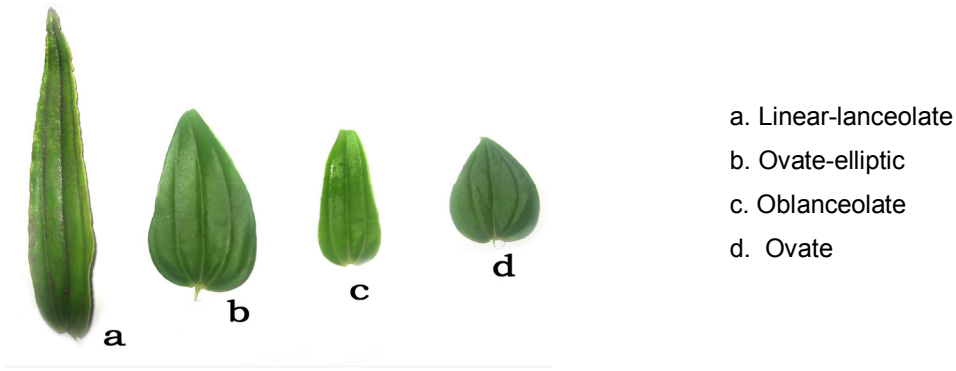

Figure 1. Leaf-shape variants of *E. bicolor*

STUDY AREAS AND METHODS

The study was carried out in the Paithal mala of Kannur district (12° 30'N and 75° 20'E) and Thirunelli forest in Wayanad district (11° 53'N and 76° 01'E) of Kerala, which are located in northern boundary of south-western Ghats at an elevation of 1375 and 1000 m respectively (Figure 2). The climatic data of the study areas are given in Table 1. The annual rainfall in Paithal mala and Thirunelli forest during the study period (2009) was c 2278 and 2554 mm respectively. The temperature ranged between 22-30°C in both areas. The soil was clay loam with a pH of 6.1 and 6.7 in Paithal mala and Thirunelli forest respectively.

Detailed phenological records of the four variants of *E. bicolor*, viz. phenophases of vegetative growth, leaf flushing, flowering, flowering with fruiting, fruiting and seed setting, were prepared from May to November 2009. (The species only appears during this time of the year.) The observations were made at monthly intervals, but during high activity periods, observations were made weekly. Observations for each variant were made on each sampling date by marking 20 randomly selected individuals in the two study areas. When a phenophase was noticed in about 10% of individuals under observation, it was considered to be initiated and peaked when it occurred in more than 80% of individuals, when phenograms were drawn [10].

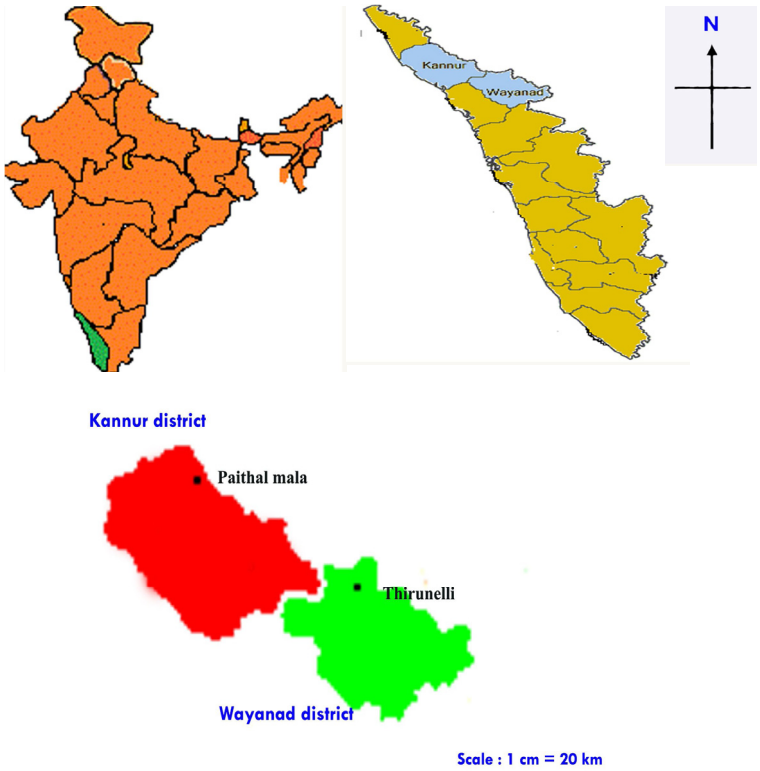

Figure 2. Location of the study areas

RESULTS AND DISCUSSION

The phenophases studied for the four variants of *E. bicolor* are shown in Figure 3. The phenophases of all four variants occurred in the same months in both study areas, indicating that all variants have responded uniformly to the environment [11] regardless of the little difference in elevation. All four variants sprouted tillers during May. Adequate rainfall at around 100 mm with more rainy days during April (Table 1) initiates tillering from the shallow root stock. Oberbauer and Billings [12] pointed out that more abundant shallow roots in the upper soil layers of certain plants favour the rapid development of tillers immediately after the occurrence of adequate rainfall.

The appearance of only 3 seedlings out of 75 individuals was noted after seed setting in the month of November for all the variants. A probable explanation is that the high rainfall occurring during November, the month of seed setting, and subsequent seed dispersal during December by severe monsoon in both study areas could not permit the seeds to complete the dormancy. Indeed, the substantial soil moisture available during this period might deteriorate the tiny seeds of *E. bicolor*. The high rainfall during this season might also wash out the seeds along the slopes of the hilly terrain, which resulted in a low appearance of seedlings in the study areas when compared to individuals recruited through rhizome sprouting. A similar kind of low seedling count has also been noted for certain Shola grassland species such as *Anaphalis elliptica, Drosera pultata* and *Ceropegia pussila* in the high hills of Nilgiris in Western Ghats [13]. A low percentage (less than 5%) of seed germination of *E. bicolor* might also be attributed to low seedling count [1].

Table 1. Climatic data of the two study areas for 2009 [14]

Month	Temperature (° C)				Rainfall (mm)		No. of rainy days		Relative humidity (%)	
	Max.		Min.							
	Paithal mala	Thirunelli	Paithal mala	Thirunelli	Paithal mala	Thirunelli	Paithal mala	Thirunelli	Paithal mala	Thirunelli
Jan	25.2	28.1	17.2	15.1	0	0	0	0	64.6	64.8
Feb	29.1	30.8	19.6	17.8	8.4	13.1	2	2	73.4	69.4
Mar	30.2	30.3	20.2	19.7	24.1	32.4	6	6	76.6	73.8
Apr	30.6	31.4	21.4	21.8	98.1	110.4	11	12	82.4	75.2
May	29.4	29.7	21.5	21.9	255.8	320.1	16	18	89.4	77.1
Jun	24.8	26.1	20.2	21.3	350.4	394.5	25	26	88.6	79.6
Jul	23.4	25.1	19.4	20.1	405.8	461.2	30	30	95.4	85.4
Aug	24.2	26.1	19.6	21.2	390.3	400.1	29	28	98.4	86.7
Sep	25.4	26.6	20.1	21.3	284.8	300.5	26	25	94.4	83.4
Oct	28.6	27.4	20.6	20.5	199.6	224.1	15	16	86.2	74.8
Nov	28.2	25.4	20.4	19.4	162.4	198.2	10	11	66.4	64.1
Dec	23.1	22.4	19.4	18.4	98.6	99.5	6	4	69.5	68.6

Leaf-blade variant shape	2009 May	Jun	Jul	Aug	Sep	Oct	Nov
Linear-lanceolate							
Ovate-elliptic							
Oblanceolate							
Ovate							

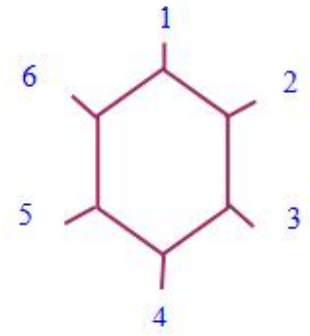

Phenophases

1. Germination and vegetative growth
2. Leaf flushing
3. Flowering
4. Flowering with fruit development
5. Fruiting
6. Seed setting

Figure 3. Phenograms for the leaf-blade variants of *Exacum bicolor* in the grasslands of Western Ghats, Kerala

Leaf maturation and expansion for all variants continued to June. The availability of adequate soil moisture by the effective south-west monsoon in this region during June facilitates leaf development. The high reserve stock of the rhizomatous part of this species might have induced leaf development in the presence of adequate soil moisture during this period with the advent of monsoon. The *Gaultheria fragrantissima* and *Ulex europaeus* species were reported [15] to have a vigorous leaf blade expansion after effective rain during south-west monsoon period in the Shola forest of high-altitude Nilgiris, the hill ranges adjoining the present study areas.

Flowering time for the four variants was during June and July. The four variants also had uniform photoperiodic responses for the other phenophases. High humidity in June and July in both study areas might influence flowering of the studied species. It has been explained that humidity as a secondary trigger may affect flowering and in combination with soil moisture induces earlier flowering in many plant species [16-18]. Similar flowering trends in New Guinea *Impatiens* with the influence of humidity were observed [19]. August-September was the period for fruit formation for all variants. Seed maturation and seed dispersal happened during October and November. The lack of seed germination in December, the month of seed setting, despite enough rainfall (above 95

mm) might be attributed to incomplete dormancy after seed dispersal. The non-matching of seed setting and seed dispersal period after proper completion of dormancy during the monsoon as well as seed deterioration by excess rain might thus account for the threatened extirpation of *E. bicolor* apart from over-exploitation. It was also reported that in Gentianaceae members, the temperature generally prevailing between 10ºC during nighttime and 30ºC during daytime is a major environmental barrier significantly reducing the seed germination process [20]. It is evident from Table I that the two study areas recorded the temperature generally between 15–31ºC throughout the year, which is considered to be an unfavourable environmental factor for seed germination of *E. bicolor*, a member of the Gentianaceae family.

CONCLUSIONS AND RECOMMENDATIONS

All four leaf-shape variants of *E. bicolor* showed no specificity in the expression of phenophases and they responded uniformly. Conservation measures adopted can therefore be non-specific. The length of dormant period of the seeds should be determined so as to find out the seed sowing time. After the completion of seed-setting period in November-December, healthy matured seeds should be collected, dried adequately and stored in a conducive environment until the completion of dormant period. Then they should be sown randomly in the soils of the plant's natural habitats to enhance its population. As enough rainfall occurs from February, moisture would not be the limiting factor in the study areas. Further, protection of the habitats of *E. bicolor* would also facilitate conservation of this species.

REFERENCES

1. U. Sreelatha, T. S. Baburaj, C. N. Kutty, P. A. Nazeem and J. Bhaskar, "Cultivation prospects of *Exacum bicolor* Roxb.–An endangered, ornamental and anti-diabetic herb", *Indian J. Nat. Prod. Resour.*, **2007**, *6*, 402-404.
2. A. Sadhale, "Studies on some endangered medicinal plants of Western Ghats of Maharashtra", Proceedings of Symposium on Rare, Endangered and Endemic Plants of the Western Ghats, **1991**, Thiruvananthapuram, India, pp.237-275.
3. V. V. Sivarajan and M. Philip, "Flora of Nilambur (Western Ghats, Kerala)", Bishen Singh Mahendra Pal Singh Publishers, Dehra Dun (India), **1996**, p.900.
4. M. R. Rao, "Flowering Plants of Travancore", Bishen Singh Mahendra Pal Singh Publishers, Dehra Dun (India), **1976**, p.484.
5. The Wealth of India, "A Dictionary of Indian Raw Materials and Industrial Products", Vol. III (Second Supplement Series), Publications and Information Directorate, New Delhi, **2009**, p.415.
6. T. V. V. S. Reddi, B. V. A. R. Naidu and S. Prasanthi, in "Herbal Remedies for Diseases" (Ed. I. Alikhan and A. Khanum), Ukay Publications, Hyderabad, **2005**, pp.67-134.
7. M. V. Jeeshna, "Evaluation of ecological variants of the endangered plant species, *Exacum bicolor* Roxb. (Gentianaceae) for effective medicinal usages and *in vitro* regeneration protocol for its conservation", *PhD Thesis*, **2011**, Bharathiar University, India.

8. J. G. Holway and R. T. Ward, "Phenology of alpine plants in northern Colorado", *Ecol.*, **1965**, *46*, 73-83.
9. R. F. Daubenmire, "Plants and Their Environment: A Text Book of Plant Ecology", 2nd Edn., John Wiley and Sons, New York, **1959**.
10. L. S. Lodhiyal, S. P. Singh and N. Lodhiyal, "Phenology, population structure and dynamics of Ringal bamboo (*Arundinaria falata*) in Nainital Hill of central Himalaya", *Trop. Ecol.*, **1998**, *39*, 109-115.
11. R. C. Sundriyal, A. P. Joshi and R. Dhasmana, "Phenology of high altitude plants at Tungnath in the Garhwal Himalaya", *Trop. Ecol.*, **1987**, *28*, 289-299.
12. S. F. Oberbauer and W. D. Billings, "Drought tolerance and water use by plants along an alpine topographic gradient", *Oecologia*, **1981**, *50*, 325-331.
13. S. Paulsamy, "Evaluation of conservation strategies for the sustainable utilization of herbaceous bioresources in the shoals of Nilgiris, the Western Ghats", Annual Progress Report, **2005**, Ministry of Environment and Forest Scheme, Government of India.
14. Report from Ground Water Department, Kannur and Wayanad, 2008-2010, in Proceedings of Directorate of Meteorological Department, Kerela State, Thiruvanandhapuram, Kerela, India, 22 Feb. **2011**, p.418.
15. K. K. Vijayakumar and S. Paulsamy, "Phenology of high altitude medicinal shrub, *Gaultheria fragrantissima* Wallich, inhabiting the shoal forests of Nilgiris, the Western Ghats", *Plant Archives*, **2010**, *10,* 435-437.
16. N. Pavon and O. Briones, "Phenological patterns of nine perennial plants in an intertropical semi-arid Mexican scrub", *J. Arid Environ.*, **2001**, *49,* 265-277.
17. D. Primack, C. Imbres, R. B. Primack, A. J. Miller-Rushing and P. D. Tredici, "Herbarium specimens demonstrate earlier flowering times in response to warming in Boston″. *Am. J. Bot.*, **2004** , *91*, 1260-1264.
18. T. A. Lee, Jr., D. L. Ketring and R. D. Powell, "Flowering and growth response of peanut plants (*Arachis hypogaea* L. var. Starr) at two levels of relative humidity", *Plant Physiol.*, **1972,** *49*, 190-193.
19. P. K. Hammer, "The New Guinea problems", *Grower Talk*, **2006**, *62*, 92.
20. R. H. Ellis, T. D. Hong and E. H. Roberts, "Handbook of Seed Technology for Genebanks", Vol. II, International Board for Plant Genetic Resources Publications, Rome, **1985**, pp.167-169.

Maejo Int. J. Sci. Technol. **2011**, *5*(03), 365-373

Maejo International Journal of Science and Technology

ISSN 1905-7873
Available online at www.mijst.mju.ac.th

Communication

Sunlight-stimulated phenylalanine ammonia-lyase (PAL) activity and anthocyanin accumulation in exocarp of 'Mahajanaka' mango

Kobkiat Saengnil [1, 2, *], Kanyarat Lueangprasert [3] and Jamnong Uthaibutra [1, 2]

[1] Department of Biology, Faculty of Science, Chiang Mai University, Chiang Mai 50200, Thailand
[2] Postharvest Technology Innovation Centre, Commission on Higher Education, Bangkok 10400, Thailand
[3] Biology Program, Faculty of Science and Technology, Kanchanaburi Rajabhat University, Kanchanaburi 71000, Thailand
* Corresponding author, e-mail: kobkiat_s@hotmail.com

Received: 7 November 2010 / Accepted: 11 November 2011 / Published: 14 November 2011

Abstract: The activity of phenylalanine ammonia-lyase (PAL) required for anthocyanin synthesis was stimulated by sunlight exposure resulting in the development of red colour in 'Mahajanaka' mango exocarp, which occurred only on the sunlight-exposed side of the fruit. The accumulation of anthocyanin was concurrent with the increase in PAL activity in the mature stage of the fruit. The exposed side of the fruit had higher PAL activity, endogenous sugar content, and anthocyanin accumulation than the unexposed side. It is concluded that sunlight increases red colour development of the mango exocarp by inducing PAL activity. Exposure to sunlight also enhances endogenous sugar accumulation in mango fruit.

Keywords: 'Mahajanaka' mango, PAL activity, anthocyanin in fruit exocarp, sunlight-induced anthocyanin synthesis, endogenous sugars

INTRODUCTION

'Mahajanaka' mango (*Mangifera indica* Linn. cv. Mahajanaka) is a hybrid cultivar between 'Nang Klang Wan' and 'Sunset' cultivars in Chiang Mai province, Thailand. The fruit is elongated and similar to 'Nang Klang Wan', with a thick exocarp and long edible portion of the thick yellowish-orange mesocarp. It is soft and has a good flavour and a thin pyrene, which makes it suitable for consuming and processing. The red colour of the exocarp is similar in intensity to

'Sunset' mango and is due to anthocyanins [1-3]. However, 'Mahajanaka' mango develops non-uniform red exocarp colouration during fruit development. This reduces the value and quality of the fruit as it is unacceptable for foreign importers and consumers in Thailand.

Light induces anthocyanin synthesis and red colour formation in plants. Sunlight increases the activity of the key enzymes for anthocyanin synthesis, especially phenylalanine ammonia-lyase (PAL), dihydroflavonol reductase (DFR), anthocyanin synthase (ANS) and UDP-glucose flavonoid 3-o-glucosyltransferase (UFGT) [4-6]. Light also induces flavonoid synthesis involving several photoreceptors such as phytochromes and the photosynthetic system [6-7]. In an experiment performed by Singh et al. [6], etiolated maize seedlings grown for six days in dark conditions were exposed to sunlight for 4 hours and transferred back to darkness. Anthocyanins were found to form in all vegetative organs with a slow increase during 4-16 hours after exposure to sunlight and a rapid increase after 16-24 hours. PAL was also found to be stimulated with two distinct peaks of activity: the first peak during 4-12 hours and the second peak during 12-24 hours after exposure. Sunlight intensity in different conditions during fruit development seems to affect anthocyanin accumulation. As reported for apple (*Malus domestica*) in China [8], the cultivars 'Starkrimson' (with red exocarp) and 'Golden Delicious' (with yellow exocarp) in a highly irradiated area had higher anthocyanin accumulation than in the same cultivars grown in a less irradiated area. In both areas, PAL activity in the red apple exocarp was also higher than in the yellow one.

Sunlight regulates anthocyanin formation in vegetative tissues and organs (root, mesocotyl, leaf and coleoptile). More anthocyanin accumulates in sun-exposed exocarp than in shaded one [7-9]. In 'Elstar', 'Jonagold', 'Elshof' and 'Red Elstar' apples, the levels of cyanidin 3-galactoside (anthocyanin) and quercetin 3-glycoside (flavonol) in the sun-exposed exocarp of individual fruit were much higher than in the shaded side [10]. Anthocyanin levels were highest in fruits borne on the top of the tree and the outer tree parts, whereas the lowest levels of anthocyanin were found in fruits from shaded parts of the tree [7]. 'Delicious' apple fruits were covered with one-, two-, or three-layered paper bags to inhibit anthocyanin accumulation in the exocarp. After the bags were opened and exposed to light for three days, the fruit treated with the three-layered bag had the highest anthocyanin accumulation [9]. In 'Early Black' cranberry fruits, natural light conditions increased total anthocyanin levels by 75.3 % and 87.2 % after 24 and 48 hours respectively of water immersion [11].

Light indirectly increases anthocyanin accumulation by increasing endogenous sugars, which induce the gene expression of key enzymes in anthocyanin biosynthetic pathways, especially PAL enzyme. In 'Comet' red radish hypocotyls during cultivation in light (~50 $\mu E/m^2s$), total sugars (glucose, fructose and sucrose) increased in 21 days after sowing, and the sugar accumulation enhanced anthocyanin production in the hypocotyl [12]. In particular, sucrose-induced anthocyanin production occurred via increased gene expression of chalcone synthase (*CHS*) and anthocyanidin synthase (*ANS*) in 'Comet' red radish hypocotyls with three times higher ratio of *CHS:ANS* expression from planting until six days after [13]. In the 'Incicle' white radish, the two anthocyanin-specific genes (*PAL* and *CHS*) responded to sucrose, and other genes such as chalcone isomerase (*CHI*), flavanone 3-hydroxylase (*F3H*), *DFR*, and *ANS* were weakly expressed, causing less anthocyanin accumulation [13]. When Lisianthus (*Eustoma grandiflorum* cv. Royal Purple), a potted

plant, was cultured in high-intensity light (15,000 lux), the petals had a higher accumulation of soluble sugars than that in a low light intensity (1,000 lux), and the high light intensity condition also induced the expression of *CHS*, *CHI* and *DFR* in anthocyanin synthesis [14]. In grape berries (*Vitis vinifera* cv. Shiraz) grown in sunlight, the total soluble solids of the fresh tissue increased during 8-16 weeks after flowering, along with an increase in anthocyanin accumulation in the berry exocarp after 10 weeks. Expression of seven anthocyanin biosynthesis genes (*PAL*, *CHS*, *CHI*, *F3H*, *DFR*, leucoanthocyanindin dioxygenase (*LDOX*) and *UFGT*) were enhanced during fruit development, especially *UFGT*, which was expressed only 10-16 weeks after flowering and coincided with anthocyanin accumulation in the berry exocarp [15]. Sunlight also promoted the synthesis of endogenous sugars, which induced the gene expression for increasing anthocyanin synthesis in *V. vinifera* cell suspension [16] and 'Comet' radish hypocotyl [12].

The two important factors affecting anthocyanin synthesis and accumulation are light and sugars. Fructose and sucrose were found to promote red colour development in the exocarp of 'Mahajanaka' mango [2], while the involvement of sunlight in red colour development has not been investigated. The objective of this study is to investigate the effects of sunlight on PAL enzyme activity, sugar accumulation, and anthocyanin accumulation during the development of 'Mahajanaka' mango exocarp.

MATERIALS AND METHODS

Plant Stock

Forty 7-year-old 'Mahajanaka' mango trees from an orchard in Chiang Mai province were used in this study. The experiment started in January and continued until the end of May 2010. Inflorescences were tagged to record the age of fruits from the day after full bloom (DAFB). After that, fruits at 70 DAFB (approximately 2 weeks prior to the beginning of red colour development in the fruit's exocarp as reported by Boonkan [1]) which hung on the outer part of the canopy were sampled at 7-day intervals until fruit maturity at 126 DAFB. The exocarp of each fruit was divided into 2 sides: the sunlight-facing side and the shaded side; the former was exposed to sunlight in the morning until midday. A total of 360 fruits were used in this experiment. The freshly harvested fruits were transported within 1 hour to Chiang Mai University laboratory for analysis. The experiment followed a completely randomised design, with each treatment being applied to 40 randomly selected trees.

Methods

Extraction and analysis of PAL activity from the exocarp (1-mm thick) was performed by a method modified of those of Faragher and Chalmer [17] and Arakawa et al. [18]. The absorbance was compared with that of standard cinnamic acid and presented as nmole/mg protein·hour. Protein quantity was measured according to the method of Lowry et al. [19] and expressed as mg/g fresh weight.

Extraction and analysis of reducing sugars and total sugar content were determined by the modified Somogyi and Nelson method [20-21] The absorbance was measured at 540 nm and

compared with standard D-glucose. Determination of total anthocyanin content was conducted according to Ranganna [22]. The absorbance of the extract was measured at 535 nm.

The exocarp colours were measured with a colourimeter. The chromaticity was measured as a* value, which measures the greenness and redness on a scale of -60 to +60. A minus a* value means a green colour and a positive value, a red colour.

The statistical packages for the social science (SPSS) software for Windows was used in this experiment for analysis of variance (ANOVA) and least-significant difference (LSD) at 95% confidence level of each variable value under a completely randomised design (CRD).

RESULTS

PAL activity on the exposed side of mango fruit exocarp increased during two periods in fruit development at 91 and 119 DAFB, and was significantly ($p = 0.05$) higher between 84-126 DAFB than the unexposed side (Figure 1). Similar results were found on the unexposed side, where PAL activity also showed two peaks, though not coinciding with those from the exposed side, at 77 and 126 DAFB, and was lower than that on the exposed side (Figure 1).

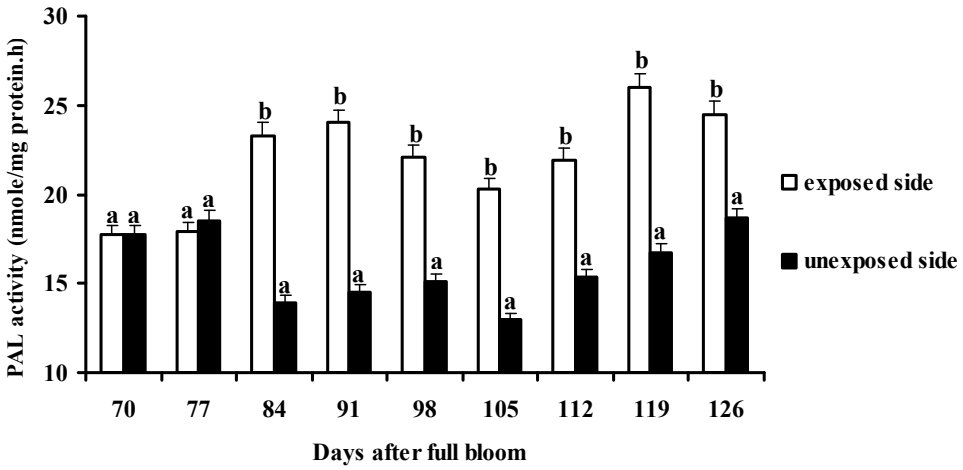

Figure 1. Effect of sunlight on PAL activity of 'Mahajanaka' mango fruit exocarp between 70-126 DAFB. Bars with different letters are significantly different ($p \leq 0.05$). Vertical bars indicate ±SE.

The reducing sugar content of the exocarp increased to the highest level at 91 DAFB and then decreased slightly and increased again at 126 DAFB (Figure 2). The exposed side had a higher reducing sugar content compared with the unexposed side throughout fruit development (significant at $p = 0.05$).

The total sugar content was relatively constant during 77-91 DAFB; after that it tended to increase. The highest content was detected at 112 DAFB for the exposed side. Total sugar content of the unexposed side had the same trend throughout fruit development (Figure 3) but was found to be lower than that of the exposed side (significant at $p = 0.05$).

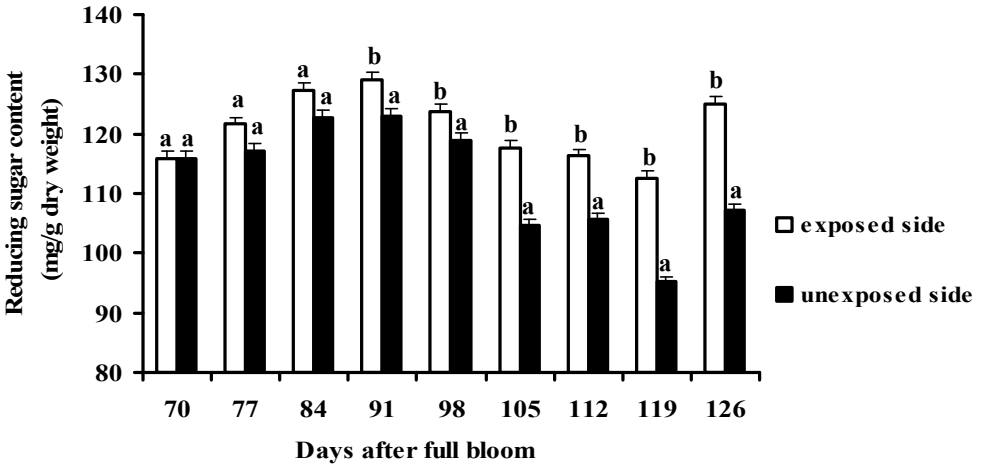

Figure 2. Effect of sunlight on reducing sugar content of 'Mahajanaka' mango fruit exocarp between 70-126 DAFB. Bars with different letters are significantly different ($p \leq 0.05$). Vertical bars indicate ±SE.

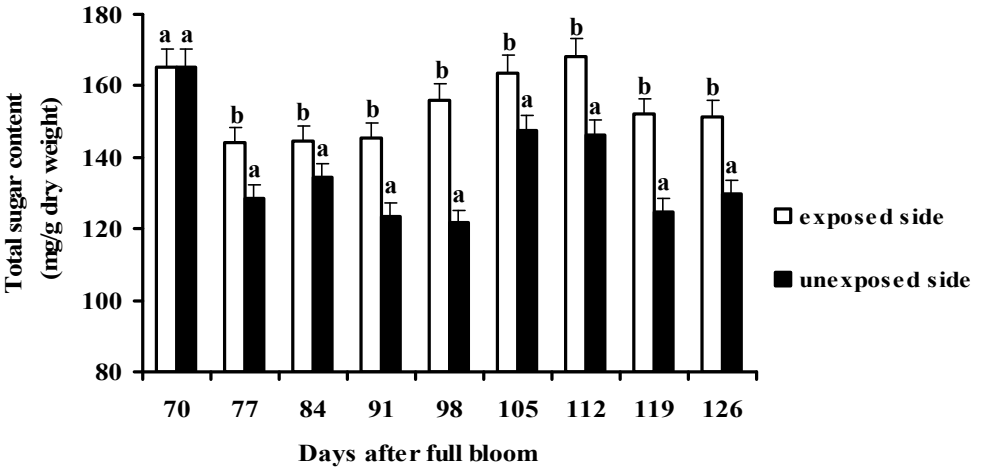

Figure 3. Effect of sunlight on total sugar content of 'Mahajanaka' mango fruit exocarp between 70-126 DAFB. Bars with different letters are significantly different ($p \leq 0.05$). Vertical bars indicate ±SE.

The total anthocyanin content of the exocarp significantly increased on the exposed side as compared with the unexposed side (Figure 4). Anthocyanin content of the exposed side started to increase at 84 DAFB and rose to its highest level at 112 DAFB, which was significantly higher than that of the unexposed side. The total anthocyanin content of the unexposed side remained relatively constant between 70-91 DAFB and then gradually decreased.

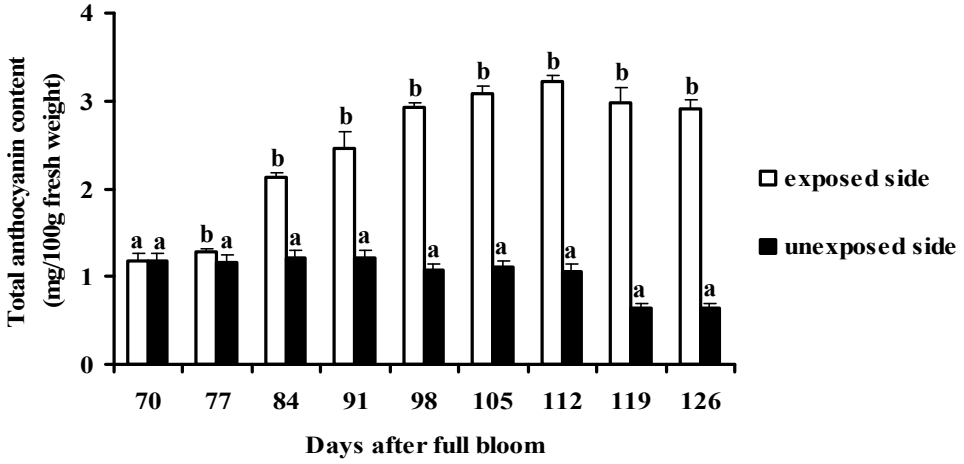

Figure 4. Effect of sunlight on total anthocyanin content of 'Mahajanaka' mango fruit exocarp between 70-126 DAFB. Bars with different letters are significantly different ($p \leq 0.05$). Vertical bars indicate ±SE.

The change of a* value of the exocarp was investigated during fruit development (Figure 5). Red colouration of the exposed side of the fruit was first observed at 84 DAFB and the highest a* value was observed at 112 DAFB, indicating maximum red colour development. The unexposed side had a minus a* value indicating a green exocarp. The a* values of all treatments were significantly different throughout the fruit development period.

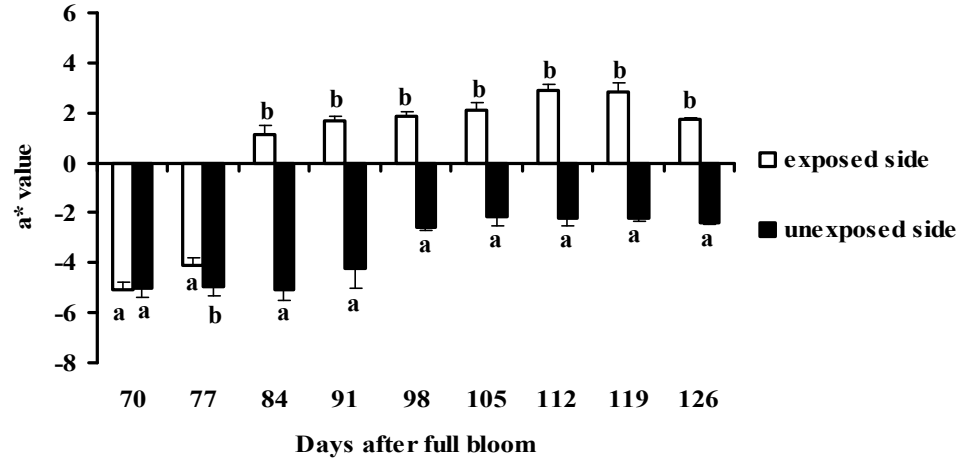

Figure 5. Effect of sunlight on a* values of 'Mahajanaka' mango fruit exocarp between 70-126 DAFB. Bars with different letters are significantly different ($p \leq 0.05$). Vertical bars indicate ±SE.

DISCUSSION

An accumulation of anthocyanin in the sunlight-exposed side of 'Mahajanaka' mango fruit exocarp was concurrent with an increase in PAL activity in the mature stage at 105-126 DAFB but not at 70-98 DAFB (Figures 1 and 4). It is possible that the first peak of PAL activity in the immature fruits is necessary for phenolic metabolism that is directed to the synthesis of simple phenols and flavonoids during fruit development. However, the relationship between PAL activity and anthocyanin accumulation varies according to the stage of fruit development, which is similar to what occurs in apple exocarp [5, 8].

Similar to our results, Awad et al. [7] found that increasing anthocyanin synthesis and development of red colour in apple exocarp depend on sunlight. This is true in apples receiving sunlight from the top of the tree, which is exposed to higher light intensity. These fruits tend to have more anthocyanin synthesis than those at other positions. Visible light (400-700 nm) and also UV-B (312 nm) have the most important role in promoting red exocarp colour development in apples [23]. A highly exposed place increases the efficiency of anthocyanin synthesis and stimulates higher anthocyanin accumulation compared to a shaded area [8]. Other studies have shown that the photosynthesis pathway stimulates the synthesis of precursors for anthocyanin production [23-24].

In our experiment, sunlight also stimulates an increase of reducing sugar and total sugar content largely on the exposed side of the exocarp, where the change in total sugar content closely follows the change in anthocyanin level except at 70-77 DAFB. Total sugar content also parallels PAL activity but only in mature fruits. Transport of sugars, especially sucrose from the source (leaf) to the sink (fruit), is stimulated by sunlight. Sucrose is translocated to fruit via phloem causing an increase in endogenous sugars [25]. This is consistent with the report of Guan and Janes [26], who found that the amount of sugar in tomato fruit (*Lycopersicon esculentum*) accumulated in light is higher than in the dark. Light stimulates uptake, metabolism and storage of sugars, especially sucrose, which is a major sugar translocated into the tomato fruit. Light-grown fruits have higher carbohydrate content than dark-grown fruits, as well as higher ADP glucose pyrophosphorylase activity, which is correlated with a high starch level in tomato fruit [27].

Endogenous sugars induce gene expression of PAL enzyme, the key enzyme in the anthocyanin synthesis pathway. According to Vitrac et al. [16], the result of *Vitis vinifera* cell suspension cultures showed that sucrose promotes anthocyanin production and recognises the general signal transduction such as Ca^{+}, calmodulin and protein kinase/phosphatases for inducing anthocyanin biosynthesis. In red radish hypocotyls treated with exogenous sucrose, the expression levels of *PAL*, *CHS*, *CHI*, *F3H*, *DFR* and *ANS* for anthocyanin biosynthesis were enhanced [13]. In corn leaves (cv. Suweon 19), sucrose, which is important for controlling *CHS*, *CHI*, *F3H*, *DFR* and *ANS*, was shown to produce the greatest stimulation of anthocyanin formation [28].

CONCLUSIONS

Sunlight induces red colour development in mango fruit exocarp by promoting anthocyanin synthesis via increasing PAL activity. Sunlight also increases endogenous sugars (reducing sugars and total sugars) during mango fruit development.

ACKNOWLEDGEMENTS

We would like to thank Mr. J. F. Maxwell of the Biology Department, Chiang Mai University for reviewing and improving the manuscript. This work is supported by a grant from the Postharvest Technology Innovation Centre, Commission on Higher Education, Bangkok. The Department of Biology, Chiang Mai University is acknowledged for providing the facilities, chemicals and equipment needed in this work.

REFERENCES

1. S. Boonkan, "Physiological and chemical changes during growth and development of 'Mahajanaka' mango fruit", *MS Thesis*, **2002**, Chiang Mai University, Thailand.
2. K. Lueangprasert, J. Uthaibutra, K. Saengnil and O. Arakawa, "The effects of sugar application on the concentrations of anthocyanin and flavonol of 'Mahajanaka' mango (*Mangifera indica* Linn. cv. Mahajanaka) fruit", *Chiang Mai J. Sci.*, **2010**, *37*, 355-362.
3. G. Mazza and E. Miniati, "Anthocyanins in Fruits, Vegetables, and Grains", CRC Press, Boca Raton, **1993**.
4. J. E. Lancaster and D. K. Dougall, "Regulation of skin color in apples", *Crit. Rev. Plant Sci.*, **1992**, *10*, 487-502.
5. Z. G. Ju, Y. B. Yaun, C. L. Liou and S. H. Xin, "Relationships among phenylalanine ammonia-lyase activity, simple phenol concentrations and anthocyanin accumulation in apple", *Sci. Hortic.*, **1995**, *61*, 215-226.
6. A. Singh, M. T. Selvi and R. Sharma, "Sunlight-induced anthocyanin pigmentation in maize vegetative tissues", *J. Exp. Bot.*, **1999**, *50*, 1619-1625.
7. M. A. Awad, P. S. Wagenmakers and A. de Jager, "Effects of light on flavonoid and chlorogenic acid levels in the skin of 'Jonagold' apples", *Sci. Hortic.*, **2001**, *88*, 289-298.
8. X. J. Li, J. H. Hou, G. L. Zhang, R. S. Liu, Y. G. Yang, Y. X. Hu and J. X. Lin, "Comparison of anthocyanin accumulation and morpho-anatomical features in apple skin during color formation at two habitats", *Sci. Hortic.*, **2004**, *99*, 41-53.
9. Z. Ju, "Fruit bagging, a useful method for studying anthocyanin synthesis and gene expression in apples", *Sci. Hortic.*, **1998**, *77*, 155-164.
10. M. A. Awad, A. de Jager and L. M. van Westing, "Flavonoid and chlorogenic acid levels in apple fruit: characterisation of variation", *Sci. Hortic.*, **2000**, *83*, 249-263.
11. Y. Zhou and B. R. Singh, "Effect of light on anthocyanin levels in submerged, harvested cranberry fruit", *J. Biomed. Biotechnol.*, **2004**, *5*, 259-263.
12. M. Hara, K. Oki, K. Hoshino and T. Kuboi, "Enhancement of anthocyanin biosynthesis by sugar in radish (*Raphanus sativus*) hypocotyl", *Plant Sci.*, **2003**, *164*, 259-265.
13. M. Hara, K. Oki, K. Hoshino and T. Kuboi, "Effects of sucrose on anthocyanin production in hypocotyl of two radish (*Raphanus sativus*) varieties", *Plant Biotechnol.*, **2004**, *21*, 401-405.
14. S. Kawabata, Y. Kusuhara, Y. Li and R. Sakiyama, "The regulation of anthocyanin biosynthesis in *Eustoma grandiflorum* under low light conditions", *J. Japan. Soc. Hort. Sci.*, **1999**, *68*, 519-526.

15. P. K. Boss, C. Devies and S. P. Robinson, "Analysis of the expression of anthocyanin pathway genes in developing *Vitis vinifera* L. cv Shiraz grape berries and the implications for pathway regulation", *Plant Physiol.*, **1996**, *111*, 1059-1066.
16. X. Vitrac, F. Larronde, S. Krisa, A. Decendit, G. Deffieux and J. M. Merillon, "Sugar sensing and Ca^{+2}-calmodulin requirement in *Vitis vinifera* cells producing anthocyanins", *Phytochem.*, **2000**, *53*, 659-665.
17. J. D. Faragher and D. J. Chalmers, "Regulation of anthocyanin synthesis in apple skin. III. Involvement of phenylalanine ammonia-lyase", *Aust. J. Plant Physiol.*, **1977**, *4*, 133-141.
18. O. Arakawa, Y. Hori and R. Ogata, "Characteristics of colour development and relationship between anthocyanin synthesis and phenylalanine ammonia-lyase activity in 'Starking Delicious', 'Fuji' and 'Mutsu' apple fruits", *J. Japan. Soc. Hort. Sci.*, **1986**, *54*, 424-430.
19. O. H. Lowry, N. J. Rosebrough, A. L. Farr and R. J. Randall, "Protein measurement with the folin phenol reagent", *J. Biol. Chem.*, **1951**, *193*, 265-275.
20. M. Somogyi, "Notes on sugar determination", *J. Biol. Chem.*, **1952**, *195*, 19-23.
21. N. J. Nelson, "A photometric adaptation of the Somogyi method for the determination of glucose", *J. Biol. Chem.*, **1944**, *153*, 375-380.
22. S. Ranganna, "Plant pigments", in "Manual of Analysis of Fruit and Vegetable Products" (Ed. S. Ranganna), Tata McGraw-Hill Publishing Co., New Delhi, **1977**, pp. 72-93.
23. O. Arakawa, Y. Hori and R. Ogata, "Relative effectiveness and interaction of ultraviolet-B, red and blue light in anthocyanin synthesis of apple fruit", *Physiol. Plant.*, **1985**, *64*, 323-327.
24. O. Arakawa, "Photoregulation of anthocyanin synthesis in apple fruit under UV-B and red light", *Plant Cell Physiol.*, **1988**, *29*, 1385-1389.
25. W. G. Hopkins and N. P. A. Hüner, "Introduction to Plant Physiology" 4th Edn., John Wiley and Sons, Danvers, **2009**.
26. H. P. Guan and H. W. Janes, "Light regulation of sink metabolism in tomato fruit. I. growth and sugar accumulation", *Plant Physiol.*, **1991**, *96*, 916-921.
27. H. P. Guan and H. W. Janes, "Light regulation of sink metabolism in tomato fruit. II. carbohydrate metabolizing enzymes", *Plant Physiol.*, **1991**, *96*, 922-927.
28. J. H. Kim, B. H. Lee, S. H. Kim, K. H. Oh and K. Y. Cho, "Responses to environmental and chemical signals for anthocyanin biosynthesis in non-chlorophyllous corn (*Zea mays* L.) leaf", *J. Plant Biol.*, **2006**, 49, 16-25.

Maejo Int. J. Sci. Technol. **2011**, *5*(03), 374-389

Maejo International Journal of Science and Technology

ISSN 1905-7873
Available online at www.mijst.mju.ac.th

Full Paper

Response surface optimisation for acetone-butanol-ethanol production from cassava starch by co-culture of *Clostridium butylicum* and *Bacillus subtilis*

Hanh Thi My Tran[1], Benjamas Cheirsilp[1,*], Kamontam Umsakul[2] and Thawien Bourtoom[3]

[1] Department of Industrial Biotechnology, Faculty of Agro-Industry, Prince of Songkla University, Hat–Yai, 90112, Thailand
[2] Department of Microbiology, Faculty of Science, Prince of Songkla University, Hat–Yai, 90112, Thailand
[3] Department of Material Product Technology, Faculty of Agro–Industry, Prince of Songkla University, Hat–Yai, 90112, Thailand

* Corresponding author, e-mail: benjamas.che@psu.ac.th ; Tel: +66–74–28–6374 ; Fax: +66–74–44–6727

Received: 15 November 2010 / Accepted: 17 November 2011 / Published: 22 November 2011

Abstract: Acetone-butanol-ethanol (ABE) production from cassava starch was enhanced by a syntrophic co-culture of *Clostridium butylicum* TISTR 1032 and high amylase producing *Bacillus subtilis* WD 161 without anaerobic pretreatment. The production of amylase and ABE using this co-culture were respectively 16 and 6 times higher than those using the pure culture of *C. butylicum* TISTR 1032. The effect of the medium components on the performance of the co-culture was investigated using response surface methodology (RSM). Among the investigated components, cassava starch and ammonium nitrate contributed a significant effect on the production of amylase and ABE, while yeast extract had less effect. Based on the optimum strategy using RSM, the ABE production by the co-culture was improved 2.2-fold compared with that obtained from the initial condition and with a minimum requirement of nitrogen source.

Keywords: acetone–butanol–ethanol fermentation, *Bacillus subtilis*, cassava starch, *Clostridium butylicum*, co-culture

INTRODUCTION

Energy derived from renewable substrates possesses a number of advantages over fossil-derived energy. These include being renewable, more environmentally friendly and more profitable.

In addition, the production of bioenergy provides new markets for the agricultural sector and turns agricultural wastes into more valuable products. Thus, it is worthwhile replacing fossil fuels by bioenergy carriers [1]. In addition to ethanol and biodiesel which are currently commonly used, butanol is one of a number of promising energy substances for future use. Compared to ethanol, butanol is more advantageous as it has a higher energy content, is less sensitive to temperature, and requires no modification for use in combustion engines [2]. Butanol is biologically produced along with small amounts of acetone and ethanol by *Clostridium* spp. from renewable materials under strictly anaerobic conditions. This process is called the acetone-butanol-ethanol (ABE) fermentation process. However, the bio-butanol has not been marketed due to its high production cost. The raw material accounts for about 63% of the cost of the fermentation product [3].

The use of starch as the substrate is probably one of the most economically feasible choices due to the low cost and the availability of starch. The ABE production from starch by *Clostridium* actually includes three processes. These are starch hydrolysis by amylolytic enzymes to produce glucose for cell growth, acid (acetic and butyric) production during the acidogenesis phase, and the conversion of these acids into ABE products during the solventogenesis phase. However, starch hydrolysis by *Clostridium* is often less effective due to its low amylase activity. The pre-hydrolysis of starch by commercial enzymes or by acids at high temperature each has its own drawback [1]. Since amylolytic enzymes were determined as a key factor in ABE production from starch, a co-culture of *Clostridium* and another organism in a way that naturally enhances amylolytic activity suggests a possibility of making starch hydrolysis more complete, providing sugar for clostridial growth, and consequently enhancing ABE production. In accord with this concept, a co-culture of *Clostridium* and an amylase producing aerobic *Bacillus* would be more profitable. This is because the *Bacillus* will not only assist the *Clostridium* in substrate hydrolysis, but will also maintain an anaerobic condition by consuming any available oxygen in the culture [4-5]. Thus, there will be less need of pre-hydrolysis of starch and anaerobic pretreatment by addition of a reducing agent and N_2 flushing of the fermentation medium. Thus, this syntrophic co-culture of anaerobic *Clostridium* and aerobic *Bacillus* might also reduce the costs of the biofuel production from starch.

The medium components such as starch concentration, nitrogen source and its content have been reported to have a great influence on ABE production from starch [6]. Although the effects of starch concentration, C/N ratio and ratio of organic/inorganic nitrogen sources on ABE production by a co-culture of *Clostridium* and *Bacillus* have been reported [7], the interactions between the variables were not considered. Response surface methodology (RSM), where the combined effects of all variables are determined through mathematical and statistical inference from experimental design to result analysis, has been applied in systems employing other cultures [8-10]. Only one work [11] employed RSM for the optimisation of ABE production, in which a pure culture of *C. acetobutylicum* P262 was used on sweet potato.

The aim of this study is to use RSM to determine the effect of some of the medium components as well as their interactions on amylase activity and ABE production using a syntrophic co-culture of *Clostridium butylicum* TISTR 1032 and amylase producing *Bacillus subtilis* WD 161 on cassava starch. It is known that starch concentration and a combination of organic-inorganic nitrogen sources are important for the enhancement of amylase activity and ABE production. In this study, yeast extract and ammonium nitrate were used as organic and inorganic nitrogen sources respectively. Yeast extract is well known for providing various amino acids, vitamins, minerals and

growth factors that promote growth of microorganisms. Ammonium nitrate supports growth and amylase production of *Bacillus* under an anaerobic condition [12]. Thus, the effects of these three factors, namely cassava starch, yeast extract and ammonium nitrate, as well as their optimum levels, were determined using RSM.

MATERIALS AND METHODS

Chemicals and Microorganisms

All chemicals used were of analytical grade and purchased from Fluka Chemical Corporation. *Clostridium butylicum* TISTR 1032 was purchased from Thailand Institute of Scientific and Technological Research (TISTR). The stock culture was maintained in the form of a spore suspension in 25% glycerol and frozen at –20°C. *Bacillus subtilis* WD 161 was a generous gift from Assoc. Prof. Dr. Poonsuk Prasertsan of the Environmental Technology Laboratory, Department of Industrial Biotechnology, Faculty of Agro–Industry, Prince of Songkla University). The stock culture was maintained at 4°C on a nutrient agar slant and subcultured monthly

Inoculum Preparation

C. butylicum TISTR 1032 was anaerobically pre-cultured in a reinforced Clostridia medium (RCM, Oxoid) (1 L RCM contains 10 g meat extract, 5 g peptone, 3 g yeast extract, 5 g glucose, 1 g soluble starch, 5 g sodium chloride, 3 g sodium acetate, and 0.5 g L-cysteine). It was then incubated under static condition at 37°C for 18–24 h. *B. subtilis* WD 161 was aerobically pre-cultured in a nutrient broth (NB) (HiMedia) under shaking condition at 200 rpm and 37°C for 12–18 h.

Fermentation Conditions

For ABE production, B medium was used (1L B medium, pH 6.5, contains 20 g cassava starch, 5 g yeast extract, 2 g NH_4NO_3, 0.5 g KH_2PO_4, 0.3 g $MgSO_4{\cdot}7H_2O$, 0.02 g $MnSO_4{\cdot}7H_2O$, 0.02 g $FeSO_4{\cdot}7H_2O$, and 0.02 g NaCl) [13]. Where noted, the concentrations of cassava starch, yeast extract and ammonium nitrate in B medium were varied to investigate their effects on ABE production. The cultures were established in 120-mL butyl-rubber-sealed serum bottles without anaerobic pretreatment which is normally done by addition of a reducing agent and flushing with N_2 gas over the medium. The working volume of all cultures was 100 mL and the fermentation process was carried out at 37°C. The co-culture was prepared by dispersing 5 mL of inoculum of each organism (6.1×10^4 CFU/mL for *C. butylicum* TISTR 1032 and 3.8×10^7 CFU/mL for *B. subtilis* WD 161) grown as previously described. For comparison purpose, the pure culture was prepared by inoculating 5 mL of inoculum of *C. butylicum* TISTR 1032. All the experiments were carried out at least in duplicate.

Optimisation of Medium Components using RSM

The effect of three variables, viz. cassava starch concentration (x_1), yeast extract concentration (x_2) and ammonium nitrate concentration (x_3), on acetone–butanol–ethanol concentration (ABE) (Y_1), butanol concentration (butanol) (Y_2) and amylase activity (amylase) (Y_3)

were investigated at three levels (low: –1; medium: 0; and high: +1). Box–Behnken design was employed for the study of interactions between the three variables [14]. Response surface plots for the models were done using the Statistica for Windows version 5.0 to plot the functions of two variables while keeping the other variable at a constant value.

Analytical Methods

Cell growth was determined by measurement of optical density at 660 nm (OD_{660}) using a spectrophotometer (Libra S22, England). During the fermentation period (72 h), a 3.0- ml sample was taken every 12 h and centrifuged at 8000 rpm and 4°C for 25 min. The supernatant was used for determination of ABE, organic acid and residual reducing sugar concentrations and amylase activity. ABE and organic acids were determined using a gas chromatograph (Hewlett Packard) equipped with a glass column (HP–INNOWax polyethylene glycol) and a flame ionisation detector with helium as the carrier gas. The operating conditions were as follows–inlet temperature: 220°C; oven temperature: initial 50°C, ramped up to 115°C at 5°C/min; detector temperature: 270°C [15]. The reducing sugars were estimated by the dinitrosalicylic acid (DNS) method [16]. Briefly, the sample solution (1 mL) was added to DNS solution (3 mL). The absorbance of the solution was measured with a spectrophotometer at 550 nm. The reducing sugars concentration was calculated using a glucose standard calibration curve. Amylase activity was determined by the starch hydrolysis method [17]. The reaction mixture consisted of 1% soluble starch (1.25 mL), 0.2M acetate buffer (pH 5.0) (0.5 mL), and tested sample (0.25 mL). After 10 min of incubation at 50°C, the reaction was stopped by boiling at 100°C for 10 min. The control was carried out in the same manner using a sample pre-inactivated by boiling for 15 min. The liberated reducing sugars were estimated by the DNS method as mentioned above. One unit (U) of amylase is defined as the amount of enzyme that releases one μmole of glucose equivalent per min under the assay condition.

RESULTS AND DISCUSSION

Syntrophic Co-culture of *C. butylicum* TISTR 1032 and *B. subtilis* WD 161 for ABE Production

The cultivation of the co-culture in this study was performed without anaerobic pretreatment as previously reported [7]. The co-culture of *C. butylicum* TISTR 1032 and high amylase producing *B. subtilis* WD 161 was established for ABE production from cassava starch compared to the pure culture of *Clostridium* itself under condition without anaerobic pretreatment (Figure 1). The medium was composed of 20 g/L cassava starch as carbon source, and 5 g/L yeast extract and 2 g/L ammonium nitrate as organic and inorganic nitrogen sources respectively. As illustrated in Figure 1A, the pure culture of *C. butylicum* TISTR 1032 produced low amounts of acids and ABE from cassava starch since it showed very low amylase activity (1.85 U/mL) and could not utilise cassava starch effectively. On the other hand, the amylase activity produced by the co-culture of *C. butylicum* TISTR 1032 and *B. subtilis* WD 161 increased 16-fold or up to 30.5 U/mL (Figure 1B). Consequently, the ABE production by the co-culture was enhanced 6-fold or up to 4.01 g/L compared to that of the pure culture of *C. butylicum* TISTR 1032. The high amylase activity in

Bacillus apparently converts starch to available sugar rapidly, which stimulates the metabolism of *Clostridium* to grow and thus enhances both the ABE production and its rate.

As it has been proved in the previous study [7] that the products from the pure culture of *B. subtilis* WD 161 without anaerobic pretreatment were only ethanol and acetic acid at very low concentrations (<0.2 g/L), it is assumed that the total acids and solvents detected in the product obtained with the co-culture result mostly from the activity of *C. butylicum* TISTR 1032.

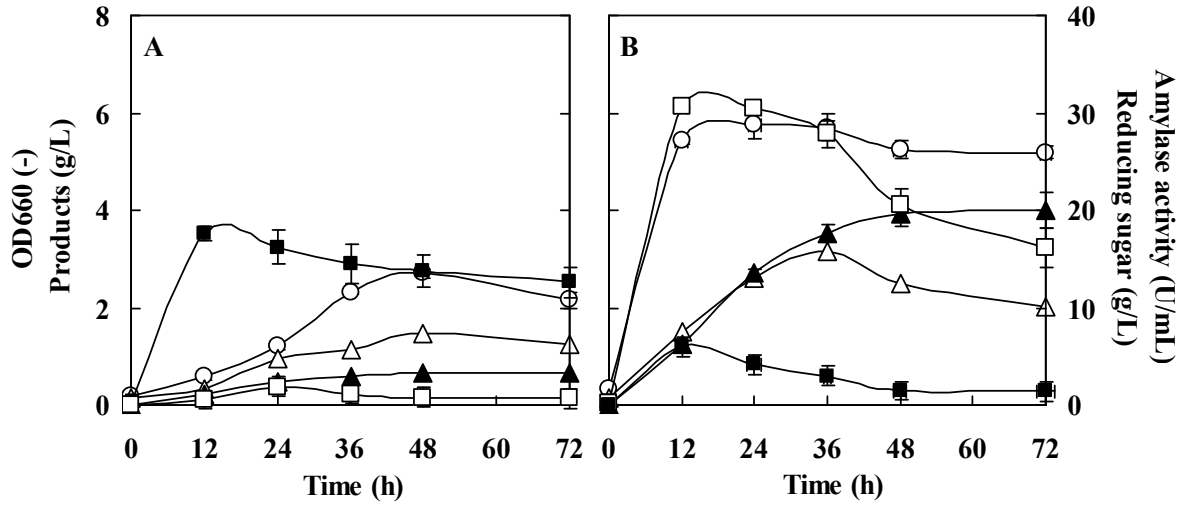

Figure 1. Growth and metabolic activity of pure culture of *C. butylicum* TISTR 1032 (A) and co-culture of *C. butylicum* TISTR 1032 and *B. subtilis* WD 161 (B) under initial condition (20 g/L cassava starch, 5 g/L yeast extract and 2 g/L ammonium nitrate). Legend: OD_{660} - open circle; amylase activity - open square; reducing sugars - filled square; acids (sum of acetic and butyric acids) - open triangle; ABE - filled triangle.

Response Surface Methodology for Optimising Co-culture of *C. butylicum* TISTR 1032 and *B. subtilis* WD 161

The syntrophic co-culture of *C. butylicum* TISTR 1032 and *B. subtilis* WD 161 was optimised using RSM. The effects of three variables, i.e. cassava starch concentration (x_1), yeast extract concentration (x_2) and ammonium nitrate concentration (x_3), were investigated. The complete design consisted of a total of 15 trials which contained three replications at the central point for estimating the purely experimental uncertainty variance. The responses observed were ABE concentration (ABE) (Y_1), butanol concentration (butanol) (Y_2) and amylase activity (amylase) (Y_3). The experimental design and respective experimental results are given in Table 1. The regression coefficients (β) and analysis of variances are shown in Table 2.

The response surface analysis was based on multiple linear regressions taking into account the main, quadratic and interaction effects in accordance with the following equation**:**

$$Y = \beta_o + \sum \beta_i x_i + \sum \beta_{ii} x^2_i + \sum \beta_{ij} x_i x_j \quad (1)$$

where Y is the predicted response, x_i and x_j are input variables which influence the response variable Y, β_o is the offset term, β_i is the ith linear coefficient, β_{ii} is the ith quadratic coefficient, and β_{ij} is the ijth interaction coefficient.

The polynomial equations for ABE (Y_1), butanol (Y_2) and amylase (Y_3) are listed as follows:

$Y_1 = -6.6998 + 0.6820x_1 - 0.0404x_2 + 0.2652x_3 - 0.0078x_1^2 + 0.0011x_2^2 - 0.0086x_3^2 + 0.0018x_1x_2 - 0.0011x_1x_3 - 0.0020x_2x_3$

$Y_2 = -4.2271 + 0.4091x_1 + 0.0614x_2 + 0.2360x_3 - 0.0049x_1^2 - 0.0027\,x_2^2 - 0.0137x_3^2 + 0.0006x_1x_2 + 0.0003x_1x_3 + 0.0008x_2x_3$

$Y_3 = -89.0804 + 6.0833x_1 - 0.7859x_2 + 5.3586x_3 - 0.0784x_1^2 + 0.0247x_2^2 - 0.1536x_3^2 + 0.0541x_1x_2 - 0.0254x_1x_3 - 0.1524x_2x_3$

Table 1. Experimental data for the effects of three variables (cassava starch concentration, yeast extract concentration and ammonium nitrate concentration) with three-level response surface analysis

Trial	Independent variable			Dependent variable		
	Cassava starch (g/L)	Yeast extract (g/L)	Ammonium nitrate (g/L)	ABE (g/L)	Butanol (g/L)	Amylase (U/mL)
	x_1	x_2	x_3	Y_1	Y_2	Y_3
1	1(60.0)	1(20.0)	0(7.0)	4.37	2.50	46.0
2	1(60.0)	-1(5.0)	0(7.0)	5.49	2.17	39.0
3	-1(20.0)	1(20.0)	0(7.0)	3.15	2.89	20.1
4	-1(20.0)	-1(5.0)	0(7.0)	3.20	2.50	25.6
5	1(60.0)	0(12.5)	1(12.0)	3.50	2.00	33.4
6	1(60.0)	0(12.5)	-1(2.0)	2.80	1.80	27.0
7	-1(20.0)	0(12.5)	1(12.0)	2.70	1.75	26.4
8	-1(20.0)	0(12.5)	-1(2.0)	1.92	1.81	15.0
9	0(40.0)	1(20.0)	1(12.0)	9.37	6.12	75.0
10	0(40.0)	1(20.0)	-1(2.0)	8.10	5.60	64.6
11	0(40.0)	-1(5.0)	1(12.0)	8.90	5.80	67.2
12	0(40.0)	-1(5.0)	-1(2.0)	6.70	5.00	36.0
13	0(40.0)	0(12.5)	0(7.0)	9.00	6.00	69.0
14	0(40.0)	0(12.5)	0(7.0)	9.05	5.90	67.3
15	0(40.0)	0(12.5)	0(7.0)	9.13	6.00	66.7

Note: Values in parentheses are uncoded independent variables.

x_1 = cassava starch concentration, x_2 = yeast extract concentration, x_3 = ammonium nitrate concentration, Y_1 = ABE concentration, Y_2 = butanol concentration, Y_3 = amylase activity

Table 2. Regression of coefficients and analysis of variance of the second-order polynomial for response variables

Coefficient	ABE (g/L) Y_1	Butanol (g/L) Y_2	Amylase (U/mL) Y_3
β_o	- 6.6998*	- 4.2271*	- 89.0804*
Linear			
x_1	0.6820*	0.4091*	6.0833*
x_2	- 0.0404	0.0614	- 0.7859
x_3	0.2652	0.2360	5.3586*
Interaction			
x_1x_2	0.0018	0.0006	0.0541*
x_1x_3	- 0.0011	0.0003	- 0.0254*
x_2x_3	- 0.0020	0.0008	- 0.1524
Quadratic			
x_1^2	- 0.0078*	- 0.0049*	- 0.0784*
x_2^2	0.0011	- 0.0027	0.0247
x_3^2	- 0.0086	- 0.0137	- 0.1536
Variability			
R^2 of model	0.99	0. 97	0.98
F value of model	63.17	4.19	29.95
$P > F$	0.016	0.002	0.032
CV of model	6.7	10.1	10.3

Note: x_1, x_2 and x_3 are cassava starch, yeast extract and ammonium nitrate concentrations respectively.

* Means significant at 5% level

Generally, the adequacy of a model is determined through R^2 (multiple correlation coefficient), CV (coefficient of variation) and P values. R^2 value closer to 1 denotes better correlation between the experimental and predicted values. As shown in Table 2, the models for ABE, butanol and amylase are adequate since their R^2 values were found close to 1: 0.99, 0.97 and 0.98 respectively. These indicated that 99%, 97% and 98% of the variability in the response could be explained by the models used for ABE, butanol and amylase respectively. The CV value as the ratio of the standard error of the estimate to the mean value of the observed response indicates the degree of precision with which the experiments are compared. A low reliability of an experiment is usually indicated by a high value of CV (> 20). In the present case, acceptable CV values (6.7, 10.1 and 10.3) are observed for the models of ABE, butanol and amylase respectively, denoting that the experiments performed were reliable. The P values (< 0.05) of these three models indicate the significance of the coefficients.

In term of the determination of interactions between the variables, the P values can provide an understanding of the pattern of the interactions as well as the effect of each variable on the investigated responses. Further statistical analysis of the effect of each variable in Table 2 shows that only cassava starch concentration (x_1) and its quadratic effect (x_1^2) have a significant effect on all the

responses (P<0.05). In the case of amylase activity, besides cassava starch concentration, ammonium nitrate (x_3) also has a significant effect (P<0.05). In addition, the interaction terms of x_1x_2 and x_1x_3 are found to be significant for amylase activity (P<0.05). In the work of Bard and Hamdy [11], RSM was employed to investigate the interactive effect of a number of medium components on ABE production by *C. acetobutylicum* P262. The obtained statistical analyses also indicated that the concentration of starch significantly affects the yield and productivity of ABE.

Optimal Conditions for ABE Production

The interaction effects and optimal levels of cassava starch, yeast extract and ammonium nitrate concentrations were determined by plotting the response surface curves. Based on the analysis of variance of the second-order polynomial model of the three investigated variables, yeast extract has the least effect on all responses (Table 2). Thus, the yeast extract concentration was fixed at selected levels (5.0, 12.5 and 20 g/L) and the response surface curves representing the interaction effects of two variables, i.e. cassava starch and ammonium nitrate concentrations, on the production of ABE, butanol and amylase were plotted. (Figures 2–4). The shapes of the response surface curves show a moderately positive interaction between these two variables on the production of ABE, butanol and amylase. Cassava starch obviously affects all the responses more than does ammonium nitrate. The increase in cassava starch from 20 g/L to approximately 40 g/L increases ABE, butanol and amylase production at all selected yeast extract concentrations.

Figure 2 shows that a maximum ABE production is obtainable at a medium concentration of cassava starch (40 g/L) and a considerably high concentration of ammonium nitrate (14 g/L). However, Figure 3 shows that a maximum butanol production is obtainable using a medium concentration of both cassava starch (40 g/L) and ammonium nitrate (8 g/L). When cassava starch concentration is increased more than the optimal level of 40 g/L, reduction in ABE, butanol and amylase is observed (Figures 2–4). This is likely to be due to the high viscosity of the culture medium, which may hinder the mass transfer of enzyme hydrolysis and microbial reactions [6, 20]. It was also reported that a high starch concentration causes a high accumulation of organic acids that would cause toxicity to cells [6]. In addition, increased starch concentration also produces a high amount of glucose or available sugars, which would possibly repress the production of amylase [21].

Since starch hydrolysis is the first step in the production of ABE from starch, the amylolytic enzymes are a key factor in ABE production [6]. As amylase activity in the culture becomes high, starch hydrolysis should be more complete and the sugars for cell growth and ABE production should be more available. Figure 4 depicts the effects of the interaction of cassava starch and ammonium nitrate on amylase activity. The shape of the response surface indicates a a large effect of both variables at low concentration of yeast extract (Figure 4A) while at high concentration of yeast extract (Figure 4C), the amylase activity mostly depends on the concentration of cassava starch. Although highest amylase activity (66 U/mL) is achieved at high concentration of yeast extract (Figure 4C), a considerably high level of amylase activity (61 U/mL) can also be obtained at low concentration of yeast extract by increasing the amount of ammonium nitrate up to 14 g/L (Figure 4A).

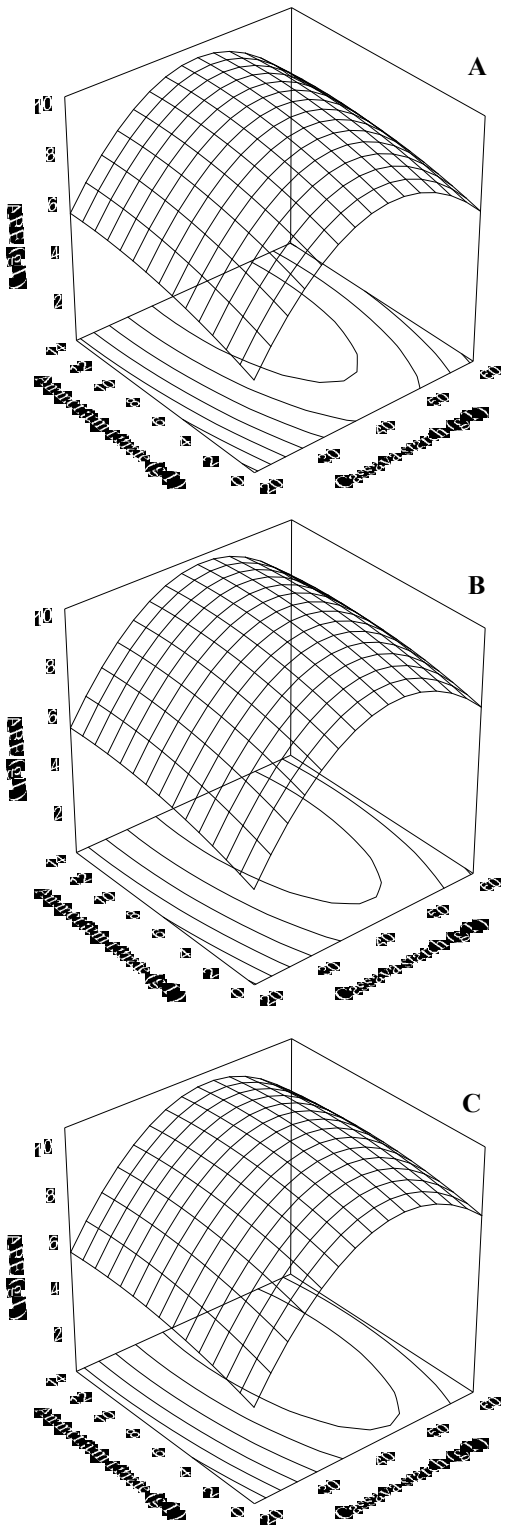

Figure 2. Response surface plots representing the interaction between cassava starch and ammonium nitrate concentrations and their effects on ABE production at given yeast extract concentrations: 5 g/L (A), 12.5 g/L (B) and 20 g/L (C)

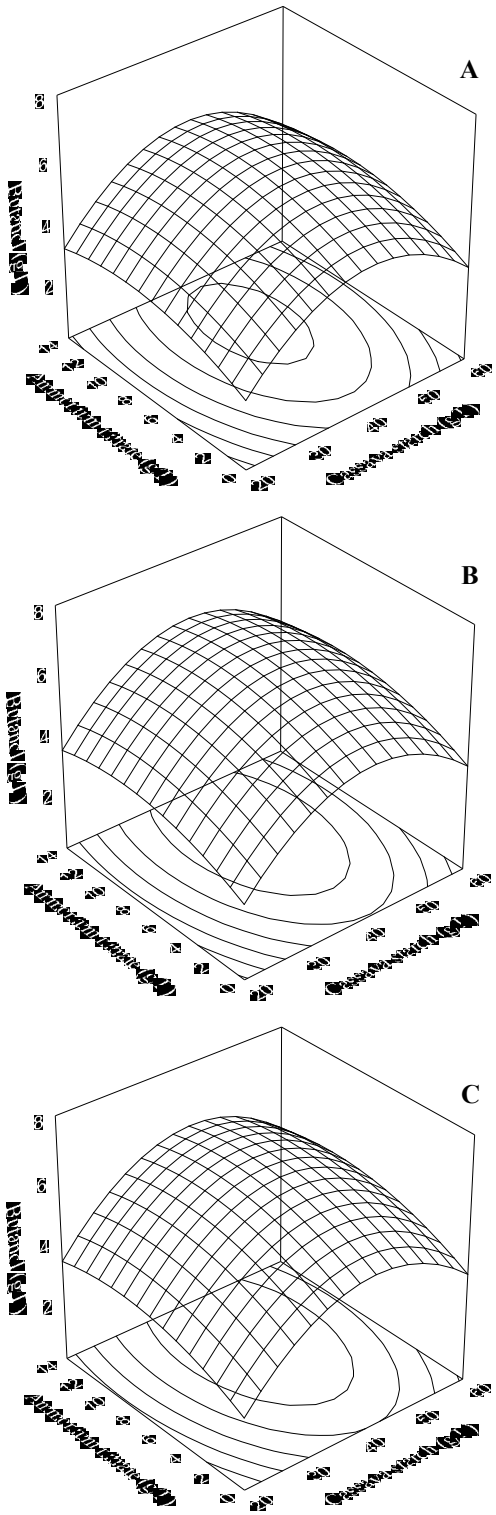

Figure 3. Response surface plots representing the interaction between cassava starch and ammonium nitrate concentrations and their effects on butanol production at given yeast extract concentrations: 5 g/L (A), 12.5 g/L (B) and 20 g/L (C)

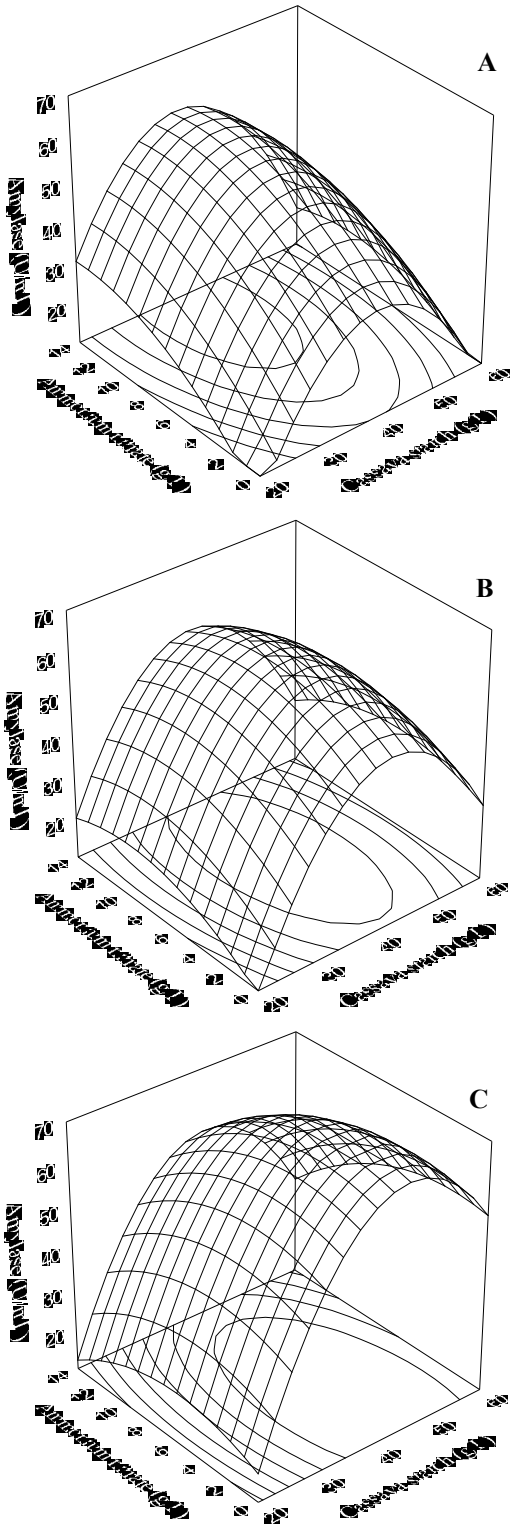

Figure 4. Response surface plots representing the interaction between cassava starch and ammonium nitrate concentrations and their effects on amylase activity at given yeast extract concentrations: 5 g/L (A), 12.5 g/L (B) and 20 g/L (C)

The increased ABE and butanol production in the co-culture with increasing ammonium nitrate concentration is probably due to the effect of ammonium nitrate on the growth and amylase production of *B. subtilis* WD 161. It was reported that *Bacillus* can grow under an anaerobic condition in the presence of ammonium nitrate since the nitrate ions from ammonium nitrate can replace oxygen as an electron acceptor in the absence of oxygen [12, 22]. Although amylase production increases with increasing concentration of ammonium nitrate, the nitrate concentration higher than 8 g/L does not show a significantly enhanced effect on amylase activity, and consequently on either ABE or butanol concentration.

From RSM, establishing that the ABE and butanol production is mainly influenced by the concentrations of cassava starch and ammonium nitrate rather than yeast extract is important information. This makes it possible to develop a strategy to maximise ABE and butanol production with a minimum requirement of costly organic nitrogen source. From Figures 2 and 3, it can be seen that the maximum ABE and butanol concentrations obtained at all levels of yeast extract are not significantly different. Thus, an optimum condition for both ABE and butanol can be determined by varying only two variables, i.e. cassava starch and ammonium nitrate, and fixing yeast extract concentration at a minimum level (5 g/L). When the concentration of starch is fixed at the optimal level (40 g/L), the concentration of ammonium nitrate can be determined at a range so as to achieve an adequate amylase activity for enhancing ABE and butanol production.

In ABE fermentation, acetone, butanol and ethanol are normally produced in the ratio of 3 : 6 : 1. Increasing ABE concentration without any reduction in the proportion of butanol is the target of most of the optimising work on ABE fermentation process. When butanol is present as a major product in the culture, its recovery process is much easier [3]. To optimise both ABE and butanol production using RSM, a superimposing of the optimal area for ABE and butanol production using Lotus Freelance Graphics at 5 g/L yeast extract concentration was carried out. The optimal points for both ABE and butanol production were in the centroid of the overlapping area as shown in Figure 5. The superimposed contour plots reveal that the optimum conditions for the production of ABE and butanol cover a large range. The central point of this area was selected for maximising both ABE and butanol production. Thus, the optimum condition for effective ABE production was: 40 g/L cassava starch, 5 g/L yeast extract and 8 g/L ammonium nitrate, at which an output of 9.43 g/L ABE, 5.80 g/L butanol and 55 U/mL amylase was predicted. The optimum condition was then experimentally tested and the results obtained are shown in Table 3.

Table 3. Predicted and observed values for optimal production of ABE, butanol and amylase

	Predicted value	Observed value ± SD	CV
ABE (g/L)	9.43	9.02 ± 0.17	1.92
Butanol (g/L)	5.80	5.60 ± 0.13	2.37
Amylase (U/mL)	55.00	56.70 ± 6.70	13.40

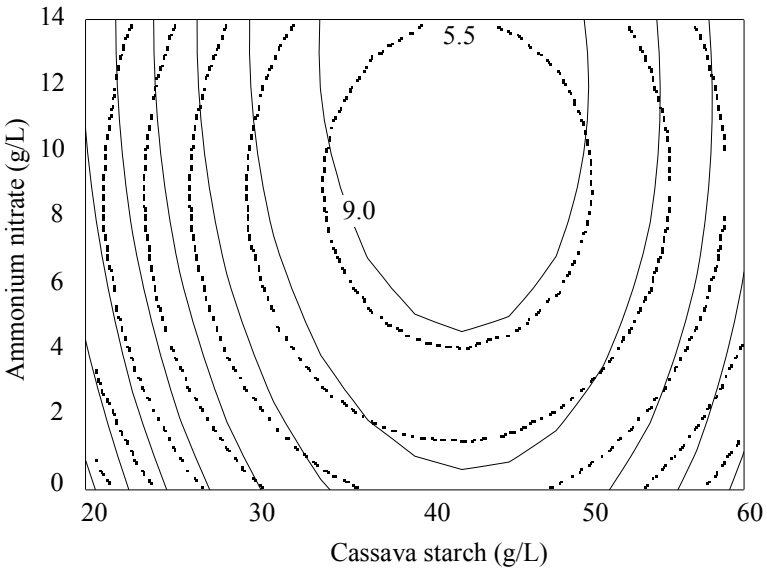

Figure 5. Superimposed contour plots of optimal areas for ABE production (solid line) and butanol production (dashed line). The centre of overlapping area is optimum for ABE and butanol production. The contour lines, 9.0 and 5.5, are the values of ABE and butanol, respectively on the contour lines closest to the centre of the optimal areas.

The low value of CV indicates a close correlation between the experimental and predicted values. The results were also compared to those of the pure culture under the same condition. Time courses of OD_{660}, amylase activity, reducing sugars, acids and ABE production are shown in Figures 6A and 6B for the pure culture and co-culture respectively. The co-culture gave a much faster rate of increase of OD_{660} and amylase activity. The latter reached 56.7 U/mL or about 11.7 times higher than that from the pure culture (4.85 U/mL). Consequently, the co-culture produced a much higher amount of ABE (9.02 g/L), i.e. about 6.9 times more than that obtained from the pure culture (1.3 g/L). Based on the medium optimisation using RSM, ABE production by the co-culture was improved 2.2-fold compared with that obtained using the initial condition in which 20 g/L cassava starch, 5 g/L yeast extract and 2 g/L ammonium nitrate were used in the medium.

The ABE production (9.02 g/L) obtained by RSM optimisation is comparable to the value (9.71 g/L) obtained in the previous study [7], in which the culture condition was conventionally optimised. The amylase activity (56.7 U/mL) from response surface optimisation is also higher than the previous result (49.3 U/mL). The optimum condition determinded by the conventional method requires 40 g/L starch, 32 g/L yeast extract and 2 g/L ammonium nitrate [7], while the optimum condition obtained by RSM requires the same amount of starch, somewhat higher amount of ammonium nitrate (8 g/L), but much lower amount of the costly yeast extract (5 g/L).

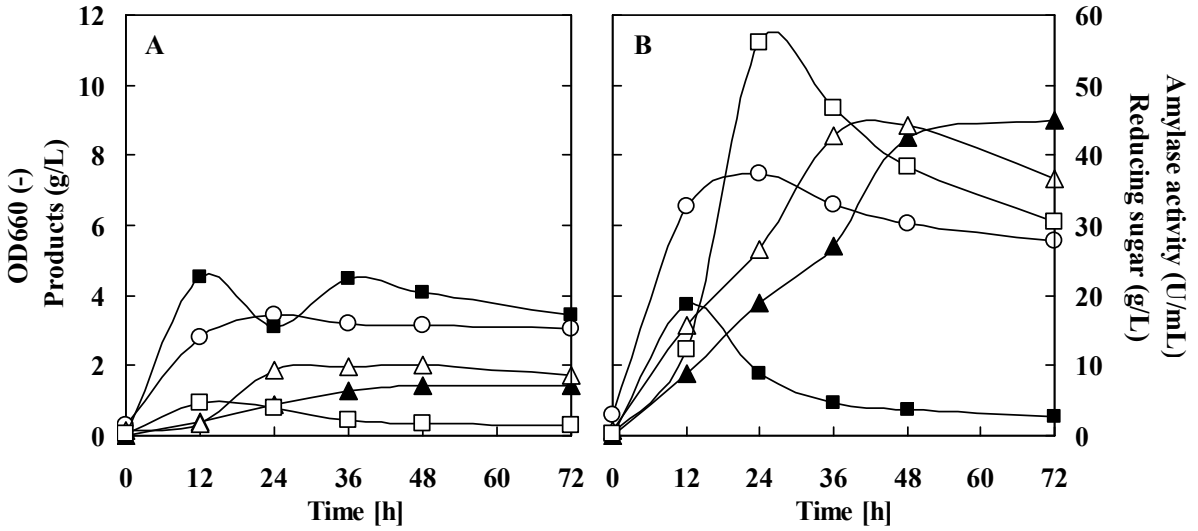

Figure 6. Growth and metabolic activity of pure culture of *C. butylicum* TISTR 1032 (A) and co-culture of *C. butylicum* TISTR 1032 and *B. subtilis* WD 161(B) under optimum condition (40 g/L cassava starch, 5 g/L yeast extract and 8 g/L ammonium nitrate). Legend: OD_{660} - open circle; amylase activity - open square; reducing sugars - filled square; acids (sum of acetic and butyric acids) - open triangle; ABE - filled triangle.

CONCLUSIONS

The optimisation by RSM has shown that starch concentration is the most important factor in ABE production from cassava starch by a co-culture of *Clostridium butylicum* and *Bacillus subtilis* without anaerobic pretreatment. Ammonium nitrate also contributes a significant effect while yeast extract has the least effect. This co-culture system with the cost-effective medium found in this study may contribute greatly to the development of industrialised ABE production.

ACKNOWLEDGEMENTS

This research was financially supported by the Graduate School of Prince of Songkla University and the Thai Government in the fiscal year of 2009–2010 through Grant AGR5311990030S. The authors would like to thank Associate Professor Dr. Poonsuk Prasertsan for providing *Bacillus subtilis* WD 161. Professor Anthony G. Hopkin is thanked for proofreading the manuscript.

REFERENCES

1. V. V. Zverlov, O. Berezina, G. A. Velikodvorskaya and W. H. Schwarz, "Bacterial acetone and butanol production by industrial fermentation in the Soviet Union: Use of hydrolyzed agricultural waste for biorefinery", *Appl. Microbiol. Biotechnol.*, **2006**, *71*, 587–597.
2. T. W. Jesse, C. T. Ezeji, N. Qureshi and H. P. Blaschek, "Production of butanol from starch-based waste packing peanuts and agricultural waste", *J. Ind.. Microbiol. Biotechnol.*, **2002**, *29*, 117–123.

3. D. T. Jones and D. R. Woods, "Acetone-butanol fermentation revisited", *Microbiol. Rev.*, **1986**, *50*, 484–524.
4. S. Kato, S. Haruta, Z. J. Cui, M. Ishii and Y. Igarashi, "Effective cellulose degradation by a mixed-culture system composed of a cellulolytic *Clostridium* and aerobic non-cellulolytic bacteria", *FEMS Microbiol. Ecol.*, **2004**, *51*, 133–142.
5. J. J. Chang, C. H. Chou, C. Y. Ho, W. E. Chen, J. J. Lay and C. C. Huang, "Syntrophic co-culture of aerobic *Bacillus* and anaerobic *Clostridium* for bio-fuels and bio-hydrogen production", *Int. J. Hydrogen Energy*, **2008**, *33*, 5137–5146.
6. M. S. Madihah, A. B. Ariff, K. M. Sahaid, A. A. Suraini and M. I. A. Karim, "Direct fermentation of gelatinized sago starch to acetone-butanol-ethanol by *Clostridium acetobutylicum*", *World J. Microbiol. Biotechnol.*, **2001**, *17*, 567–576.
7. H. T. M. Tran, B. Cheirsilp, B. Hodgson and K. Umsakul, "Potential use of *Bacillus subtilis* in a co-culture with *Clostridium butylicum* for acetone-butanol-ethanol production from cassava starch", *Biochem. Eng. J.*, **2010**, *48*, 260-267.
8. V. Bhornsmithikun, P. Chetpattananondh, R. Yamsaengsung and K. Prasertsit, "Continuous extraction of prebiotics from jackfruit seeds", *Songklanakarin J. Sci. Technol.*, **2010**, *32*, 635-642.
9. J. A. Macedo, L. D. Sette and H. H. Sato, "Optimization of medium composition for transglutaminase production by a Brazilian soil *Streptomyces* sp.", *Electron. J. Biotechnol.*, **2007**, *10*, 618-626.
10. S. Dagbagli and Y. Goksungur, "Optimization of β-galactosidase production using *Kluyveromyces lactis* NRRL Y-8279 by response surface methodology", *Electron. J. Biotechnol.*, **2008**, *11*, 1-12.
11. H. R. Badr and M. K. Hamdy, "Optimization of acetone-butanol production using response surface methodology", *Biomass Bioenergy*, **1992**, *3*, 49–55.
12. L. D. Clements, B. S. Miller and U. N. Streips, "Comparative growth analysis of the facultative anaerobes *Bacillus subtilis, Bacillus licheniformis,* and *Escherichia coli*", *Syst. Appl. Microbiol.*, **2002**, *25*, 284–286.
13. S. Chauvatcharin, C. Siripatana, T. Seki, M. Takagi and T. Yoshida, "Metabolism analysis and on-line physiological state diagnosis of acetone-butanol fermentation", *Biotechnol. Bioeng.*, **1998**, *58*, 561-571.
14. G. E. P. Box and D. W. Behnken, "Some new three level designs for the study of quantitative variables", *Technometrics*, **1960**, *2*, 455–475.
15. J. R. Gapes, D. Nimcevic and A. Friedl, "Long-term continuous cultivation of *Clostridium beijerinckii* in a two-stage chemostat with on-line solvent removal", *Appl. Environ. Microbiol.*, **1996**, *62*, 3210-3219.
16. G. L. Miller, "Use of dinitrosalicylic acid reagent for determination of reducing sugar", *Anal. Chem.*, **1959**, *31*, 426-429.
17. B. N. Okolo, L. I. Ezeogu and C. N. Mba, "Production of raw starch digesting amylase by *Aspergillus niger* grown on native starch sources", *J. Sci. Food Agric.*, **1995**, *69*, 109–115.

18. H. R. Badr, R. Toledo and M. K. Hamdy, "Continuous acetone-ethanol-butanol fermentation by immobilized cells of *Clostridium acetobutylicum*", *Biomass Bioenergy*, **2001**, *20*, 119–132.
19. N. Božić, J. Ruiz, J. López-Santín and Z. Vujčíc, "Production and properties of the highly efficient raw starch digesting α–amylase from a *Bacillus licheniformis* ATCC 9945a", *Biochem. Eng. J.*, **2011**, *53*, 203–209.
20. M. M. Nakano and F. M. Hullet, "Adaptation of *Bacillus subtilis* to oxygen limitation", *FEMS Microbiol. Lett.* **1997**, *157*, 1–7.

Maejo Int. J. Sci. Technol. **2011**, *5*(03), 390-400

Maejo International Journal of Science and Technology

ISSN 1905-7873
Available online at www.mijst.mju.ac.th

Full Paper

Development of Job's tears ice cream recipes with carrot juice and pumpkin paste

Waraluck Khongjeamsiri, Wiwat Wangcharoen*, Suthaya Pimpilai and Wichittra Daengprok

Faculty of Engineering and Agricultural Industry, Maejo University, Chiang Mai 50290, Thailand

*Corresponding author, e-mail: wiwat@mju.ac.th

Received: 17 January 2011 / Accepted: 6 November 2011 / Published: 25 November 2011

Abstract: Carrot juice and pumpkin paste were used as ingredients in Job's tears ice cream. Carrot juice or pumpkin paste added at 50% was equally preferred by 100 consumers compared to the original Job's tears ice cream. The new types of ice cream were lower in antioxidant capacity and higher in total phenolic content but could still be considered as potential antioxidant products. Purchase intent was significantly increased ($p \leq 0.05$) if consumers were informed about the nutritional and antioxidant capacity of these products.

Key words: Job's tears, Job's tears ice cream, antioxidant capacity, purchase intent

INTRODUCTION

Job's tears or adlay (*Coix lacryma-jobi* L.) is a grass native to tropical Asia [1]. It is classified into 4 varieties: *lacryma-jobi*, *stenocarpa* Stapf, *monilifer* Watt, and *ma-yuen* (Rom.) Stapf [2]. Job's tears has been used in traditional Chinese and Indian medicine [3-5]. Kanglaite, a neutral lipid extract from the endosperm of Job's tears, has been endorsed as a treatment for lung, liver, stomach and breast cancers by the Chinese government [6]. Medicinally beneficial compounds in Job's tears seeds have been discovered. For example, coixenolide [7], palmitic acid, stearic acid, oleic acid and linoleic acid [8] have antitumour activity. Benzoxazinones show anti-inflammatory activity [9] and coixan A, B and C possess hypoglycemic activity [10]. Six phenolic compounds, viz. coniferyl alcohol, syringic acid, ferulic acid, syringaresinol, 4-ketopinoresinol and mayuenolide, have strong antioxidant effects [11]. Owing to its beneficial components, Job's tears is considered a functional food ingredient.

Job's tears (*Coix lacryma-jobi* L var. *ma-yuen* (Rom.) Stapf) is grown in Thailand [2]. The hulled grains are edible in the same way as cereal foods and can be ground into flour [12]. Unfortunately, Thai people rarely consume Job's tears. There are only one conventional dessert made from Job's tears mixed with sugar and coconut milk, and a few of non-dairy drinks with Job's tears, alone or mixed with other cereals, available in the market. More Job's tears products should be introduced to Thai consumers for consumption.

Ice cream, a favourite dessert for everyone, is a frozen combination of milk, sweeteners, stabilisers, emulsifiers and flavourings. This mixture is pasteurised and homogenised before rapid freezing with agitation to incorporate air to make a smooth and soft frozen product [13]. In Thailand, a Thai-style ice cream called "i-tim ga ti" is made from coconut milk. Its taste is different from a milk-based ice cream whilst its texture is between milk ice cream and sorbet. Thais and foreigners relish its unique flavour and texture [14-15]. A trial using Job's tears together with coconut milk for making ice cream was done and 64 of 100 Thai participants preferred Job's tears-based ice cream [16]. A recipe of Job's tears-based ice cream was developed [17].

To promote consumption of the healthful Job's tears by introducing its new acceptable and easy-to-eat products, this study aims to make new Job's tears-based ice cream recipes by adding carrot juice or pumpkin paste. This should make for more colourful and flavoured products with more health benefits to consumers due to the phenolic compounds present in carrot [18] and pumpkin [19]. The effect of awareness of the nutritional and antioxidant capacities of the ingredients on the intention to buy Job's tears-based ice cream was also studied.

MATERIALS AND METHODS

Ice Cream Mix Preparation

Job's tears seeds (Rai Tip brand) were washed, soaked in water for 2 hours, boiled for 40 minutes, and blended with water in a weight ratio of 1:2 (boiled seeds:water) by means of a blender. Water was added to adjust the total solids of blended Job's tears to 8% (w/w). Coconut milk (Chaokoh brand), glucose syrup (5 Star Elephant brand), sucrose (Mitr Phol brand) and salt (Prung Thip brand) at 50, 32, 20 and 0.4% respectively of the 8% Job's tears blend were added to the mixture to make the Job's tears ice cream mix [17], which was blended, heated at 80°C for 15 minutes, cooled rapidly and stored overnight in a refrigerator before being made into ice cream by means of an ice cream maker (JCS Technic Line Co., Ltd.).

Carrot juice, prepared from fresh orange carrot (bought from a local market) by a fruit juice extractor, was added to the Job's tears ice cream mix above at 0, 25, 50, 75 and 100% (w/w) of the 8% Job's tears blend. The mixture was blended, pasteurised, stored in the refrigerator overnight and ice cream was made.

Pumpkin paste, prepared by steaming fresh pumpkin (bought from a local market) for 25 minutes and blending the steamed pumpkin flesh with water in a ratio of 1:1 (steamed pumpkin flesh:water) by means of a blender, was added to the Job's tears ice cream mix above at 0, 20, 35, 50 and 65% (w/w) of the 8% Job's tears blend before mixing, pasteurising, overnight chill storage, and ice cream making in that order.

Sensory Property Measurement

One hundred consumers were requested to evaluate the sensory attributes of the products, viz. colour (orange and yellow), hardness (the resistance of the ice cream to deformation when it is in the mouth), sweetness, saltiness, Job's tears flavour, coconut milk flavour, richness, carrot or pumpkin flavour, and smoothness, together with their overall preference of each product, by scoring each item on a 10-cm line scale (0 = least, 10 = most). After product evaluation, consumers were asked for their purchase intention before and after informing them about the nutritional and antioxidant capacity of the products.

Chemical Analysis

Nutritional data, antioxidant capacity and total phenolic content of the ice cream of all three formulas (original, with 50% carrot juice, and with 50% pumpkin paste) were determined. Moisture, protein, fat, ash and crude fibre content were determined in accordance with AOAC methods [20] while carbohydrate content was calculated by subtraction. Antioxidant capacity was evaluated by 3 different methods, namely ferric reducing/antioxidative power (FRAP) assay [21], improved ABTS radical cation decolorisation assay [22], and DPPH free radical scavenging activity [23]. Total phenolic content was analysed by Folin-Ciocalteau micro method [24]. All analyses of antioxidant capacities and total phenolic content were done with some modification as previously described [17].

Statistical Analysis

Sensory-attribute rating scores of the products were reduced by principal component analysis (PCA) and the results were used to create a product positioning map. The equation for predicting preference direction was calculated from the product position and overall preference scores [25-27]. Overall preference and chemical analysis data were analysed by analysis of variance and Duncan's new multiple range test was applied to compare means. The McNemar test was used to compare the purchase intention before and after information concerning nutritional and antioxidant capacities of the products. All statistical analysis was done by SPSS 16.0 Family.

RESULTS AND DISCUSSION

Job's Tears Ice Cream with Carrot Juice

Sensory attributes of the ice cream with carrot juice at different percentages were reduced by principal component analysis to 2 principal components (PCs) with 54.5% variance explained. A product positioning map was created on 2 PCs as shown in Figure 1. Sweetness, saltiness, Job's tears flavour, coconut milk flavour, richness and smoothness were related to PC1 with 28.3% variance explained, whilst orange colour, hardness and carrot flavour were related to PC2 with 26.2% variance explained. Addition of carrot juice thus affected the colour and hardness of the ice cream. Ice cream hardness, the resistance to deformation when an external force is applied, is affected by many factors such as overrun (amount of air in ice cream), ice crystal size, ice phase volume, fat content, fat globule destabilisation and temperature [28-30]. The addition of carrot juice

increased moisture content and decreased fat content of the ice cream (Table 5), which made the products harder.

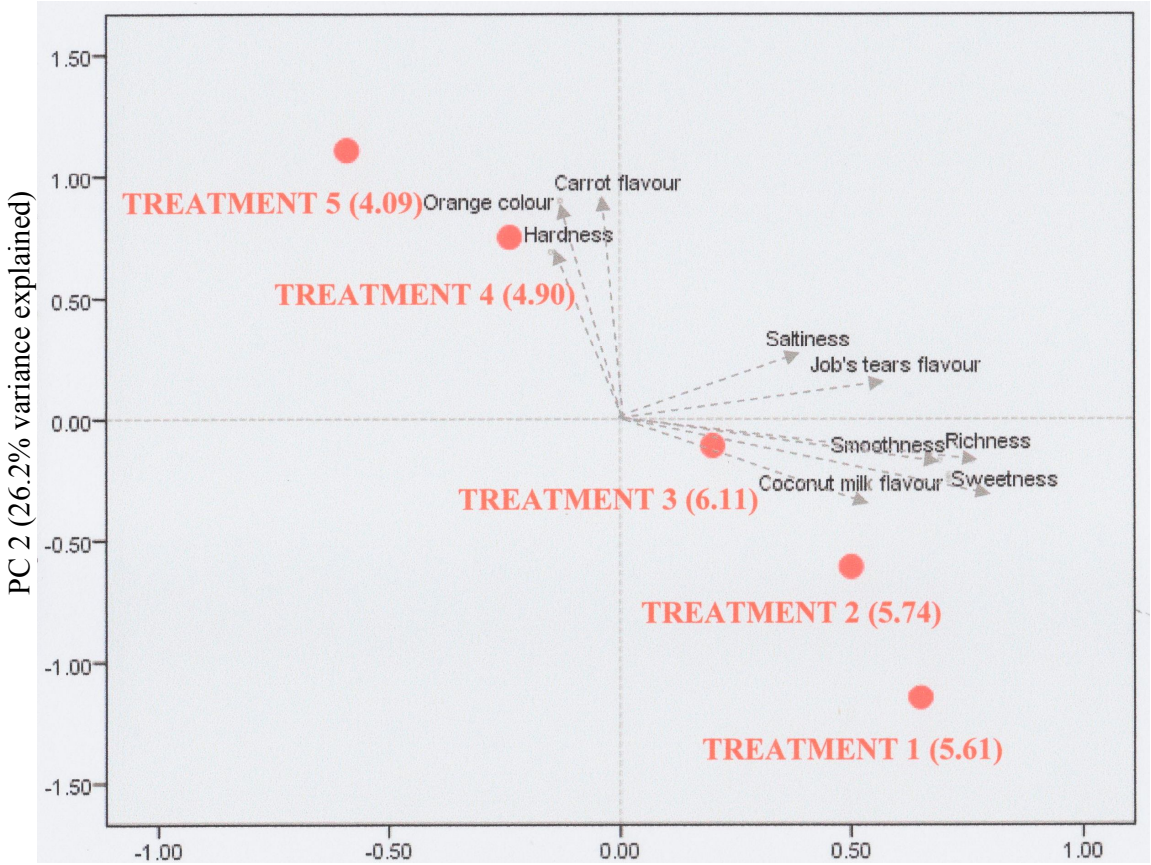

Figure 1. Product positioning map of ice cream made from Job's tears mixed with carrot juice at 0, 25, 50, 75, and 100% (treatments 1–5 respectively; the number after each treatment is its mean overall preference score.) (Overall preference score = 4.78 + 6.14 PC1 + 2.58 PC2; $r^2 = 0.87$)

The equation for predicting preference direction, which was calculated from the overall preference data and product scores on PC1 and PC2 for this recipe, was a linear model: Overall preference score = 4.78 + 6.14 PC1 + 2.58 PC2. This means that the products located on the plus area of PC1 and PC2 would be preferred to products in other areas. Both Job's tears and carrot flavours made better products, but it was impossible to increase both of them at the same time. Since Job's tears was used as a main raw material and it affected the overall preference scores rather than carrot juice (the coefficient of PC1 (6.14), which is related to Job's tears flavour was higher than that of PC2 (2.58), which is related to carrot flavour), the quantity of carrot juice added should be considered.

An overall preference data showed that the products with 25 and 50% carrot juice were not significantly preferred ($p>0.05$) to that without carrot juice, while all of them were significantly

preferred ($p \leq 0.05$) to products with 75 and 100% carrot juice (Table 1). The addition of carrot juice at 25-50% did not significantly increase consumer preference but made the product different in colour and flavour (Figure 3). The composition with 50% carrot juice was then selected as suggested recipe for optimum health benefits from both the carrot and the Job's tears, and chemical analysis was performed on it.

Awareness on nutritional and antioxidant capacity of the products influenced the purchase intent. The number of consumers who had the intention to buy these products significantly increased ($p \leq 0.05$) from 70 to 88% (Table 2) after the nutritional and antioxidant capacity were explained. The awareness effect of a product's health benefits on the purchase intent of consumers was found previously, but the intent is also affected by other factors such as degree preference, product price, perceived value, and consumer characteristics [31-33].

Table 1. Overall preference scores of Job's tears ice cream with carrot juice

Treatment	Score (mean ± SD)
1 (0% carrot juice added)	$5.61^{a} \pm 2.04$
2 (25% carrot juice added)	$5.74^{a} \pm 2.26$
3 (50% carrot juice added)	$6.11^{a} \pm 3.05$
4 (75% carrot juice added)	$4.90^{b} \pm 1.83$
5 (100% carrot juice added)	$4.09^{c} \pm 2.09$

Note: Means with different letters were significantly different ($p<0.05$).
(0 = least preferred, 10 = most preferred)

Table 2. Number of consumers with intention to buy Job's tears ice cream with carrot juice before and after informing them about the nutritional and antioxidant capacity of the product

	Buy	Not buy	Total
Before informing	70	30	100
After informing	88	12	100

Note : McNemar test = 16.05 ($p<0.05$)

Job's Tears Ice Cream with Pumpkin Paste

The principal component analysis of sensory attributes of Job's tears ice cream with added pumpkin paste at 0, 20, 35, 50 and 65% showed that these data could be reduced to 2 PCs with 43.3% variance explained. Both of them were used to create a product positioning map (Figure 2). Yellow colour, hardness and pumpkin flavour were related to PC1 with 22.8% variance explained,

whilst sweetness, saltiness, Job's tears flavour, coconut milk flavour, richness and smoothness were related to PC2 with 20.5% variance explained. This means that the addition of pumpkin paste affected the colour and hardness of the ice cream, which was similar to adding carrot juice. Pumpkin paste increased the moisture content of the products and made them harder, but there was no effect from the fat content (Table 5) because pumpkin flesh contains 1.5% fat [34].

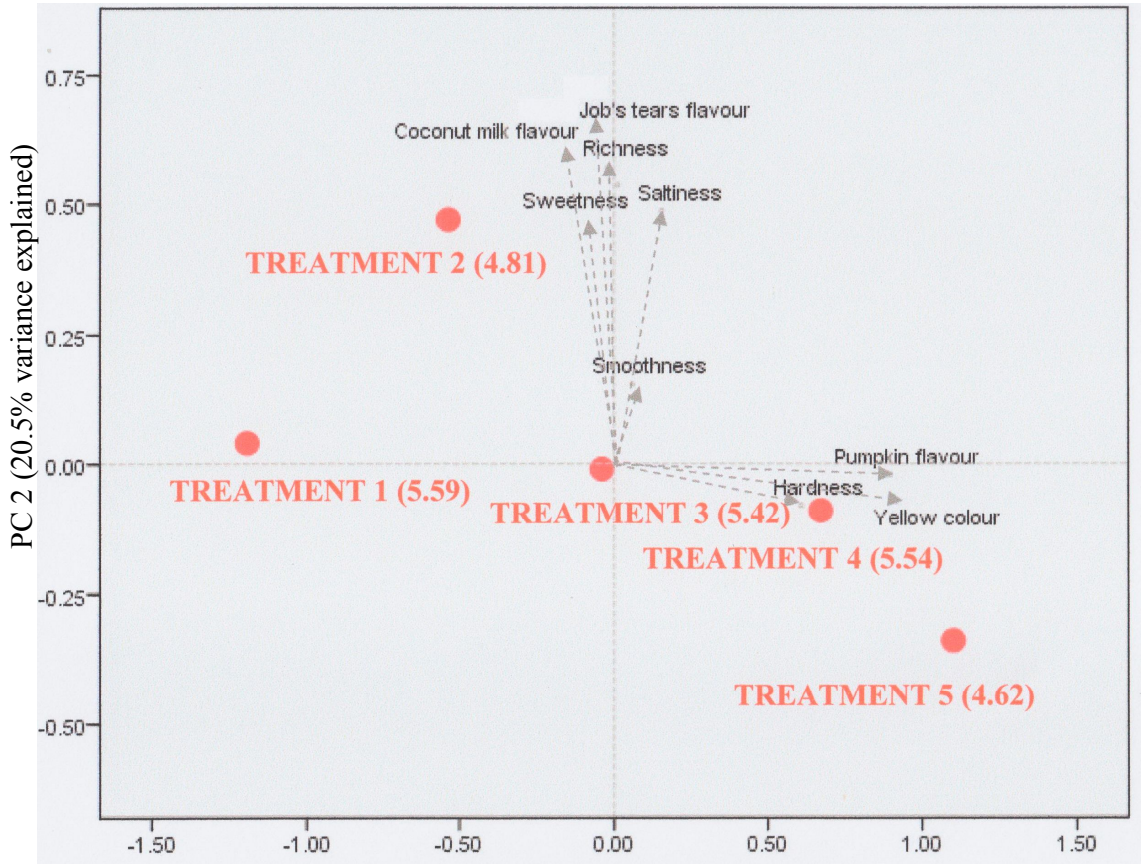

Figure 2. Product positioning map of Job's tears ice cream with pumpkin paste at 0, 20, 35, 50, and 65% (Treatments 1–5 respectively; the number after each treatment is its mean overall preference score.) (Overall preference score = 5.56 - 0.13 $PC1^2$ - 3.96 $PC2^2$; $r^2 = 0.75$)

To predict preference inclinations, the overall preference data were regressed on PC scores of products. The equation for pumpkin paste recipe was an elliptical model: Overall preference score = 5.56 - 0.13 $PC1^2$ - 3.96 $PC2^2$. This means that a product located at point (0,0) of PC1 and PC2 scores was most preferred, and a product at a minus or plus value of both PCs was less preferred. This kind of model showed that the addition of more or less quantities of pumpkin paste made the products less desirable.

The overall preference mean scores of the products with 35 and 50% pumpkin paste were almost equal to that without pumpkin paste. All of them were significantly preferred ($p \leq 0.05$) to

products with 20 and 65% pumpkin paste (Table 3). Although pumpkin paste addition did not significantly increase the consumer preference of Job's tears ice cream, adding pumpkin paste at 35 and 50% did make the products different in colour and flavour similar to adding carrot juice (Figure 3). The composition with 50% pumpkin paste was then selected as suggested recipe for optimum health benefits from both the pumpkin and the Job's tears, and chemical analysis was performed on it.

For purchase intent, the number of consumers who had the intention to buy the products significantly increased ($p \leq 0.05$) from 75 to 88% (Table 4) when consumers were informed about the nutritional and antioxidant capacity of the products. This result was similar to that on the carrot juice ice cream.

Table 3. Overall preference scores of Job's tears ice cream with pumpkin paste

Treatment	Score (mean ± SD)
1 (0% pumpkin paste added)	$5.59^{a} \pm 2.14$
2 (20% pumpkin paste added)	$4.81^{b} \pm 2.35$
3 (35% pumpkin paste added)	$5.42^{a} \pm 2.24$
4 (50% pumpkin paste added)	$5.54^{a} \pm 2.08$
5 (65% pumpkin paste added)	$4.62^{b} \pm 2.37$

Note : Means with different letters in the same column were significantly different ($p<0.05$). (0 = least preferred, 10 = most preferred)

Table 4. Number of consumers with intention to buy Job's tears ice cream with pumpkin paste before and after informing them about the nutritional and antioxidant capacity of the product

	Buy	Not buy	Total
Before informing	75	25	100
After informing	88	12	100

Note : McNemar test = 8.47 ($p \leq 0.05$)

Figure 3. Job's tears ice cream (white – original; orange – with carrot juice; yellow – with pumpkin paste)

Chemical Analysis

Nutritional data, antioxidant capacity and total phenolic content of selected ice cream products are shown in Table 5. Job's tears ice cream with 50% carrot juice contained more moisture, ash and total phenolics, but less fat, carbohydrate and crude fibre than the original Job's tears ice cream. The antioxidant capacity of the ice cream with carrot was found to be lower than that of the original product. Similarly, the ice cream with 50% pumpkin paste contained more moisture, crude fibre and total phenolics, and less carbohydrate than the original ice cream. The ABTS value of the ice cream with pumpkin was observed to be higher, while the FRAP and DPPH values lower, than the corresponding values of the original product. This difference was possibly due to the different mechanisms involved in the reactions in the three methods. The FRAP assay measures the total reducing power of electron donating substances [21] whilst ABTS and DPPH assays are based on the ability of antioxidant molecules to quench ABTS radical cation [22] or DPPH free radical [23]. Phenolic compounds in Job's tear, carrot and pumpkin are different [11, 18-19] and most likely there are other compounds in these ingredients which also possess antioxidant activity. These phenolic and other compounds in Job's tears, carrot and pumpkin could provide other health benefits as well.

The lowest value of antioxidant capacity in this study was 26.50 mg vitamin C equivalent/100 grams, which is more than 40% of the daily value (60 mg) of vitamin C [35]. Vitamin C is one of the antioxidant vitamins used for claims of antioxidant nutrient content. A product must contain 20% or more of the daily value of vitamin C, vitamin E, or β-carotene for the claim of 'high in antioxidant vitamin C, vitamin E, or β-carotene' [36]. Although other ingredients are not allowed to be used for this antioxidant claim, a comparison of the antioxidant capacity of a product with such antioxidant vitamins as vitamin C may be used to express the product's antioxidant potential.

Table 5. Nutritional data, antioxidant capacity and total phenolic content (mean ± SD) of Job's tears ice cream

	Job's tears ice cream	Job's tears ice cream with 50% carrot juice	Job's tears ice cream with 50% pumpkin paste
Moisture (%w/w)	$67.66^{c} \pm 0.36$	$72.24^{a} \pm 0.23$	$71.07^{b} \pm 0.03$
Protein (%w/w) ^{ns}	1.00 ± 0.06	0.88 ± 0.05	0.98 ± 0.01
Fat (%w/w)	$0.48^{a} \pm 0.12$	$0.17^{b} \pm 0.09$	$0.43^{a} \pm 0.12$
Ash (%w/w)	$0.34^{b} \pm 0.01$	$0.40^{a} \pm 0.01$	$0.35^{b} \pm 0.01$
Carbohydrate (%w/w)	$30.52^{a} \pm 0.56$	$26.3^{c} \pm 0.06$	$27.17^{b} \pm 0.09$
Crude fibre (%w/w)	$0.04^{b} \pm 0.01$	$0.02^{c} \pm 0.01$	$0.07^{a} \pm 0.01$
FRAP (mg vitamin C equivalent /100 grams product)	$47.12^{a} \pm 2.63$	$26.50^{c} \pm 3.13$	$30.4^{b} \pm 1.38$
ABTS (mg vitamin C equivalent /100 grams product)	$228.54^{b} \pm 20.48$	$94.38^{c} \pm 8.64$	$372.15^{a} \pm 32.13$
DPPH (mg vitamin C equivalent /100 grams product)	$251.38^{a} \pm 8.61$	$209.20^{b} \pm 20.36$	$192.80^{b} \pm 15.24$
Total phenolic content (mg gallic acid equivalent /100 grams product)	$9.06^{c} \pm 0.07$	$25.14^{a} \pm 1.83$	$15.21^{b} \pm 0.42$

Note : Means with different letters in the same row were significantly different ($p \leq 0.05$).
^{ns} = There is no significant difference ($p > 0.05$).

CONCLUSIONS

It has been shown that consumers' acceptance of the original and the two new flavours of Job's tears ice cream developed in this study is similar. Although the antioxidant capacity of Job's tears ice cream with carrot juice or pumpkin paste may be somewhat lessened, this is compensated by a higher phenolic content and a lower carbohydrate content, and all formulas can be considered as antioxidant products.

The development of Job's tears ice cream is an approach to promoting the consumption of Job's tears because ice cream is a popular product for people, especially in tropical areas like Thailand. Incorporation of carrot juice and pumpkin paste into the recipe makes Job's tears ice cream more colourful and varied in flavour as well as in health benefits, which may be more attractive to consumers.

ACKNOWLEDGEMENTS

This work is a part of a research project supported by a grant from the Faculty of Engineering and Agro-Industry, Maejo University.

REFERENCES

1. Encyclopedia Britannica, "Micropedia Ready Reference", Vol. 6, 15th Edn, Encyclopedia Britannica Inc., Chicago, **1997**.

2. S. Vacharotayan, J. Jan-orn, P. Charoen, S. Titatarn and S. Kingkaew, "Job's Tears Production and Marketing in Thailand", Japan Trade Centre and Agricultural and Marine Produce Group of the Japanese Chamber of Commerce, Bangkok, **1982**.
3. J. A. Duke and E. S. Ayensu, "Medicinal Plants of China", Reference Publications, Michigan, **1985.**
4. H. Yeung, "Handbook of Chinese Herbs and Formulas", Institute of Chinese Medicine, Los Angeles, **1985.**
5. R. N. Chopra, S. L. Nayar and I. C. Chopra, "Glossary of Indian Medicinal Plants" (including the supplement), Council of Scientific and Industrial Research, New Delhi, **1986.**
6. W. W. Gibbs, "Healing cancer", *Sci. Am.*, **1998**, *279*, 40-41.
7. T. Ukita and A. Tanimura, "Studies on the antitumor components in the seeds of *Coix lacryma-jobi* L. var. ma-yuen (Roman) Stapf. 1. Isolation and antitumor activity of coixenolide", *Chem. Pharm. Bull.*, **1961**, *9*, 43-46.
8. M. Numata, A. Yamamoto, A. Moribayashi and H. Yamada, "Antitumor components isolated from the Chinese herbal medicine *Coix lacryma-jobi*", *Planta Med.*, **1994**, *60*, 356-359.
9. T. Nagao, H. Otsuka, H. Kohda, T. Sato and K. Yamasaki, "Benzoxazinones from *Coix lacryma-jobi* L. var. ma-yuen", *Phytochem.*, **1985**, *24*, 2959-2962.
10. M. Takahashi, C. Konno and H. Hikino, "Isolation and hypoglycemic activity of coixan A, B and C, glycans of *Coix lacryma-jobi* var. ma-yuen seeds", *Planta Med.*, **1986**, *52*, 64-65.
11. C. C. Kuo, M. C. Shih, Y. H. Kuo and W. Chiang, "Antagonism of free-radical-induced damage of adlay seed and its antiprolifrative effect in human histolytic lymphoma U237 monocytic cells", *J. Agric. Food Chem.*, **2001**, *49*, 1564-1570.
12. J. W. Purseglove, "Tropical Crops Monocotylendons", Longman Scientific Technical, Harlow, **1972**.
13. R. T. Marshall and W. S. Arbuckle, "Ice Cream", 5th Edn., Chapman and Hall, New York, **1996**.
14. M. Moore, "Ice cream: Thailand's version", http://www.wheretoeat-bangkok.com/Assets/Articles/thai_ice_cream.pdf (Retrieved: Dec 23, **2010**).
15. M. Badcock, "Ice cream, Thai-style", http://thaifoodandtravel.com/blog/thai-ice-cream/, **2010** (Retrieved: Dec 23, 2010).
16. W. Khongjeamsiri, W. Wangcharoen, S. Pimpilai and W. Daengprok, "Preference direction study of Job's-tears ice cream", *Maejo Int. J. Sci. Technol.*, **2007**, *1*, 137-144.
17. W. Khongjeamsiri, W. Wangcharoen, S. Pimpilai and W. Daengprok, "Development of Job's-tears ice cream recipe", *Maejo Int. J. Sci. Technol.*, **2009**, *3*, 388-399.
18. D. Zhang and Y. Hamauzu, "Phenolic compounds and their antioxidant properties in different tissues of carrots (*Daucus carota* L.)", *J. Food Agr. Environ.*, **2004**, *2*, 95-100.
19. M. Yadav, S. Jain, R. Tomar, G. B. K. S. Pasad and H. Yadav, "Medicinal and biological potential of pumpkin: An updated review", *Nutr. Res. Rev.*, **2010**, *23*, 184-190.
20. AOAC Internatioanl, "Official Method of Analysis of AOAC International", 17th Edn., Gaithersburg, Maryland, **2000**.
21. I. F. Benzie and J. J. Strain, "Ferric reducing / antioxidant power assay: Direct measure of total antioxidant activity of biological fluids and modified version for simultaneous measurement of total antioxidant power and ascorbic acid concentration", *Methods Enzymol.*, **1999**, *299*, 15-27.

22. M. J. Arts, G. R. Haenen, H. P. Voss and A. Bast, "Antioxidant capacity of reaction products limits the applicability of the Trolox equivalent antioxidant capacity (TEAC) assay", *Food Chem. Toxicol.*, **2004**, *42*, 45-49.
23. W. Brand-William, M. Cuelier and M. E. Berset, "Use of a free radical method to evaluate antioxidant activity", *Lebensm. Wiss. Technol.*, **1995**, *28*, 25-30.
24. A. Waterhouse, "Folin-Ciocalteau micro method for total phenol in wine", http://waterhouse. ucdavis.edu/phenol/folinmicro.htm (Retrieved: May 4, **2005**).
25. A. A. Williams, in "Food Acceptability" (Ed. D. M. H. Thomson), Elsevier Science Publishers, Essex, **1988**, pp.297-309.
26. H. J. H. MacFie and D. M. H Thomson, "Measurement of Food Preferences", Blackie Academic & Professional, Glasgow, **1994**.
27. H. R. Moskowitz, "Product testing 2: Modeling versus mapping and their integration", *J. Sens. Stud.*, **1994**, *9*, 323-336.
28. A. M. Roland, L.G. Phillips and K. J. Boor, "Effects of fat content on the sensory properties, melting, color, and hardness of ice cream" *J. Dairy Sci.*, **1999**, *82*, 32-38.
29. M. R. Muse and R. W. Hartel, "Ice cream structural elements that affect melting rate and hardness", *J. Dairy Sci.*, **2004**, *87*, 1-10.
30. K. Inoue, H. Ochi, K. Habara, M. Taketsuka, H. Saito, N. Ichihashi and K. Iwatsuki, "Modeling of the effect of freezer conditions on the hardness of ice cream using response surface methodology", *J. Dairy Sci.*, **2009**, *92*, 5834-5842.
31. J. A. Bower, M. A. Saadat and C. Whitten, "Effect of liking, information and consumer characteristics on purchase intention and willingness to pay more for a fat spread with a proven health benefit", *Food Qual. Prefer.*, **2003**, *14*, 65-74.
32. J. Walker, C. A. Boeneke, S. Sriwattana, J. Herrera-Corredor and W. Prinyawiwatkul, "Consumer acceptance and purchase intent of a novel low-fat sugar-free sherbet containing soy protein", *J. Food Qual.*, **2010**, *33*, 27-41.
33. M. R. Shaharudin, J. J. Pani, S. W. Mansor and S. J. Elias, "Purchase intention of organic foods; perceived value overview", *Can. Soc. Sci.*, **2010**, *6*, 70-79.
34. Nutrition Division, "Nutrient Composition per 100 grams Edible Portion" (in Thai), Department of Health, Ministry of Public Health, Bangkok, **1987**.
35. Center for Food Safety and Applied Nutrition, "Guidance for industry: A food labeling guide", http://www.cfsan.fda.gov/guidance.html, **2008** (Retrieved: April 15, 2008).
36. U.S. Food and Drug Administration, "Food labeling; Nutrient content claims: Definition for 'high potency' and definition of 'antioxidant' for use in nutrient content claims for dietary supplements and conventional foods", *Fed. Regist.*, **1997**, *62*, 49868-49881.

Maejo Int. J. Sci. Technol. **2011**, *5*(03), 401-412

Maejo International Journal of Science and Technology

ISSN 1905-7873
Available online at www.mijst.mju.ac.th

Full Paper

Identification of *Pfdhfr* mutant variants in *Plasmodium berghei* model

Wachiraporn Tipsuwan [1,2], Somdet Srichairatanakool [2], Sumalee Kamchonwongpaisan [1], Yongyuth Yuthavong [1] and Chairat Uthaipibull [1,*]

[1] National Centre for Genetic Engineering and Biotechnology (BIOTEC), National Science and Technology Development Agency (NSTDA), 113 Thailand Science Park, Pathumthani 12120, Thailand
[2] Department of Biochemistry, Faculty of Medicine, Chiang Mai University, 110 Inthawaroros Road, Sriphum, Amphur Muang, Chiang Mai 50200, Thailand

* Corresponding author, e-mail: chairat@biotec.or.th

Received: 24 May 2011 / Accepted: 4 November 2011 / Published: 2 December 2011

Abstract: Parasite resistance to antimalarials is a major burden in controlling malaria disease. Genetic mutations within the parasites are found to be the factor in conferring resistance to drugs. In this study, the power of random mutant library and transgenic parasite systems were employed to identify mutations on the antimalarial drug target, viz. *Plasmodium falciparum* dihydrofolate reductase (DHFR), which could contribute to resistance, and to elucidate the functionality of resistant mutant parasites in *P. berghei*. Using the moderate drug-resistant *Pfdhfr*^{S108N} gene as template, we generated a library of *Pfdhfr* mutants by error-prone PCR followed by transfection and selection in *P. berghei*. Two clones of transgenic *P. berghei* expressing *Pf*DHFR of interest due to the position of mutations, i.e. *PbPf*DHFR3m1 (M55I+S108N+S189C) and *PbPf*DHFR3m2 (C50Y+S108N+F116S), were selected for drug sensitivity test. Although these transgenic parasite clones showed similar reproducibility with the parental transgenic *P. berghei*, expressing *Pf*DHFR with mutation at S108N (*PbPf*S108N) in response to antifolate pyrimethamine, this study reconfirms that this *P. berghei* model is effective in predicting the evolution of *Pfdhfr* mutations in vivo. This approach can be applied during the development of new antifolates with better effective properties against drug resistant parasites.

Keywords: *Plasmodium berghei*, transfection, malaria, dihydrofolate reductase, antifolate resistance

INTRODUCTION

Malaria is one of the devastating diseases endemic to tropical and subtropical areas of the world. It is caused by parasites in the genus *Plasmodium*, of which *P. falciparum* is the most virulent species that infects humans. The current major issue for malaria control is the increasing resistance to the available antimalarial drugs. Although efforts are being made in the discovery of novel antimalarial drugs by research groups, understanding of current drug resistance mechanism developed by the parasites is necessary for the design of new compounds that are effective against drug resistant parasites and for averting further possible resistance in the future.

A bi-functional dihydrofolate reductase-thymidylate synthase (DHFR-TS) enzyme is a well-defined target of antimalarial drugs such as pyrimethamine, cycloguanil and methotrexate [1]. Dihydrofolate reductase (DHFR) catalyses the production of tetrahydrofolate from dihydrofolate while thymidylate synthase (TS) is in charge of transferring a methyl group from methylene-tetrahydrofolate to deoxyuridine monophosphate (dUMP), thereby generating deoxythymidine monophosphate (dTMP) and tetrahydrofolate [2]. Resistance to pyrimethamine, cycloguanil and methotrexate was reported to be associated with mutations in *dhfr* gene [3]. Despite the possibility to develop more mutations, thus becoming more resistant to the drugs, the availability of target-based screening models [4-5] and detailed crystal structure [6] makes DHFR still an attractive drug target for malaria.

Recently, our group has reported the use of transgenic *P. berghei* model to predict the evolution of drug-resistant *Pfdhfr* mutations [7]. The system utilised the power of *P. berghei* transfection technology to identify possible novel drug-resistant mutants that could arise against the antifolate drug. Using our system, we have successfully identified S108N (serine, S, at amino acid position 108 changed to asparagine, N) mutant of *Pf*DHFR, which was the first reported pyrimethamine-resistant mutation isolated from the field. It was reported that the accumulation of amino acid substitutions on DHFR enzyme at positions 51, 59, 164 and 108 increases the level of the parasites' resistance to the drug [8].

In this study, in order to predict possible evolutionary changes within the DHFR enzyme, which may increase the level of drug resistance, we have used the moderate drug-resistant $Pfdhfr^{S108N}$ mutant as a template to generate a random mutant library of *Pfdhfr* and transfected the mutant library to the *P. berghei* parasite. After pyrimethamine selection, a number of $Pfdhfr^{S108}$-based variants were identified and tested for pyrimethamine resistant level. This study reconfirms the power of the random mutant library and transgenic *P. berghei* systems to predict the drug-resistant *Pfdhfr* mutations in an in vivo setting.

MATERIALS AND METHODS

Experimental Animals and *P. berghei* Parasite

Female BALB/c mice (National Laboratory Animal Centre, Mahidol University) 4-6 weeks old and weighing 20-25 grams were used in all experiments. The transgenic *P. berghei* parasite line MRA-867, stably expressing green fluorescent protein (PbGFP) and kindly provided by Drs. Andrew Waters and Chris Janse of Malaria Research Group, Leiden University Medical Centre, the Netherlands, was used [9]. The animal study protocol was approved by the Ethical Committee of

Animal Experimentation at the Faculty of Medicine, Chiang Mai University (Protocol Number 18/2553). Animal experiments conformed to international and national guidelines for ethical conducts on the care and use of animals.

Transfection Plasmid

The plasmid for *P. berghei* transfection, designated pY005^{S108N}, was modified from the original plasmid pL0017 [10], which was kindly provided by Drs. Andrew Waters and Chris Janse (Leiden University Medical Centre, the Netherlands). The pY005^{S108N} plasmid contained *Pfdhfr*^{S108N}*-ts* gene flanked with 2.3 and 1.0 kilobases (kb) of 5' and 3' untranslated region (UTR) sequences of *Pbdhfr-ts* respectively, which also served as homologous recombination sites. *Bam*HI and *Afl*II restriction sites introduced at 5' and 3' ends of the *Pfdhfr* domain respectively served as cloning sites for the randomly mutated *Pfdhfr* library.

Random Mutagenesis of *Pfdhfr* Library

The *Pfdhfr* mutant library was generated by error prone PCR [11]. The PCR reaction contained 1 ng pY005^{S108N} [7], 10 µM of sense primer F1 (CGGTGGATCCATGATGGAACAAG; *Bam*HI site is underlined) and antisense primer R1 (CTTTGTCATCATTCTTAAGAGGC; *Afl*II site is underlined), 0.1 mM dGTP, 0.1 mM dATP, 0.5 mM dCTP, 0.5 mM dTTP, 1x mutagenesis buffer [12] and 5 units of GoTaq® DNA polymerase. The thermocycle condition was: 1 cycle at 95ºC for 3 min, 30 cycles at 95ºC for 1 min, 50ºC for 1 min and 72ºC for 1 min. The PCR products of the random mutant *Pfdhfr* library of about 0.7 kb were cloned into *Bam*HI/*Afl*II sites of pY005^{S108N}. Variant clones were randomly picked and the mutant *Pfdhfr* genes were sequenced (BioDesign sequencing service, Thailand).

Transfection, Selection and Identification of *Pfdhfr* Random Mutant Library

The bacterial clones with plasmids containing *Pfdhfr* mutation library were pooled and grown in Luria Bertani broth containing 100 µg/ml ampicillin at 37ºC with shaking for 12-16 hr. Plasmids were extracted and purified using a Qiaprep Spin Miniprep kit (Qiagen) according to the manufacturer's protocol. Extracted plasmids were pooled, precipitated by isopropanol and resuspended in 10 µl TE buffer (10 mM Tris and 1 mM EDTA, pH 8.0). In vitro culture of PbGFP and transfection was performed as described [13]. Briefly, parasitised blood was collected from a donor animal and cultured overnight in RPMI 1640 medium containing 20% heat-inactivated fetal calf serum, 50 IU/ml neomycin and 25mM Hepes. Schizont stage parasites were purified from the culture by Nycodenz gradient centrifugation [13], transfected with plasmid DNA containing mutant library using the Amaxa Nucleofector protocol [13] and re-infected into the animals by intravenous injection. Twenty-four hr after transfection, the infected mice were daily treated by intraperitoneal (i.p.) injection with 0.25 mg/kg of pyrimethamine. When the parasitemia reached 3%, tail blood was drawn from the infected animals on alternate days for genomic DNA extraction until parasitemia reached 8-10%. The obtained genomic DNA was transformed into *E. coli* DH5α. The transformed bacterial colonies were picked, the plasmid DNA extracted and the sequence of *Pfdhfr* mutants obtained by DNA sequencing as described above.

Generation and Cloning of Transgenic *P. berghei* Expressing *Pf*DHFR Mutants

Plasmids containing *Pfdhfr* mutants of interest were selected and re-introduced into *P. berghei*. The plasmids were linearised for double crossover recombination at the 5' and 3' UTR. In vitro culture of PbGFP and transfection was performed as described above. Twenty-four hr after transfection, 0.25 mg/kg of pyrimethamine was used to treat the infected mice by i.p. injection daily until the resistant parasites reappeared in the blood. The animals were sacrificed and infected blood was collected for genomic analysis. The integrated transgenic mutant parasite clones were obtained by the limiting dilution method [14].

Genomic Analysis of Transgenic *P. berghei* Parasites

To determine the correct integration of mutant vector into the genome of the transgenic parasites, a 4.0-kb DNA fragment spanning the endogenous 5' UTR *Pbdhfr-ts* gene and the introduced *Pfdhfr* in the vector was detected by PCR using F2 (TTGAGCTACATAACTTCCATACAT) and R1 primers (described above). A 3.0-kb DNA fragment spanning the *Pfdhfr-ts* in the vector and the endogenous 3' UTR *Pbdhfr-ts*, indicative of a 3' integration event, was detected by PCR using F1 (described above) and R2 (CGATCTACACCTCTTCAT) primers (Figure 2).

The correct integration of the mutant *Pfdhfr* transgenic parasites was further confirmed by Southern analysis [15]. Genomic DNA of the transgenic mutant parasites was digested with *Eco*RI restriction enzyme and hybridised with *Pfdhfr* probe labelled with Digoxigenin-11-dUTP (using DIG high prime DNA labelling and detection starter kit II, Roche Applied Science). The pattern of hybridisation was detected using alkaline phosphatase-conjugated anti-DIG antibody and CSPD reagent according the manufacturer's protocol (Roche Applied Science).

Sensitivity of Transgenic *P. berghei* Expressing *Pf*DHFR Mutant to Pyrimethamine

The 4-day suppressive test [16] was used to determine the level of susceptibility of the mutant parasites to pyrimethamine. Six groups of four BALB/c mice per group were infected intravenously with $1x10^7$ parasitised erythrocytes. The experimental groups were treated with different concentration of pyrimethamine by i.p. injection four hr after infection. The control group was treated with 5%(v/v) DMSO in PBS. The treated groups were administered daily with pyrimethamine through the same route for 3 days. Twenty-four hr after the last treatment (day 4), blood smears were made from all groups for microscopic screening after Giemsa staining to determine the percentages of parasitemia. The difference between the mean value of the control group (taken as 100%) and those of the experimental groups was calculated and expressed as per cent inhibition.

Statistical Analysis

The non-linear regression for sigmoidal dose-inhibition (variable slope) was used to calculate the 50% effective dose (ED_{50}) value. Per cent inhibition was calculated using the formula below. The unpaired *t*-test was used to compare the mean ED_{50} value. All data were subjected to statistical analysis using the SigmaPlot software.

% Inhibition = 100 – {[mean parasitemia (treated) / mean parasitemia (control)] x 100}

RESULTS AND DISCUSSION

Generation of *Pfdhfr* Random Library Using *Pfdhfr*^{S108N} as Template

Approximately 8,300 bacterial colonies containing random mutant *Pfdhfr* library were generated. Twelve colonies were randomly picked from the pool of colonies and sequenced to check mutations within the *Pfdhfr* gene. Apart from the sequence at amino acid position 108 (serine, S; AGC changed to asparagine, N; AAC), which was used as template, up to 5 base substitutions per gene were found. The mutation frequency in this study was 0.27%, which is equivalent to approximately 2 base substitutions per 700 base pairs (bp) of *Pfdhfr* gene. It was within the criteria of functional mutation frequency of 2-5 base substitutions per gene [17].

Selection of Transgenic Parasite Lines Expressing Pyrimethamine-Resistant Phenotype

Plasmid DNA containing random mutant *Pfdhfr* library were purified and transfected to *P. berghei* parasite. Two mice were infected with the transfected parasite and treated with pyrimethamine to select transgenic parasite lines. Reappearance of pyrimethamine-resistant parasites was observed six days after transfection. The genomic DNA of the parasites were extracted and transformed to *E. coli*. Colonies from the transformation were picked, cultured and the extracted plasmids were subjected to sequencing analysis. Results from the sequencing analysis indicated the presence of *Pfdhfr* mutant genes that might contribute to pyrimethamine resistance of the transfected parasites. Many variations of *Pfdhfr* mutants were observed as shown in Table 1.

Table 1. Variation of *Pfdhfr* mutation compared with S108N template after transfection to *P. berghei* parasite and selection with 0.25 mg/kg

Clone #	Amino acid #																			
	4	6	11	22	24	29	31	36	50	55	80	97	102	**108**	116	117	157	164	189	192
Template	Q	C	I	S	N	N	V	T	C	M	Y	K	V	N	F	K	N	I	S	E
1														N						
2								*T*		I				N					C	
3						F	F							N						
4	*Q*	S												N						
5				C					S					N						
6			T		D									N						
7														N		R	D			
8											C			N				*I*		
9														N						G
10									Y					N	S					
11													A	N						
12												*K*		N						

Note: Silent mutations are in italics. Mutations of interest are in red.

From the list, clone #2 (M55I+S108N+S189C) and clone #10 (C50Y+S108N+F116S), designated *Pf*DHFR3m1 and *Pf*DHFR3m2 respectively, were selected for further study since their positions of mutation might be associated with drug resistance. The *Pf*DHFR3m1 mutant contained mutation at Met55, which was an amino acid at the entry of catalytic cleft [18] and corresponded to Phe31 of human DHFR that was reported to account for resistance to antifolate methotrexate in human colon cancer cell lines [19]. The *Pf*DHFR3m2 mutant contained mutations at Cys50, which was previously reported to be associated with a high level of pyrimethamine resistance in field isolates [20-21], and at Phe116, which was positioned around the entry of catalytic cleft of the enzyme [18]. Figures 1A and 1B show the positions of those mutations on the models of *Pf*DHFR3m1 and *Pf*DHFR3m2 superimposed on the double mutant *Pf*DHFR-TS (C59R+S108N) complexed with pyrimethamine. These two mutants were further assessed for their level of pyrimethamine resistance in the transgenic *P. berghei* model.

(A)

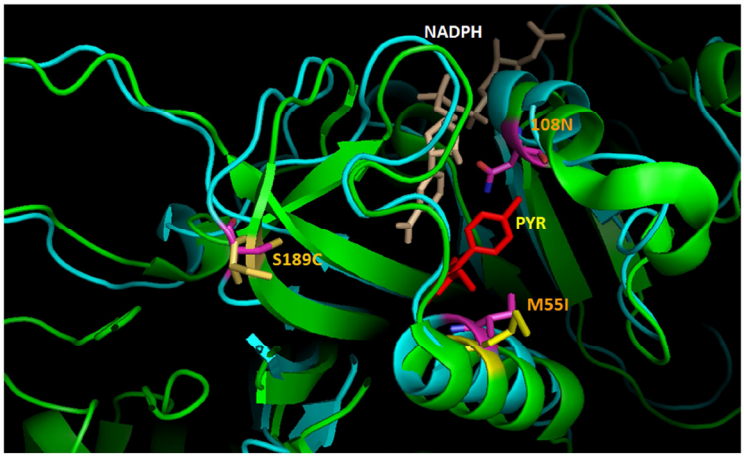

(B)

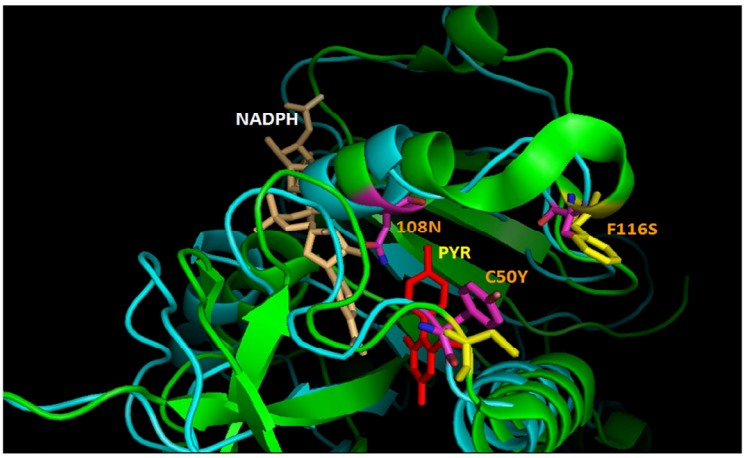

Figure 1. Superimposition of *Pf*DHFR(C59R+S108N)/NADPH/pyrimethamine complex (green - structure; yellow - amino acids) on (A) *Pf*DHFR3m1 (M55I+S108N+S189C) or (B) *Pf*DHFR3m2 (C50Y+S108N+F116S) (cyan – structure; pink - amino acids). Each image presents a clear visualisation, in different views, of the locations of amino acid of interest. The numbers indicate positions with mutation. The models were created by Geno3D program (http://geno3d-pbil.ibcp.fr). Figures were generated with PyMOL program [22].

Generation of Transgenic *P. berghei* Expressing *Pf*DHFR3m Mutants

Transgenic *P. berghei* parasites stably expressing *Pf*DHFR3m1 and *Pf*DHFR3m2, designated *PbPf*DHFR3m1 and *PbPf*DHFR3m2 respectively, were generated. Endogenous *Pbdhfr-ts* was replaced with either *Pfdhfr*3m1 or *Pfdhfr*3m2 mutant genes by double homologous recombination. The allelic replacement strategy is shown in Figure 2. Correct integration was investigated by PCR analysis on genomic DNA of the transgenic parasites using specific primer pairs. The expected 4.0- and 3.0-kb PCR products were obtained, thus confirming 5' and 3' integration respectively of the introduced *Pfdhfr*3m mutants replacing *Pbdhfr-ts* in the transgenic *P. berghei* (Figure 3A). Additional evidence for proper genomic integration was investigated by Southern analysis of digested genomic DNA of the transgenic parasites using a *Pfdhfr* probe (Figure 2). As shown in Figure 3B, a 4.8-kb band of *Eco*RI digested fragment confirmed the correct integration of *Pfdhfr*3m gene in the transgenic parasites. The digested plasmid DNA pY005^{S108N} control produced a 7.5-kb product while the digested genomic DNA of transgenic parasite PbGFP was used as negative control.

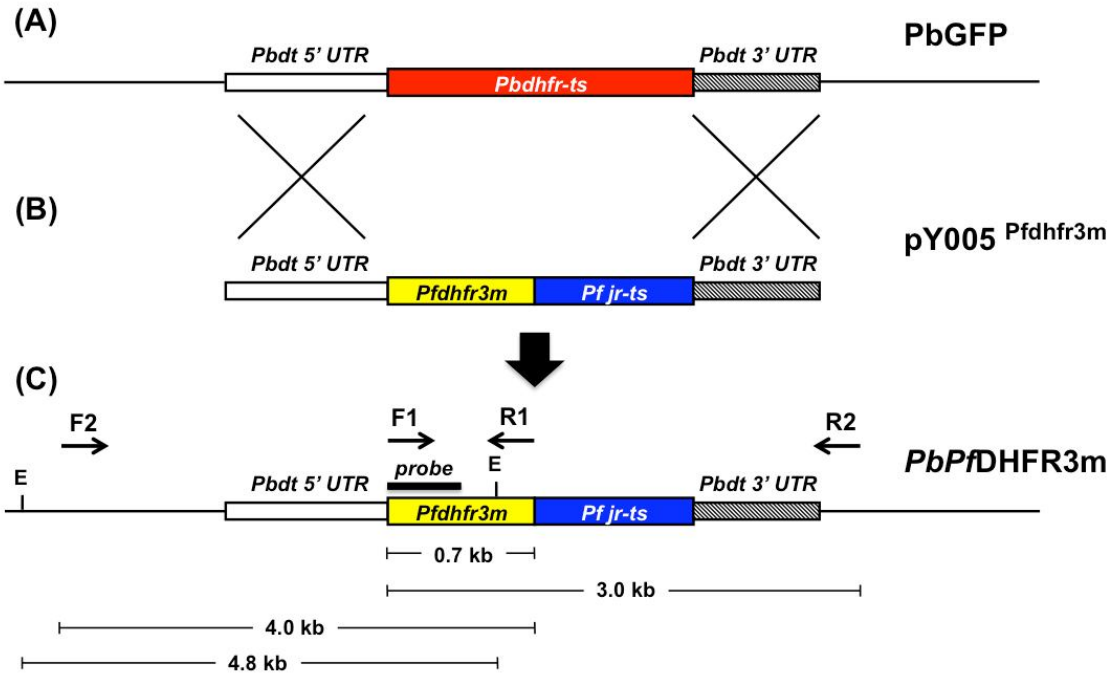

Figure 2. Double-crossover homologous recombination of *Pfdhfr-ts* into *Pbdhfr-ts* locus: (A) endogenous *Pbdhfr-ts* gene in PbGFP parasite; (B) linearised plasmid containing mutant *Pfdhfr3m* gene; (C) correct integration of the construct contributing to the replacement of mutant *Pfdhfr3m* gene. Positions of the primers used for PCR analysis are indicated by arrows. *Pfdhfr* probe is shown as solid bar. E represents *Eco*RI restriction site.

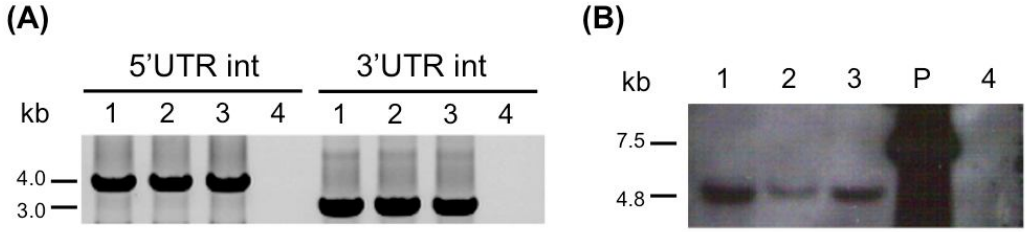

Figure 3. Genotype analysis of transgenic *P. berghei* expressing *Pf*DHFR3m mutants: (A) PCR analysis of 5' and 3' UTR integrations; (B) Southern analysis of transgenic parasites: *PbPf*S108N (1), *PbPf*DHFR3m1 (2) and *PbPf*DHFR3m2 (3), and genomic DNA of control parasite, PbGFP, as negative control (4). The pY005^{S108N} plasmid (P) serves as positive control in Southern analysis.

Growth Rate and Susceptibility to Pyrimethamine of Transgenic Parasites

The transgenic *PbPf*DHFR3m1 and *PbPf*DHFR3m2 parasites were infected into naive mice and the growth rates were compared with the parental PbGFP parasite. As shown in Figure 4, the growth rates of both transgenic parasites were not significantly different from each other or from the parental PbGFP parasite. Accumulation of 3 mutations in *Pf*DHFR expressed in the newly generated transgenic parasites in this study did not cause a significant defect to the function of *Pf*DHFR-TS in complementing endogenous *Pb*DHFR-TS. The ED_{50} values of pyrimethamine against the transgenic *PbPf*S108N [7], *PbPf*DHFR3m1 and *PbPf*DHFR3m2 parasites were 1.08 ± 0.23, 1.61 ± 0.70 and 1.07 ± 0.39 mg/kg respectively (Figure 5). The results showed that the combination of S108N mutation with M55I and S189C, or with C50Y and F116S mutations did not significantly confer a higher resistance to pyrimethamine compared with the starting S108N mutant as expected. Using the unpaired *t*-test to compare the means of the transgenic parasite clones with that of the parental *PbPf*S108N parasite clone, the *P*-values of *PbPf*DHFR3m1 and *PbPf*DHFR3m2 against *PbPf*S108N were 0.28 and 0.99 respectively.

The active site region of *Pf*DHFR contains amino acid residues that have earlier been identified by studies in other species as important in the activity of DHFR [6]. Methionine at position 55 of *Pf*DHFR corresponds to Phe31 of *h*DHFR and has been shown to be present in the active site region of DHFR [6, 23]. It was reported that the mutation of this Phe31 residue of *h*DHFR to Ser or Arg confers resistance to methotrexate [19] while variant isolates with mutations of F31L, F31V and F31T were not resistant to methotrexate [24-25]. Another report in yeast complementation system [4] demonstrated that an additional mutation of N51I+S108N with S189R in *Pf*DHFR increases resistance to pyrimethamine and a prodrug WR99210 at a level higher than a double mutant template. This effect may be related to the fact that Ser189 is within a region in close proximity to the key substrate or to the drug [26].

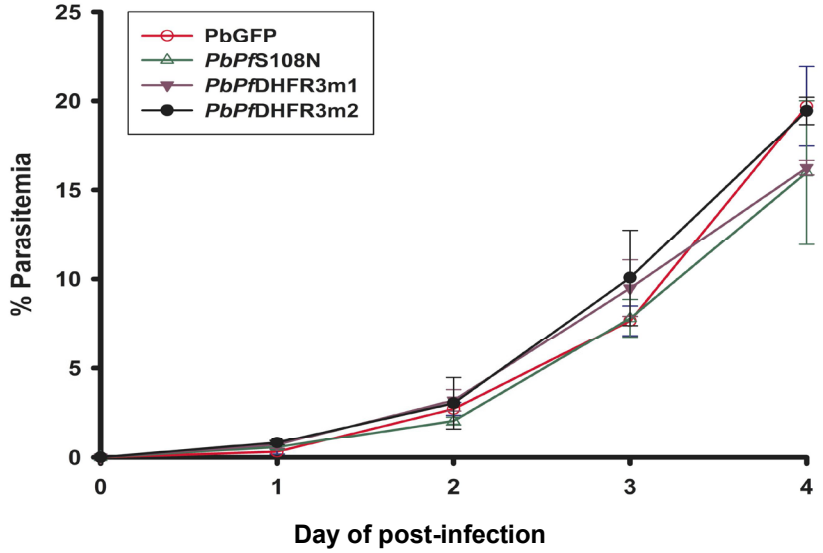

Figure 4. Growth profile of transgenic parasites expressing *Pf*DHFR mutant enzymes: parental PbGFP (red line), *PbPf*S108N (green line), *PbPf*DHFR3m1 (M55I+S108N+S189C) (purple line) and *PbPf*DHFR3m2 (C50Y+S108N+F116S) (black line). The experiments were performed in mice in three independent experiments and the data represent mean ± SD values.

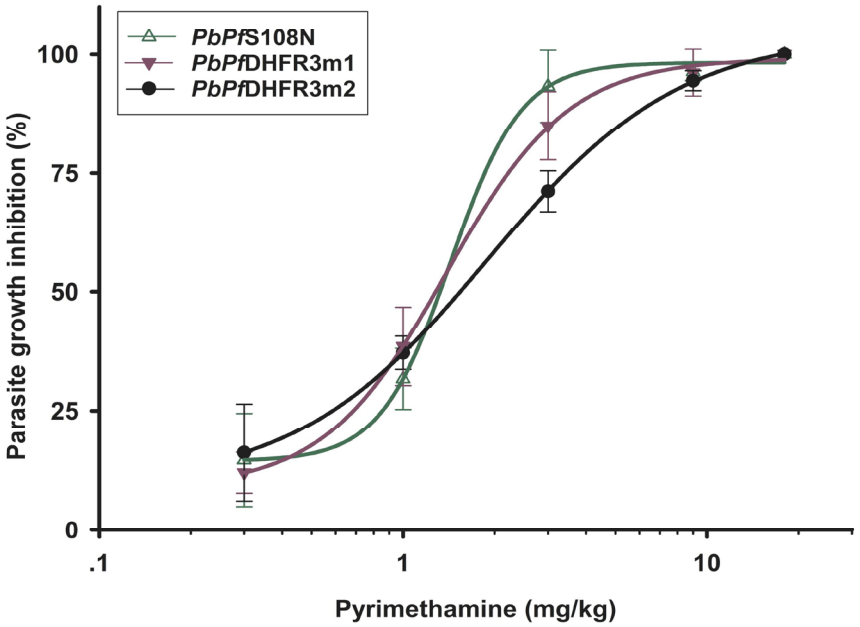

Figure 5. Pyrimethamine susceptibility profile of transgenic *PbPf*S108N, *PbPf*DHFR3m1 and *PbPf*DHFR3m2 parasites. The data represent mean ± SD of percentage of growth inhibition for 4 mice per group from three independent experiments. The average ED_{50} values of pyrimethamine against *PbPf*S108N [7], *PbPf*DHFR3m1 and *PbPf*DHFR3m2 are 1.08 ± 0.23, 1.61 ± 0.70 and 1.07 ± 0.39 mg/kg respectively. Using the unpaired *t*-test, the *P*-values of *PbPf*DHFR3m1 and *PbPf*DHFR3m2 against *PbPf*S108N are 0.28 and 0.99 respectively.

Cysteine at position 50 of *Pf*DHFR is located around the active site region of the enzyme [6]. Previous study on *Pf*DHFR random library in yeast complementation system [27] using a *Pf*DHFR triple mutant (N51I+C59R+S108N) as a template has identified a quadruple mutant C50S+N51I+C59R+S108N that confers resistance to chlorcycloguanil at a level higher than the quadruple mutant N51I+C59R+S108N+I164L, a common antifolate-resistant allele found in field isolates. In *E. coli* complementation system [11, 28], C50R mutation was identified from *Pf*DHFR quadruple mutation library selected by WR99210. The C50R mutation was also reported to confer resistance to sulfadoxine-pyrimethamine in Venezuela and Brazil [20-21]. There was no previous report revealing any mutations at Phe116 of *Pf*DHFR located on the entry of catalytic cleft of the enzyme in the field or any complementation systems. In this study, both transgenic *PbPf*DHFR3m1 and *PbPf*DHFR3m2 lines showed comparable pyrimethamine resistance level with the transgenic *P. berghei* line expressing *Pf*DHFR with mutation at S108N (*PbPf*S108N) previously reported by our group [7]. The results confirm that although additional mutations do not affect the function of the enzyme, a proper combination of mutations is required to confer resistance to the drug, which shows that the *Pf*DHFR mutant library expressed by our *P. berghei* surrogate model can be used as an appropriate model to study the drug resistance level and the evolution of *Pfdhfr* mutations in vivo. The only limitation of this system is host tolerance to the drug. If the animals could tolerate a high dose of drug without toxicity, selection of mutant clones with a higher level of drug resistance would be possible.

CONCLUSIONS

The power of random mutant library and transgenic parasite system to elucidate the functionality of resistant mutant parasites in real situation of *Plasmodium* species has been demonstrated. The approach adopted in this system sets to find and predict such mutations at different positions not only around or at the active sites, but also away from the enzyme catalytic region. Using a moderate drug-resistant $Pfdhfr^{S108N}$ mutant gene as template, a library of *Pfdhfr* mutants was generated and subsequently transfected and selected in *P. berghei* parasite. Two clones of major interest of transgenic *P. berghei* parasites *PbPf*DHFR3m1 (M55I+S108N+S189C) and *PbPf*DHFR3m2 (C50Y+S108N+F116S), expressing *Pf*DHFR with mutations at such positions, showed a similar level of growth rate and resistance to pyrimethamine with the parental transgenic *P. berghei* expressing *Pf*DHFR with mutation at S108N (*PbPf*S108N). The study has reconfirmed that this transgenic *P. berghei* model expressing a random mutant library is an effective model for studying the accumulation of *Pfdhfr* mutations in vivo. The approach of our system is very adaptable and can serve as a better tool than the complementation systems in mimicking possible mutations in nature. The approach can be applied during the development of new antifolates with better effective properties against drug-resistant parasites.

ACKNOWLEDGEMENTS

This work is financially supported by the UNICEF/UNDP/World Bank/WHO Special Programme for Research and Training in Tropical Diseases (TDR) (to C.U.), the Howard Hughes Medical Institute (HHMI, USA) (to S.K.), and the Faculty of Medicine Research Fund, Chiang Mai

University (to S.S. and W.T.). W.T. was in receipt of Thailand Graduate Institute of Science and Technology (TGIST) studentship. We thank Dr. Philip Shaw for sharing his experience in the course of this study and Dr. Deanpen Japrung for technical support.

REFERENCES

1. Y. Yuthavong, "Basis for antifolate action and resistance in malaria", *Microbes Infect.*, **2002**, *4*, 175-182.
2. I. M. Kompis, K. Islam and R. L. Then, "DNA and RNA synthesis: Antifolates", *Chem. Rev.*, **2005**, *105*, 593-620.
3. A. Gregson and C. V. Plowe, "Mechanisms of resistance of malaria parasites to antifolates", *Pharmacol. Rev.*, **2005**, *57*, 117-145.
4. J. T. Ferlan, S. Mookherjee, I. N. Okezie, L. Fulgence and C. H. Sibley, "Mutagenesis of dihydrofolate reductase from *Plasmodium falciparum*: analysis in *Saccharomyces cerevisiae* of triple mutant alleles resistant to pyrimethamine or WR99210", *Mol. Biochem. Parasitol.*, **2001**, *113*, 139-150.
5. S. Bunyarataphan, U. Leartsakulpanich, S. Taweechai, B. Tarnchompoo, S. Kamchonwongpaisan and Y. Yuthavong, "Evaluation of the activities of pyrimethamine analogs against *Plasmodium vivax* and *Plasmodium falciparum* dihydrofolate reductase-thymidylate synthase using in vitro enzyme inhibition and bacterial complementation assays", *Antimicrob. Agents Chemother.*, **2006**, *50*, 3631-3637.
6. J. Yuvaniyama, P. Chitnumsub, S. Kamchonwongpaisan, J. Vanichtanankul, W. Sirawaraporn, P. Taylor, M. D. Walkinshaw and Y. Yuthavong, "Insights into antifolate resistance from malarial DHFR-TS structures", *Nat. Struct. Biol.*, **2003**, *10*, 357-365.
7. W. Tipsuwan, S. Srichairatanakool, S. Kamchonwongpaisan, Y. Yuthavong and C. Uthaipibull, "Selection of drug resistant mutants from random library of *Plasmodium falciparum* dihydrofolate reductase in *Plasmodium berghei* model", *Malar. J.*, **2011**, *10*, 119.
8. A. F. Cowman, "Mechanisms of drug resistance in malaria", *Aust. New Zealand J. Med.*, **1995**, *25*, 837-844.
9. C. J. Janse, B. Franke-Fayard and A. P. Waters, "Selection by flow-sorting of genetically transformed, GFP-expressing blood stages of the rodent malaria parasite, *Plasmodium berghei*", *Nat. Protoc.*, **2006**, *1*, 614-623.
10. B. Franke-Fayard, H. Trueman, J. Ramesar, J. Mendoza, M. van der Keur, R. van der Linden, R. E. Sinden, A. P. Waters and C. J. Janse, "A *Plasmodium berghei* reference line that constitutively expresses GFP at a high level throughout the complete life cycle", *Mol. Biochem. Parasitol.*, **2004**, *137*, 23-33.
11. S. Chusacultanachai, P. Thiensathit, B. Tarnchompoo, W. Sirawaraporn and Y. Yuthavong, "Novel antifolate resistant mutations of *Plasmodium falciparum* dihydrofolate reductase selected in *Escherichia coli*", *Mol. Biochem. Parasitol.*, **2002**, *120*, 61-72.
12. L. Giver, A. Gershenson, P. O. Freskgard and F. H. Arnold, "Directed evolution of a thermostable esterase", *Proc. Natl. Acad. Sci. USA*, **1998**, *95*, 12809-12813.
13. C. J. Janse, J. Ramesar and A. P. Waters, "High-efficiency transfection and drug selection of genetically transformed blood stages of the rodent malaria parasite *Plasmodium berghei*", *Nat. Protoc.*, **2006**, *1*, 346-356.
14. A. P. Waters, A. W. Thomas, M. R. van Dijk and C. J. Janse, "Transfection of malaria parasites", *Methods*, **1997**, *13*, 134-147.
15. E. M. Southern, "Detection of specific sequences among DNA fragments separated by gel electrophoresis", *J. Mol. Biol.*, **1975**, *98*, 503-517.
16. W. Peters and B. L. Robinson, "Malaria", in "Handbook of Animal Models of Infection" (Ed. O. Zak and M. A. Sande), Academic Press, New York, **1999**, pp.757-773.

17. P. C. Cirino, K. M. Mayer and D. Umeno, "Generating mutant libraries using error-prone PCR", *Methods. Mol. Biol.*, **2003**, *231*, 3-9.
18. T. Lemcke, I. T. Christensen and F. S. Jorgensen, "Towards an understanding of drug resistance in malaria: Three-dimensional structure of *Plasmodium falciparum* dihydrofolate reductase by homology building", *Bioorg. Med. Chem.*, **1999**, *7*, 1003-1011.
19. B. I. Schweitzer, S. Srimatkandada, H. Gritsman, R. Sheridan, R. Venkataraghavan and J. R. Bertino, "Probing the role of two hydrophobic active site residues in the human dihydrofolate reductase by site-directed mutagenesis", *J. Biol. Chem.*, **1989**, *264*, 20786-20795.
20. K. F. Vasconcelos, C. V. Plowe, C. J. Fontes, D. Kyle, D. F. Wirth, L. H. Pereira da Silva and M. G. Zalis, "Mutations in *Plasmodium falciparum* dihydrofolate reductase and dihydropteroate synthase of isolates from the Amazon region of Brazil", *Mem. Inst. Oswaldo. Cruz.*, **2000**, *95*, 721-728.
21. L. Urdaneta, C. Plowe, I. Goldman and A. A. Lal, "Point mutations in dihydrofolate reductase and dihydropteroate synthase genes of *Plasmodium falciparum* isolates from Venezuela", *Am. J. Trop. Med. Hyg.*, **1999**, *61*, 457-462.
22. R. Wernersson, K. Rapacki, H. H. Staerfeldt, P. W. Sackett and A. Molgaard, "FeatureMap3D– a tool to map protein features and sequence conservation onto homologous structures in the PDB", *Nucleic Acids Res.*, **2006**, *34*, W84-W88.
23. J. P. Volpato and J. N. Pelletier, "Mutational 'hot-spots' in mammalian, bacterial and protozoal dihydrofolate reductases associated with antifolate resistance: Sequence and structural comparison", *Drug Resist. Updat.*, **2009**, *12,* 28-41.
24. N. J. Prendergast, J. R. Appleman, T. J. Delcamp, R. L. Blakley and J. H. Freisheim, "Effects of conversion of phenylalanine-31 to leucine on the function of human dihydrofolate reductase", *Biochem.*, **1989**, *28*, 4645-4650.
25. S. K. Chunduru, V. Cody, J. R. Luft, W. Pangborn, J. R. Appleman and R. L. Blakley, "Methotrexate-resistant variants of human dihydrofolate reductase. Effects of Phe31 substitutions", *J. Biol. Chem.*, **1994**, *269*, 9547-9555.
26. D. C. Warhurst, "Antimalarial drug discovery: development of inhibitors of dihydrofolate reductase active in drug resistance", *Drug Discov. Today*, **1998**, *3*, 538-546.
27. E. G. Hankins, D. C. Warhurst and C. H. Sibley, "Novel alleles of the *Plasmodium falciparum dhfr* highly resistant to pyrimethamine and chlorcycloguanil, but not WR99210", *Mol. Biochem. Parasitol.*, **2001**, *117*, 91-102.
28. D. Japrung, U. Leartsakulpanich, S. Chusacultanachai and Y. Yuthavong, "Conflicting requirements of *Plasmodium falciparum* dihydrofolate reductase mutations conferring resistance to pyrimethamine-WR99210 combination", *Antimicrob. Agents Chemother.*, **2007**, *51*, 4356-4360.

Maejo Int. J. Sci. Technol. **2011**, *5*(03), 413-425

Maejo International Journal of Science and Technology

ISSN 1905-7873
Available online at www.mijst.mju.ac.th

Full Paper

Culture condition, inoculum production and host response of a wild mushroom, *Phlebopus portentosus* strain CMUHH121-005

Naritsada Thongklang [1], Kevin D. Hyde [2, 3], Boonsom Bussaban [1] and Saisamorn Lumyong [1,*]

[1] Department of Biology, Faculty of Science, Chiang Mai University, Chiang Mai 50200, Thailand
[2] School of Science Mae Fah Luang University, Chiang Rai 57100, Thailand
[3] Botany and Microbiology Department, College of Science, King Saud University, Riyadh, Saudi Arabia

* Corresponding author, e-mail: scboi009@chiangmai.ac.th

Received: 7 July 2010 / Accepted: 15 November 2011 / Published: 9 December 2011

Abstract: The optimal media and growth conditions of an edible wild mushroom, *Phlebopus portentosus* strain CMUHH121-005, were investigated for inoculum production. The optimum temperature for mycelial growth was 30ºC and the optimum pH was 4.0. Malt extract and yeast extract as carbon and nitrogen sources respectively, with a C:N ratio of 10:1, were most suitable. The biomass production in 16 types of cereal grain media was investigated. The fungus was found to grow best in barley grain mixed with Murashige and Skoog solution over 30 days following inoculation. Further incubation at 30°C for 60 days in the dark caused numerous agglomerations of mycelia as if fruiting bodies were being formed. The data presented provide growth requirements that will be useful in a future development of *P. portentosus* as a cultivatable mycorrhizal mushroom.

Keywords: *Phlebopus portentosus*, mushroom cultivation, mycorrhizae, mushroom inoculum

INTRODUCTION

The edible wild mushroom *Phlebopus portentosus* belongs to the order Boletales and in Thailand is commonly known as *hed har* or *hed tubtaodum*. It is a highly sought-after and valued edible mushroom, especially in northern and north-eastern Thailand [1]. It forms ectomycorrhizal associations with host plants such as elaeocarpus (*Elaeocarpus hygrophilus*), jambul (*Syzygium cumini*), longan (*Dimocarpus longan*) and giant mimosa (*Mimosa pigra*) [2] and is sold as a tree inoculum [3].

Ectomycorrhizal fungi are difficult to cultivate as they need to grow in association with their host. However, *Phlebopus portentosus* is unusual among the Boletales and possibly most mycorrhzal fungi as it produces clamp connections and can be easily isolated in culture. It thus has the potential to produce fruiting bodies in vitro and to be a cultivatable species without a host plant [4]. Because it is easy to isolate and can grow readily in culture it is also possible to inoculate various hosts with this fungus and these associations improve host growth and health. Furthermore, since many of its hosts are fruit trees, the establishment of a symbiosis with *P. portentosus* may increase fruit yield and result in a yearly mushroom yield of considerable value.

Most cultivatable mushrooms have specific requirements for growth in axenic culture [5-10]. The main factors affecting growth are nutrient sources and environmental factors such as temperature and pH [11-14]. The media generally contain a carbon source, nitrogen source and vitamins. The carbon source is especially important and should be in greater quantities than other essential nutrients, and generally in the range of 3-28% [15]. Mushrooms can be grown on different carbon sources such as glucose, galactose, mannose, fructose, sucrose, cellulose, dextrin and starch [15-18]. Nitrogen sources such as ammonium nitrate, calcium nitrate, yeast extract, soya bean, arginine and glutamic acid have been used to promote mycelium growth [10, 15-17]. The optimum temperature and pH of mycelial growth varies with the strain or species of mushroom. For example, *Volvariella volvacea* grows well at 35°C, *Pleurotus eryngii* at 25°C, *Pleurotus ostreatus* and *Pleurotus pulmonarius* at 30°C, *Agrocybe aegerita* at 25°C or 30°C, *Lentinus strigosus* at 35°C and *Lentinula edodes at* 20°C or 30°C [13-20]. Yamanaka [13] reported that the optimum pH of ammonia fungi, saprobic mushrooms and mycorrhiza mushrooms are pH 7, 7-8 and 5 or 6 respectively. *Phlebopus portentosus* CMU 2210 grows well on modified Gamborg medium over 26 days and the optimum condition for growth is 30°C and pH 4 [21]. The work by Sanmee et al. [21] did not establish a suitable strain for cultivation since the fruiting bodies produced in vitro were deformed when compared to natural basidocarps.

Production of many ectomycorrhizal and cultivated mushroom inocula (spawn) frequently involves using cereal grains such as millet, wheat, corn, rice, barley [22-23], sawdust + barley grain and sawdust + rice grain [24] or sorghum grain as the substrate [2]. The advantages of cereal-grain-based media are production in large scale due to their general low cost and ease of handling [25].

In this study, fast-growing strain selection, culture conditions for mycelial growth, and evaluation of suitable solid media for growth of selected *P. portentosus* strains are investigated for better inoculum production.

MATERIALS AND METHODS

Fungal Strain Isolation and Preparation of Starting Culture

Fruiting bodies of *P. portentosus* were collected from different sites in Chiang Mai, Lamphun and Chiang Rai provinces, Thailand. Their morphological structure was recorded. Dried specimens were numbered in sealed plastic bags with silica gel and deposited in the herbarium of the Laboratory of Applied Microbiology, Department of Biology, Chiang Mai University.

Mycelia were isolated from the fruiting bodies and cultured on potato dextrose agar (PDA) medium (Labscan Asia Co.,Ltd, Thailand). The pure cultures were named as CMUHH in a code series and the colony diameters were measured. CMUHH121-005 grew faster than other isolates and was chosen as a presentative strain for investigating a suitable basal growth medium. It was grown on 12 types of agar media, viz. corn meal agar, glucose peptone yeast extract agar, malt extract agar, oat meal agar, potato carrot agar, potato dextrose agar (PDA), potato sucrose agar [26], Fries agar, Murashige & Skoog (MS) agar medium [27], fungus-host medium [28], modified Gamborg medium [21], and modified Schenk & Hildebrandt medium [29]. All cultures were incubated at 30°C for 21 days. Colony morphology and dry weight were recorded at 3-day intervals during incubation. Stock cultures were kept on PDA slants at 4°C.

A mycelium plug (0.5-mm diameter) of *P. portentosus* CMUHH121-005 grown on PDA for 14 days was inoculated in Murashige & Skoog (MS) agar medium. All cultures were incubated at 30°C in the dark.

Effect of Temperature and pH

MS agar medium plates were centrally inoculated with mycelial plugs of approximately 0.5-mm diameter cut from an actively growing mycelia colony and incubated at 20, 25, 30, 37, 40 and 45°C. The medium was melted and washed away with hot water, leaving the fungal mycelia. Growth of the mycelia was evaluated by determination of dry weight in triplicate every 3 days.

The optimal pH was evaluated in MS medium broth that was adjusted to pH 2, 4, 4.5, 5, 5.5, 6, 6.5, 7, 8 and 10 with 1N HCl or 1N NaOH before autoclaving. The MS broth (50 ml) was inoculated with a mycelial plug of approximately 0.5 mm in diameter from an actively growing mycelia colony. All cultures were incubated at 30°C, followed by incubation on a rotary shaker at 140 rpm in the dark. Mycelial growth was evaluated by dry weight determination every 3 days for 14 days. The experiment was conducted in triplicate.

Effect of Different Carbon and Nitrogen Sources

In the testing of different carbon sources, MS agar media (without glucose) was supplemented separately with a 3% (w/v) carbon source comprising one of the following: glucose, fructose, sucrose, starch or malt extract. The pH of the medium was adjusted to 4 with 1N HCl. All cultures were incubated at 30°C in the dark. The medium was melted and washed away with hot water, leaving the fungal mycelia. Mycelial growth was evaluated by determination of the dry weight every 3 days for 21 days. The experiment was done in triplicate.

In the testing of different nitrogen sources, MS agar media (without NH_4NO_3) was supplemented separately with a 3.55% (w/v) nitrogen source comprising one of the following: NH_4NO_3, KNO_3, NH_4NO_3 + KNO_3, peptone, or yeast extract. The pH of the medium was adjusted to 4 with 1N HCl. All cultures were incubated at 30°C in the dark. The medium was melted and washed away with hot water, leaving the fungal mycelia. Mycelial growth was evaluated by determination of the dry weight every 3 days for 21 day. The experiment was done in triplicate.

Effect of C:N Ratio

The best carbon and nitrogen sources (malt extract and yeast extract respectively) were mixed up in a ratio of 1:1, 1:2, 1:3, 1:10, 2:1, 3:1 and 10:1. Each medium was adjusted to pH 4 with 1N HCL. Five ml of the MS broth was inoculated with a mycelium plug of approximately 0.5 mm in diameter from the actively growing mycelia colony. All cultures were incubated at 30°C, followed by incubation on a rotary shaker at 140 rpm in the dark. Mycelial growth of was evaluated by dry weight determination after 7 days. The experiment was done in triplicate.

Effect of Cereal Media for Inoculum Production

Sixteen types of cereal media were used as substrates for mycelial growth (Table 1). Tissue culture bottles containing 100 g of each medium were inoculated with 3 mycelial plugs of approximately 0.5 cm in diameter from the actively growing mycelia colony. The cultures were incubated in the dark at room temperature and growth rate was estimated from the linear expansion of mycelia growing through the medium. The experiment was done in triplicate.

Table 1. Growth of *P. portentosus* CMUHH121-005 on various cereal grain media

Cereal grain media	Ratio	Growth of mycelia (days*)
Sorghum grain	-	70.00±1.00
Barley grain	-	55.67±0.58
Corn grain	-	95.00±1.00
Wheat grain	-	89.33±0.58
Sorghum grain: barley grain: wheat grain	1:1:1	89.33±0.58
Green bean peel: water	10: 3	No growth
Green bean	-	74.67±0.58
Ground nut peel: water	10: 3	72.00±0.00
Ground nut peel: MS solution (modified from MS agar)	10: 3	59.67±0.58
Barley grain: MS solution	100: 1	41.00±1.00
Barley grain: MS solution	10: 3	30.33±0.58
Barley grain: sawdust: MS solution	5: 5: 3	60.67±0.58
Barley grain: sawdust: MS solution	5: 1: 1	50.00±1.00
Barley grain: synthetic solution [24]	10: 3	44.67±0.58
Barley grain: sawdust: synthetic solution	5: 5: 3	120.00±1.00
Barley grain: sawdust: synthetic solution	5: 1: 1	120.33±0.58

* no. of days for mycelia to cover all of cereal grain medium in the container

Host Responce to Fungal Inoculum

Four host plant seedlings (*Elaeocarpus hygrophilus* Kurz, *Adenanthera pavonina* L., *Clausena lansium* (Lour) Skeels, and *Sauropus androgynus* Merr.) were grown in pots filled with sterile soil mixed with sand in the ratio of 2:1 (w/w) and were inoculated with 25 g of *P. portentosus* CMUHH121-005 inoculum and incubated in an open green house. The pots were watered everyday for 6 months. Root infection was determined once every month after staining with trypan blue and examining under light microscope [29].

RESULTS AND DISCUSSION

Strain Isolation and Selection

Twenty two basidiocarp samples associated with different host plants were collected from forests, orchards, roadsides and other locations (Figure 1). They were observed to have different characteristics (Figure 2). Each isolated strain was grown on PDA and incubated in culture for 14 days. Strain CMUHH 121-005, isolated from a basidiocarp sample bought from a roadside market in Wiang Pa Pao district, Chiang Rai province, grew faster than other isolates (data not shown) based on colony diameter. This strain was selected for further study. Among the 12 media tested, the strain grew in all media at different rates (Figure 3). The fastest growth rate was observed when the isolate was grown on MS agar medium, with the colony reaching 8 cm in diameter after 21 days (data not shown). It is unusual amongst mycorrhizal fungi as it can be isolated and cultured in agar media and forms clamp connections in the media (Figure 1d). With the discovery that the taxon can be cultivated, there has been avid interest in trying to cultivate this species at an industrial scale [21]. It is also believed that the taxon can form mycorrhizal association with various trees including some fruit trees and thus has potential to be 'farmed' as a mycorrhizal edible fungus (Figure 1b).

Effect of Temperature and pH on Mycelial Growth

Mycelia of *P. portentosus* CMUHH 121-005 grew in the range of 20–37°C, but did not grow at 40 or 45°C (Table 2). Optimal dry growth weight occurred at 30°C with an average dry growth weight of 0.2050 g in 21 days.

Various cultivated mushrooms have different temperature optima (e.g. *Volvariella volvacea* at 35°C, *Pleurotus eryngii* at 25°C [19]), while the temperature for optimum growth of *P. portentosus* CMUHH121-005 is 30°C. This makes sense as the fruiting bodies of this fungus are produced from May to July when the air temperature ranges between 23-34°C [30].

Strain CMUHH121-005 grew very slowly at pH 2, 6, 6.5, 7, 8 and 10 (Table 2). The optimal pH was 4-5.5, with a maximum average dry weight of 0.0959 g at pH 4 in 14 days. These results agree with reports on other mycorrhizal species. Niitsu et al. [31] reported the optimum pH of 4 for the growth of *Mycena chlorophos* while most other mushrooms produce fruiting bodies in neutral or slightly acidic pH of 6-7 [32-33]. Many ectomycorhizal mushrooms grow at acidic pH [34].

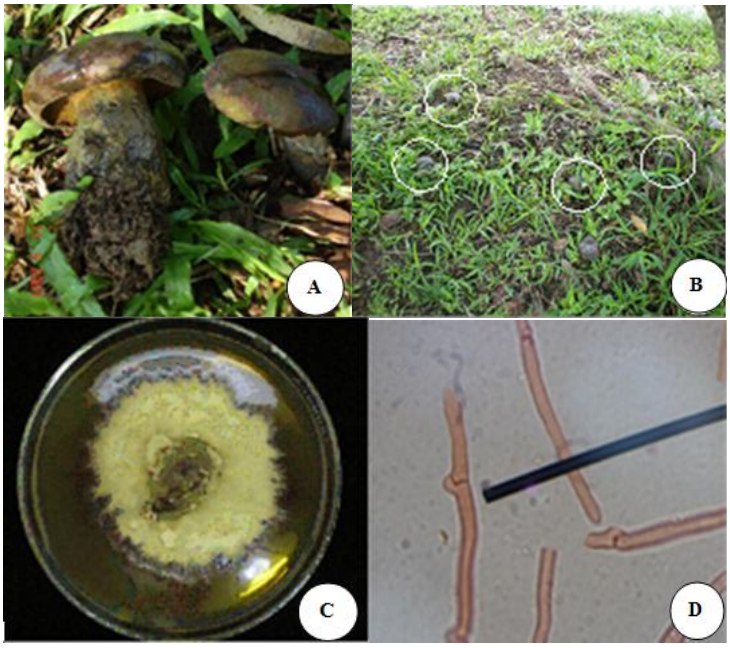

Figure 1. *Phlebopus portentosus*: A) olive brown to dark olive brown fruit body; B) fruit-body forming associate with host plant; C) mycelium growth on medium; D) clamp connection of *P. portentosus* in medium

Figure 2. Different macrocharacteristics of *P. portentosus*

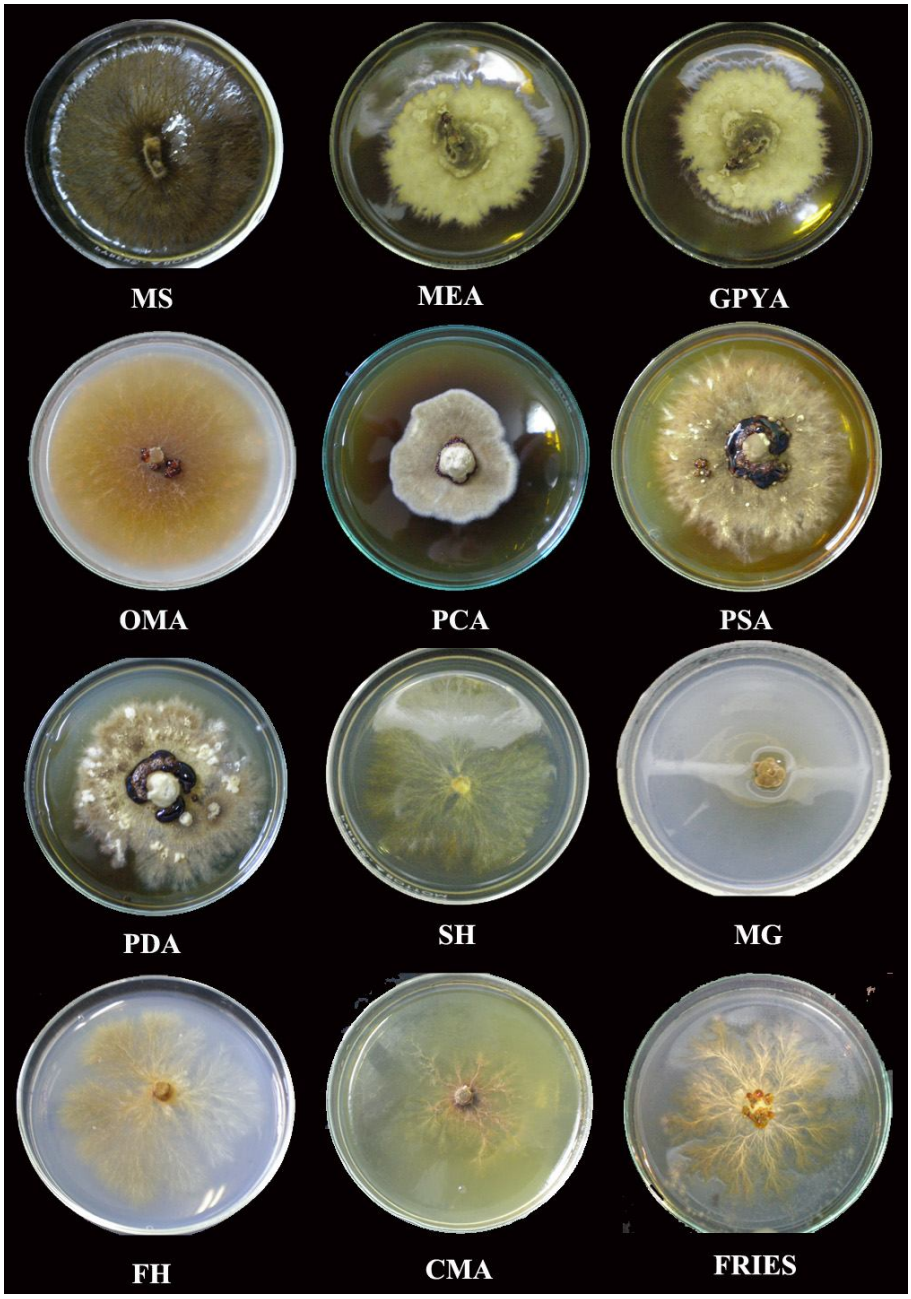

Figure 3. Mycelial growth on various solid media when incubated for 21 days at 30°C (MS = Murashige & Skoog agar, MEA = malt extract agar, GPYA = glucose-peptone-yeast extract agar, OMA = oat meal agar, PCA = potato carrot agar, PSA = potato sucrose agar, PDA = potato dextrose agar, SH = modified SH medium, MG = modified Gamborg, FH = fungus-host medium, CMA = corn meal agar, FRIES = Fries agar)

Effect of Carbon and Nitrogen Sources on Mycelial Growth

Phlebopus portentosus CMUHH 121-005 was observed to grow in all media at varying rates. Maximum growth occurred on malt extract agar (Table 2). The average dry growth weight was 0.2868 g in 21 days. The strain also grew well in starch with 0.1583 g dry weight of mycelia produced. The lowest growth occurred on media supplemented with glucose, sucrose and fructose (0.0925 g, 0.1004 g and 0.1128 g respectively).

Carbon is an essential nutrient needed by fungi and affects mycelial growth. *Pleurotus ostreatus*, for example, grows well on medium that contains millet extract [10] while broth media that contain dextrose are good for *Pleurotus florida* mycelial growth [17]. Jonathan and Fasidi [15] reported that the edible mushroom *Psathyerella atroumbonata* grows well on glucose. Growth of *P. portentosus* CMUHH121-005, on the other hand, was observed to be significantly enhanced in MS medium that contained 3% malt extract in this study.

Table 2. Dry weight of mycelium grown in axenic culture under various conditions for 21 days

Parameter	Dry weight + Standard error (g)
Temp (°C)	
20	0.0229±0.0008^{c}
25	0.1043±0.0112^{b}
30	**0.2050±0.0104^{a}**
37	0.1241±0.0103^{b}
40	0.0000±0.0000^{c}
45	0.0000±0.0000^{c}
pH	
2	0.0020±0.0001^{c}
4	**0.0959±0.0027^{a}**
4.5	0.0928±0.0016^{ab}
5	0.0915±0.0015^{ab}
5.5	0.0869±0.0018^{b}
6	0.0081±0.0001^{c}
6.5	0.0062±0.0002^{c}
7	0.0027±0.0004^{c}
8	0.0020±0.0002^{c}
10	0.0020±0.0002^{c}
Carbon source	
Glucose	0.0925±0.0038^{c}
Malt extract	**0.2868±0.0165^{a}**
Sucrose	0.1004±0.0046^{c}
Fructose	0.1128±0.0056^{c}
Starch	0.1583±0.0009^{b}

Table 2. (Continued)

Parameter	Dry weight + Standard error (g)
Nitrogen source	
NH_4NO_3	0.1550±0.0037[b]
KNO_3	0.1413±0.0107[b]
Yeast extract	**0.3273±0.0213[a]**
Peptone	0.2939±0.0085[a]
NH_4NO_3+KNO_3	0.1241±0.0103[b]
C:N ratio	
1:1	0.0108±0.0056[b]
1:2	0.0139±0.0015[b]
1:3	0.0224±0.0081[b]
3:1	0.0188±0.0073[b]
2:1	0.0121±0.0017[b]
1:10	0.0074±0.0009[b]
10:1	**0.1035±0.0197[a]**

Note: Values with the same letter are not significantly different (p=0.05) according to Tukey's multiple range test.

Inorganic nitrogen such as NH_4NO_3, KNO_3 and NH_4NO_3+KNO_3 were poor sources of nitrogen for growth of the CMUHH121-005 strain. The best mycelia growth was found in the medium that contained organic nitrogen, viz. yeast extract and peptone, with an average dry mycelial weight of 0.3273 g and 0.2939 g respectively in 21 days (Table 2). Hatakeyama and Ohmasa [16] reported that ammonium tartrate was the best nitrogen source for *Boletinus* sp. On the other hand, *Pleurotus florida* grew well on a basal medium that contained casein, which was better than the basal medium that contained urea, yeast extract and peptone [17]. The optimal C:N ratio for growth of mycelium also seems to depend on the fungal species. A suitable C:N ratio for *P. florida* was 5:3 [17] while Jonathan and Fasidi [15] reported that a suitable C:N ratio for *Psathyerella atroumbonata* was 2:3. In this study, *Phlebopus portentosus* grew best in MS medium with a C:N ratio of 10:1 (Table 2).

Effect of Cereal Media on Inoculum Production

In the cultivation of many mushrooms, inocula comprising cereal grains such as sawdust + barley grain, sawdust + rice grain, and sorghum grain are frequently used [2, 24]. Cereal-grain-based media are advantageous for large scale production as the cost is low and the media are easy to manage [25]. This study confirms that the fungus can grow in all types of media except green bean peel (Table 1). Optimal growth was found in barley grain mixed with MS solution. After further incubation at 30°C over 60 days in the dark, numerous primordia-like structures were formed (Figure 4), although no fully-formed fruiting bodies developed. Other strains of *P. portentosus* grew

well on sorghum grain media [2]. Kawagishi et al. [35] reported that *Tricholoma matsutake* grew better when D-isoleucine was added to the media.

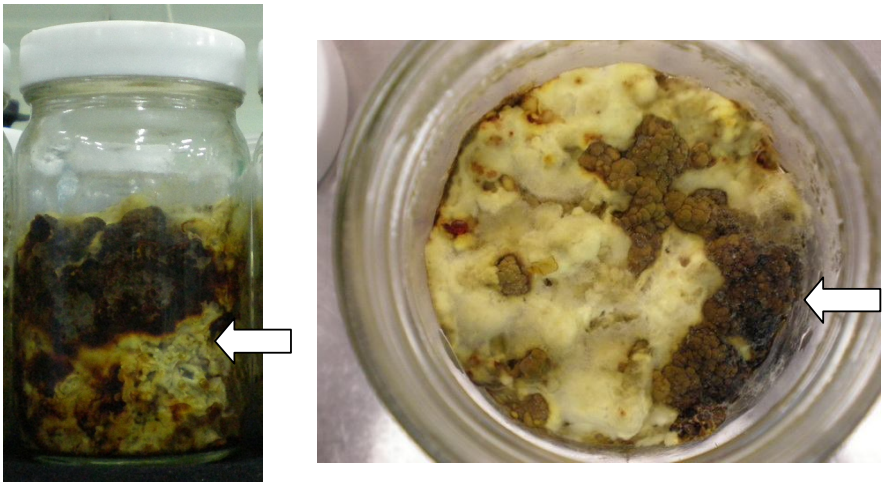

Figure 4. Primordia-like structures of *P. portentosus* (strain CMU121-005) in barley grain mixed with MS solution when incubated in the dark at 30°C for 90 days

Host Response for Fungal Inoculum

Inoculation of four plant species with the fungus resulted in root associations only in *Elaeocarpus hygrophilus* after 6 months. Mycelial infection of the host roots was observed under a stereo microscope, although a mantle sheath was not observed (Figure 5). The effect of inoculating the hosts with *P. portentosus* needs to be better evaluated since it was not clear in this experiment if the host really formed a mycorrhizal association with the fungus. It is also desirable to establish whether inoculating the host plants with this mushroom results in a continuous future production of the fruiting bodies. Some researchers have succeeded in inoculating different hosts in pots with different strains of this mushroom [4, 21].

CONCLUSIONS

Optimal conditions for mycelial growth are important when inducing fruiting body formation in vitro on solid media without the host plant. As yet we have not managed to obtain fruiting bodies of *P. portentosus* CMUHH 121-005 in vitro. However, by providing data on conditions for optimum growth, it is expect that it will eventually be possible to achieve this aim. Growth in culture may lead to commercialisation of the fungus. Pure cultures of the fungus can be established in cereal media that can then be used as inocula for saplings in nurseries or even established orchards so that fruit farmers can reap the reward of a mushroom in addition to the fruit harvest.

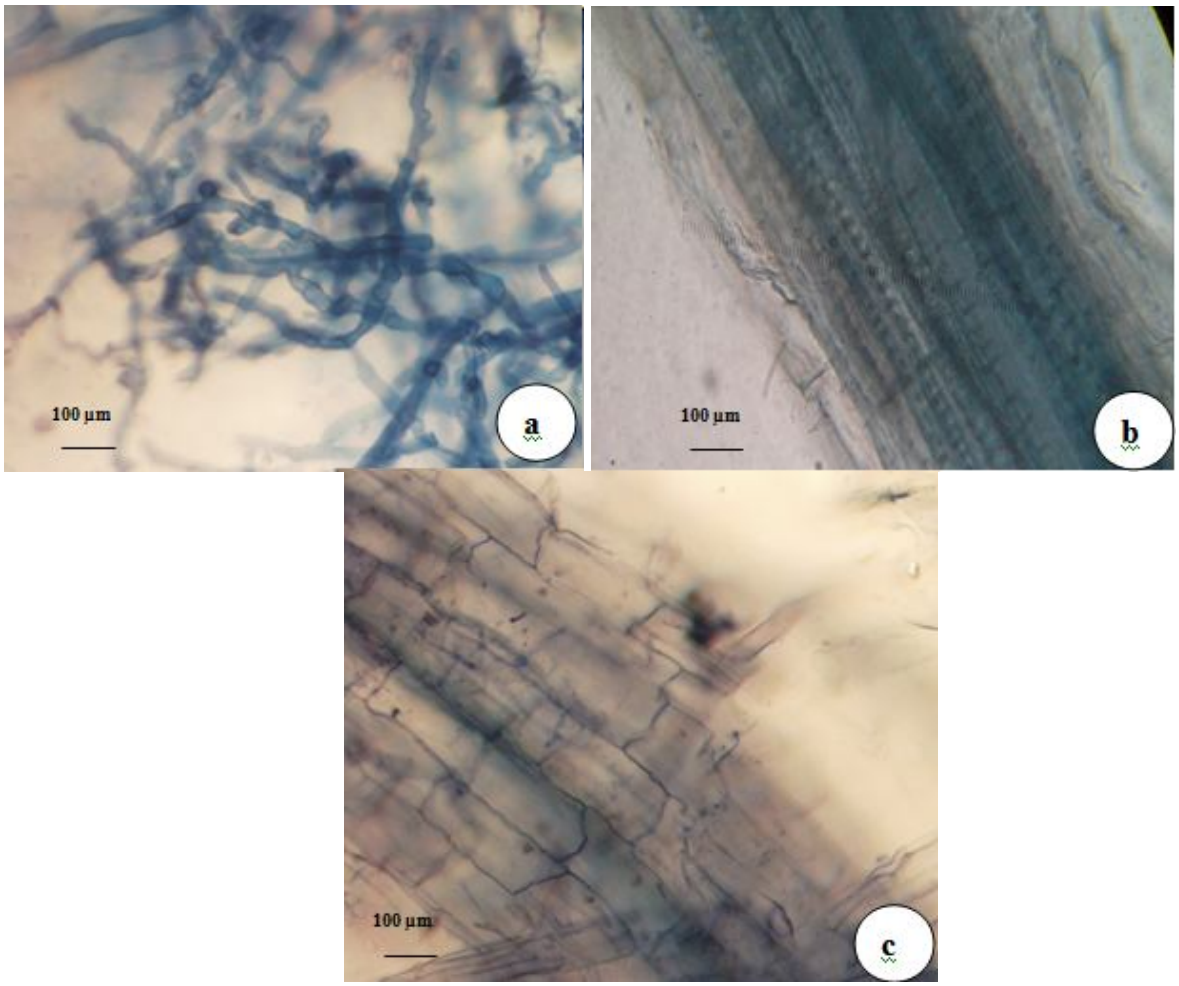

Figure 5. a) *P. portentosus* mycelia; b) and c) root infection, 6 months after inoculation with *P. portentosus* CMUHH121-005 in *E. hygrophilus*

ACKNOWLEDGEMENTS

The Graduate School of Chiang Mai University is thanked for providing financial support and the Department of Biology of Chiang Mai University is acknowledged for providing facilities. Preparation of this manuscript was partially supported by the 'Value-added products from basidiomycetes: putting Thailand's biodiversity to use' project (BRN049/2553) and the Commission on Higher Education, National Research University Program.

REFERENCES

1. R. Sanmee, B. Dell, P. Lumyong, K. Izumori and S. Lumyong, "Nutritive value of popular wild edible mushrooms from Northern Thailand", *Food Chem.*, **2003**, *82*, 527-532.
2. S. Lumyong, R. Sanmee and P. Lumyong, "Is large scale cultivation of boletes possible?", *Opera Mycol.*, **2007**, *1*, 34-37.

3. Agriculture Technology Training Club, "Hed Tub Tao off-season selling" (in Thai), http://www.thaiagro.com/index_library_detail.php?show=196 (accessed: March 2010).
4. K. P. Ji, C. X. Zhang, Y. Zeng, C. F. Liu, M. X. He and W. B. Wang, "Artificial fungal colony and its fruiting of *Phlebopus portentosus* (Boletaceae) in pot", *Acta Bot. Yunn.*, **2007**, *29*, 554-558.
5. S. T. Chang and T. H. Quimio, "Tropical Mushrooms: Biological Nature and Cultivation Methods", The Chinese University Press, Hong Kong, **1982**.
6. P. Stamets and J. S. Chilton, "The Mushroom Cultivator: A Practical Guide to Growing Mushrooms at Home", Agarikon Press, Washington, **1985**.
7. G. Nasim, S. H. Malik, R. Bajwa, M. Afzal and S. W. Mian, "Effect of three different culture media on mycelia growth of oyster and Chinese mushrooms", *J. Biol. Sci.*, **2001**, *1*, 1130-1133.
8. T. Sangtiean and S. Schmidt, "Growth of subtropical ECM fungi with different nitrogen sources using a new floating culture technique", *Mycol. Res.*, **2002**, *106*, 74-85.
9. B. S. Inglet, M. Song, C. L. Hansen and S. Hwang, "Cultivation of *Lentinus edodes* mycelia using whey permeate as an alternative growth substrate", *J. Dairy Sci.*, **2006**, *89*, 1113-1115.
10. V. I. Lbekwe, P. I. Azubuike, E. U. Ezeji and E. C. Chinakwe, "Effects of nutrient sources and environmental factors on the cultivation and yield of oyster mushroom (*Pleurotus ostreatus*)", *Pakistan J. Nutr.*, **2008**, *7*, 349-351.
11. L. L. Hung and J. M. Trappe, "Growth variation between and within species of ectomycorrhizal fungi in response to pH *in vitro*", *Mycologia*, **1983**, *75*, 234-241.
12. M. O. Garraway and R. C. Evans, "Fungal Nutrition and Physiology", Wiley, New York, **1984**.
13. T. Yamanaka, "The effect of pH on the growth of saprotrophic and ectomycorrhizal ammonia fungi *in vitro*", *Mycologia*, **2003**, *95*, 584-589.
14. B. J. Akinyele and F. C. Adetuyi, "Effect of agowastes, pH and temperature variation on the growth of *Volvariella volvacea*", *African J. Biotechnol.*, **2005**, *4*, 1390-1395.
15. S. G. Jonathan and I. O. Fasidi, "Effect of carbon, nitrogen and mineral sources on growth of *Psathyerella atroumbonata* (Pegler), a Nigerian edible mushroom", *Food Chem.*, **2001**, *72*, 479-483.
16. T. Hatakeyama and M. Ohmasa, "Mycelial growth of strains of the genera *Suillus* and *Boletinus* in media with a wide range of concentrations of carbon and nitrogen sources", *Mycoscience*, **2004**, *45*, 169-176.
17. O. D. Adejoye, B. C. Adebayo-Tayo, A. A. Ogunjobi, O. A. Olaoye and F. I. Fadahunsi, "Effect of carbon, nitrogen and mineral sources on growth of *Pleurotus florida,* a Nigeria edible mushroom", *African J. Biotechnol.*, **2006**, *5*, 1355-1359.
18. A. Daza, J. L. Manjón, M. Camacho, L. R. de la Osa, A. Aguilar and C. Santamaría, "Effect of carbon and nitrogen sources, pH and temperature on *in vitro* culture of several isolates of *Amanita caesarea* (Scop.:Fr.) Pers", *Mycorrhiza*, **2006**, *16*, 133-136.
19. G. Zervakis, A. Philippoussis, S. Ioannidou and P. Diamantopoulou, "Mycelium growth kinetics and optimal temperature conditions for the cultivation of edible mushroom species on lignocellulosic substrates", *Folia Microbiol.*, **2001**, *46*, 231-234.
20. V. I. Ruby and K. I. Noemia, "Optimal conditions of *in vitro* mycelial growth of *Lentinus strigosus* an edible mushroom isolated in the Brazilian Amazon", *Mycoscience*, **2008**, *49*, 215-219.

21. R. Sanmee, P. Lumyong, B. Dell and S. Lumyong, "In vitro cultivation and fruit body formation of the black bolete, *Phlebopus portentosus*, a popular edible ectomycorrhizal fungus in Thailand", *Mycoscience*, **2010**, *51*, 15-22.
22. S. M. Barreto, M. V. López and L. Levin, "Effect of culture parameters on the production of the edible mushroom *Grifola frondosa* (maitake) in tropical weathers", *World J. Microbiol. Biotechnol.*, **2008**, *24*, 1361-1366.
23. B. Elhami and N. A. Ansari, "Effect of substrates of spawn production on mycelium growth of oyster mushroom species", *J. Biol. Sci.*, **2008**, *8*, 474-477.
24. A. Ohta and N. Fujiwara, "Fruit-body production of an ectomycorrhizal fungus in genus *Boletus* in pure culture", *Mycoscience*, **2003**, *44*, 295-300.
25. M. Brundrett, N. Bougher, B. Dell, T. Grove and N. Malajczuk, "Working with Mycorrhizas in Forestry and Agriculture", ACIAR Monograph, Pirie Printers, Canberra, **1996**.
26. R. M. Atlas and L. C. Parks, "Handbook of Microbiological Media", CRC Press, Raton, **1993**.
27. E. Danell, "*Cantharellus cibarius*: Mycorrhiza formation and ecology", *PhD Thesis*, **1994**, University of Uppsala, Sweden.
28. L. M. Vaario, W. M. Gill, M. Tanaka, Y. Ide and K. Suzuki, "Aseptic ectomycorrhizal synthesis between *Abies firma* and *Cenococcum geophilum* in artificial culture", *Mycoscience*, **2000**, *41*, 395-399.
29. A. G. Laguette, L. M. Vaario, W. M. Gill, F. Lapeyrie, N. Matsushita and K. Suzuki, "Rapid in vitro ectomycorrhizal infection on *Pinus densiflora* roots *by Tricholoma matsutake*", *Mycoscience*, **2000**, *41*, 389-393.
30. P. Sysouphanthong, S. Thongkantha, R. Zhao, K. Soytong and K. D. Hyde, "Mushroom diversity in sustainable shade tea forest and the effect of fire damage", *Biodivers. Conserv.*, **2010,** *19*, 1401-1415.
31. H. Niitsu, N. Hanyuda and Y. Sugiyama, "Cultural properties of a luminous mushroom, *Mycena chlorophos*", *Mycoscience*, **2000**, *41*, 551-558.
32. K. Kinugawa, "Physiology and the breeding of *Flamminula velutipes*", in "Genetics and Breeding of Edible Mushrooms" (Ed. S. T. Chang, J. A. Buswell and P. G. Milles), Gordon and Breach, Y-Parc (Switzerland), **1998**, pp. 87-109.
33. U. Kües and Y. Liu, "Fruiting body production in basidiomycetes", *Appl. Microbiol. Biotechnol.*, **2000**, *54*, 141-152.
34. A. Ohta, "Fruit-body production of two ectomycorrhizal fungi in the genus *Hebeloma* in pure culture", *Mycoscience*, **1998**, *39*, 15-19.
35. H. Kawagishi, K. Hamajima, R. Takanami, T. Nakamura, Y. Sato, Y. Akiyama, M. Sano and O. Tanaka, "Growth promotion of mycelia of the matsutake mushroom *Tricholoma matsutake* by D- isoleucine", *Biosci. Biotechnol. Biochem.*, **2004**, *68*, 2405-2407.

Maejo Int. J. Sci. Technol. **2011**, *5*(03), 426-435

Maejo International Journal of Science and Technology

ISSN 1905-7873
Available online at www.mijst.mju.ac.th

Full Paper

An economical ultrasonic-assisted extraction for the spectrophotometric determination of anionic surfactants

Sarawut Somnam [1,*], Praweena Novichai [1], Jaroon Jakmunee[2] and Kate Grudpan[2]

1Chemistry Program, Department of Science, Faculty of Science and Technology, Chiang Mai Rajabhat University, Chiang Mai 50300, Thailand

2 Department of Chemistry and Centre for Innovation in Chemistry, Faculty of Science, Chiang Mai University, Chiang Mai 50200, Thailand

* Corresponding author, e-mail: sarawut_som@cmru.ac.th; tel. +66-5388-5621; fax +66-5388-5620

Received: 11 December 2010 / Accepted: 15 December 2011 / Published: 21 December 2011

Abstract: An economical ultrasonic-assisted extraction system was developed for the extraction / spectrophotometric determination of anionic surfactants based on methylene blue method. A low-cost ultrasonic cleaner was employed to enhance extraction efficiency and also to reduce chemical consumption, time and cost of analysis. Optimum conditions for extraction and detection were determined. Extraction time of 30 seconds and a volume ratio of aqueous sample to organic solvent of 8:1 were found to be optimum. Concentrations of methylene blue and Na_2SO_4 were selected at 10^{-5} and 10^{-2} M respectively. Simultaneous parallel extraction of 12 samples could be carried out. Standard solutions of sodium dodecyl sulphate (0.10 mg L^{-1}) were evaluated for reproducibility and the relative standard deviation was found to be 4.8%. The method was applied to the analysis of 7 real water samples. The concentrations of AS were found in the range of 0.054–0.123 mg L^{-1}. The results obtained were compared to those from the standard method and no significant difference was observed. Recovery was found to be 106–112%.

Keywords: ultrasonic-assisted extraction, methylene blue, anionic surfactants

INTRODUCTION

Anionic surfactants (AS) are widely used in household, cosmetic and industrial products as well as in research laboratories [1-3]. Because of their difficult biodegradation, the resulting contamination of water source can affect water quality and aquatic animals [4]. In order to determine the content of the surfactants accurately, an effective analytical method is needed. The official method for determination of AS in water is based on the formation of an ion-associated complex between an anionic surfactant and methylene blue (MB) cationic-dye molecules in the

stoichiometric ratio of 1:1. The complex is extracted into chloroform and determined spectrophotometrically at 654 nm [5]. This method involves multiple steps and tedious extraction procedure which is time-consuming and consumes a large volume of organic solvent [2-3, 6].

Ultrasonic-assisted extraction (UAE) is expeditious and inexpensive compared to conventional extraction [e.g. 7-8]. When the ultrasonic wave passes through a liquid medium, the liquid is compressed and decompressed leading to the generation of bubbles. Numerous micro-bubbles form, grow, oscillate quickly and collapse violently, thus producing shock wave, a phenomenon called cavitation [9-13]. The phenomenon can be applied for various purpose, e.g. cleaning [9-10], stripping [11], accelerating liquid-liquid or solid-liquid extraction [12-13], digesting [14-15], emulsifying [16-17], homogenising [18], degassing [19], filtering [20] and crystallising [21].

UAE method can be achieved by various types of ultrasonic devices such as ultrasonic probe [17, 22-23], ultrasonic bath [24-25], sonoreactor [26] and cup horn [27]. Although an ultrasonic probe provides the highest intensity of sonication because it immerses directly into the solution [28-29], the extraction can only be done for individual samples and with a risk of contamination. While a sonoreactor, cup horn and ultrasonic bath give lower sonication intensities because the ultrasonic wave needs to cross the medium solution or the wall of the container, a simultaneous extraction without contamination is possible [11, 29].

The scientific ultrasonic instruments of various types as described above are of large size and expensive. In this work, a small ultrasonic cleaner that is generally used for cleaning small objects was applied as a UAE system. This instrument is simple, low-cost and small in size. The system was used for the extraction of anionic surfactants based on MB method employing dichloromethane as organic solvent. The main factors affecting the extraction efficiency were optimised with emphasis on extraction efficiency and reduction of organic solvent volume and time needed for extraction.

MATERIALS AND METHODS

Chemicals and Standard Solutions

Deionised water from a Milli Q & Elix 10 element system (Millipore, USA) were used throughout. Sodium dodecyl sulphate (SDS) (98.0%, Fluka) and dichloromethane (99.8%, Lab-scan) were used as standard anionic surfactant and organic solvent respectively. Methylene blue (MB, 95.0%) was purchased from Riedel-de Haën. Other chemicals used for preparing the working MB solution were sodium sulphate (99.5%, Fluka), potassium dihydrogen phosphate (99.5%, Merck) and sulfuric acid (98.0%, Lab-scan). Chemicals used for interference study were sodium chloride (99.0%, Lab-scan), potassium bromide (99.5%, Rankem), sodium nitrite (99.0%, Merck), sodium nitrate (99.5%, Merck), sodium thiocyanate (98.0%, Fluka), sodium sulphate (99.0%, Fluka) and sodium phosphate (98.0%, Rankem).

Stock standard solution (1000 mg L^{-1}) of SDS was prepared by dissolving the anionic surfactant (0.1109 g) in water and diluting to 100 mL. Working standard solutions were prepared daily by diluting the stock standard solution with water to obtain desired concentrations.

A stock solution (1.0×10^{-3} M) of MB was prepared by dissolving the dye (0.0333 g) in water (100 mL). A working MB solution (1.0×10^{-5} M) was prepared by mixing the following together: MB stock solution (2.5 mL), Na_2SO_4 (0.3552 g), KH_2PO_4 (0.25 g) and H_2SO_4 (0.5 mL), and adjusting the volume to 250 mL with water [30]. This solution was then pre-extracted with dichloromethane (1/5 volume) to prevent a background level when partitioning MB into the organic phase. The organic solvent was also shaken with water (1/5 volume) before use to saturate the solvent with water.

Apparatus and Operation Procedure

The extraction of anionic surfactants was carried out by mixing aqueous solutions of SDS and MB in a test tube (10 x 1.7 cm) followed by adding a small volume (1 mL) of dichloromethane. The volume ratio of the aqueous solution to organic solvent was kept at 8:1. The test tubes were placed on a rack that was immersed in the bath of a simple ultrasonic cleaner (dimension: 10.5 × 18 × 9 cm; DADI DA-968, Ling Tong Electronic Factory, China) for the extraction under a sonication frequency of 40 KHz (50 W). After extraction, the two phases were separated by centrifugation. The organic phase was subjected to measurement by a UV-VIS spectrophotometer (Shimadzu UV 1600, Japan) at 660 nm.

Because of the small volume of extracting solvent, the use of a general cuvette for measurement was not possible. A flow cell with an internal volume of 400 µL was then used by connecting to PTFE tubing (i.d. 0.030 inch) and a simple hypodermic syringe (Figure 1). The PTFE tubing was dipped into the organic phase and the solution was sucked into the flow cell by the syringe until it filled the flow cell. After the absorbance was read, the solution was pushed out of the flow cell. The absorbance obtained for the standard or sample solution was substracted by that of a blank solution before being used for plotting a calibration curve.

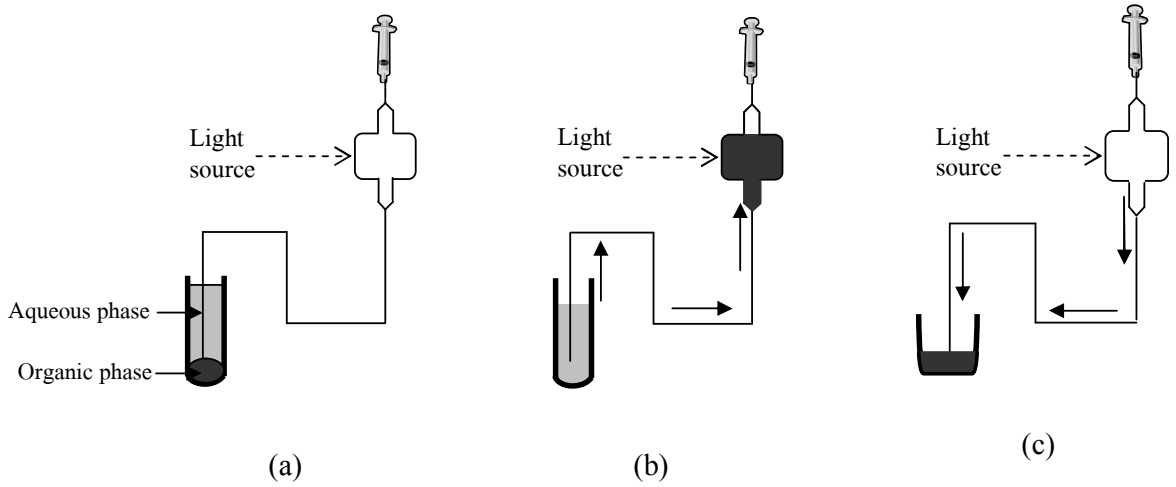

Figure 1. The flow cell and steps for use: (a) PTFE tube was dipped into organic phase; (b) solution was sucked up to fill flow cell for spectrophotometric measurement; (c) extract was pushed out of flow cell.

RESULTS AND DISCUSSION

Optimisation of Influencing Factors

Some factors that affected the extraction efficiency were studied, viz. extraction time, cationic dye (MB) concentration, volume ratio of aqueous solution to organic solvent, and salting-out effect. The effect of extraction time was first studied by using the initial condition: 10^{-5}M MB, 0.05M Na_2SO_4, and 5:1 volume ratio of aqueous phase to organic phase. The extraction time was varied at 15, 30, 45, 60 and 75 seconds. A series of standard solutions of SDS (0.020-0.50 mg L^{-1}) was extracted in order to construct calibration graphs. Then the slope of the calibration graph versus extraction time was plotted as shown in Figure 2. Although it was found that the slopes (sensitivity) at different extraction times were not much different, an extraction time of 30 seconds which provided the highest sensitivity and lowest blank signal was chosen as optimum.

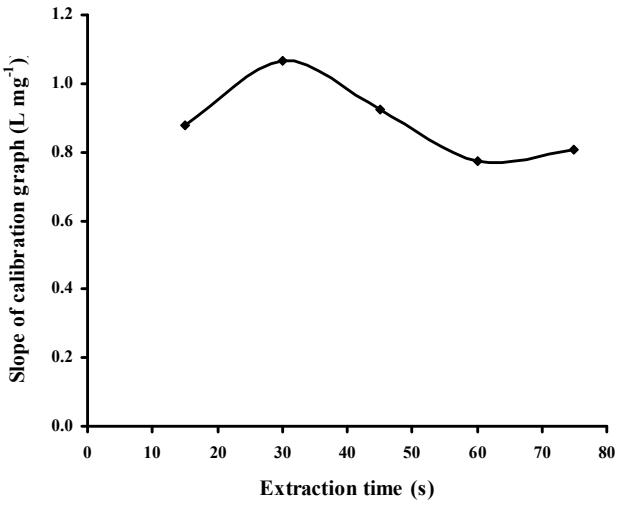

Figure 2. Effect of extraction time on slope of calibration graph

The influence of MB concentration was examined to observe the change in efficiency of extraction of the SDS-MB ion pair into the organic phase. The MB concentrations of 10^{-6}, 10^{-5}, 10^{-4} and 10^{-3}M were used and a plot of concentration of MB as p-function (pMB) versus sensitivity (slope of the calibration graph) is illustrated in Figure 3. The result indicates that 10^{-5}M MB gave the highest sensitivity.

Using conditions previously selected, the effect of volume ratio of aqueous to organic phase was investigated. The volume of dichloromethane was fixed at 1 mL while the aqueous volume was increased to obtain the aqueous:organic ratios of 1:1, 2:1, 5:1, 8:1 and 10:1. The obtained calibration graph (Figure 4) shows that the sensitivity increased with increasing aqueous volume. Although at the ratio of 10:1 gave the highest slope, the blank signal was also highest while the blank signals of the other ratios were much lower. Thus, the 8:1 ratio of was selected as optimum.

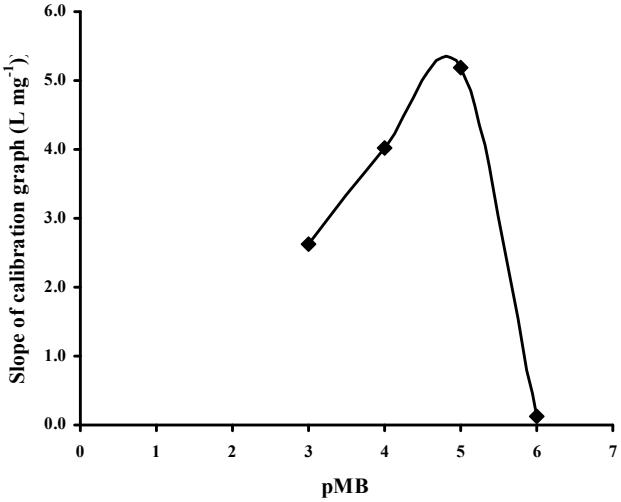

Figure 3. Effect of MB concentration on slope of calibration graph

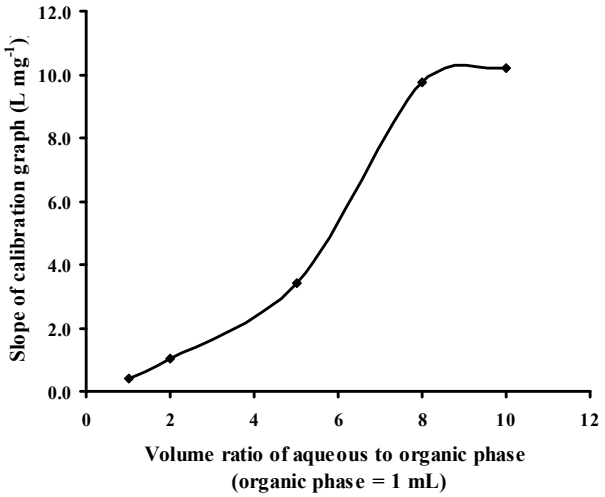

Figure 4. Effect of volume ratio of aqueous to organic phase on slope of calibration graph

A higher ionic strength was reported to greatly enhance the extraction efficiency of organic compounds from aqueous solutions to the organic phase and thus improve the sensitivity and precision of the determination, i.e. the so-called salting-out effect [31-32]. Various salts can be employed while Na_2SO_4 was used in this work because it gives a high ionic strength and is readily available. Different concentrations of Na_2SO_4 (5.0, 10.0, 50.0, 100.0 and 200.0 mM) were added to the working standard solution of SDS. The result in Figure 5 shows that a sharp increase in sensitivity occurred between 5.0-10.0 mM Na_2SO_4. The sensitivity enhancement then slightly decreased between 10-100 mM and steadily decreased after that. The solutions were also observed to be turbid due to the high concentration of salt. Thus, Na_2SO_4 at 10 mM was selected as optimum.

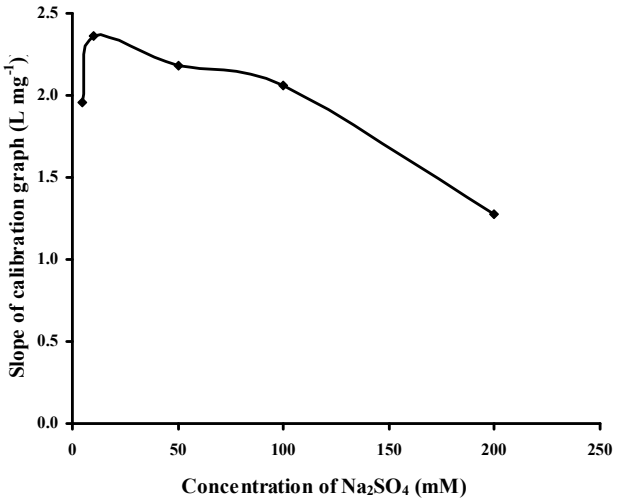

Figure 5. Salting-out effect of Na_2SO_4

Analytical Characteristics

Under the selected set of conditions, i.e. extraction time of 30 seconds, ratio of aqueous to organic solutions of 8:1, and concentrations of MB and Na_2SO_4 of 10^{-5} M and 10 mM respectively, a series of standard solutions of SDS after treatment with MB solution were extracted as described above. The organic phase was separated and analysed spectrophotometrically. The calibration graph was then constructed by plotting absorbance versus concentration of SDS (0.0, 0.020, 0.10, 0.20 and 0.50 mg L^{-1}). A linear calibration graph ($y = 1.5151x + 0.1218$, $R^2 = 0.9920$) was obtained. The limit of detection (LOD) calculated from 3 × standard deviation of blank / slope of the calibration graph [33] was found to be 0.010 mg L^{-1}.

The reproducibility of the ultrasonic-assisted extraction was examined by performing 11 simultaneous extractions of 0.10 mg L^{-1} SDS solutions under the optimum conditions. The average signal of absorbance was obtained and the relative standard deviation was 4.8%. The result showed good precision even though the extraction vessels were placed at different positions in the ultrasonic bath. The procedure consumed only 1 mL of organic solvent for each extraction and several extractions (up to 12 samples) could be performed simultaneously.

Interference Study

Interference from foreign ions usually found in water samples was investigated. Various ions, namely Cl^-, Br^-, NO_2^-, NO_3^-, SCN^-, SO_4^{2-} and PO_4^{3-}, of known concentrations were separately added to a solution containing a fixed concentration of SDS (0.20 mg L^{-1} or 6.93×10^{-7} M, the mean concentration of the calibration range). The tolerance limit, defined as the maximum concentration of a foreign ion per a fixed concentration of SDS that causes a deviation of absorbance not higher than ± 5% of the mean value of the absorbance due to the SDS solution without foreign ion, is summarised in Table 1.

Table 1. Maximum tolerance concentration ratio of various ions in AS determination

Species	Tolerance limit (C_{ion} / C_{AS})
Cl^-, Br^-, NO_2^-, SCN^-, SO_4^{2-}	140
NO_3^-, PO_4^{3-}	1400

It was found that ions normally found in water samples did not interfere in the extraction of AS under the proposed conditions. The concentration ratios of these ions to surfactant in water samples are usually lower than the tolerance limit. Moreover, these ions which are of smaller size than the surfactant may not form a strong ion association with MB and the small ion-pair compounds are unlikely to be effectively extracted into the organic layer.

Analysis of Water Samples

Water samples (500 mL) were collected from various sources around Chiang Mai city (defined area of about 40 km^2), the sampling sites being about 5 km apart. All samples were filtered through a 0.45-μm membrane filter and analysed within 24 h without any preservation. Table 2 summarises the results on the AS content obtained by UAE under the determined optimum conditions compared to those obtained by the standard method carried out by batch extraction [5].

Table 2. Results of AS determination by UAE and standard methods

Sample number	Source	Amount of AS (± SD) (mg L^{-1})	
		UAE method*	Standard method*
1	Canal	0.082 ± 0.004	0.0520 ± 0.0002
2	Canal	0.069 ± 0.007	0.0580 ± 0.0002
3	Drain	0.123 ± 0.005	0.1160 ± 0.0002
4	Drain	0.072 ± 0.006	0.0510 ± 0.0009
5	River	0.058 ± 0.015	0.0420 ± 0.0004
6	River	0.054 ± 0.002	0.0350 ± 0.0000
7	River	0.065 ± 0.017	0.0380 ± 0.0004

* Mean of triplicate determinations

The values of AS content found by UAE method (x) agreed well with those found by the standard method (y), as indicated by the fact that the slope, intercept and coefficient of determination (R^2) of the correlation graph between the two methods were close to 1, 0 and 1 respectively ($y = 1.1508x + 0.0300$, $R^2 = 0.9279$). According to the paired t-test at 95% confidence level [33], there was no significant difference between the results from the two methods.

Recovery Study

Three water samples in Table 2 were randomly taken for recovery study by addition of SDS standard solution (0.10 mg L^{-1}). This concentration was used because it was close to those found in

most of the samples. Recoveries were found to be 106-112% with a relative standard deviation of 2.8%.

CONCLUSIONS

The UAE technique using a simple ultrasonic cleaner for determination of AS based on MB method was found to be effective. Up to 12 samples can be simultaneously determined with low consumption of chemicals and time. Application to real samples gave results which were comparable to those obtained conventionally.

ACKNOWLEDGEMENTS

The Thailand Research Fund (TRF) is gratefully acknowledged for financial support to this research. We thank PERCH-CIC for providing partial support.

REFERENCES

1. E. Chirila, I. Carazeanu and S. Dobrinas, "Spectrometric studies about some dyes-anionic surfactant interactions in aqueous solutions", *Talanta*, **2000**, *53*, 271-275.
2. E. M. El-Nemma, N. M. Badawi and S. S. M. Hassan, "Cobalt phthalocyanine as a novel molecular recognition reagent for batch and flow injection potentiometric and spectrophotometric determination of anionic surfactants", *Talanta*, **2009**, *78*, 723-729.
3. E. Ródenas-Torralba, B. F. Reis, A. Morales-Rubio and M. de la Guardia, "An environmentally friendly multicommutated alternative to the reference method for anionic surfactant determination in water", *Talanta*, **2005**, *66*, 591-599.
4. Y. Y. Hu, Y. Z. He, L. L. Qian and L. Wang, "On-line ion pair solid-phase extraction of eletrokinetic multicommutation for determination of trace anion surfactants in pond water", *Anal. Chim. Acta*, **2005**, *536*, 251-257.
5. G. H. Jeffery, J. Bassett, J. Mendham and R. C. Denney, "Vogel's Textbook of Quantitative Chemical Analysis", 5th Edn., Longman, London, **1994**, pp. 706-707.
6. M. Koga, Y. Yamamichi, Y. Nomoto, M. Irie, T. Tanimura and T. Yoshinaga, "Rapid determination of anionic surfactants by improved spectrophotometric method using methylene blue", *Anal. Sci.*, **1999**, *15*, 563-568.
7. I. Rezić, "Optimization of ultrasonic extraction of 23 elements from cotton", *Ultrason. Sonochem.*, **2009**, *16*, 63-69.
8. D. A. Lambropoulou, I. K. Konstantinou and T. A. Albanis, "Sample pretreatment method for the determination of polychlorinated biphenyls in bird livers using ultrasonic extraction followed by headspace solid-phase microextraction and gas chromatography-mass spectrometry", *J. Chromatogr. A*, **2006**, *1124,* 97-105.
9. O. V. Abramov, V. O. Abramov, S. K. Myasnikov and M. S. Mullakaev, "Extraction of bitumen, crude oil and its products from tar sand and contaminated sandy soil under effect of ultrasound", *Ultrason. Sonochem.*, **2009**, *16*, 408-416.
10. V. Sivakumar and P. G. Rao, "Application of power ultrasound in leather processing: An eco-friendly approach", *J. Clean. Product.*, **2001**, *9*, 25-33.

11. R. A. Munoz, P. V. Oilveira and L. Angnes, "Combination of ultrasonic extraction and stripping analysis: An effective and reliable way for the determination of Cu and Pb in lubricating oils", *Talanta*, **2006**, *68*, 850-856.
12. A. Marin, A. López-Gonzálvez and C. Barbas, "Development and validation of extraction methods for determination of zinc and arsenic speciation in soils using focused ultrasound: Application to heavy metal study in mud and soils", *Anal. Chim. Acta*, **2001**, *442*, 305-318.
13. J. L. Capelo, M. M. Galesio, G. M. Felisberto, C. Vaz and J. C. Pessoa, "Micro-focused ultrasonic solid-liquid extraction (mμFUSLE) combined with HPLC and fluorescence detection for PAHs determination in sediments: Optimization and linking with the analytical minimalism concept", *Talanta*, **2005**, *66*, 1272-1280.
14. F. Priego-Capote and M. D. Luque de Castro, "Ultrasound-assisted digestion: A useful alternative in sample preparation", *J. Biochem. Biophys. Methods*, **2007**, *70*, 299-310.
15. G. Vale, R. Rial-Otero, A. Mota, L. Fonseca and J. L. Capelo, "Ultrasonic-assisted enzymatic digestion (USAED) for total elemental determination and elemental speciation: A tutorial", *Talanta*, **2008**, *75*, 872-884.
16. S. Freitas, B. Rudolf, H. P. Merkle and B. Gander, "Flow-through ultrasonic emulsification combined with static micromixing for aseptic production of microspheres by solvent extraction", *Eur. J. Pharm. Biopharm.*, **2005**, *61*, 181-187.
17. R. S. Juang and K. H. Lin, "Ultrasound-assisted production of W/O emulsions in liquid surfactant membrane processes", *Colloids Surf. A: Physicochem. Eng. Aspects*, **2004**, *238*, 43-49.
18. M. D. L. de Castro and F. Priego-Capote, "Ultrasound-assisted preparation of liquid samples", *Talanta*, **2007**, *72*, 321-334.
19. F. Chemat, Z. Huma and M. K. Khan, "Applications of ultrasound in food technology: Processing, preservation and extraction", *Ultrason. Sonochem.*, **2011**, *18*, 813-835.
20. M. Mantysalo and E. Mantysalo, "Extraction and filtering in ultrasonic field: Finite element modeling and simulation of the processes", *Ultrasonics*, **2000**, *38*, 723-726.
21. A. Patist and D. Bates, "Ultrasonic innovations in food industry: From the laboratory to commercial production", *Innov. Food Sci. Emerg. Tech.*, **2008**, *9*, 147-154.
22. M. Villar, R. Fernández-Torres, M. Callejón, P. Villar and J. C. Jiménez, "Application of probe sonication extraction for the determination of linear alkylbenzene sulfonates from sewage sludge. Comparison with other extraction methods", *Microchem. J.*, **2008**, *90*, 164-170.
23. G. M. Greenway and Q. J. Song, "An ultrasound accerelated sequential extraction method and its application for element partitioning studies in compost from mixed waste streams", *J. Environ. Monit.*, **2002**, *4*, 950-955.
24. N. Jalbani, T. G. Kazi, B. M. Arain, M. K. Jamali, H. I. Afridi and R. A. Sarfraz, "Application of factorial design in optimization of ultrasonic-assisted extraction of aluminum in juices and soft drinks", *Talanta*, **2006**, *70*, 307-314.
25. M. Toma, M. Vinatoru, L. Paniwnyk and T. J. Mason, "Investigation of the effects of ultrasound on vegetal tissues during solvent extraction", *Ultrason. Sonochem.*, **2001**, *8*, 137-142.

26. S. Ueno, T. Fujita, D. Kuchar, M. Kubota and H. Matsuda, "Ultrasound assisted extraction and decomposition of Cl-containing herbicide involved in model soil", *Ultrason. Sonochem.*, **2009**, *16*, 169-175.
27. G. Cravotto, L. Boffa. S. Mantegna, P. Perego, M. Avogadro and P. Cintas, "Improved extraction of vegetable oils under high-intensity ultrasound and/or microwaves", *Ultrason. Sonochem.*, **2008**, *15*, 898-902.
28. H. M. Santos and J. L. Capelo, "Trends in ultrasonic-based equipment for analytical sample treatment", *Talanta*, **2007**, *73*, 795-802.
29. R. Rial-Otero, R. J. Carreira, F. M. Cordeiro, A. J. Moro, H. M. Santos, G. Vale, I. Moura and J. L. Capelo, "Ultrasonic assisted protein enzymatic digestion for fast protein identification by matrix-assisted laser desorption/ionization time-of-flight mass spectrometry: Sonoreactor versus ultrasonic probe", *J. Chromatogr. A*, **2007**, *1166*, 101-107.
30. R. Burakham, J. Jakmunee and K. Grudpan, "Development of sequential injection-lab-at-valve (SI-LAV) micro-extraction instrumentation for the spectrophotometric determination of an anionic surfactant", *Anal. Sci.*, **2006**, *22*, 137-140.
31. G. M. Nikolić, J. M. Perović, R. S. Nikolić and M. D. Cakić, "Salting-out extraction of catechol and hydroquinone from aqueous solutions and urine samples", *Facta Univers.*, **2003**, *2*, 293-299.
32. B. Jiménez, J. C. Moltó and G. Font, "Influence of dissolved humic material and ionic strength on C8 extraction of pesticides from water", *Chromatographia*, **1995**, *41*, 318-324.
33. G. D. Christian, "Analytical Chemistry", 6th Edn., Wiley, New York, **2004**, pp. 93-98.